JAEA-Review
2006-012

JP0650380

JAEA-Review

Progress of Nuclear Safety Research—2005

(Eds.) Editorial Committee on Nuclear Safety Research Results

Nuclear Safety Research Center

March 2006

Japan Atomic Energy Agency

日本原子力研究開発機構

JAEA-Review 2006-012

Progress of Nuclear Safety Research – 2005

(Eds.) Editorial Committee on Nuclear Safety Research Results※

Nuclear Safety Research Center
Japan Atomic Energy Agency
Tokai-mura, Naka-gun, Ibaraki-ken

(Received February 15, 2006)

The Japan Atomic Energy Research Institute (JAERI), one of the predecessors of the Japan Atomic Energy Agency (JAEA), had conducted nuclear safety research primarily at the Nuclear Safety Research Center in close cooperation with the related departments in accordance with the Long Term Plan for Development and Utilization of Nuclear Energy and Five-Years Program for Safety Research issued by the Japanese government. The fields of conducting safety research at JAERI were the engineering safety of nuclear power plants and nuclear fuel cycle facilities, and radioactive waste management as well as advanced technology for safety improvement or assessment. Also, JAERI had conducted international collaboration to share the information on common global issues of nuclear safety and to supplement own research. Moreover, when accidents occurred at nuclear facilities, JAERI had taken a responsible role by providing technical experts in assistance to conducting accident investigations or emergency responses by the government or local government. These nuclear safety research and technical assistance to the government have been taken over as an important role by JAEA.

This report summarizes the nuclear safety research activities of JAERI from April 2003 through September 2005 and utilized facilities.

Keywords: Nuclear Safety, Nuclear Power Plant, Nuclear Fuel Cycle, Radioactive Waste Management, Experiment, Analysis

---

※ Supervisor: Kiyomi Ishijima, Director, Nuclear Safety Research Center
Editors: Yoshinari Anoda (Chief editor), Masaki Amaya, Junichi Saito, Sato Atsushi, Hiroki Sono, Hitoshi Tamaki, Kotaro Tonoike, Yoshiyuki Nemoto, Yasuo Motoki, Kiyofumi Moriyama, Tetsuji Yamaguchi, Fumimasa Araya

JAEA-Review 2006-012

原子力安全性研究の現状（平成１７年）

日本原子力研究開発機構安全研究センター
(編)安全性研究成果編集委員会※

(2006年2月15日受理)

日本原子力研究開発機構の前身の一機関である日本原子力研究所（原研）は、国の定める原子力エネルギー開発・利用に関する長期計画や安全研究年次計画に沿って、安全性試験研究センターを中心に関連部門との密接な連携のもとで、原子力安全性研究を実施してきた。研究対象の分野は、原子炉施設及び燃料サイクル施設の工学的安全性研究、放射性廃棄物安全性研究、安全性向上及び評価に関する先進技術の研究等である。また、世界共通の原子力安全課題に関する情報の共有を図ると共に、原研の研究を補完する目的で国際協力を実施してきた。さらに、原子力施設の事故等に際し、国や地方自治体が行う原因究明や緊急時対応等の作業を技術面で支援することは、原研に求められる重要な役割の一つである。これらの安全研究及び原子力安全規制に係る技術支援は、日本原子力研究開発機構の重要な役割として継承されている。

本報告書は、平成15年4月から平成17年9月までの2年半の間に原研において実施された原子力安全性研究の概要及び研究に用いられた施設について記載している。

原子力科学研究所（駐在）：〒319-1195　茨城県那珂郡東海村白方白根２－４
※　監修：安全研究センター長　石島清見
編集委員：安濃田良成（委員長）、天谷政樹、齋藤順市、佐藤篤司、曽野浩樹、玉置等史、外池幸太郎、根本義之、元木保男、森山清史、山口徹治、新谷文將

Contents

目次

Authors

1. Kiyomi ISHIJIMA, Director, Nuclear Safety Research Center
2. Masahide SUZUKI, Senior Principal Researcher, Nuclear Safety Research Center
2.1 Toyoshi FUKETA, Unit Manager, Reactor Safety Research Unit, Nuclear Safety Research Center
2.1.1 Motoe SUZUKI and Jinich NAKAMURA, Fuel Safety Research Gr., Reactor Safety Research Unit
2.1.2 Takehiko NAKAMURA, Fuel Safety Research Gr., Reactor Safety Research Unit
2.1.3 Fumihisa NAGASE, Fuel Safety Research Gr., Reactor Safety Research Unit
2.2 Kunio ONIZAWA, Gr. Leader, Reactor Component Reliability Research Gr., Reactor Safety Research Unit
2.2.1 Kunio ONIZAWA, Hideharu SUGINO and Hiroto ITOH, Reactor Component Reliability Research Gr., Reactor Safety Research Unit
2.2.2 Yutaka NISHIYAMA, Tohru TOBITA, Noriya EBINE and Kunio ONIZAWA, Reactor Component Reliability Research Gr., Reactor Safety Research Unit
2.2.3 Takashi TSUKADA, Gr. Leader, Research Group for Corrosion Damage Mechanism, Division of Fuels and Materials Engineering, Nuclear Science and Engineering Directorate
2.3 Hideo NAKAMURA, Gr. Leader, Thermohydraulic Safety Research Gr., Reactor Safety Research Unit
2.3.1 Takeshi TAKEDA, Thermohydraulic Safety Research Gr., Reactor Safety Research Unit
2.3.2 Masaya KONDO, Thermohydraulic Safety Research Gr., Reactor Safety Research Unit
2.3.3 Hideaki ASAKA, Thermohydraulic Safety Research Gr., Reactor Safety Research Unit
2.4 Ken MURAMATSU, Senior Principal Researcher, Nuclear Safety Research Center
2.4.1 Tamotsu KUDO, Fuel Safety Research Gr., Reactor Safety Research Unit; Kiyofumi MORIYAMA, Thermohydraulic Safety Research Gr., Reactor Safety Research Unit
2.4.2 Toshimitsu HOMMA, Gr. Leader and Jun ISHIKAWA, Risk Analysis and Applications Research Gr., Nuclear Facility Safety Research Unit
2.4.3 Toshimitsu HOMMA, Gr. Leader and Sohei SATO, Risk Analysis and Applications Research Gr., Nuclear Facility Safety Research Unit
2.4.4 Ken MURAMATSU, Senior Principal Researcher, Nuclear Safety Research Center
2.5 Norio WATANABE, Risk Analysis and Applications Research Gr., Nuclear Facility Safety Research Unit
2.5.1 Norio WATANABE, Risk Analysis and Applications Research Gr., Nuclear Facility Safety Research Unit
2.5.2 Yoshiyuki KAJI, Research Group for Corrosion Damage Mechanism, Division of Fuels

and Materials Engineering, Nuclear Science and Engineering Directorate

3. Hiroshi YANAGISAWA, Gr. Leader, Fuel Cycle Facility Safety Research Gr., Nuclear Facility Safety Research Unit

3.1 Hiroshi YANAGISAWA, Gr. Leader, Fuel Cycle Facility Safety Research Gr., Nuclear Facility Safety Research Unit

3.1.1 Shouichi WATANABE, Fuel Cycle Facility Safety Research Gr., Nuclear Facility Safety Research Unit

3.1.2 Kenya SUYAMA, Fuel Cycle Facility Safety Research Gr., Nuclear Facility Safety Research Unit

3.1.3 Mikio SAKAI and Toshihiro YAMAMOTO, Fuel Cycle Facility Safety Research Gr., Nuclear Facility Safety Research Unit

3.1.4 Yuichi YAMANE and Hiroshi OKUNO, Fuel Cycle Facility Safety Research Gr., Nuclear Facility Safety Research Unit

3.1.5 Minoru MURASAKI, Fuel Cycle Facility Safety Research Gr., Nuclear Facility Safety Research Unit; Hiroki SONO, Dept. of Criticality and Fuel Cycle Research Facilities

3.2 Yasuji MORITA, Gr. Leader, Research Group for Aqueous Separation Process Chemistry, Division of Fuels and Materials Engineering, Nuclear Science and Engineering Directorate

3.2.1 Toshihide ASAKURA, Research Group for Aqueous Separation Process Chemistry, Division of Fuels and Materials Engineering, Nuclear Science and Engineering Directorate

3.2.2 Toshihide ASAKURA, Research Group for Aqueous Separation Process Chemistry, Division of Fuels and Materials Engineering, Nuclear Science and Engineering Directorate

3.3 Kiyoshi KIUCHI, Gr. Leader, Corrosion resistant Materials Development Gr., Division of Fuels and Materials Engineering, Nuclear Science and Engineering Directorate

3.3.1 Ichiro TSUKATANI, Corrosion resistant Materials Development Gr., Division of Fuels and Materials Engineering, Nuclear Science and Engineering Directorate

3.3.2 Chiaki KATO, Corrosion resistant Materials Development Gr., Division of Fuels and Materials Engineering, Nuclear Science and Engineering Directorate

3.4 Kazuo YOSHIDA and Hitoshi TAMAKI, Risk Analysis and Applications Research Group, Nuclear Facility Safety Research Unit

3.4.1 Kazuo YOSHIDA and Hitoshi TAMAKI, Risk Analysis and Applications Research Group, Nuclear Facility Safety Research Unit

3.4.2 Kazuo YOSHIDA, Risk Analysis and Applications Research Group, Nuclear Facility Safety Research Unit

3.5 Hiroshi OKUNO and Koji WATANABE, Fuel Cycle Facility Safety Research Group, Nuclear Facility Safety Research Unit

3.5.1 Hiroshi OKUNO and Koji WATANABE, Fuel Cycle Facility Safety Research Group, Nuclear Facility Safety Research Unit

4. Shinichi NAKAYAMA, Gr. Leader, Waste Disposal and Decommissioning Safety Research Group, Nuclear Facility Safety Research Unit

4.1 Hideo KIMURA, Waste Disposal and Decommissioning Safety Research Group, Nuclear Facility Safety Research Unit

4.1.1 Masahiro MUNAKATA, Waste Disposal and Decommissioning Safety Research Group, Nuclear Facility Safety Research Unit

4.1.2 Masayuki MUKAI, Takeshi FUJIWARA and Tetsuji YAMAGUCHI, Waste Disposal and Decommissioning Safety Research Group, Nuclear Facility Safety Research Unit

4.2 Tetsuji YAMAGUCHI, Waste Disposal and Decommissioning Safety Research Group, Nuclear Facility Safety Research Unit

4.2.1 Dai MIZUNO and Toshikatsu MAEDA, Waste Disposal and Decommissioning Safety Research Group, Nuclear Facility Safety Research Unit

4.2.2 Yoshifumi SAKAMOTO and Tetsuji YAMAGUCHI, Waste Disposal and Decommissioning Safety Research Group, Nuclear Facility Safety Research Unit

4.2.3 Yoshihisa IIDA, Waste Disposal and Decommissioning Safety Research Group, Nuclear Facility Safety Research Unit

4.2.4 Seiji TAKEDA, Waste Disposal and Decommissioning Safety Research Group, Nuclear Facility Safety Research Unit

4.3 Seiji TAKEDA, Waste Disposal and Decommissioning Safety Research Group, Nuclear Facility Safety Research Unit

4.4 Takenori SUKEGAWA, Waste Disposal and Decommissioning Safety Research Group, Nuclear Facility Safety Research Unit

4.4.1 Taro SHIMADA, Waste Disposal and Decommissioning Safety Research Group, Nuclear Facility Safety Research Unit

4.4.2 Masataka TANIMOTO, Waste Disposal and Decommissioning Safety Research Group, Nuclear Facility Safety Research Unit

5. Fumiya TANABE, Supreme Researcher, Nuclear Safety Research Center

5.1 Fumiya TANABE, Supreme Researcher, Nuclear Safety Research Center

5.2 Fumiya TANABE, Supreme Researcher, Nuclear Safety Research Center

6. Yoshinari ANODA, Research Planning and Co-ordination Office, Nuclear Safety Research Center

6.1 Hidetoshi AMANO, Director, Dept. of Hot Laboratories and Facilities

6.1.1 Atsushi SATO, Hot Material Examination Section, Dept. of Hot Laboratories and Facilities

6.1.2 Hiroyuki KANAZAWA, Nonirradiated Fuel Management Section, Dept. of Hot Laboratories and Facilities

6.1.3 Masahiro NISHI, Nuclear Fuel Control Section, Dept. of Hot Laboratories and Facilities
6.2 Shigeru DOJIRI, Director, Dept. of Criticality and Fuel Cycle Research Facilities
6.2.1 Koichi SAKURABA, General Manager, Critical Facility Operation and Engineering Section I, Dept. of Criticality and Fuel Cycle Research Facilities
6.2.2 Shiro KUROBANE, General Manager, Fuel Cycle Research Facility Management Section, Dept. of Criticality and Fuel Cycle Research Facilities
6.3 Teruo NAKAJIMA, Director, Dept. of JMTR
6.3.1 Michihiro NAKA, JMTR Project Engineering Section, Dept. of JMTR; Satoshi HANAWA, Irradiation Technology Section, Technology Development Dept.
6.3.2 Toshimitsu ISHII, Irradiation Technology Section, Technology Development Dept.
7. Yoshinari ANODA, Research Planning and Co-ordination Office, Nuclear Safety Research Center

1. INTRODUCTION

To ensure the safe development and utilization of nuclear energy, the Japan Atomic Energy Research Institute (JAERI), one of the predecessors of the Japan Atomic Energy Agency (JAEA), conducted nuclear safety research in close cooperation with nuclear utilities, venders, universities, and governmental research organizations. The safety research at JAERI concerned the safety of nuclear power plants, nuclear fuel cycle facilities, and radioactive waste management, placing highest priority in establishing technical bases necessary for safety regulation by the government. At the same time, continuous efforts had been made by JAERI to provide technically sound and reliable data and information to the public. Moreover, when accidents occurred at nuclear facilities, JAERI had taken a responsible role by providing technical experts in assistance to conducting accident investigations or emergency responses by the government or local government. JAERI took neutral positions on issues pertaining to governmental regulatory bodies and the nuclear industry. These nuclear safety research and technical assistance to the government have been taken over as an important role by JAEA.

The scope of this safety research was based on the Long Term Plan for Development and Utilization of Nuclear Energy issued by the Atomic Energy Commission and the Five-Years Program for Nuclear Safety Research issued by the Nuclear Safety Commission. The Five-Years Program from 2001 to 2005 specified research items on radioactive waste disposal, MOX fuel processing, fuel safety, aging and decommissioning of nuclear power plants, fuel reprocessing, probabilistic safety assessments, radiation effects, severe accidents and nuclear emergency preparedness to be performed by government organizations to ensure the safety of nuclear facilities. These items were selected because they were needed to develop safety criteria and to establish a technical basis for licensing procedures.

Nuclear safety research at JAERI was conducted primarily at the Nuclear Safety Research Center of the Tokai Research Establishment of JAERI. Various items of safety research were performed by different research divisions within JAERI to optimize the use of facilities and the expertise of JAERI personnel. In addition to administrative offices and research divisions, technical advisory committees were established by JAERI. Japanese experts were invited to offer advice and comments to maximize the utilization of the research results and to improve the quality of research. The organizations engaged in nuclear safety research at JAERI are shown in Fig. 1-1.

This report summarizes the nuclear safety research activities in JAERI from April 2003 through September 2005.

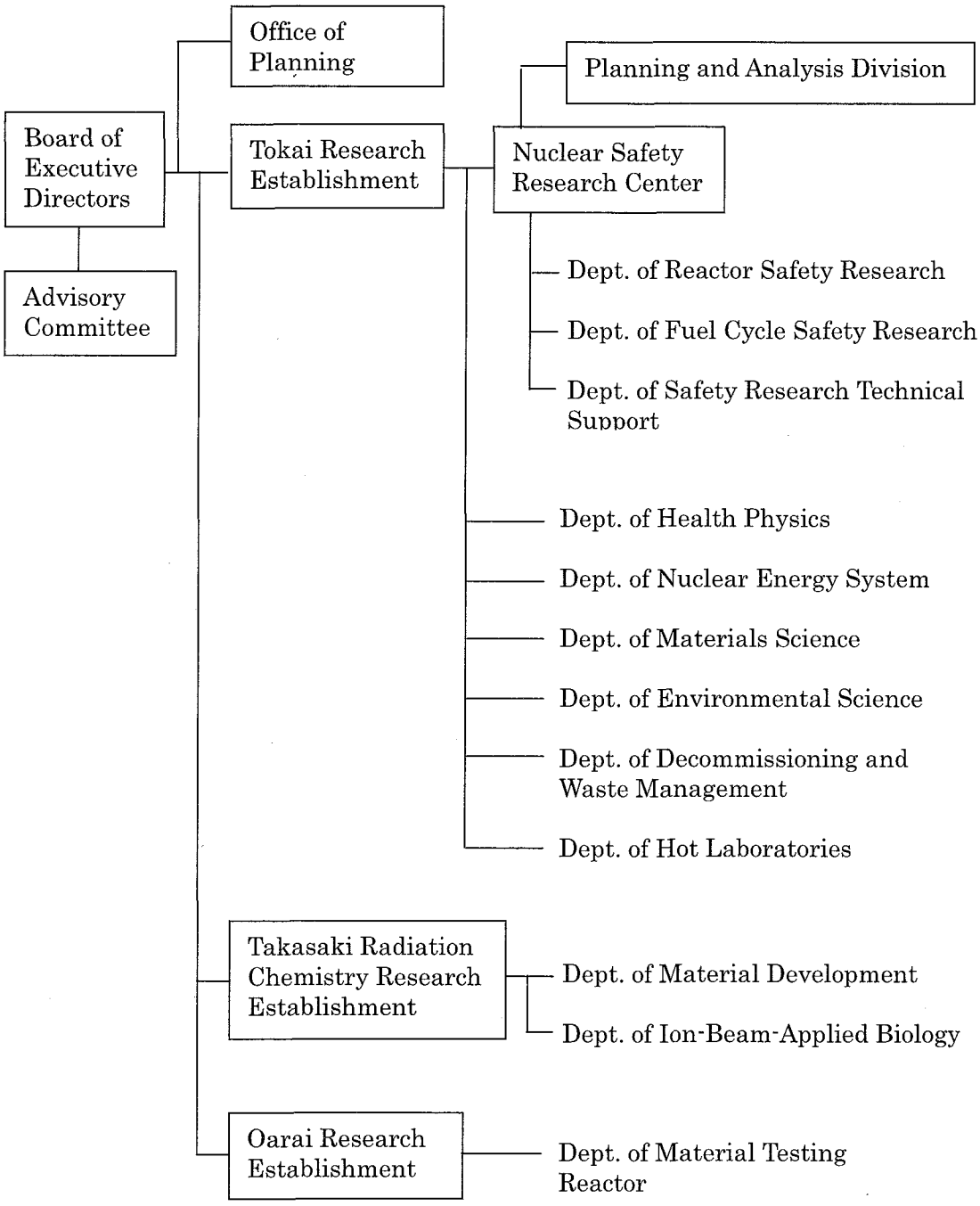

Fig. 1-1 Organizations engaged in nuclear safety research at JAERI

2. REACTOR SAFETY RESEARCH

While light water reactor (LWR) is expected to remain a major nuclear power generation system for a considerable time period up to the middle of 21st century, steady progress has been made for use of high burnup fuels which could lead to reducing the amount of spent fuels and improving the efficiency of fuel usage. For BWR, for example, high burnup UO_2 fuels of 55GWd/t have been utilized. Also for PWR, the ones with improved cladding materials have been used up to the burnup of 55GWd/tU. For the use of mixed oxide (MOX) fuels in LWR, the utilities are planning to initiate using them in several nuclear power plants in the near future. Under the situation now stands, the confirmation of the safety in relation to further burnup extension of UO_2 fuels and the utilization of MOX fuels is an urgent issue to the nuclear safety regulation.

In the area relating to aging of nuclear power plant, a series of important reforms has been made after two big incidents, so called TEPCO problem (2002) and Mihama accident (2004). The former was concerning the cover-up of inspection records performed as self imposed tests by utilities. The latter was the secondary coolant pipe failure accident caused by flow accelerated corrosion, which became the most serious accident in the history of Japanese nuclear power generation. In the new framework of nuclear safety regulation enforced on October 2003, periodic safety review (PSR) has been specified in the law, and the review from the point of plant life management (PLM) for aged plants reaching 30 years operation was incorporated to PSR. In the review, technical assessment of aging and preparation of long term maintenance plan are to be made. After the Mihama accident, regulatory actions for general aging management have further been strengthened, and a general guideline to be followed by licensees for aging management, including that for pipe wall thickness, is under preparation. Hence, in the filed of structural reliability, development of the methodology for evaluating the effect of aging on the integrity of reactor components and/or improving the precision of the evaluation are the matter of great concern.

In the USA, risk informed regulation (RIR) is in the process of being incorporated and reflected to regulatory guides. While in Japan, an issue on the safety goal has extensively been reviewed by the Nuclear Safety Commission (NSC). The interim report issued on August 2003 indicated the quantitative goal as well the qualitative one. Furthermore, fundamental policy on introducing RIR was determined on November 2003 by NSC, clarifying the significance of utilizing risk for the benefit of 1) improvement of rationality, consistency and transparency in the nuclear safety regulation, and 2) proper allotment of the resource among regulatory activities. Corresponding to these activities, the Nuclear and Industrial Safety Agency (NISA) summarized the report concerning RIR on December 2003. Hence, in the area of probabilistic safety assessment (PSA), the establishment of PSA methodology including public risk evaluation, quantitative analysis of the uncertainty

involved in the methodology, making a better use of risk information in the regulatory activities and so on are expected. In the area of thermal hydraulic research, in particular, highly accurate evaluation method is necessary to set more appropriate safety margin.

For the safety assessment of advanced reactor systems, the workshop on "Advanced Nuclear Reactor Safety Issues and Research Needs" held under the auspices of OECD/NEA emphasized the necessity to prepare for new needs. Although urgent safety issues have not been emerged yet in Japan, the technical basis should be accumulated for the future.

As for the analysis and evaluation of accidents that occurred in Japan or abroad, the one on the Davis Besse plant (USA, PWR) should be specially referred to, because unprecedentedly sever damage was produced at the upper head of the reactor pressure vessel due to boric acid corrosion. The use of lessons learned from operating experience is particularly important for improving safety.

Considering the background described above, the activities of reactor safety research in JAEA (JAERI) include:

1) Fuel behavior at high burnup under normal and accident condition,
2) Aging degradation and reliability of structures and components,
3) Thermal hydraulic phenomena in passive safety systems for next generation LWR and coupled neutronic-thermal hydraulic instability in BWR,
4) Assessment and management of risks of LWRs,
5) Operating experience at actual nuclear power plants.

The outline of these activities and main results are shown in the following chapters.

2.1 Fuel Safety Research

From the view points of maintenance and improvement of competitive power in the use of nuclear energy, reduction of environmental load, and maintenance of international trust to our country, burnup extension of light water reactor (LWR) fuel and introduction of mixed oxide (MOX) fuel are being promoted.

In order to supply the evaluation technologies for nuclear safety which are needed to regulate these processes properly; studies concerning normal operation, abnormal transients, reactivity-initiated accident (RIA) and loss-of-coolant accident (LOCA) are being performed at the Japan Atomic Energy Agency (JAEA).

2.1.1 Research on Evaluation of Fuel Behavior during Normal Operation and Abnormal Transients

In this study, PIE in a hot laboratory, irradiation tests in the Halden Rector and development of fuel analysis code on the basis of the data obtained from the above tests and an international collaboration have been carried out for confirming the safety and integrity of high burnup fuel rods.

(1) Fuel behavior study based on irradiation test and PIE

To clarify the fundamental properties of high burnup fuel, disc pellets were irradiated in JRR-3 up to about 130GWd/t, and the burnup analysis of the fuel confirmed that the planned burnup was achieved in the irradiation tests. PIE tests such as density measurement, thermal diffusivity measurements, lattice constant measurement, gas analysis and ceramography were conducted, and the fuel property data between 60 and 130 GWd/t were obtained.

At the Halden Reactor Project, in which JAERI participated, various irradiation tests on high burnup fuel and MOX fuel are conducted as international collaboration research. For example, the fuel center temperature of UO_2 fuel and MOX fuel is measured by means of in-pile instrumentation up to high burnup to evaluate the degradation of thermal conductivity with burnup. A model of fuel thermal conductivity change with burnup is also proposed on the basis of the in-pile measurement.

The internal pressure increase due to fission gas release may result in over pressure conditions which open the pellet-cladding gap, resulting in fuel temperature rise as a thermal feed back effect. This is called a Lift-off behavior. The Lift-off test at the Halden reactor revealed that the over pressure higher than 15MPa is necessary to start the Lift-off behavior. The PIE on the tested rod clarified that the gap was closed due to bonding between pellet and cladding even after the Lift-off. This result suggests that the fuel temperature increase is due to the increase in thermal resistivity within the pellet due to increase of cracks and relocation

of pellet fragments.

In addition, in-pile LOCA tests with high burnup fuel has been started to study the relocation effect during ballooning of cladding, which compromises the out pile LOCA tests with cladding.

As the cooperative researches with several Japanese agencies and companies by means of the Halden Reactor, advanced BWR fuel test (Nuclear Fuel Industries, Ltd.), MOX fuel tests (Mitsubishi Heavy Industries, Ltd. and Nippon Nuclear Fuel Development Co., Ltd.), high–worth control rod material test (Hitachi, Ltd.) and irradiation test to study the effect of additive elements for cladding corrosion (Tokyo Electric Power Company) were conducted.[1]

(2) Development of computer codes for the analysis of fuel rod behavior in normal and abnormal transient conditions

In series of the FEMAXI codes for analysis of fuel behavior in normal and abnormal transient conditions, the latest version FEMAXI-6[2] has been developed. This version is designed particularly for the behaviors in the burnup range above 50GWd/t. In the FEMAXI-6 code, a simultaneous solution is obtained in each time step by coupling thermal analysis and mechanical analysis through iteration process. In the former, temperature distribution, fission gas release and internal pressure are calculated, and in the latter deformation of pellet and cladding are calculated. This coupled solution enables us to obtain more accurate predictions of temperature and deformation of fuel rod.

Models for pellet-clad bonding and for fission gas bubble swelling etc. have been introduced into the code. The bonding model simulates the effect of bonding layer on the enhanced gap thermal conductance and the axial restraint between pellet outer and cladding inner surfaces. Materials properties for MOX fuel have been also extended, and a new function has been incorporated to generate result-file of initial conditions for the accident analysis of the RANNS code. The source code, detailed description, and I/O manual of the FEMAXI-6 code have been released to external users, and to the Japan Nuclear Energy Safety Organization (JNES) to be utilized as a cross-check reference tool for the safety licensing procedure.

The FEMAXI-6 code has been validated from low to high burnup region with the irradiation data which were obtained in the commercial reactor and in the Halden reactor, which proved that the code succeeded in predicting the rod diameter increase by fission gas bubble fuel swelling during power ramp,[3] fuel temperature reduction due to the enhanced thermal conductance in the bonding layer,[4] etc. Figure 2.1-1 shows a comparison between predicted and measured fuel center temperatures in the Lift-Off test in the Halden reactor.[4] The bonding enhances gap thermal conductance, and reduced fuel temperature. Accordingly, the bonding model (BD-gap) predicts a much closer temperature to the measured data (open circles connected by thick line) than the Ross-Stoute model (RS-gap). Further

verification and improvements on the code are in progress.

2.1.2 Research on Fuel Behavior under RIA Conditions

RIA-simulating pulse irradiation experiments have been conducted at the NSRR on short fuel segments, which were irradiated in commercial or research reactors.[5-7),(9-17] The experimental data have been utilized to establish the Safety Evaluation Guidelines for RIAs. From the beginning of fiscal year of 2003 until September 2005, five pulse irradiation tests on irradiated fuel rods and fifteen tests on fresh fuels were performed in the NSRR. Three types of domestic PWR fuel rods with new cladding alloys, MDA[*1], ZIRLO[*2] and NDA[*3], at burnups from 58 to 61 GWd/t were subjected to RIA simulating transients in Tests OI-10, 11[8] and 12, respectively. Another PWR fuel rod irradiated abroad to higher burnup of 78 GWd/t with the new cladding was examined in Test VA-1, using that shipped from Europe in 2004. Fundamental behavior of mechanical energy generation caused by solid fuel/water interaction was studied in 8 tests with fresh fuel powders of various sizes, simulating fragmented fuel. Fuel rod integrity and hydrogen dissociation of the TRIGA fuel for research reactors were examined in 4 fresh fuel tests.

Fuel behavior under instability power oscillation arising during anticipated transient without scram (ATWS) is examined in Test JMH-8 with a fuel at a burnup 19 GWd/t. Transition to film boiling occurred locally at top end of the fuel stack, resulting in the cladding temperature to reach the peak of 743 K (470 ^{0}C) locally measured by one of thermocouples on the cladding. Cladding integrity was maintained after the seven power oscillation which peaked to 89 kW/m in 2 s intervals reaching to the estimated peak fuel enthalpy of 470 J/g, although small plastic deformation was observed at the burn out location.

A computer code RANNS was developed for the quantitative analysis of fuel behavior in the NSRR pulse-irradiation experiments and in hypothetical RIA conditions. Having succeeded the basic structure of the FEMAXI-6 code, the RANNS code uses a geometry which consists of eight ring elements in cladding wall and thirty-six ring elements in a pellet and can perform an accurate calculation of temperature and stress-strain induced by the pellet-cladding mechanical interaction (PCMI) in both pellet and cladding.

Tests performed in NSRR during the period are listed in Table 2.1-1. Main results are described in the following paragraphs from the domestic PWR fuel rod tests, i.e. OI-10, 11 and 12. The test VA-1 on the PWR fuel rod irradiated abroad, was conducted as a part of contract program sponsored and organized by the Nuclear and Industrial Safety Agency, the Ministry

---

[*1] Mitsubishi Developed Alloy (Zr-0.8Sn-0.2Fe-0.1Cr-0.5Nb) was developed by Mitsubishi Heavy Industries, Ltd.[18]

[*2] ZIRLO (Zr-1.0Sn-0.1Fe-1.0Nb) was developed by Westinghouse Electric Corporation.[19]

[*3] New Developed corrosion resistance Alloy (Zr-1.0Sn-0.27Fe-0.16Cr-0.1Nb-0.01Ni) was developed by Nuclear Fuel Industries, Ltd. and Sumitomo Metal Industries, Ltd.[20]

of Economy, Trade and Industry (NISA/METI).

In Test OI-10, PWR fuel rod at burnup of 60GWd/t (segment average in the section) was subjected to a peak fuel enthalpy of 435 J/g (104 cal/g) by a pulse irradiation. The rod had MDA cladding for high burnup application. Oxide thickness of the cladding was approximately 27 μm. The fuel remained intact in the Test OI-10. Fission gas release during the RIA transient was measured by gas analysis of the rod after the pulse irradiation. The release was approximately 2.6% and smaller than those measured in earlier tests, as shown in Fig. 2.1-2. The rod had pellets with larger grain size of approximately 28 μm. Limited accumulation of fission gases was expected in grain boundaries during power-reactor operation owing to the larger grain size, which could make the transient release smaller in the test.

A fuel rod with ZIRLO cladding at a burnup of 58 GWd/t was pulse irradiated in Test OI-11. Oxide thickness of the cladding was approximately 28 μm. The test fuel rod was subjected to the largest pulse-condition available in the NSRR, which could give the peak fuel enthalpy of 657 J/g (157 cal/g). The rod failed when the fuel enthalpy reached 500 J/g (120 cal/g), then pellets fragmentation and mechanical energy generation were observed. As shown in Fig. 2.1-3, a long axial crack was observed in the post-test cladding over the active fuel length and the crack reached to the bottom end fitting resulting in separation. The characteristics of the crack were common to those failed due to PCMI in earlier tests. The fuel enthalpy at the time of failure, however, was higher than those in the earlier tests with Zircaloy-4 cladding, as shown in Fig. 2.1-4, suggesting larger safety margins for the new cladding material with improved corrosion resistance. The rod had pellets with a conventional grain size and the fission gas release during the RIA test was comparable to those in the earlier tests, as shown in Fig.2.1-2.

A fuel rod with NDA cladding at a burnup of 61 GWd/t was subjected to a peak fuel enthalpy of 600 J/g (143 cal/g). The cladding had a little thicker oxidation of approximately 41 μm formed during the 4 cycles' operation. The fuel remained intact in the Test OI-12. The rod contained pellets with conventional grain size of approximately 8 μm and the fission gas release during the test was 22.4% comparable to those in earlier tests and larger than that in Test OI-10 with large grain.

The Test VA-1 was performed with an MDA-cladded PWR rod irradiated up to 78GWd/t in Spain, and resulted in PCMI failure at a fuel enthalpy of 255 J/g (61 cal/g). As shown in Fig. 2.1-4, the result indicates conservativeness of the current PCMI failure threshold even at a higher burnup than the defined range.

The results from recent NSRR RIA-simulating Tests reflect the better performance of the new cladding materials in terms of corrosion, the thinner oxides and accordingly lower hydrogen content generated during irradiation in the PWR. It can be accordingly concluded that these rods with improved corrosion resistance have larger safety margin against the

PCMI failure than conventional Zircaloy-4 rods. The tests will be extended to higher burnups using the UO_2 and MOX fuel rods of PWRs and BWRs transported from Europe.

2.1.3 Research on Fuel Behavior under LOCA Conditions

In safety analysis for the postulated loss-of-coolant accident (LOCA) in a light water reactor (LWR), fuel rods would be exposed to high-temperature steam for several minutes until the emergency core cooling water quenches the fuel bundle. The fuel cladding, therefore, might be severely oxidized and lose ductility, resulting in possible degradation of fuel rods by thermal shock during the quench. The Japanese criterion on fuel safety for LOCA is based on fracture/no-fracture threshold of oxidized cladding which was experimentally determined under simulated LOCA conditions. Coolable geometry of the reactor core is ensured if fuel rods survive the quench after the high-temperature oxidation phase. Accordingly, it is one of the most important issues to clarify thermal shock resistance (fracture/no-fracture threshold) of oxidized fuel cladding in order to confirm the safety of LWRs under LOCA conditions. Fuel burnup has been extended and it will be continued in future. Thickness of metallic part of the cladding is decreased and hydrogen concentration is increased with progress of water-side corrosion. These may enhance cladding embrittlement under LOCA conditions and reduce the thermal shock resistance of the fuel cladding during quench.

In order to evaluate burnup effect on the thermal shock resistance of the fuel cladding, LOCA-simulated tests have been conducted with irradiated PWR cladding specimens. The specimens were sampled from two PWR fuel rods which were irradiated to 39 and 44GWd/t (rod average) at Takahama unit-3 reactor, Kansai Electric Power Co., Inc. The cladding material is Zircaloy-4 containing 1.3 wt% of Sn. The initial outer diameter and thickness were 9.50 and 0.57 mm, respectively. The initial oxide layer thickness ranged 15 to 25 μ m Hydrogen concentration is estimated to range from 120 to 210 ppm assuming that 15% of hydrogen generated by corrosion was absorbed. Test rods were fabricated with the cladding specimens, alumina dummy pellets and Zircaloy end plugs, and were heated in steam flow. The rods ruptured at temperatures ranging from 1050 to 1100 K due to increase of the internal pressure and decrease of the cladding strength. The rods were heated to pre-determined temperatures from 1303 to 1451 K, and isothermally oxidized for 120 to 2195 s. After the isothermal oxidation, the rods were cooled in the steam flow to about 970 K and finally quenched with water flooding from the bottom. Both ends of the test rods were fixed at the termination of the isothermal oxidation to simulate possible loading applied to the cladding between grid-spacers on cladding shrinkage. Tensile load generated by restraining cladding shrinkage is controlled not to exceed 540 N. The maximum restraining load was conservatively determined based on previous reports regarding the restrained conditions in bundle geometry.[21,22]

Six tests were successfully performed with the irradiated cladding specimens. Two cladding specimens, oxidized to about 26 to 29% ECR, were fractured during the quench. The post-test appearance of one of the fractured specimens is shown in Fig. 2.1-5.[23] It is considered that cracking initiated at the rupture opening and propagated circumferentially. There is no difference in fracture position and direction of crack propagation between irradiated and non-irradiated cladding specimens.[24,25] Fracture/no-fracture conditions of irradiated cladding specimens are compared with those of unirradiated cladding specimens in Fig. 2.1-6, relevant to the ECR value and the initial hydrogen concentration.[23] Since the failure boundary of non-irradiated cladding lies at about 28% ECR at about 200 ppm, the fracture of the irradiated cladding is consistent with the fracture criteria for non-irradiated cladding with a similar hydrogen concentration. Therefore, the fracture boundary appears not to be reduced so significantly by irradiation to the examined burnup level, except for the hydrogen effect. Four claddings oxidized to about 16 to 22% ECR survived the quench. Hence, the fracture boundary is between 22 and 26% ECR for these high burnup fuel claddings, and it is higher than the limit in the Japanese ECCS acceptance criterion (15% ECR).

It is planned to perform the LOCA-simulated tests with PWR and BWR cladding specimens (MDA, NDA, ZIRLO, M5 and Zircaloy-2), highly irradiated to about 79 GWd/t. The influence of further burnup extension and new alloys will be investigated in detail.

References

(1) H. Uetsuka, *et al.*, *Fuel Irradiation Research of Japan at Halden Reactor*, JAERI-Tech 2004-023(2004).

(2) M. Suzuki and H. Saitou, *Light Water Reactor Fuel Analysis Code FEMAXI-6 (Ver.1)*, JAERI-Data/Code 2003-019 (2003).

(3) M. Suzuki, H. Uetsuka and H. Saito, "Analysis of Mechanical Load on Cladding Induced by Fuel Swelling during Power Ramp in High Burn-up Rod by Fuel Performance Code FEMAXI-6," *Nucl. Eng. Design*, 229, 1 (2004).

(4) M. Suzuki, K. Kusagaya, H. Saitou, *et al.*, "Analysis on Lift-Off Experiment in Halden Reactor by FEMAXI-6 Code," *J. Nucl. Mater.* 335, 417 (2004).

(5) T. Nakamura, H. Sasajima, H. Ikehata, *et al.*, "Hydride Effects on Failure of High Burnup LWR Fuel Rods under RIA Conditions", *2003 Int. Congress on Advances in Nuclear Power Plants (ICAPP '03)*, May, Spain, Cordoba, (2003).

(6) T. Fuketa, T. Sugiyama, T. Nakamura, *et al.*, "Effects of Pellet Expansion and Cladding Hydrides on PCMI Failure of High Burnup LWR Fuel during Reactivity Transients", *Proc. of Nuclear Safety Research Conference 2003*, October, Washington, USA, (2003).

(7) T. Sugiyama, F. Nagase and T. Fuketa, "LOCA and RIA Studies at JAERI", *Proc. Fuel and Materials Sessions, Enlarged Halden Programme Group Meeting*, Sandefjord, Norway,

May 9-14, 2004, HPR-362, Vol 2 (2004).

(8) T. Sugiyama, T. Fuketa, M. Ozawa, *et al.*, "RIA-simulating Experiments on High Burnup PWR Fuel Rods with Advanced Cladding Alloys", *Proc. of 2004 International Meeting on LWR Fuel Performance, September*, Orlando, Florida, USA, (2004).

(9) T. Fuketa, F. Nagase and T. Sugiyama, "RIA- and LOCA-Simulating Experiments on High Burnup LWR Fuels", *Proc. of IAEA Technical Meeting on Fuel Behavior Modelling under Normal, Transient and Accident Conditions, and High Burnup*, September, Kendal, UK, (2005).

(10) M. Amaya, T. Sugiyama and T. Fuketa, "Fission Gas Release in Irradiated UO_2 Fuel at Burnup of 45GWd/t during Simulated Reactivity Initiated Accident (RIA) Conditions", *J. Nucl. Sci. Technol.*, 41[10], 966 (2004).

(11) T. Sugiyama and T. Fuketa, "Effect of Cladding Surface Pre-oxidation on Rod Coolability under Reactivity Initiated Accident Conditions", *J. Nucl. Sci. Technol.*, 41[11], 1083 (2004).

(12) F. Nagase and T. Fuketa, "Influence of Hydride Re-orientation on BWR Cladding Rupture under Accident Conditions", *J. Nucl. Sci. Technol.*, 41[12], 1211 (2004).

(13) F. Nagase and T. Fuketa, "Investigation of Hydride Rim Effect on Failure of Zircaloy-4 Cladding with Tube Burst Test", *J. Nucl. Sci. Technol.*, 42[1], 58 (2004).

(14) T. Nakamura, T. Fuketa, T. Sugiyama, *et al.*, "Failure Thresholds of High Burnup BWR Fuel Rods under RIA Conditions", *J. Nucl. Sci. Technol.*, 41[1], 37 (2004).

(15) T. Sugiyama, T. Nakamura, K. Kusagaya, *et al.*, *Behavior of Irradiated BWR Fuel under Reactivity-Initiated-Accident Conditions [Results of Tests FK-1,-2 and -3]*, JEARI-Research 2003-033, (2003).

(16) T. Fuketa, et al., *Proceedings of Fuel Safety Research Meeting 2004*, JAERI-Review 2004-021 (2004).

(17) H. Sasajima, T. Sugiyama, T. Nakamura, *et al.*, *Behavior of Irradiation PWR Fuel under Simulated RIA Conditions [Results of the NSRR Tests GK-1 and GK-2]*, JAERI-Research 2004-022, (2004).

(18) S. Doi, S. Suzuki, M. Mori, *et al.*, "Advanced Fuel Design and Performance for Burnup Extension," *Proc. 2000 Int. Topical Mtg on LWR Fuel Performance*, Park City, Utah, April 10-13 (2000).

(19) G. P. Sabol, R. J. Comstock, G. Schoenberger, *et al.*, "In reactor Fuel Cladding Corrosion Performance at Higher Burnups and Higher Coolant Temperature," *Proc. 1997 Int. Topical Mtg on LWR Fuel Performance*, Portland, Oregon, March 2-6 (1997).

(20) K. Goto, S. Matsumoto, T. Murata, *et al.*, "Update on the Development of Japanese Advanced PWR Fuels," *Proc. 2000 Int. Topical Mtg on LWR Fuel Performance*, Park City, Utah, April 10-13 (2000).

(21) K. Honma, S. Doi, M. Ozawa *et al.*, "Thermal-Shock Behavior of PWR High-Burnup Fuel Cladding Under Simulated LOCA Conditions," *Proc. ANS Annual Meeting*, Milwaukee, Wisconsin (2001).

(22) T. Murata, Y. Taniguchi, S. Urata *et al.*, "LOCA Simulation Test of the Cladding for High-Burnup Fuel," *Proc. ANS Annual Meeting*, Milwaukee, Wisconsin (2001).

(23) F. Nagase and T. Fuketa, "Embrittlement and fracture behavior of pre-hydrided cladding under LOCA conditions," *Proc. 2005 Water Reactor Fuel Performance Meeting*, Kyoto, Japan, October 2-6, 2005.

(24) F. Nagase and T. Fuketa, "Effect of Pre-Hydriding on Thermal Shock Resistance of Zircaloy-4 Cladding under Simulated Loss-of-Coolant Accident Conditions," *J. Nucl. Sci. Technol.*, 41[7], 723 (2004).

(25) F. Nagase and T. Fuketa, "Behavior of Pre-hydrided Zircaloy-4 Cladding under Simulated LOCA Conditions," *J. Nucl. Sci. Technol.*, 42[2], 209 (2005).

Table 2.1-1 NSRR tests conducted from April 2003 through September 2005

Test ID	Test Fuel		Objectives and remarks
	Burnup (GWd/t)	Fuel type	
OI-10	60	PWR 17x 17, MDA cladding	RIA transient behavior of high burnup PWR fuel rods with new cladding alloys (domestic), PCMI failure threshold and consequences
OI-11	58	PWR 17x 17, ZIRLO cladding	
OI-12	61	PWR 17x17, NDA cladding	
VA-1	78	PWR 17x 17, MDA cladding	RIA transient behavior of higher burnup PWR fuel rod with new cladding alloy (irradiated abroad), PCMI failure threshold and consequences
Powder fuel tests	fresh	Powders with cladding	Mechanical energy generation by thermal interaction of solid fuel and water
TRIGA	fresh	TRIGA(U-$ZrH_{1.6}$), Incoloy-800H	Integrity and performance of research reactor fuel
JMH-8	19	PWR 14x14, 19.5%E pre-irradiated in JMTR	Fuel integrity & performance under power oscillation ATWS
Power oscillation	fresh	PWR 14x14, 4.1%E Pre-oxidized Zry-4	

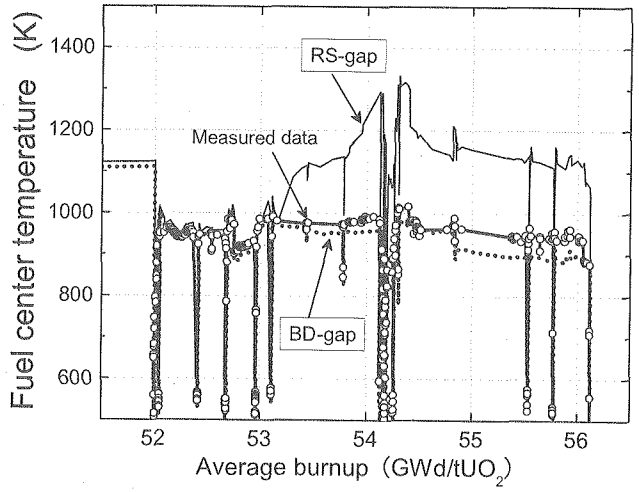

Fig.2.1-1 Comparison between predicted and measured fuel center temperatures in the Lift-Off experiment in the Halden reactor (The bonding model (BD-gap) predicts a much closer temperature to the measured data than the Ross-Stoute model (RS-gap).)

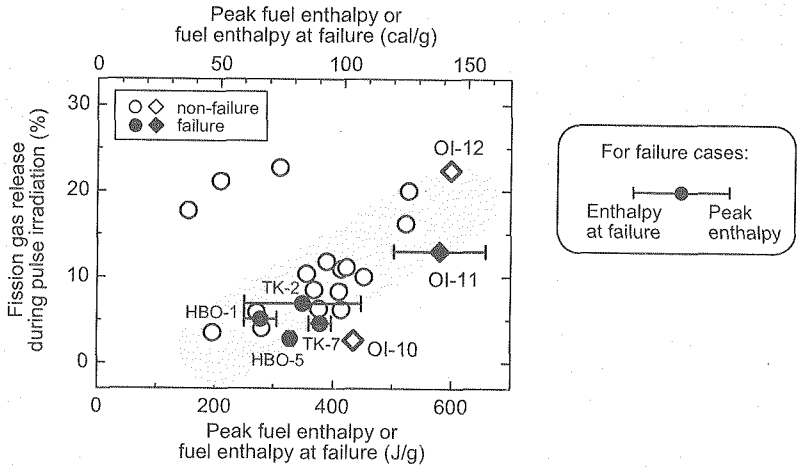

Fig.2.1-2 Fission gas release during pulse irradiation for PWR fuel rods

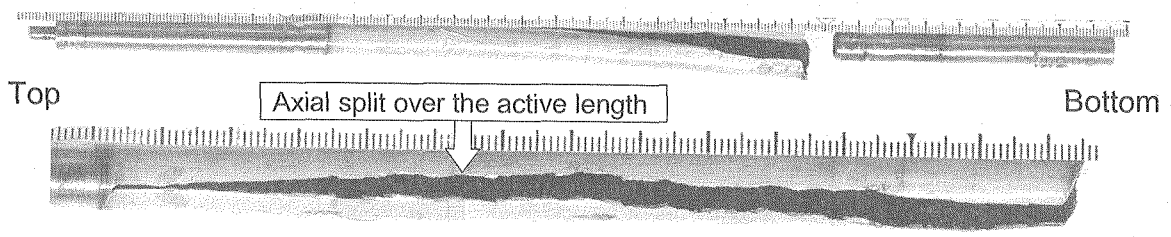

Fig. 2.1-3 Appearance of PWR fuel rod failed in Test OI-11 under a simulated RIA condition

This is a blank page.

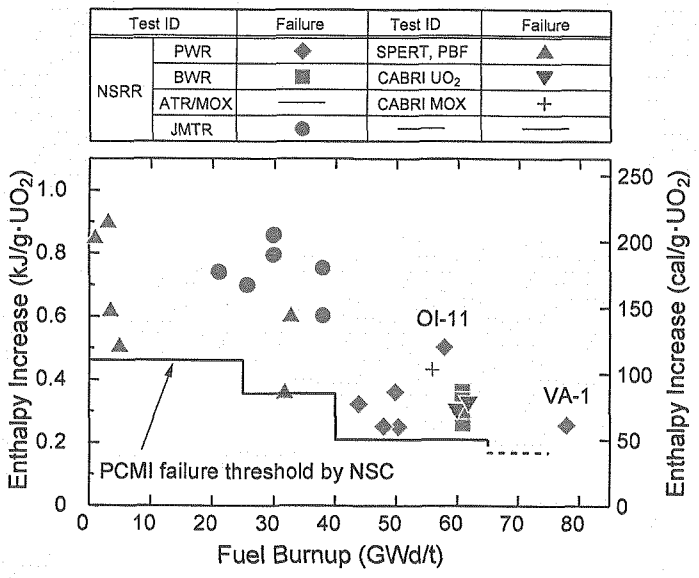

Fig. 2.1-4 Fuel failure enthalpies as a function of fuel burnups

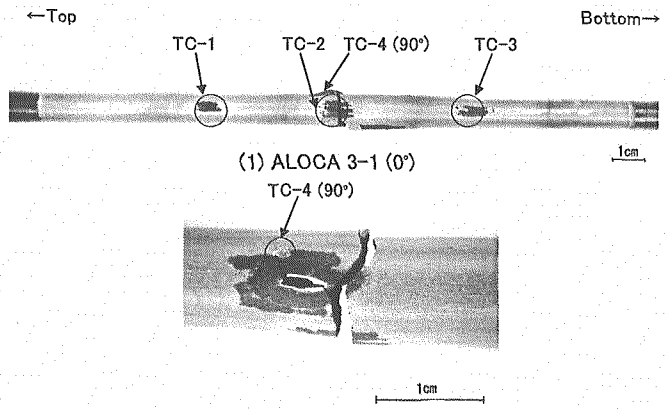

Fig. 2.1-5 Post-test appearance of 48GWd/t PWR cladding, oxidized to 29% ECR and quenched

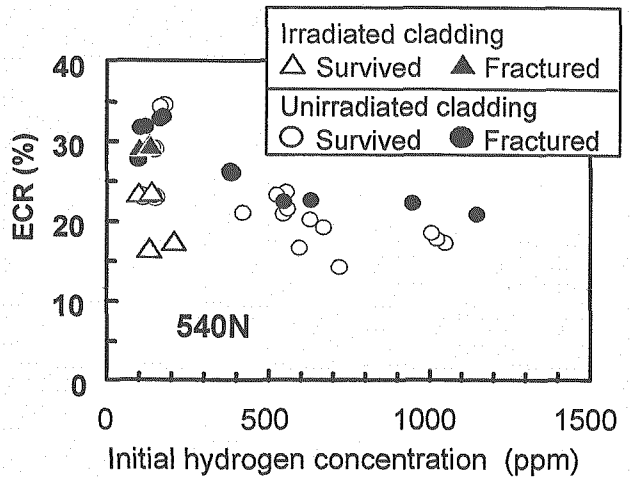

Fig. 2.1-6 Fracture/no-fracture conditions relevant to ECR and hydrogen concentration, obtained from integral thermal shock test

This is a blank page.

2.2 Structural Reliability and Material Degradation of Aged Structures and Components

Fifty-three plants of light water reactors (LWRs) in Japan including seven plants which have already reached a 30-year operation have been operated as of August 2005. The LWRs, which over the years have proven themselves to be safe, have come to be considered a highly reliable type of reactor. The LWRs will be the mainstream of nuclear power generation for a considerably long period. It is, therefore, necessary for the aged reactors to further operate when aging phenomena are readily manageable. The domestic countermeasures designated to cope with the aging of LWRs have been already taken expecting a 60-year operation. It is particularly important to maintain the integrity of the safety-related structures and components subjected to aging during long-term operation. Before reaching 30-year operation, a regulatory body, the Nuclear and Industrial Safety Agency (NISA) reviews the technical evaluation report for the aging management of safety-related components in the plant which submitted by the utility. The report includes feedbacks of operating experiences, management and countermeasures for aging degradation, and a long-term maintenance program.

To maintain the integrity of the major components during the service life, it is important to consider the aging degradation of the material and defect initiation and growth. When the defect is detected on the components at the in-service inspection, the integrity evaluation of the components should be performed based on fracture mechanics method. The probabilistic fracture mechanics (PFM) method has been recently highlighted to rationally incorporate the uncertainties arising from the material properties, defect distribution, inspection quality and so on, unlike the conventional deterministic method. A failure probability is obtained through the PFM analysis by imputing the material strength, cracking size, load and so on as probabilistic distribution. We investigate how this PFM method is applied to the domestic regulation, codes and standards. In the meantime, we are developing analytical codes for PFM analysis of RPV and piping under design base loading conditions such as transient loading and seismic loading. The PFM codes developed in JAEA are called as PASCAL (PFM Analysis of Structural Components in Aging LWRs) series.

In addition to the analytical study above, the detection and evaluation of aging degradation are investigated for structures and components which are important from the safety standpoint and difficult in replacing and repairing, e.g. RPV and internal core.

For the RPV, the ductile-to-brittle transition temperature (DBTT) should be lower than its operation temperature to prevent the brittle fracture. In general, neutron exposure of the vessel steels reduces the ductility, resulting in the shift in DBTT to higher temperatures. This is called "irradiation embrittlement". To monitor this, surveillance capsules filled with standard Charpy specimens made of the material representative of the vessel steels have been installed in the vicinity of the core of the reactor. They are periodically retrieved from the plant and tested. The surveillance results based on Charpy impact tests have been used for the estimation of fracture toughness of the vessel steels according to the present regulation of the surveillance program, which assumes that the degree of irradiation embrittlement measured from Charpy impact tests is equivalent to that from fracture toughness tests. Recently, many efforts have been made to develop a fracture toughness testing method

called the "Master Curve" (MC) method and this has been accepted and introduced in regulations in the EU and the US. The MC method can determine the temperature dependence of fracture toughness using at least 6 specimens only. The research on the MC method to improve the accuracy in evaluating the irradiation embrittlement of the Japanese RPV has been conducted using JMTR. It is also necessary to investigate the effects of neutron dose rate, γ-ray irradiation, phosphorus contents as impurity atom on irradiation embrittlement to precisely predict the degree of the irradiation embrittlement in the long-term operation of the RPV. The use of nondestructive evaluation method of irradiation embrittlement, which has been widely under research and development, will also contribute to the integrity assessment of RPV.

It is known that irradiation-assisted stress corrosion cracking (IASCC) occurs in the austenite stainless steel for the internal core structures exposed to high fluence under tensile stress in high temperature water environment. Since cracking thought to be due to IASCC has been often observed in foreign and domestic aged LWRs, IASCC becomes one of the important issues for prolonged operation of domestic reactors. Understanding the mechanism(s) of IASCC, in particular, to identify the controlling factors and to predict the crack growth rates are the area where JAEA is concentrating on.

The typical results of the researches performed during the period from FY2003 to 2005 are described in the following sections.

2.2.1 Development of Reliability Evaluation Code of Structural Components

(1) Reactor pressure vessel integrity under pressurized thermal shock*1

PASCAL code developed in JAEA can evaluate the conditional probabilities of crack initiation and fracture of an RPV under transient conditions such as pressurized thermal shock (PTS)[1][2]. PASCAL version 1 has been registered and available from OECD/NEA Databank.

Using PASCAL version 1, the flaw acceptance standard of ASME Code Sec. XI was examined with some concerns weather the failure probability is uniform for flaws with various aspect ratios (=crack depth / crack half length)[3]. A PTS transient prescribed by NRC/EPRI PTS benchmark study was used as an applied load for the study. Analysis results showed that the conditional failure probability of an RPV with an initial flaw of acceptable depth significantly depends on the aspect ratio. In the case flaw shape is close to semi-circular, the failure probability is higher than that of the cases aspect ratios are less than 0.6 by one order of magnitude due to the difference of fracture behavior at the surface point. Flaw depths with different aspect ratios which gave a constant failure probability were determined under the PTS transient at the neutron fluence of 5×10^{19} (n/cm^2, E>1MeV) as shown in Fig. 2.2-1, This flaw gave a reasonably uniform failure probability against other fluences and another transient.

PASCAL has also been modified into version 2 in order to improve the functions and reliability in failure analysis. For calculating the stress intensity factor (SIF) of an embedded crack, the CRIEPI method in addition to JSME method was introduced into the PASCAL code[4]. The CRIEPI method

*1 This work includes results obtained under an entrustment from the Ministry of Economy, Trade and Industry of Japan.

enables us to calculate the SIF values at three points on the crack tip, namely outermost and innermost tips in thickness direction and a crack tip in length direction. Under a PTS loading, the stress discontinuity near the interface between cladding and base metal of an RPV is caused by the difference in their thermal expansion coefficients. So the SIF of a surface crack close to the interface should be calculated taking account of the stress discontinuity. SIF calculations have to be performed many times in Monte Carlo simulation of PFM analysis. To avoid the time consuming process from the SIF calculation in the PFM analysis, the influence coefficients were developed based on FEM analyses to calculate the SIF easily and accurately corresponding to the stress distributions in the cladding and base metal. Using the coefficients, the SIF values at the crack tips at both surface and deepest points of a surface crack are evaluated accurately and in a reasonable time [5].

To evaluate precisely the fracture toughness after neutron irradiation, the new fracture toughness curves based on the Weibull distribution were incorporated into the PASCAL code. One is the Master Curve based on the weakest link theory. Another is a statistical Weibull-type curve proposed by ORNL. When a severe PTS transient is considered, the calculated results with these new curves showed little difference in the conditional probabilities of RPV fracture as compared to the curve currently used in the USA. A new function on the frequency of in-service inspection and an optimized Monte Carlo analysis method were also introduced into PASCAL.

Using the updated PASCAL, sensitivity analyses on some parameters for some typical PTS transients have been performed. The probabilities of crack initiation and through-wall crack during typical PTS transients were calculated applying two kinds of probability of crack detection (POD) models for pre-service and in-service inspections. The results showed that the difference in the POD models affected the fracture probability significantly and that repeating the inspection decreases the failure probability even in the case of low POD. The exponential-type Marshall distribution for a surface crack and the empirical distribution for an embedded crack developed by PNNL were compared. Considering the existence probability for both type cracks, the fracture probability could be the same order of magnitude.

(2) Piping reliability evaluation method under seismic loading

After Hyogo-ken-Nanbu Earthquake in 1995, the seismic safety of a nuclear power plant (NPP) has become a great concern. In addition, as the NPPs continue to be operated for a longer period, it becomes more important that the safety of aging-degraded NPPs be verified by conducting a technical evaluation of the safety and reliability of structural components. Therefore, it is necessary to establish the rational and precise method of a seismic reliability evaluation for structural components considering the aging degradation and uncertainty of seismic motion.

In JAEA, we established the structural reliability evaluation method for aged piping considering uncertainty of seismic motion[6]. This method is composed of three phases as shown in Fig.2.2-2. Phase 1 is a seismic hazard assessment to calculate probability of seismic occurrence and input seismic motion at NPP site. Phase 2 is a fragility assessment to calculate failure probability of piping considering the

aging such as SCC(Stress Corrosion Cracking) and fatigue crack extension by seismic load. And phase 3 is a quantitative failure assessment of aged piping by combination of phase1 and phase 2. For this method, we developed a seismic hazard evaluation code SHEAT-FM[7] using a seismic motion prediction method based on fault model, and a piping failure probability evaluation code PASCAL-SC[8] mentioned later.

Using this method, we evaluated the seismic reliability of a welded joint of PLR (Primary Loop Recirculation system) piping using a BWR model plant, but in-service inspection (ISI) was not considered. As a result, as the operation time passes, the failure probability of aged piping (Pf) has increased and the failure probability by SCC (Pscc) became more predominant than the failure probability by seismic load (Peq|scc) as shown in Fig. 2.2-3. To establish a more realistic reliability evaluation method, we improve these evaluation codes considering latest knowledge.

(3) Developments of PFM analysis codes for aged piping

As a part of the aging and structural integrity research for LWR components, new PFM codes PASCAL-SC (PASCAL – Stress Corrosion Cracking) and PASCAL-EQ (PASCAL – EarthQuake) have been developed for piping[8]. These codes evaluate the failure probability of an aged welded joint by a Monte Carlo method. PASCAL-SC treats Stress Corrosion Cracking (SCC) in austenitic piping, while PASCAL-EQ takes fatigue crack growth by seismic load into account in austenitic and carbon steel piping. The development of these codes has been aimed to improve the accuracy and reliability of analysis by introducing new analysis methodologies and algorithms considering the recent development in the fracture mechanics methodologies and computer performance. The crack growth by an irregular stress due to seismic load in detail is considered in these codes. They also includes latest stress intensity factor solutions and fracture criteria of piping. In addition, a user's friendly GUI (Graphical User Interface) which generates input data, supports calculations and plots analysis results has been developed.

The pipe rupture of the main feedwater pump suction line elbow of the secondary system due to FAC has occurred at Surry-2 in USA on December 1986. After the Surry-2 accident occurred, the wall thickness management guideline for PWR secondary system pipes was established based on the measured data in 1990 in Japan. On August 2004, however, the secondary system pipe ruptured at Unit 3 of Mihama nuclear power station of the Kansai Electric Power Co. The reliability of piping subjected to wall thinning due to flow accelerated corrosion (FAC) has become important from a viewpoint of aging management of LWRs. Although these ruptured piping were less safety significant and located outside the reactor containment, the wall thinning behavior due to FAC is not well-predicted at this moment and has a large scatter between measured rates and predicted ones. Therefore, by extending PFM analysis method, PASCAL-EC (PASCAL – Erosion/Corrosion) has been developed[9]. This code evaluates the failure probability of an aged piping with a wall thinning based on a wall thinning prediction equation available and some fracture criteria for wall-thinned pipe.

2.2.2 Research on Neutron Irradiation Embrittlement and Non-destructive Evaluation of Reactor Pressure Vessel

(1) Integranular embrittlement*2

Neutron irradiation induces hardening, resulting in the increase in the ductile-brittle transition temperature (DBTT) for reactor pressure vessel (RPV) steels. The present embrittlement prediction is based on this hardening mechanism. One of the other possible embrittlement at high neutron fluence in the long-term operation is caused by grain boundary phosphorous (P) segregation, called intergranular embrittlement. The segregation of impurity such as P is promoted by neutron irradiation and the presence of P at grain boundaries weakens a cohesive strength of grain boundaries, leading to an increase in DBTT through intergranular failure. However, a P concentration at grain boundaries for intergranular embrittlement to be operative, how to evaluate fracture toughness for intergranular fracture, and underlying mechanism of neutron-induced P segregation are not fully understood.

A study on intergranular embrittlement of reactor pressure vessel steels due to grain boundary P segregation has been performed[10], in particular, to estimate the effect of grain boundary P (Pgb) concentrations on embrittlement in terms of shifts in Charpy ductile-to-brittle transition temperature and fracture toughness. Three kinds of A533B steel plates doped with different bulk phosphorus contents of 0.013 wt.%, 0.026 wt.% and 0.057 wt.% were prepared. The initial Pgb concentrations of these materials after post-welding heat treatment determined by scanning Auger microscopy (SAM) were 9 %, 17 % and 32 % in average, respectively. The materials thermally aged at 450°C~550°C to 10,000 h exhibited increases in Pgb concentration. A linear correlation was obtained between Pgb concentration and Charpy 41J transition temperature; 10 % increase in the Pgb concentration corresponded to shift in transition temperature by 40°C with an increase in intergranular fracture. Fracture toughness tests in the ductile-to-brittle transition temperature region have been conducted by the Master Curve method using 25 mm-thick compact tension (CT) specimens. A fractography by scanning electron microscope on the fractured CT specimens having fracture toughness around 80 MPa$\sqrt{m}$ revealed 36 % of fraction of intergranular fracture appearance to the cleavage one for the material with the highest Pgb concentration, while 3% for the lowest one. Fracture toughness data are well agreed with the Master Curve determined by a reference temperature T_0, corresponding to the fracture toughness temperature at 100 MPa$\sqrt{m}$. A comparison between the T_0 and Charpy ductile-to-brittle transition temperature shows that fracture toughness shift is about the same as the Charpy shift.

(2) Reaction kinetics calculation of electron irradiation effect in Fe based model alloy

It is an important subject to investigate the mechanisms of irradiation embrittlement in reactor pressure vessel steel (RPVs). The impurities in RPVs materials have been known to have a storing effect on the irradiation embrittlement. The Cu precipitates which grow during irradiation cause

*2 This work includes results obtained under an entrustment from the Ministry of Economy, Trade and Industry of Japan.

irradiation hardening. We developed a numerical calculation code based on the reaction kinetics, which gives the time-varying concentration of the various defects by calculating the interaction among an interstitial, a vacancy and a Cu atom. The following equations are employed.

$$dC_{V,I}/dt = P_{V,I} - C_S M_{V,I} C_{V,I} \pm Z_{V,I+VN,IN}\ C_{VN,IN} \times M_{V,I} C_{V,I}, \quad (1)$$

$$dC_{Cu}/dt = C_{Cu} \pm Z_{Cu,V+CuN}\ C_{CuN} \times M_V C_V C_{Cu}, \quad (2)$$

where C: a concentration, V: vacancy, I: interstitial, Cu: Cupper, t: time, P: a Frenkel pair generation frequency ($P_{V,I}$ is equivalent to the dpa rate at electron irradiation), Cs: a sink concentration, M: a jump frequency, Z: number of a reaction site, and N: number of atoms in the defect cluster. There are many combinations of reactions: for example, [$V_N + V_1 \rightarrow V_{N+1}$, $V_N + I_1 \rightarrow V_{N-1}$, $V_N \rightarrow V_1 + V_{N-1}$]. The parameters we used, such as migration energy, binding energy, reaction site number, etc. were quoted from the literature[11].

We tried to make a comparative study of this calculation code and experiment. We used the Fe-0.6wt%Cu alloy, electron irradiation and the electrical resistivity measurements. The Fe-Cu alloys were fabricated as pure as possible to eliminate the effects of impurities. After the heat treatment at 850°C for 10 min, the materials were gas-quenched to keep the Cu atoms in supersaturated solid solution at room temperature. In order to investigate irradiation dose and dose rate effects, 2MeV electron irradiation was performed at two different dose rates, 2.7×10^{-9} and 3×10^{-10} dpa/s. We measured electrical resistivity as an index of irradiation effects. The accumulation of vacancy increases the resistivity, while Cu clustering decreases the resistivity. The electrical resistivity is very sensitive to defects concentration and the obtained information is the average over the measured region of a specimen.

Fig.2.2-4 shows the dose dependence of calculated value and measured the electrical resistivity change for the dose rates, 2.7×10^{-9} and 3×10^{-10} dpa/s. Both the calculated and measured resistivity decreases steadily with dose. There is a transient peak in the measured values at 2.7×10^{-9} dpa/s, but we can not explain this phenomenon yet. For the effect of dose rate on the resistivity change, the same trend is observed in both the calculated and measured values: a low dose rate induces electron resistivity change effectively. It is suggested that the present reaction kinetics calculation is qualitatively adequate to simulate defect behavior.

(3) Nondestructive evaluation of material properties of RPV steels by magnetic measurement

Nondestructive technique to measure the degree of material degradation of RPV is a prospective inspection method to increase the safety and reliability of aging nuclear power plants. Development of a monitoring technique to evaluate the degradation of RPV by nondestructive method has started using changes of magnetic hysterisis of RPV steel. A few studies have been done on the correlation between magnetic properties and neutron radiation damage. In the present study, continuous measurements of the magnetic properties of RPV steels under irradiation were taken as a step to make correlations between magnetic properties and neutron radiation damage.

To measure the magnetic properties, the ring-shaped specimens were prepared. A

mineral-insulated, stainless steel-sheathed, two-core cable was wound on the specimen. The one of the core was used for excitation and the other was for measurement of induced voltage. The specimens were installed into the irradiation capsule. Irradiations were performed in JMTR (Japan Material Testing Reactor). Total fast neutron fluence was 5.3 x 10^{19} n/cm^2 (E>1.0 MeV), and an irradiation temperature was controlled at 563 K by using an electrical heater wound around the inner capsule. During irradiation experiment, measurement cables and equipments worked well and we could obtain measurement data continuously. After irradiation, magnetization curves became very slightly wider. This means that magnetic properties changed. As an example of the results, Fig.2.2-5 shows coercivity changes during irradiation[12]. The increasing coercivity is consistent with domain-wall pinning theory. Hysteresis loss also showed almost the same trend as coercivity one. In near future we have a plan of mechanical experiments of this irradiated sample to correlate magnetic properties and mechanical properties to establish material evaluation methods.

(4) Fracture toughness evaluation of the RPV steels by means of the master curve approach

For the Master Curve (MC) approach, we investigated the MC method adopted in the ASTM E1921 standard test method to evaluate the reference temperature of ferrite steels. The materials used are five ASTM A533B class 1 steels and one weld metal. Neutron irradiation for Charpy-size fracture toughness test specimens and standard Charpy-V specimens was carried out at JMTR. A correlation between the reference temperature on fracture toughness and Charpy transition temperatures before and after irradiation is established. Based on this correlation, the optimum test temperature for fracture toughness testing was suggested. The method to determine a lower bound fracture toughness curve was also discussed[13].

On the application of the MC to the RPV integrity assessment based on surveillance results, we participated in the coordinated research project (CRP) organized by the International Atomic Energy Agency (IAEA). The objectives of the CRP are to assess the use of small size surveillance specimens such as the precracked Charpy specimens loaded in three-point bending and to make a guideline to apply the MC method to RPV integrity assessment. The project has started in 2000 participating eighteen laboratories from the world. According to the project plan, we tested and evaluated fracture toughness values of a common material, JRQ at several temperatures. We also studied the loading rate effect of our own materials varying the loading rate from static to dynamic, and the effect of specimen size on the MC method with analyzing our previous results. After summarizing the results gathered from all participants of the CRP, IAEA have published the summary report and the guideline of the MC method for the RPV integrity assessment[14][15].

2.2.3 Research on Stress Corrosion Cracking of Core Internal Structural Materials

From the view point of the life management of the core components of the aged LWR, the irradiation assisted stress corrosion cracking (IASCC) is concerned to be one of the key issues, so that the following various experiments were carried out at JAERI to investigate the IASCC behavior and

mechanism of core structural materials.

In 2000, METI has begun the project for IASCC technology development as a part of the more comprehensive program for technological development of countermeasures for the aged LWRs. In the project, JAERI is engaged in the BWR related testing and research program, which includes the neutron irradiation at JMTR and post-irradiation examinations (PIEs) shared by industries, and the austenitic stainless steels have been irradiated up to four levels of neutron fluence of $5x10^{24}$, $1x10^{25}$, $3x10^{25}$ and $1x10^{26}$ n/m^2 (E>1 MeV). To obtain the crack propagation rate data on the irradiated material, in March 2004, a new IASCC test machine having two autoclaves was installed in the concrete cell of JMTR hot laboratory (see 6.3.2). The crack growth length is measured by means of the DC potential drop method during the test and after the test it is calibrated by the observation of fracture surface of specimen[16].

To investigate the behavior of IASCC crack initiation, the in-situ observation of irradiated specimen was conducted during the slow strain rate testing (SSRT) in high temperature water by using a test facility installed in the hot cell of WASTEF (Fig.2.2-6)[17]. A special design of this test machine is an equipment of a window for in-situ observation of the specimen during SSRT. The window is made of sapphire glass that is durable in high temperature water. Specimens of type 304 stainless steel were treated by solution annealing, thermal sensitization or cold working. Specimens were irradiated to $1x10^{26}$ n/m^2 (E>1 MeV) at JMTR and examined by SSRT in oxygenated high purity water at 561 K. The gage length section of specimen was observed through a window during SSRT. As common features of the specimens, it was known that a crack initiation was observed immediately after the maximum stress and one or two cracks were propagated[18].

Three dimensional atom probe (3DAP) is the analytical instrument which provides the highest spatial resolution among the various micro-analytical techniques which are used in the material science. Therefore, it is expected to obtain more detailed information about the solute distribution due to segregation, precipitation and clustering in matrix or at grain boundaries. 3DAP has a depth resolution of a single atomic layer and sub nanometer (~0.2 nm) lateral resolution. For the mechanistic understanding of IGSCC of low carbon austenitic stainless steel, the 3DAP analyses on the material, type 316L stainless steel, extracted from a core shroud of Japanese BWR were conducted by 3DAP facility at the Institute for Material Research of Tohoku University. Analyses of the concentration profile near grain boundary obtained from 3DAP dataset results in the random distribution of Cr and Mn, enrichment of Si, Mo at grain boundary[19].

Since the synergies of neutron/gamma radiation, stress and high temperature water are significant to understand IASCC behavior in the core but those are not reproducible by PIEs, the in-pile IASCC testing is one of the key experiments to understand IASCC behavior of core internal materials. A high temperature water loop facility was designed to be installed at JMTR to carry out material irradiations and in-pile IASCC testing in the framework of cooperative research program between JAERI and the Japan Atomic Power Company[20]. Using the loop facility, in-pile IASCC tests have been successfully carried out which included the IASCC initiation and growth tests. Fig. 2.2-7 shows the schematic

drawing of the crack initiation and growth test unit for in-pile testing[21][22]. The in-pile SCC tests using pre-irradiated materials in the JMTR core were started from FY2004. Result to be obtained from the in-pile IASCC tests will be compared with test results from PIEs and it will reveal the synergy of the radiation, stress and high temperature water in core.

References

(1) K. Onizawa, K. Shibata, D. Kato and Y. Li, "Probabilistic Fracture Mechanics Analyses of Reactor Pressure Vessel Under PTS Transients," *JSME International Journal Series A*, Vol. 47, No.3,2004, pp. 486-493(2004).

(2) K. Shibata, K. Onizawa, Y. Li and D. Kato, "Importance of fracture criterion and crack tip material characterization in probabilistic fracture mechanics analysis of an RPV under a pressurized thermal shock," *International Journal of Pressure Vessels and Piping*, Vol. 81, Issue 9, September 2004, pp. 749-756(2004).

(3) K. Shibata, K. Onizawa, Y. Li, *et al.*, "Study on Flaw Acceptance Standard of ASME Code Sec. XI Based on Failure Probability," *PVP-Vol. 480, Pressure Vessel and Piping Codes and Standards*, San Diego, California USA, The American Society of Mechanical Engineers, July 25-29, 2004.

(4) K. Onizawa, K. Shibata and M. Suzuki, "Embedded crack treatments and fracture toughness evaluation methods in probabilistic fracture mechanics analysis code for the PTS analysis of RPV," *PVP-Vol. 481, RPV Integrity and Fracture Mechanics*, San Diego, California USA, The American Society of Mechanical Engineers, July 25-29, 2004.

(5) K. Onizawa, K. Shibata and M. Suzuki, "Development of Stress Intensity Factor Coefficients Database for a Surface Crack of an RPV Considering the Stress Discontinuity between Cladding and Base Metal," PVP2005-71371, *Proceedings of PVP2005, ASME Pressure Vessels and Piping Division Conference*, Denver, Colorado USA, The American Society of Mechanical Engineers, July 17-21, 2005.

(6) H. Sugino, H. Itoh, K. Onizawa and M. Suzuki, "Development of structural reliability evaluation method for aged piping considering uncertainty of seismic motions," *J. Nucl. Sci. Technol.*, 4[4], 1~9, (2005), [in Japanese].

(7) H. Sugino, K. Onizawa and M. Suzuki, *User's Manual of a Computer Code for Seismic Hazard Evaluation for Assessing the Threat to a Facility by Fault Model: SHEAT-FM*, JAERI-Data/Code 2005-008, Japan Atomic Energy Research Institute, (2005), [in Japanese].

(8) H. Itoh, K. Onizawa and K. Shibata, *User's Manual of Probabilistic Fracture Mechanics Codes PASCAL-SC and PASCAL-EQ*, JAERI-Data/Code 2005-007, Japan Atomic Energy Research Institute, (2005), [in Japanese].

(9) H. Itoh, K. Onizawa and K. Shibata, *User's Manual of Probabilistic Fracture Mechanics Code PASCAL-EC*, to be published as JAEA-Data/Code , Japan Atomic Energy Agency, (2006), [in Japanese].

(10) Y. Nishiyama, *et al.*, "Research on Intergranular Phosphorus Segregation and Embrittlement of

Reactor Pressure Vessel Steels (2) - Thermal Aging Results –," *Proc. of AESJ Fall Meeting*, G50(2004), [in Japanese].

(11) S. Yanagita, *et al.*, *Mat. Trans.*, 43, pp.1663-1669(2002).

(12) N.Ebine *et al.*, "In-situ Magnetic Property Measurement of the RPV Steel under Irradiation," *Proc. of 30 the MPA-Seminar in conjunction with the 9th German-Japanese Seminar*, Vol.1, pp.12.1-12.8(2004).

(13) K. Onizawa and M. Suzuki, "Correlation Between Cleavage Fracture Toughness and Charpy Impact Properties in the Transition Temperature Range of Reactor Pressure Vessel Steels", *JSME International Journal Series A*, Vol. 47, No.3, 2004, pp. 479-485(2004).

(14) IAEA, "Application of Surveillance Programme Results to Reactor Pressure Vessel Integrity Assessment," IAEA-TECDOC-1435, April 2005.

(15) IAEA, "Guidelines for Application of the Master Curve Approach to Reactor Pressure Vessel Integrity in Nuclear Power Plants," Technical Report Series No. 429, March 2005.

(16) T. Ishii, M. Ohmi, M. Shimizu, *et al.*, "Current Activities in Development of PIE Techniques in JMTR Hot Laboratory," *Proc. 5th JAERI-KAERI Joint Seminar on Advanced Irradiation and PIE Technologies*, Oarai, Japan, Nov. 2005 (to be published).

(17) J. Nakano, T. Tsukada, M. Kikuchi, *et al.*, *Development of SSRT facility with ability of in-situ observation during SCC test in high temperature water for irradiated materials*, JAERI-Conf 2003-001, Japan Atomic Energy Research Institute, (2003), [in Japanese].

(18) J. Nakano, Y. Miwa, T. Tsukada, *et al.*, "In-situ SCC Observation on Neutron Irradiated Thermally-sensitized Austenitic Stainless Steel," *International Conference on Fusion reactor Materials, Santa Barbara, California*, Dec. 2006 (to be presented).

(19) Y. Miwa, Y. Nemoto, K. Kondo, *et al.*, "Microstructural Observation of Core Shroud Sample and Correlation of SCC Mechanism," *Proc. 52nd Japan Conf. on Materials and Environments, JSCE*, pp.189-192 (2005) ,[in Japanese].

(20) H. Takiguchi, K. Dozaki, N. Nagata, *et al.*, "Program of in-pile IASCC testing under the simulated BWR plant condition - Overview -," *Proc. of the 11th International Conference on Nuclear Engineering (ICONE-11)*, ICONE11-36324, Tokyo, Japan, April 20-23, 2003.

(21) H. Ugachi, Y. Kaji, J. Nakano,*et al.*, "Development of Test Techniques for In-Pile SCC Initiation and Growth tests and The Current Status of In-Pile Testing at JMTR," *Proc. 12th International Conference on Environmental Degradation of Materials in Nuclear Power Systems – Water Reactors*, Salt Lake City, Aug., 2005 (to be published).

(22) Y. Kaji, M. Ohmi, Y. Matsui, *et al.*, "Program of in-pile IASCC testing under the simulated actual plant condition -Development of techniques for in-pile IASCC growth test in JMTR-," *Proc. of the 11th International Conference on Nuclear Engineering (ICONE-11)*, ICONE11-36119, Tokyo, Apr., 2003.

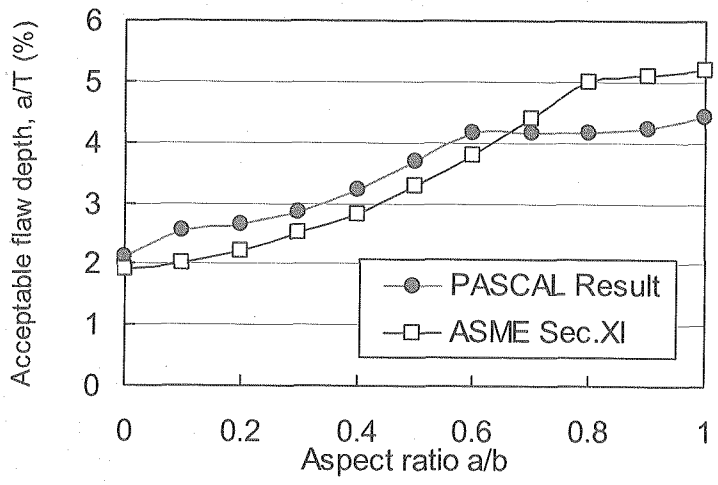

Fig. 2.2-1 Comparison of acceptable flaw depths in ASME code Sec. XI and PASCAL results (Flaw depths with different aspect ratios which gave a constant failure probability were calculated using PASCAL under a PTS transient at the neutron fluence of 5×10^{19} (n/cm^2, E>1MeV).)

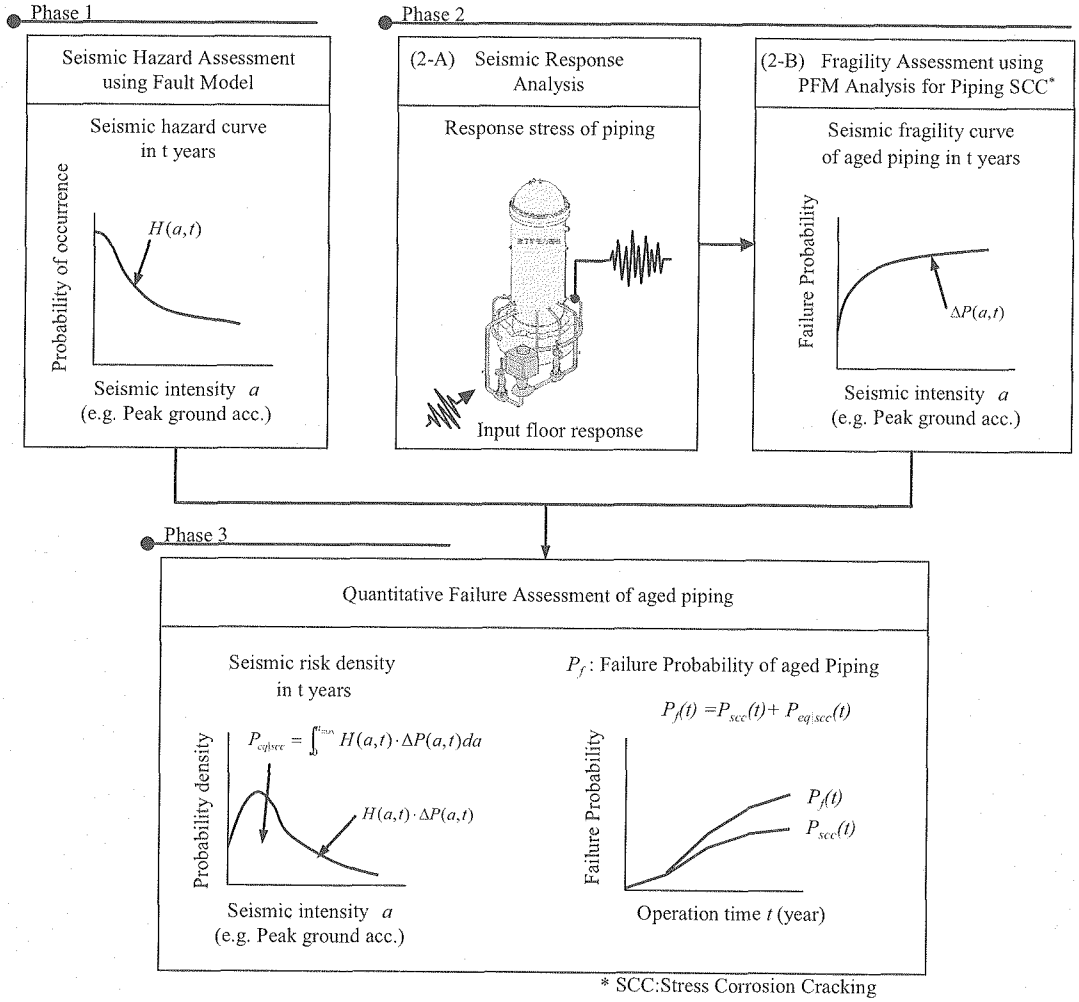

Fig. 2.2-2 Seismic reliability evaluation for aged piping

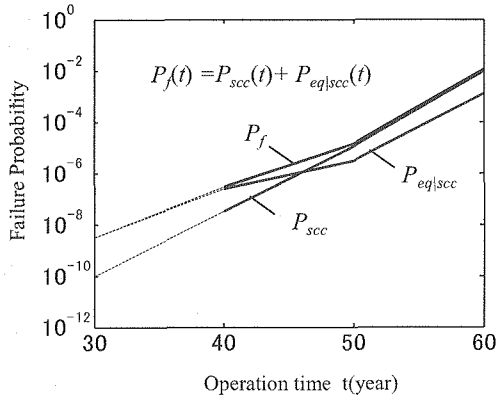

Fig. 2.2-3 Example of failure probability of a welded joint of PLR piping using a BWR model plant (The point at t = 30 was determined assuming $Pscc$=1×10^{-10} and $\Delta P(a)$= 1×10^{-10}(constant).)

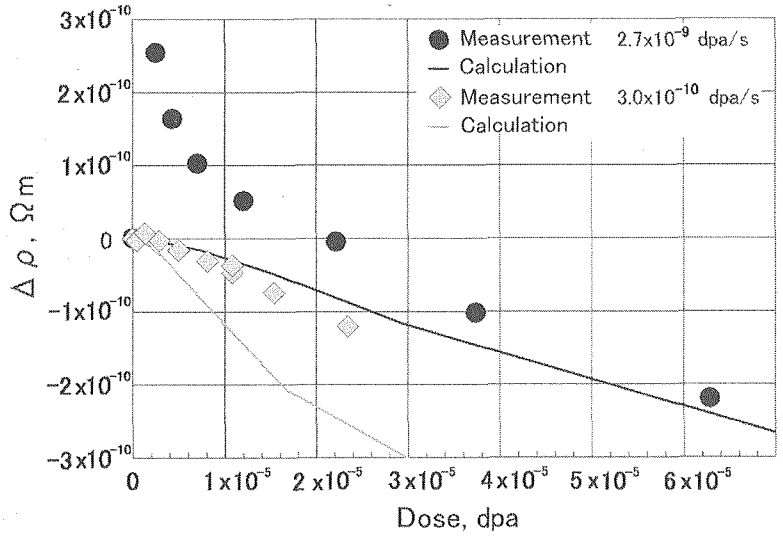

Fig.2.2-4 Comparison of measured and calculated electrical resistivity changes of Fe-0.6%Cu alloy by different dose rate electron irradiation at 300K

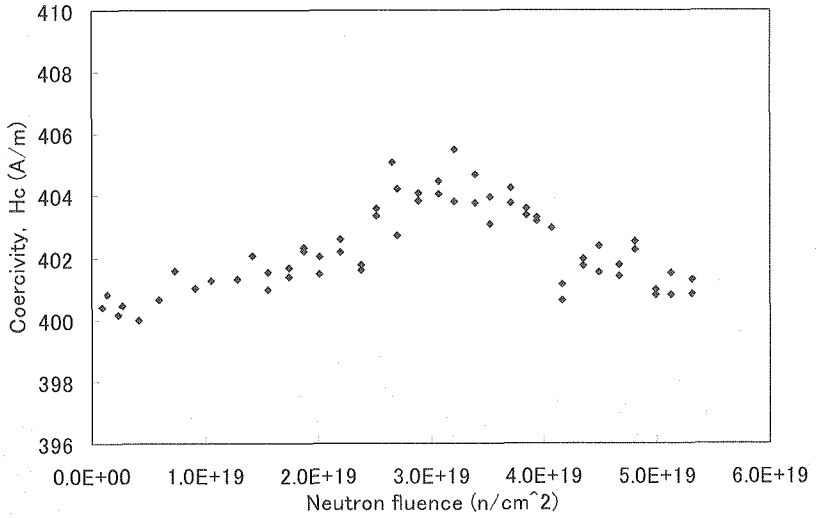

Fig. 2.2-5 An example of coercivity changes of the ring-shaped specimen during irradiation at JMTR

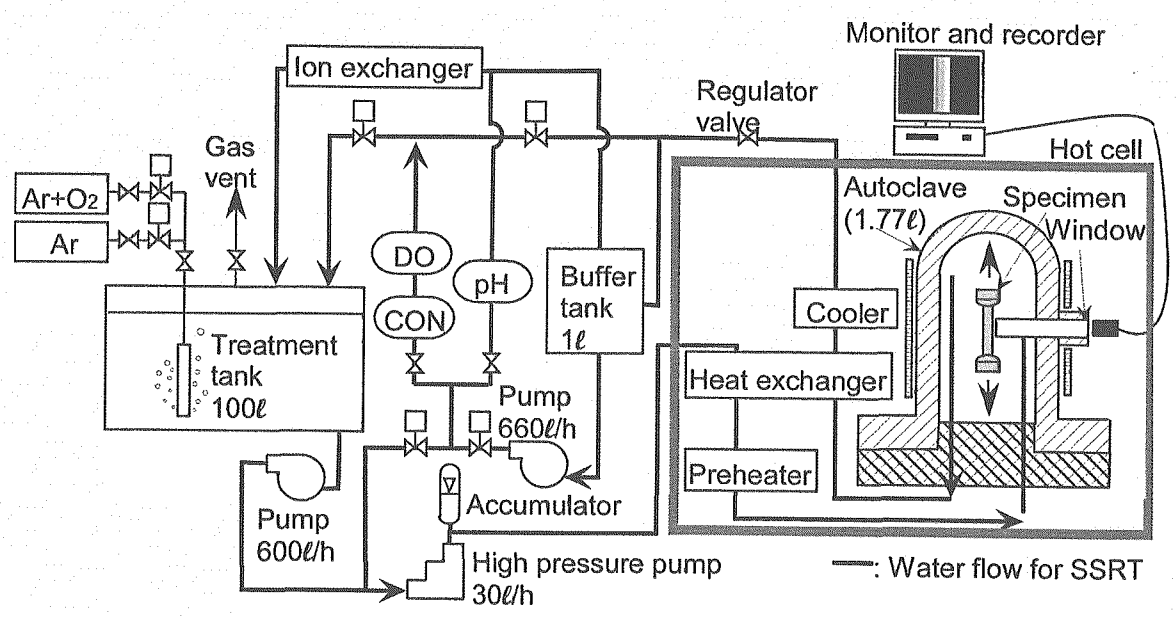

Fig. 2.2-6 SSRT facility for in-situ observation test on irradiated specimen

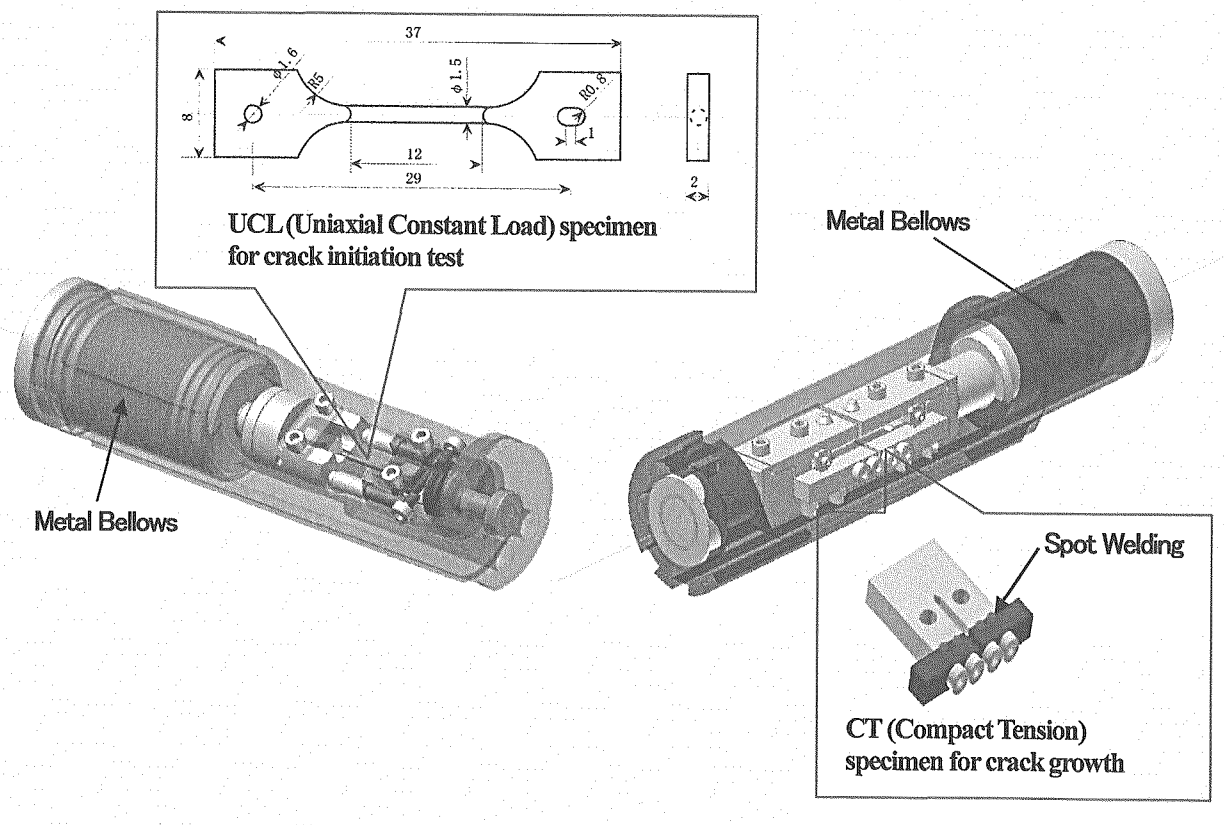

Fig. 2.2-7 In-pile testing units for IASCC initiation and growth tests at JMTR

This is a blank page.

2.3 Reactor Thermal Hydraulics Safety Research

Effectiveness of passive safety features has been investigated in JAEA to incorporate reactor accident management (AM) measures and concepts into the new reactor design for both PWR and BWR. Effectiveness of several candidates for passive safety features is under investigation through the ROSA/LSTF experiments after ROSA-AP600 program which was performed as a cooperative research with USNRC until 2001. A passive containment cooling system (PCCS) for BWR is investigated using a prototypical scale horizontal heat exchanger model composed of U-shaped condenser tubes, especially concerning the degradation of heat removal capability because of low water level in the secondary-side water pool and accumulation of various kinds of aerosols onto inner wall of condenser tubes. Effectiveness of AM measures themselves is also investigated especially for steam generator (SG) secondary side depressurization to cool and depressurize primary system during small-break loss-of-coolant accident (LOCA) to assure long-term core cooling by using low-pressure coolant injection system under influences of non-condensable gas from accumulator system. Thermal hydraulic data obtained from LSTF experiments, which include the data of multi-dimensional and parallel channel non-uniform behavior, are extensively used for the development and improvement of safety analyses codes for the safety evaluation of water reactors.

BWR nuclear-thermal hydraulic coupling experiments are performed using THYNC facility to clarify the mechanisms and influences of the flow and power stability in BWR core furnished with MOX fuel and high-burnup fuel. Margin to induce instability is quantitatively evaluated for channel stability through the THYNC experiments and analyses using the JAERI-developed three-dimensional nuclear-thermohydraulic coupling code TRAC/SKETCH. Transient void behavior experiments simulating reactivity initiated accident (RIA) in BWR core furnished with high-burnup fuel were started using a single heater rod simulating BWR fuel to provide transient void data for the validation of models.

2.3.1 Research on Effectiveness of Accident Management in PWR

Total failure of the high pressure injection (HPI) system of the emergency core cooling system (ECCS) of PWR may lead to severe core damage in a small break loss-of-coolant accident (SBLOCA). This is because the primary coolant mass continues to decrease while the primary pressure is kept high. Steam generator (SG) secondary-side depressurization, by means of steam discharge through the relief valves, is one of effective Phase-I accident management (AM) measures for the prevention of severe accident from occurring during such a SBLOCA in case of the total failure of the HPI system. The SG secondary-side depressurization induces the primary depressurization because of steam condensation in the U-tubes and actuates the accumulator (ACC) system to furnish coolant. However, non-condensable gas may enter the primary loops after the ACC system becomes empty of liquid and accumulate in the SG U-tubes.

Table 2.3-1 summaries ROSA/LSTF[1] experiments performed to verify the effectiveness of several AM measures when the ingress of non-condensable gas into SG U-tubes takes place during SBLOCA. A series of experiments simulating pressure vessel (PV) bottom SBLOCA were conducted first under the assumption of total failure of the HPI system to study the influences of timing and rate of the SG secondary-side depressurization and non-condensable gas from the ACC system on the actuation timing of the low pressure injection (LPI) system for long-term core cooling.[2] All of non-condensable gas from the ACC system may remain in the primary system in this type of LOCA.

In Experiment SB-PV-05, the break of nine 0.4-inch ID instrument-tubes at the PV bottom was simulated, which was equivalent to 0.18% cold leg break. SG secondary-side depressurization to achieve depressurization rate of 55 K/h in the primary system was initiated 10 min after the generation of safety injection (SI) signal when the primary pressure decreased to 12.27 MPa. Non-condensable gas inflow was not assumed due to the isolation of the ACC system. It was confirmed that long-term core cooling is ensured by the actuation of the LPI system before the initiation of core boil-off.

Three experiments of SB-PV-03, -04 and -06 were performed further to investigate the effectiveness of various AM measures when inflow of non-condensable gas from the ACC system is assumed to take place. In Experiment SB-PV-03, SG secondary-side depressurization to provide 55 K/h in the primary system was initiated 10 min after the SI signal generation. Inflow of non-condensable gas caused the degradation in the steam condensation in the SG U-tubes. Core uncovery because of boil-off, thus, resulted at about 8500s after the break, far before the initiation of the LPI system. In Experiment SB-PV-04, SG secondary-side depressurization rate was increased by fully opening the relief valves at the same operation timing as in SB-PV-03 Experiment. The LPI system was actuated before the initiation of core boil-off while non-condensable gas inflow took place from the ACC system. In Experiment SB-PV-06, SG secondary-side depressurization to achieve 55 K/h in the primary system was initiated first 10 min after the generation of SI signal, and switched to full opening of the relief valves as second AM action when the PV liquid level decreased to the hot leg bottom. Core boil-off was found to occur before the initiation of the LPI system.

Figure 2.3-1 compares the primary pressure transients in these three experiments of SB-PV-03, -04 and -06. It took very long time to start the LPI system after non-condensable gas entered the primary loops. It was found that the fast primary depressurization by fully opening the SG relief valves has a merit to make the primary coolant loss rate small and thus contributes to maintain core cooling more effectively.

2.3.2 Passive Containment Cooling System for Next Generation BWR

A series of experiments and analytical studies are performed to study the thermal-hydraulic response of a horizontal heat exchanger for a Passive Containment Cooling

System (PCCS) for BWR containment,[3,4] which prevents the containment over-pressurization during a severe accident. The PCCS heat exchanger condenses steam in the containment generated by decay heat and transfers the decay heat to PCCS secondary-side water pool located in the containment outside as shown in Fig. 2.3-2.

The experiments are performed using a prototypical-scale horizontal heat exchanger that is composed of U-shaped horizontal condenser tubes. The experimental results showed that the horizontal heat exchanger used for the experiments has enough heat removal capacity, even when the collapsed liquid level in the PCCS pool greatly decreased. Figure 2.3-3 compares the total heat removal rates of the heat exchanger and the condenser tubes in terms of the collapsed liquid level. When the collapsed level is decreased to the bundle center, the total heat removal rate of the whole heat exchanger is still almost equal to that at the fully flooded condition. The heat exchanger is partially exposed to atmosphere, causing that the heat removal rate of partial-exposed condenser tubes decreases. The total heat removal rate of tubes that were fully covered by coolant under mixture level increases instead, maintaining the total heat removal rate by the heat exchanger. Consequently, it was confirmed that a shallow PCCS pool may fit well to horizontal heat exchanger, considering such effective heat removal capability.

A large amount of aerosols composed of fission products (FPs) and structural materials may pass through a PCCS heat exchanger during a severe accident. It is anticipated that the heat transfer capability of the PCCS is degraded by the deposition of the aerosols onto the inner surface of condenser tubes. Stepwise analytical studies were conducted in order to evaluate the comprehensive effectiveness of the PCCS with a horizontal heat exchanger. As the first step, based on a series of analyses with a computational fluid-dynamics (CFD) code (STAR-CD code), a correlation was developed for the aerosol deposition in a piping system and a header of the heat exchanger located at the upstream of the tube bundle. Aerosol characteristics flowing into the tube bundle can be evaluated with this correlation. In the second step, correlations for aerosol deposition in each of the condenser tubes of heat exchanger were fabricated through combined analyses with a CFD code (FLUENT code) and ART code developed at JAERI for analyses of FP behavior in pipes during severe accidents. Condensation of water vapor in condenser tubes was taken into account in the FLUENT/ART combined analyses. An example of the correlations is shown in Fig. 2.3-4. The correlation was a function of Reynolds number (Re) and dimensionless water vapor concentration (R_{vp}) at the entrance of condenser tubes along with Stokes number (St). The correlations developed in the first and second steps were introduced into a coupled code system with TRAC code for thermal-hydraulic analyses and MAAP code for severe accident analyses. The results of the TRAC/MAAP coupled analyses indicated that the aerosol deposition onto the inner surface of the heat transfer tubes did not largely degrade the heat transfer capability of the PCCS horizontal heat exchanger, indicating that the suppression of containment vessel

pressurization is comparable to cases without the aerosol deposition.

2.3.3 Research on Coupled Neutronic-thermal Hydraulic Phenomena in BWR

Thermal-hydraulic and neutronic dynamics are closely interrelated in BWR core, being referred as thermal-neutronic (T/N) coupling. It is known that the BWR core stability depends on the T/N coupling characteristics. Precise stability analysis method has been required due to the utilization of high-burnup fuel or MOX fuel, which may reduce the stability margin which is defined as margin between certain system status and the stability boundary. JAEA has, thus, been conducting BWR stability experiments using Thermal-hydraulic and Neutronic Coupling loop (THYNC)[5,6], and developing a three-dimensional T/N coupling code TRAC-BF1/ SKETCH-N[7].

(1) Experiments for channel stability (Effect of T/N coupling) [8]

The THYNC facility shown in Fig. 2.3-5 consists of three 2x2 bundle test sections and one 4x4 bundle test section. Each of 2x2 bundle test sections is composed of three electrically heated rods and one unheated rod. The diameter and heated length of the heater rods are the same as those of conventional BWR fuels. The cross-sectional area-averaged void fraction in the test section is measured instantaneously with impedance-type void fraction meters[9,10]. Electric power to the heater rods is dynamically controlled simulating void reactivity feedback based on point neutron kinetics equation by using measured void fraction.

Similarity of channel stability of THYNC against BWR channel was evaluated. Figure 2.3-6 shows calculated channel stability boundary of density-wave oscillations for the THYNC and prototypical BWR. Variables N_{ph} , N_{sub} and N_{ph} - N_{sub} plane are phase change number, subcooling number and stability plane introduced by Ishii and Zuber[11]. The calculated results show that a stability boundary of THYNC is almost identical to that of a BWR channel. The solid and dashed lines in the figure nearly fall on a straight line with the inclination of 45 degree, i.e., N_{ph} - N_{sub} is constant, which means that the system is destabilized at a constant exit quality, when the pressure is constant.

The effect of T/N coupling on channel instability was investigated with THYNC facility under the conditions of pressure = 2 to 7 MPa, subcooling = 10 to 40 K, and time-averaged mass flux = 270 to 660 kg/m^{2}s. Figure 2.3-7 shows comparison of exit quality at onset of channel instability in the experiments performed with and without T/N coupling. It was clarified that the T/N coupling gives a tendency to destabilize the channel under the experimental conditions. However, the measured decrease in the channel power at the onset of the channel instability under T/N coupling was less than 10% under the T/N coupling at 7MPa.

(2) Transient subcool boiling experiment simulating RIA[12] *1

Postulated reactivity-initiated accident (RIA) in BWR involves abrupt peaking of nuclear power that would jeopardize the integrity of nuclear fuel rods. During RIA, vapor void is formed around fuel rods that may have an effect to reduce the core power and thereby to lower the possibility of fuel failure. This favorable effect, however, has been neglected in the licensing calculations because it is difficult to obtain experimental data to validate models that predict the void formation transient with accuracy.

A series of experiments for fast transient void behaviors during RIA is thus performed with a single simulated fuel rod under conditions simulating a cold stand-by. Schematic diagram of the experimental setup is illustrated in Fig. 2.3-8. Experimental apparatus consists of a test section and a water heating system connected to a water circulation loop, an electric power source, and control and data acquisition systems. The maximum voltage, current and current increasing rate of the electric power are 40 V, 10 kA and 500 A/ms, respectively. A fast-response impedance technique developed through THYNC experiments is applied to the void fraction measurement.

Accuracy of the impedance technique is confirmed through the comparison with x-ray attenuation technique simultaneously measured in transient boiling tests. Maximum voltage and current for the x-ray source are 300 kV and 3 mA, respectively. Figure 2.3-9 compares results of both techniques for two tests with inlet water temperatures at 313 K and 353 K, indicating that the difference between the two methods is within a range of 20 % which is an allowable accuracy when the void fraction is larger than 0.1.

Figure 2.3-10 compares the experimental results with the Saha and Zuber model for steady subcool boiling.[13] Tendency of the experimental results that follows the model prediction suggests that net vapor generation is dominated by thermal conditions with small influences of liquid flow to mechanically strip voids away from the heating surface.

References

(1) The ROSA-V Group, *ROSA-V Large Scale Test Facility (LSTF) System Description for the Third and Fourth Simulated Fuel Assemblies*, JAERI-Tech 2003-037, Japan Atomic Energy Research Institute, (2003).

(2) M. Suzuki, T. Takeda, H. Asaka *et al.*, "Effects of Secondary Depressurization on PWR Bottom Small Break LOCA Experiments in Case of HPI Failure and Non-condensable Gas Inflow," *Proc. 6th Int. Topical Mtg. on Nuclear Reactor Thermal Hydraulics, Operation and Safety (NUTHOS-6)*, Nara, Japan, Oct. 4-8, 2004, (CD: N6P255) (2004).

(3) M. Kondo, *et al.*, "Experimental Observation of Thermal-hydraulic Behavior in PCCS

*1 This work was entrusted from the Nuclear and Industrial Safety Agency, Ministry of Economy, Trade and Industry of Japan.

Horizontal Heat Exchanger", *Proc. GENES4/ANP2003*, Kyoto, (2003).

(4) M. Kondo, *et al.*, "Confirmation of effectiveness of horizontal heat exchanger for PCCS", *Proc. Int. Conf. Nuclear Engineering (ICONE13)*, Beijin, (2005).

(5) Y. Anoda, *et al.*, "Status of BWR thermal-hydraulic instability tests 6.Thermal hydraulic test on BWR instability," *Proc. 2000 AESJ annual meeting*, Matsuyama, (2000), [In Japanese].

(6) T. Iguchi, *et al.*, "Core thermal hydraulic test (14) -Status of instability test-", *Proc. 2000 AESJ annual meeting*, Matsuyama, (2000), [In Japanese].

(7) H. Asaka, V. G. Zimin, T. Iguchi, *et al.*, "Coupling of the Thermal-Hydraulic TRAC Codes with 3D Neutron Kinetics Code SKETCH-N," *Proc. OECD/CSNI Workshop on Advanced Thermal-Hydraulic and Neutronics Codes: Current and Future Applications*, Barcelona, Spain, April 10-13, (2000).

(8) T. Iguchi, *et al.*, "Experimental study on thermal-hydraulics and neutronics coupling effect on flow instability in a heated channel with THYNC facility", *Proc. 10th Topical Mtg. on Nuclear Reactor Thermal Hydraulics (NURETH-10)*, Seoul, Korea, October 5-9, (2003).

(9) H. Watanabe, *et al.*, *Development of quick-response area-averaged void fraction meter*, JAERI-Research 2000-043, Japan Atomic Energy Research Institute, (2000). [In Japanese]

(10) T. Iguchi, *et al.*, *Development of quick-response area-averaged void fraction meter -Application to BWR condition-*, JAERI-Research 2001-032, (2001). [In Japanese]

(11) M. Ishii and N. Zuber, "Thermally induced flow instabilities in two phase mixture", *Proc. 4th Int. Heat Transfer Conf.*, B5.11 (1970).

(12) Y. Maruyama, *et al.*, "Experimental Study on Transient Void Behavior in Subcooled Water during Reactivity Initiated Accidents under Low Pressure Conditions", *Proc. Int. Conf. Nuclear Engineering (ICONE13)*, Beijing, China, May 16-20, (2005).

(13) P. Saha and N. Zuber, "Point of Net Vapor Generation and Vapor Void Fraction in Subcooled Boiling", *Proc. 5th Int. Heat Transfer Conf.*, 175-179, (1974).

Table 2.3-1 Summary of ROSA/LSTF experiments with several AM measures

Run ID	Break Location	Size	AM Measure & Timing
SB-PV-03	PV bottom	0.2%	SG secondary-side depressurization to achieve 55K/h in primary system being initiated 10 min after SI signal generation
SB-PV-04	PV bottom	0.2%	SG secondary-side depressurization by fully opening relief valves being initiated 10 min after SI signal generation
SB-PV-05	PV bottom	0.18%	SG secondary-side depressurization to achieve 55K/h in primary system being initiated 10 min after SI signal generation
SB-PV-06	PV bottom	0.2%	SG secondary-side depressurization to achieve 55 K/h in primary system being initiated first 10 min after SI signal generation, and switch to full opening of SG relief valves as second AM action after PV liquid level decreases to hot leg bottom

Note: Non-condensable gas inflow (except for SB-PV-05)

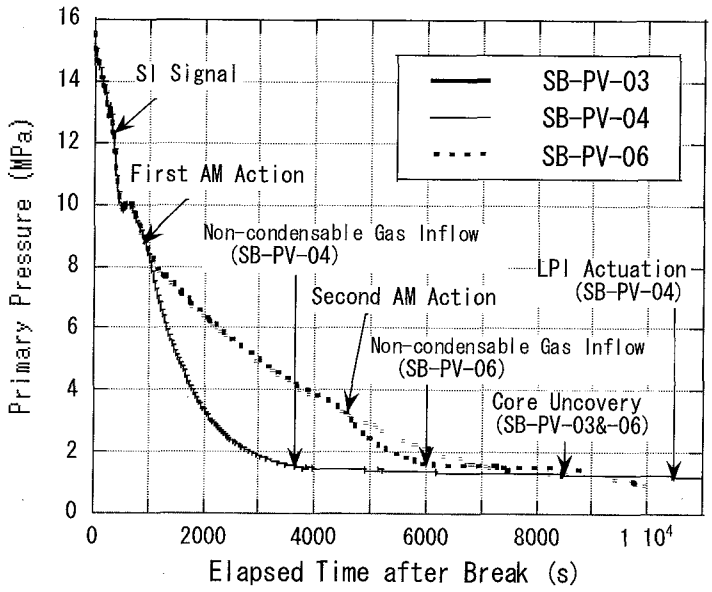

Fig. 2.3-1 Primary pressure transients in 0.2% PV bottom SBLOCA experiments with different SG secondary-side depressurization rates (Long-term core cooling by LPI system was achieved only in Experiment SB-PV-04 where full opening of SG relief valves was assumed.)

This is a blank page.

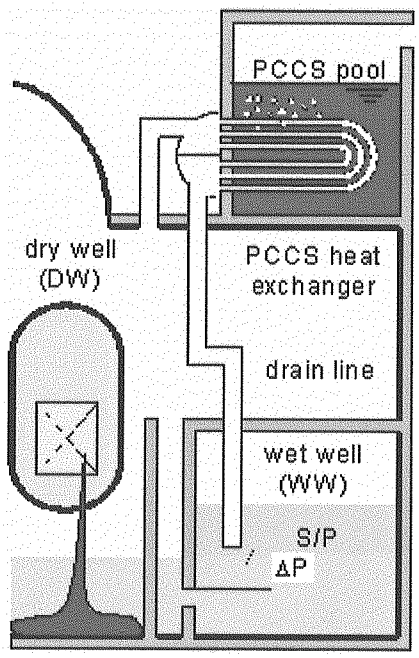

Fig. 2.3-2 Schematic of PCCS using a horizontal heat exchanger

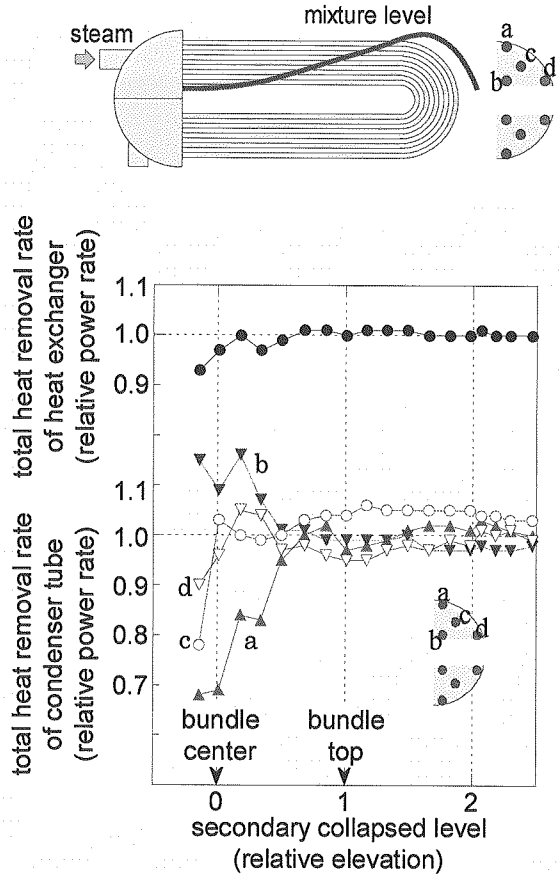

Fig. 2.3-3 Comparison of total heat removal rates of whole heat exchanger and several condenser tubes

This is a blank page.

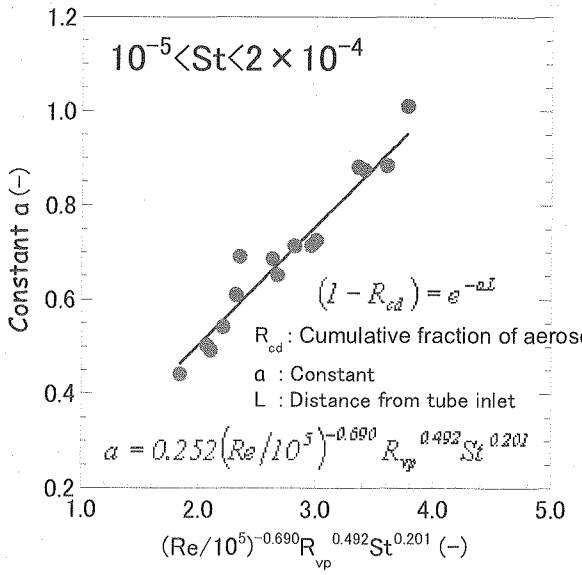

Fig. 2.3-4 Correlation for aerosol position in heat transfer tubes of PCCS for St from 10^{-5} to $2x10^{-4}$

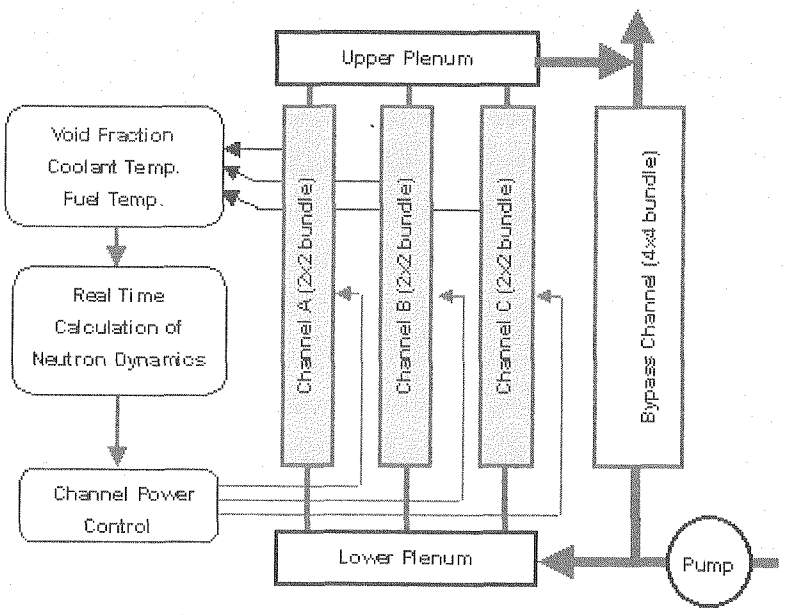

Fig. 2.3-5 Thermal-HYdraulic and Neutronic Coupling loop (THYNC)

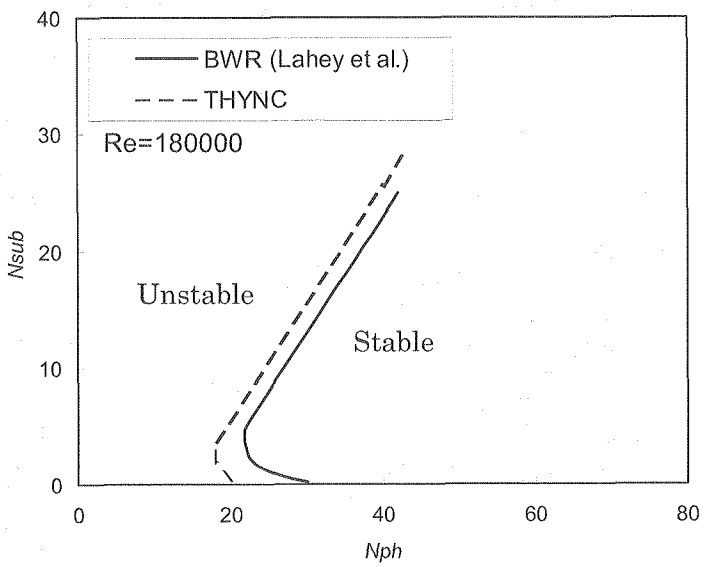

Fig. 2.3-6 Preliminary analysis of stability boundary

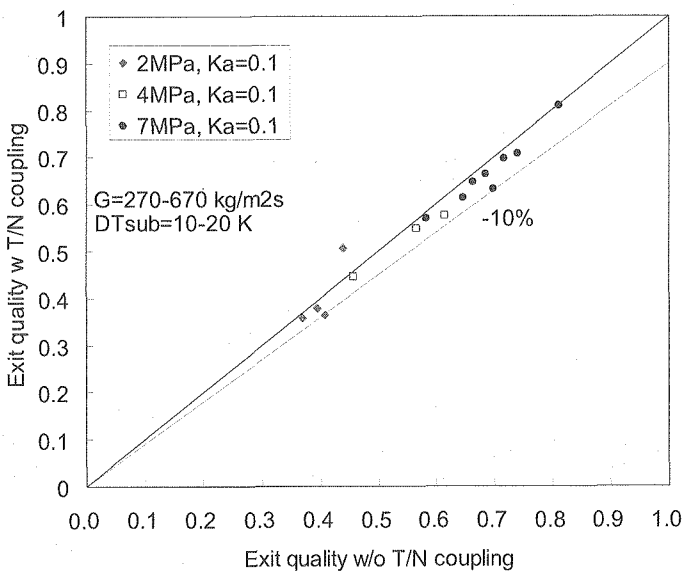

Fig. 2.3-7 Comparison of exit quality at onset of channel instability with T/N coupling against without T/N coupling (THYNC)

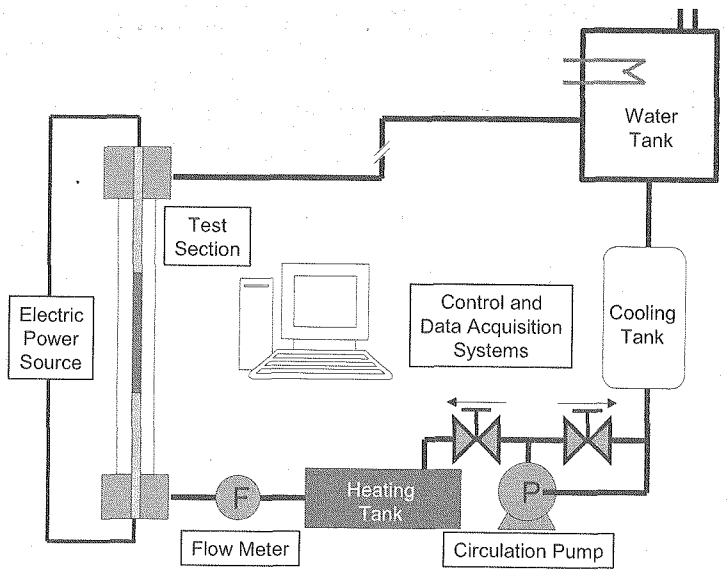

Fig. 2.3-8 Schematic diagram of experimental setup

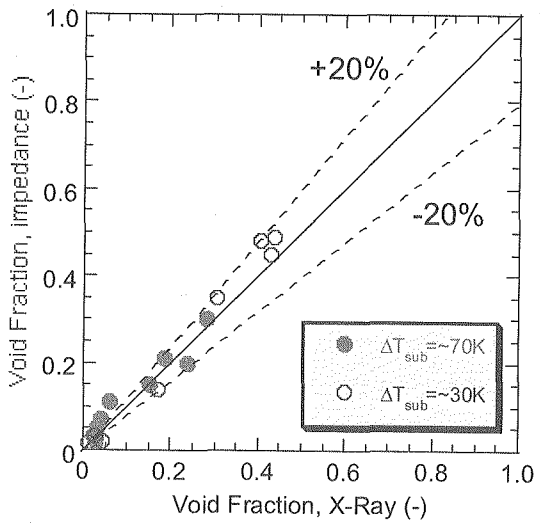

Fig. 2.3-9 Comparison of void fractions measured by impedance and x-ray techniques

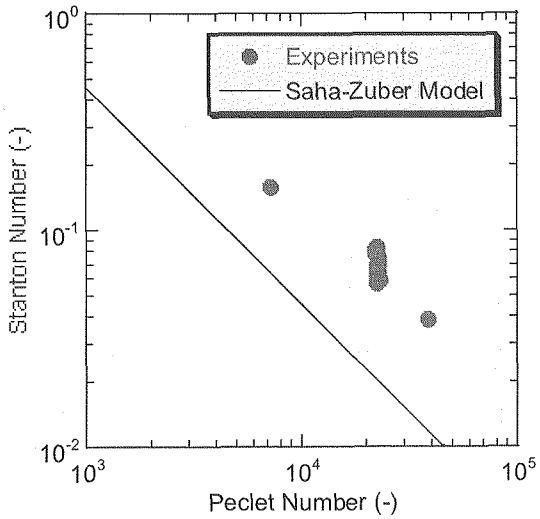

Fig. 2.3-10 Comparison of onset of net vapor generation between experiments and prediction by Saha and Zuber model

2.4 Research on Assessment and Management of Risks of LWRs

The following four research programs are in progress at JAERI to develop methodologies for the effective and efficient management of severe accident risks of LWRs. These programs are aimed at enhancing the technical basis for the introduction of risk-informed regulations and strengthening the effectiveness of emergency measures in Japan.

1) Experimental Validation and Improvement of Severe Accident Analysis Codes: This program consists of two activities. One is to validate and improve the models for radionuclide release from irradiated fuel by performing experiments at the VEGA facility of JAERI and the other is to validate and improve the simulation codes for fuel coolant interaction(FCI) processes by performing a separate effect test on the coarse mixing phase of the FCI.
2) Assessment and Uncertainty Analysis of Severe Accident Risks: Under this program, uncertainty analysis methodologies are developed and applied in level 2 and level 3 PSAs. The outputs of this program such as the information on the public risk are used to assist the Nuclear Safety Commission in their discussions for the establishment of safety goals for LWRs.
3) Research on Emergency Countermeasures: Under this program, the methodologies and results of level 3 PSA are used to examine the technical issues related to emergency countermeasures such as the more rational determination of the emergency protection zone (EPZ) and intervention levels for protective actions.
4) Research on Management of Seismic Risk: Under this program, the methodologies and results of seismic PSA are used to examine the technical issues related to seismic design of nuclear power plants and development of rational approaches for reduction and management of seismic risks.

2.4.1 Experimental Validation and Improvement of Severe Accident Analysis Codes

(1) Fuel-coolant interactions*1

During a severe accident of LWRs, fuel-coolant interactions (FCIs) including steam explosions may occur, if the molten core material contacts with coolant. Mechanical loads caused by a steam explosion would threaten the integrity of containment vessel. Also, the melt break-up process in the FCIs is important in relation to debris bed formation and its coolability. The FCIs may occur in several stages during severe accident, i.e. when the molten core relocates into a coolant pool inside the reactor vessel (in-vessel), or when the molten core ablates through the reactor vessel and drops into a coolant pool in the containment vessel (ex-vessel). Analytical and experimental studies on FCIs have been done

---

*1 This work includes results obtained under an entrustment from the Ministry of Education, Culture, Sports, Science and Technology of Japan.

at JAERI.

Since fiscal year 2003, experiments on break-up of a molten jet in a water pool[1], development and verification of a steam explosion analysis code, JASMINE[2], and its application on level-2 PSA[3][4] have been done.

A series of experiments on the break-up of high temperature oxide and steel melt jets in a water pool were conducted[1], to obtain data for the jet break-up length and size distribution of the droplets produced by the jet break-up. Also, information on the mechanism governing the melt jet break-up, such as flow intensity of the steam column surrounding the melt jet, and its relation with the droplet size were pursued. In the experiments, a zirconia-alumina mixture or stainless steel melt jet with diameter 17mm and velocity 7.8m/s at the water surface was dropped into a deep (2.1m) or shallow (0.6m) water pool with various subcool (Fig. 2.4-1). From the results of the present experiments and by referring existing data in literature[5][6], we obtained empirical correlation equations for the jet break-up length, the fraction of jet broken-up in a shallow pool where the jet was not completely broken-up, and the droplet size. These correlation equations can be used as constitutive models in FCI simulation codes.

A steam explosion simulation code JASMINE was developed at JAERI for the assessment of steam explosion impacts on the integrity of containment vessel during severe accidents in light water reactors. For the verification and tuning of JASMINE, we performed simulation of selected steam explosion experiments with alumina and corium melt[2], KROTOS-44, 42, 37 and FARO-L33[5][7]. The experimentally observed difference of the steam explosion intensity with the two materials, i.e. alumina often shows typical strong explosions but corium shows much weaker interactions, was reproduced in the simulation without changing the model parameters related to the explosion process, but based on the difference in the premixing behavior predicted by the simulations. The simulation of corium experiments showed more fractions of the melt droplets frozen during premixing, as well as more void fractions, and those two points were likely to be the primary reasons of weak interactions in corium experiments. Based on this result, we decided to apply JASMINE code with explosion parameters tuned for typical alumina explosion to reactor analysis.

The containment failure probability due to ex-vessel steam explosions was evaluated for Japanese LWR model plants(Fig.2.4-2)[3][4]. A stratified Monte Carlo technique (Latin Hypercube Sampling (LHS)) was applied for the evaluation of steam explosion loads, in which JASMINE was directly used as a physics model. The evaluation was made for three scenarios: a steam explosion in the pedestal area and in the suppression pool of a BWR model plant with a Mark-II containment, and a steam explosion in the reactor cavity of a PWR model plant. The scenario connecting the generation of steam explosion loads and the containment failure was assumed to be the displacement of the reactor vessel and pipes, and failure at the penetration in the containment boundary. The conditional containment failure

probabilities (CCFPs) per occurrence of steam explosion were 6.4×10^{-2} (mean) and 3.9×10^{-2} (median) for the BWR suppression pool case, 2.2×10^{-3} (mean) and 2.8×10^{-10} (median) for the BWR pedestal case, and 6.8×10^{-2} (mean) and 1.4×10^{-2} (median) for the PWR cavity case. Note that the CCFPs were based on the preconditions of failure of the accident termination within the reactor vessel, relocation of the core melt into the ex-vessel water pool without significant interference, and a strong triggering with maximized premixing mass. The CCFPs on the basis of core melt event, with these factors included, should be lower than the values given above. The obtained failure probabilities were most dependent on the assumed range of melt flow rates and on the fragility curves. More detailed examination of the assumed probability distribution of the melt jet diameter and structural failure process would narrow the range of the failure probabilities.

In parallel with the development and application of JASMINE code described above, we participated in OECD/SERENA program that was an international cooperative study on the analytical capability of energetic steam explosions[8]. We contributed with analytical results by JASMINE on premixing and explosion experiments, and plant scale phenomena. Discussions and exchanges in the program as well as experimental data obtained were profitable for our work on the development and verification of JASMINE.

(2) Radionuclides release from irradiated fuel under severe accident conditions

The experimental program VEGA (Verification Experiments of radionuclide Gas/Aerosol release) had been performed at JAEA. The program was comprised of series of experiments on radionuclides release from UO_2 and MOX fuel at temperatures up to melting point of fuel under pressures up to 1.0 MPa and model development for numerical calculations[9]. In the test called VEGA-M1*2 [10][11], MOX fuel (43GWd/tHM) irradiated in the ATR (Advanced Thermal Reactor) Fugen was heated up to about 3150K in helium (He) atmosphere at 0.1 MPa to enlarge limited data base for radionuclides release from MOX.

The schematic diagram of the VEGA apparatus is shown in Fig. 2.4-3 with a photograph through a lead glass window. The apparatus consists of an induction furnace to heat up the fuel specimen, a gas supply system, thermal gradient tubes (TGT), aerosol filters, a condenser, a dryer and a cold charcoal trap. Tungsten was used as crucible material in inert atmosphere. Three sets (Trains A, B and C) of TGTs and filters were switched sequentially to collect radionuclides released during three fuel temperature plateaus (fuel temperature histories were indicated in Fig. 2.4-4). Fission gas was collected in the cold charcoal trap maintained at 210 K.

---

*2 This work was entrusted from the Ministry of Education, Culture, Sports, Science and Technology of Japan.

The fractional release of cesium (Cs) from the MOX fuel in comparison with test VEGA-3 was evaluated from gamma-ray measurement of the fuel as shown in Fig. 2.4-4. Test VEGA-3 was performed using PWR UO_2 fuel (47GWd/tU). Conditions of the two tests were almost same. The Cs release started at about 1000K from the MOX fuel and at about 1600K from the UO_2 fuel. Since the fission gas release (FGR) of the MOX fuel was large during normal operation, certain amount of Cs migrated at grain boundary. On the other hand, the FGR of the UO_2 fuel was very small. The possible reason of this discrepancy of release is due to the release from grain boundary.

The fractional releases of plutonium (Pu) from MOX fuel were evaluated for three temperature regions (A: - 2300 K, B: 2300 - 2800 K, C: 2800 - 3150 K) from alpha-ray measurements of leaching solutions of TGTs, filters and connecting pipes of VEGA apparatus (Fig. 2.4-5). The Pu release above 2800 K was higher by nearly three orders of magnitude than that at lower temperature. Since the existing ORNL Booth model underestimated this Pu release at the high temperature, an empirical formulation was prepared based on these experimental data. The release fractions of Pu into a containment vessel during major severe accident sequences were evaluated using the JAEA's source term analysis code, THALES-2 with the empirical release formulation. The analyses showed the fractional releases into the containment vessel were less than 1%, indicating that the assumption of 1% release of Pu into the containment vessel used in the Japanese site evaluation is conservative enough.

2.4.2 Assessment and Uncertainty Analysis of Severe Accident Risks[*3]

In the research for uncertainty analysis of severe accident, the improvement of methods of uncertainty analysis for the estimation of core damage frequency through the assessment of accident consequences and collection of necessary information were made for performing uncertainty analysis for a BWR (a 1100MWe BWR5/Mark-II). As for a PWR(a 1100MWe four-loop PWR with dry containment), important accident sequences were identified by the uncertainty evaluations of containment failure frequency. Analyses on accident progression and source terms were made for major accident sequences.

(1) Uncertainty analysis of core damage frequency

Uncertainty analysis of core damage frequency was performed by SAPHIRE code developed by U.S.NRC. Uncertainty of core damage frequency is caused by the propagation of uncertainties, in which exists component failure data, through the calculation model composed of the front line system event tree and the fault tree. The improvement of the event tree was performed to consider accident management mitigation. On the uncertainty

---

[*3] This work was entrusted from the Ministry of Education, Culture, Sports, Science and Technology of Japan.

analysis, the influence on the core damage sequence caused by whether the accident management mitigation was considered in the calculation model or not was evaluated. From the result of uncertainty analyses, it was found that 1) a dominant sequence for total core damage frequency is TQUX which is transient with loss of ECCSs and failure of depressurization, 2) total core damage frequency was reduced on the usage of accident management, and 3) uncertain range between 5% and 95% value is double figures.

(2) Uncertainty analysis of containment failure frequency

The containment event tree (CET) is a calculation model for evaluating the containment failure frequency following core damage accidents. CET is structured by the combination of the branch on physical phenomena such as steam explosion, operation of the safety systems and recovery control by operator and is quantified by adding appropriate probabilities to the branches. Uncertainty of containment failure frequency results from not only the propagation of uncertainties in branch probabilities but also uncertainties in the core damage frequency through the CET.

Concerning BWR analysis, some of tree structure and of branch probabilities have been altered with the investigation results on the latest PSA knowledge, especially including quantitative analysis for in-vessel and ex-vessel steam explosion from the previous CET model originally developed by JAERI for BWR. From the result of uncertainty analyses, it was found that 1) total containment failure frequency(/reactor year) is 5.13E-7(average value)、1.59E-7(5%)、3.96E-7(50%)、1.20E-6(95%), and 2) the uncertainty of total containment failure frequency caused by more uncertainties of the core damage frequency than uncertainties of the branch probabilities in CET.

Concerning energetic in-vessel explosion in BWR, it has been decided to quantify the outcome likelihood, considering that it has become an issue because of large uncertainty involved and large early FP release potential. For this purpose, probabilistic analysis method with uncertainty treatment has been developed through the whole process sequence of the event for BWR by combining mechanistic and probabilistic approaches based on ROAAM (Risk Oriented Accident Analysis Methodology) proposed by T.G.Theofanous. The models are incorporated from the associated mechanistic studies (JASMINE code analysis etc.) for molten fuel-coolant interaction (FCI) and energy dissipation/partition. The analysis results show such a very skewed distribution as almost all is localized at zero or extremely low probability ($\sim 10^{-4}$ or lower) while only a very little portion spreads out up to higher order probability (~ 1.0) just like long tail for failure likelihood and thus containment failure probability (conditional on core melt) has been estimated to be 3.2×10^{-4} (95percentile) and 1.2×10^{-2} (average (expected value)).

Concerning PWR analysis, CET has been analyzed using a method developed by reflecting the latest knowledge and quantitative analysis results on the physical phenomena-

related branches in the CET, as an extension of the previous study by NUPEC. As a result, estimated containment failure frequency (per reactor-year) is 1.37×10^{-8} on average and 1.69×10^{-9} (5 percentile) to 4.58×10^{-8} (95 percentile) for variation range. It is found that dominant failure mode is containment bypass event due to interface LOCA.

(3) Uncertainty analysis of source terms

As for the estimation of source terms, the uncertainty analysis for source terms performed by severe accident analysis code THALES2 for BWR-5/Mark-II plant. The procedure of uncertainty analysis for source terms with THALES2 is shown in Table 2.4-1.

At first it needs to determine uncertain terms of source terms, such as released FPs in reactor vessel and transfer of FPs from in-vessel to ex-vessel, which are dominant factor for source terms. These uncertain terms determined by surveying preceding PSAs, which is expert's opinions in the NUREG-1150.

It needs to determine associated parameters, which are selected in THALES2 inputs, for above uncertain terms. Uncertainty analysis is performed by being had a uncertain distribution on each associated parameter. The uncertain distribution of these associated parameters are assessed by surveying recent experimental and analytical studies as well as by our experiences on analyzing severe accidents with THALES2. But release mechanism of non-volatile FPs is not fully understood for the difficulty of measurement in experiments. There exist uncertainties in the model. Therefore, the distribution of several parameters, which is difficult to assess the distribution, are applied to NUREG-1150's uncertain range defined by experts.

The uncertainty analysis performed for the BWR identified 14 accident scenarios as important in terms of containment failure frequencies and severity of consequence. As a result of uncertainty analysis for these scenarios, information of uncertainties, such as those in the timing of release and release fraction of CsI to the environment, was obtained. From the result of these analyses, it was found that 1) release fraction of CsI to the environment (average value) of 14 scenarios is 10% for initial core inventory except for containment venting scenario, which is an accident management measure to avoid the containment overpressure failure by a controlled release of containment atmosphere to the environment and 2) the timing of FP release to the environment depends on the core damage sequence.

(4) Uncertain and sensitivity analyses with OSCAAR [12]

The uncertainty and sensitivity methodology has been successfully implemented for the probabilistic accident consequence assessment code OSCAAR developed at JAERI. This study addressed the uncertainty in the predicted individual risks of early fatality and latent cancer fatality in the population near a nuclear power plant, which might be relevant to the safety goal application in Japan. There are two types of parameter uncertainties in

probabilistic accident consequence assessments. The first type of uncertainty (stochastic uncertainty) includes those parameters for which there is no single value but for which a probability distribution of values can be specified. The weather condition at the time of an accident is an example of this type of uncertainty and this is usually summarized in the form of complementary cumulative distribution function (CCDF) in probabilistic consequence assessments. The second type of uncertainty (subjective uncertainty) indicates that there is a correct value but it is not known because of a lack of information about a deterministic process. This type of uncertainty is in general expressed by confidence interval for the CCDFs. The distinction between these two types of uncertainties in the accident consequence assessment is important for decision-making because an increased effort in gathering information can improve the quality of decision-making by reducing the subjective uncertainties, while it would be ineffective for the stochastic uncertainties. The following three questions were investigated:

- How do we deal with the stochastic uncertainty (weather conditions) in accident consequence assessments and how much is the statistical variability?
- How much is the uncertainty with respect to imprecisely known variables in the model and what are the main contributors to the uncertainty in individual risks of early and latent cancer fatality?
- How much of the overall uncertainty about individual risks is attributable to stochastic uncertainty and how much to subjective (parameter) uncertainty?

The stratified sampling scheme appropriate for the atmospheric dispersion model used in OSCAAR has been developed for identifying a representative sample of meteorological sequences for use in the accident consequence assessment. It has been found that the 99th percentile of the CCDF for early health effects was uncertain by a factor about two. The parameter uncertainty propagation analyses performed with OSCAAR provide quantitative information on the uncertainties of individual fatality risks of the probabilistic accident consequence assessment. Figs. 2.4-6 and 2.4-7 show the resulted distributions of the expected values for the average individual risks of early and latent cancer fatality in the form of box plots. The uncertainty factor defined by the ratio of the 95th percentile value to the mean value of the expected value of the CCDF for individual risks of early and latent cancer fatality were both less than about four close to the site. This result could give valuable insights for the discussion of safety goal. In the sensitivity analyses, the parameters whose uncertainties make important contributions to the overall uncertainty were identified as the parameters which related to the inhalation dose. This result might be relevant to the situation considered. Therefore, further analyses will be needed for different situations. Finally, it was found that the contribution of stochastic uncertainty due to weather scenarios to the overall uncertainty for individual fatality risks was less than about 25% at all

distances. This quantitative information could also emphasize further research aiming at reducing the uncertainties due to lack of knowledge about the important parameter values.

2.4.3 Research on Emergency Countermeasures

It is recognized that good preparedness in advance of an emergency can substantially improve the emergency response to a nuclear accident. Probabilistic accident consequence assessment models are being applied for providing a technical basis for discussing the effective emergency planning including intervention levels and emergency planning zones for appropriate protective actions such as sheltering, evacuation, stable iodine prophylaxis and relocation.

The study [13] has been conducted to investigate the sensitivity of the predicted consequences to the variation of intervention levels and return criteria in the assumed long-term relocation countermeasure. The probabilistic accident consequence calculations suggested that the collective dose saved by relocation was not greatly affected by the choice of relocation and return criteria but the time integral of numbers of people relocated was strongly dependent on the chosen relocation and return criteria. Avertable per caput dose per unit time, which was a key index for justification of protective measures, was less sensitive to the chosen intervention levels but quite sensitive to the specific return criteria. These results will provide a valuable insight for establishing the intervention level and return criteria for relocation in the emergency response planning.

If an accident occurs in a nuclear power plant (NPP), early protective actions are carried out. To implement these actions more effectively, emergency preparedness and emergency planning are important, and especially prompt evacuation is expected to reduce a large amount of radiation exposures. To examine the effect of early protective measures by using a PSA method, estimation of the parameter uncertainty related to the time for early protective actions is needed. For this purpose, we have developed a computer code for estimating time needed to implement urgent protective actions using Geographic Information System (GIS), and estimated the distribution of the distances from the residence area to the transient points for preparing evacuation[14]. For this analysis, we used the temporary gathering locations data and the emergency shelter data shown on each regional emergency response plans for disaster prevention which will be used in actual emergency situations and the targeted area is the residence area inside Emergency Planning Zone (EPZ). The travel distance during an evacuation is assumed as the shortest distance on the road network from each residence area to the temporary gathering locations or the emergency shelter. The accumulation gathering number of people as the function of the travel distance for each these gathering locations is calculated. By applying this method for Tokai village, we estimated the distribution of the travel distance during an evacuation and the maximum value is 4,650m

(Fig. 2.4-8). We are preparing the data for each NPP sites to apply this method and to investigate evacuation time for each sites.

2.4.4 Research on Management of Seismic Risk

JAERI developed procedures and computer codes for performing level 1 seismic PSAs and demonstrated their usefulness by performing a seismic PSA for a BWR model plant by 1999[15]. The current program aims at proposing effective applications of seismic PSAs for design and risk management of nuclear facilities. In FY2002 and 2003, a trial study was conducted for seismic PSA of a multi-unit site to examine potential combinations of core damage sequences and the effectiveness of an accident management measure, namely, the cross connection of emergency diesel generators (EDGs) between adjacent units.

In this study, twin units (BWR-5 with Mark-II Containment) were assumed to be located closely in one site and each of them has two EDGs. Credit was taken for the success of operating procedure on cross-connection.

This study used the SECOM2 code[16] developed at JAERI for the calculation of core damage frequencies (CDFs) with consideration of the effect of correlation of failure of components which is an important issue of seismic PSA especially for this study which needed to examine the accident conditions in similar units located in the same site under a seismic event. The correlation of failure arises from the similarity in seismic responses or seismic capacities of components of similar conditions such as the similarity in design, location, or natural frequency. For example, if a pump fails by seismic motion, then the failure probability of another pump of the same design would be high. Therefore the simultaneous occurrence of similar accident scenarios would be higher if we consider the effect of correlations. In this study, correlation coefficients for responses of components were determined by the methods of NUREG-1150[17] and capacities of components were assumed to be completely independent.

It was suggested from this analysis that, even if two units simultaneously have core damage, it is more likely for them to have different accident sequences than to have the same sequence. It was indicated that, for the case with the cross-connection of EDGs unavailable, the CDFs estimated for individual units were about 2 times higher than that for single unit site and, for the case with the cross-connection of EDGs available, the CDFs estimated for individual units were lower than that for single unit site. Since most of Japanese nuclear power stations have more than one units, it seems to be beneficial to use seismic PSA methodology for examining the likely accident scenarios and effective accident management measures.

References

(1) K. Moriyama, Y. Maruyama, T. Usami, et al., *Coarse break-up of a stream of oxide and steel melt in a water pool*, Japan Atomic Energy Research Institute, JAERI-Research 2005-017 (2005).

(2) K. Moriyama, H. Nakamura and Y. Maruyama, "Simulation of alumina and corium steam explosion experiments with JASMINE v.3", *Proc. the 6th Int. Conf. on Nuclear Reactor Thermal Hydraulics, Operations and Safety*, Nara, Japan (CD-ROM: Paper ID.264) (2004).

(3) K. Moriyama, S. Takagi, K. Muramatsu, et al., "Evaluation of ex-vessel steam explosion induced containment failure probability for Japanese BWR", *Proc. 2005 Int. Congress on Advances in Nuclear Power Plants (ICAPP2005)*, Seoul, Korea (CD-ROM: Paper no.5632) (2005).

(4) Japan Atomic Energy Research Institute, "FY2004 Report of the research for technical knowledge base for the legal system for the compensation of nuclear damage" (2005), [in Japanese].

(5) D. Magallon, S. Basu and M. Corradini, "Implications of FARO and KROTOS experiments for FCI issues", *Proc. OECD Workshop on Ex-Vessel Debris Coolability*, Karlsruhe, Germany (FZKA 6475), 268-276 (1999)

(6) A. Kaiser, W. Sch tz and H. Will, "PREMIX: Experiments PM12--PM18 to investigate the mixing of a hot melt with water", Forschungszentrum Karlsruhe, FZKA 6380 (2001).

(7) I. Huhtiniemi, D. Magallon and H. Hohmann, "Results of recent KROTOS FCI tests: alumina versus corium melts", Nuclear Engineering and Design, 189, 379-389 (1999).

(8) D. Magallon, K.H. Bang, S. Basu et al., "Status of international programme SERENA on fuel-coolant interaction", *Proc. Int. Congress on Advances in Nuclear Power Plants (ICAPP'05)*, Seoul, Korea, (CD-ROM:Paper 5382), (2005).

(9) A. Hidaka, T. Kudo, T. Ishigami, et al., "Proposal of Simplified Model of Radionuclide Release from Fuel under Severe Accident Conditions Considering Pressure Effect," J. Nucl. Sci. Technol., 41(12), pp.1 (2004).

(10) A. Hidaka, T. Kudo and T. Fuketa, "Radionuclides Release from Mixed-Oxide Fuel under Severe Accident Conditions," Trans. of 2004 ANS Winter Mtg. (2004).

(11) A. Hidaka, T. Kudo, J. Ishikawa, et al. "Radionuclide Release from Mixed-Oxide Fuel under High Temperature at Elevated Pressure and Influence on Source Terms," J. Nucl. Sci. Technol., 42(5), pp.451 (2005).

(12) T. Homma et al., Uncertainty and Sensitivity Studies with the Probabilistic Accident Consequence Assessment Code OSCAAR, Nucl. Eng. Technol. 2005. (to be published)

(13) T. Homma et al., "Technical Analysis for Off-site Emergency Planning with a Probabilistic Accident Consequence Assessment model," *Proc. The 11th Int. Radiation Protection Association*, Madrid , June 6-7, (2004).

(14) S. Sato et al., "Development of a computer program for analyzing evacuation delay time using Geographic Information System," *Proc. The 38th Annual Meeting of the Japan Health Physics Society*, Kobe, April, (2004), [in Japanese].

(15) Risk Analysis Laboratory, *Summary report of seismic PSA of BWR model plant*, JAERI-Research 99-035 May (1999), [in Japanese].

(16) Y. Watanabe, et. al., "Development of the DQFM method to consider the effect of correlation of component failures in seismic PSA of nuclear power plant," Reliability Engineering and System Safety 792, 65–279, (2003).

(17) J.A. Lambright, et. al., *Analysis of core damage frequency: Peach Bottom Unit 2 external event*, NUREG/CR-4550, (1989).

Table 2.4-1 Procedure of uncertainty analysis

Procedure of uncertainty analysis
1) Determination of uncertain terms - base on expert's opinions in the NUREG-1150
2) Determination of associated parameters for uncertain terms - THALES2 inputs
3) Determination of uncertain range of associated parameters - Parameter survey in recent experimental and analytical studies - Application of NUREG-1150's uncertain ranges
4) Execution of uncertainty analysis

This is a blank page.

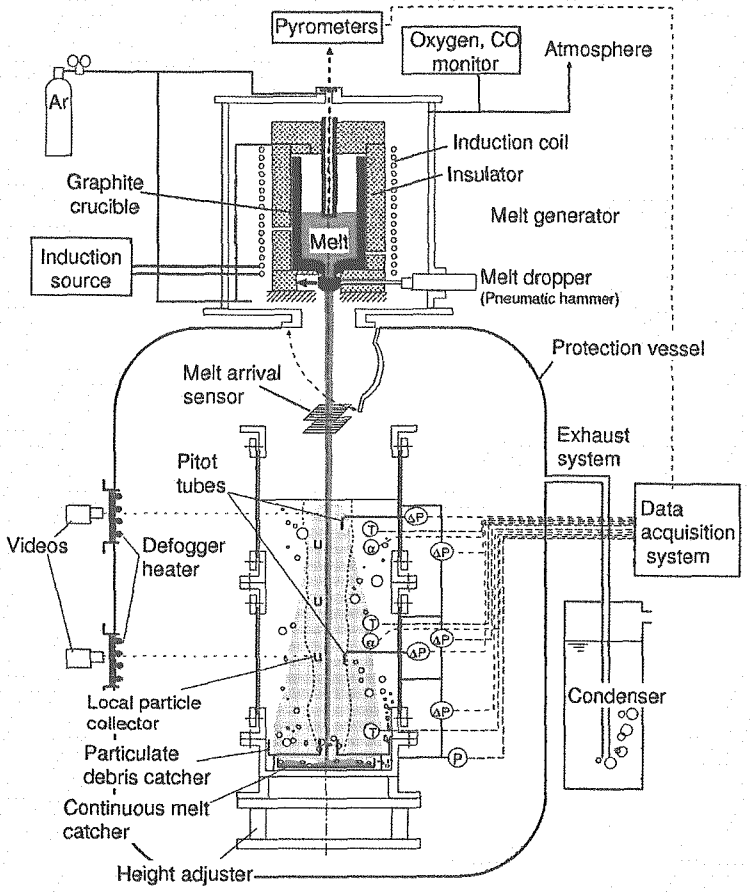

Fig. 2.4-1 Schematic diagram of melt jet break-up experiment

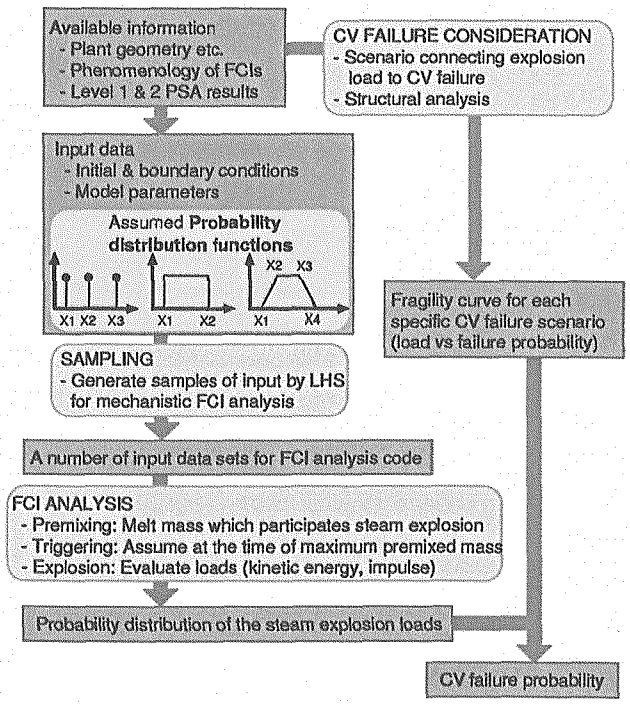

Fig. 2.4-2 Method of probabilistic application of a mechanistic model for evaluation of containment failure probability due to ex-vessel steam explosions

This is a blank page.

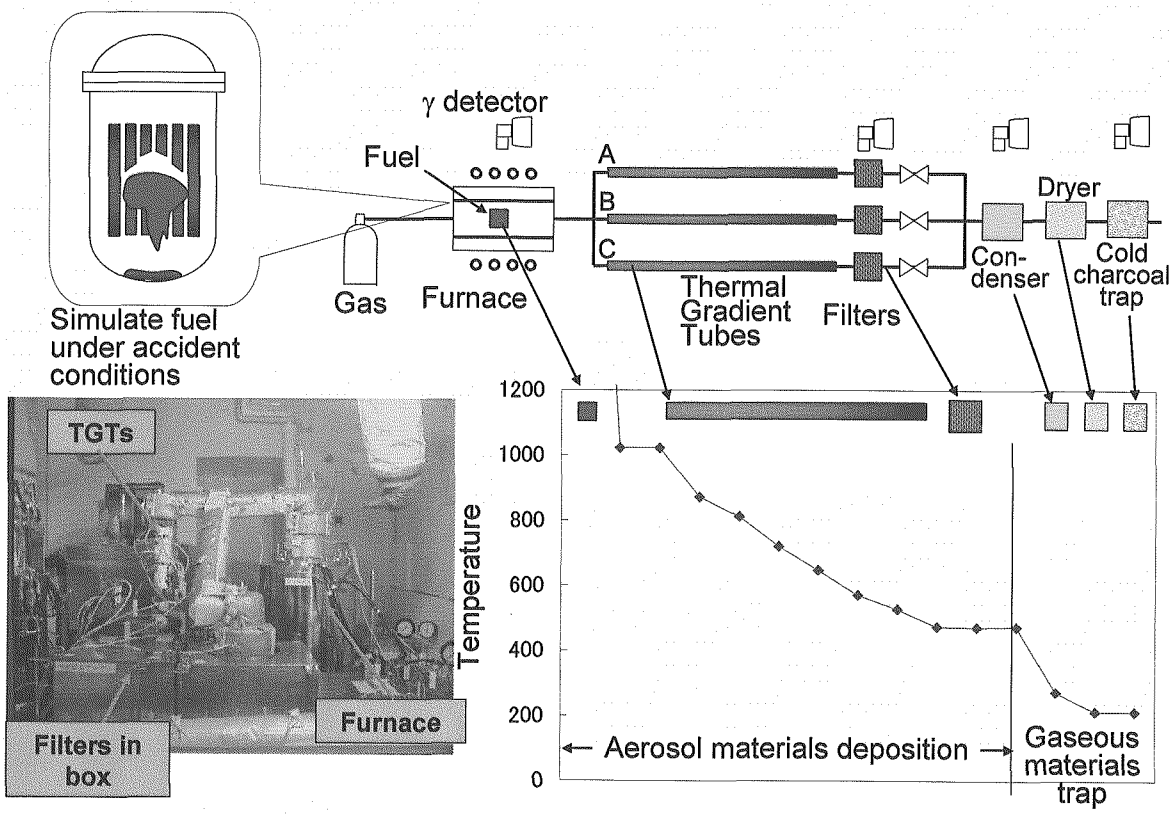

Fig. 2.4-3 Schematic diagram of VEGA facility

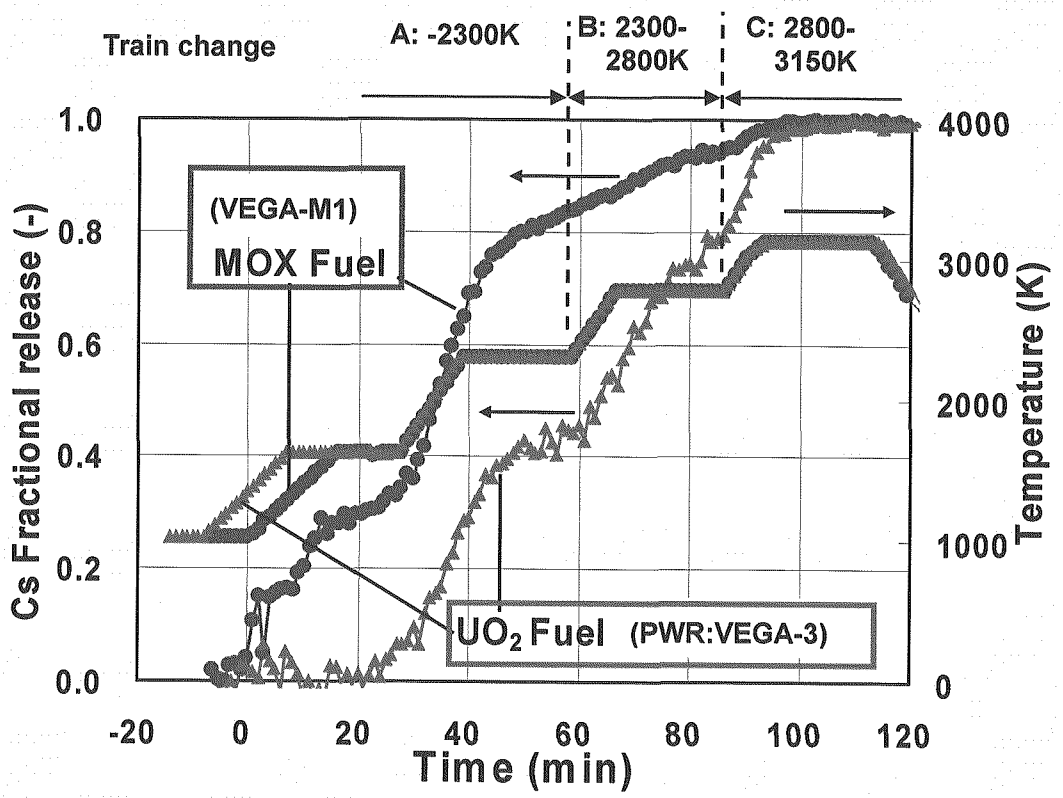

Fig. 2.4-4 Comparison of Cs fractional release between MOX and PWR UO_2

This is a blank page.

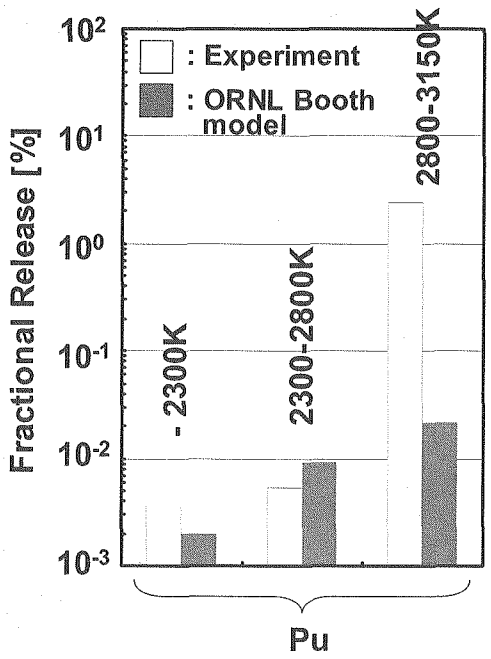

Fig. 2.4-5 Comparison of fractional release of Pu for three temperature regions between experiment and ORNL Booth model calculation

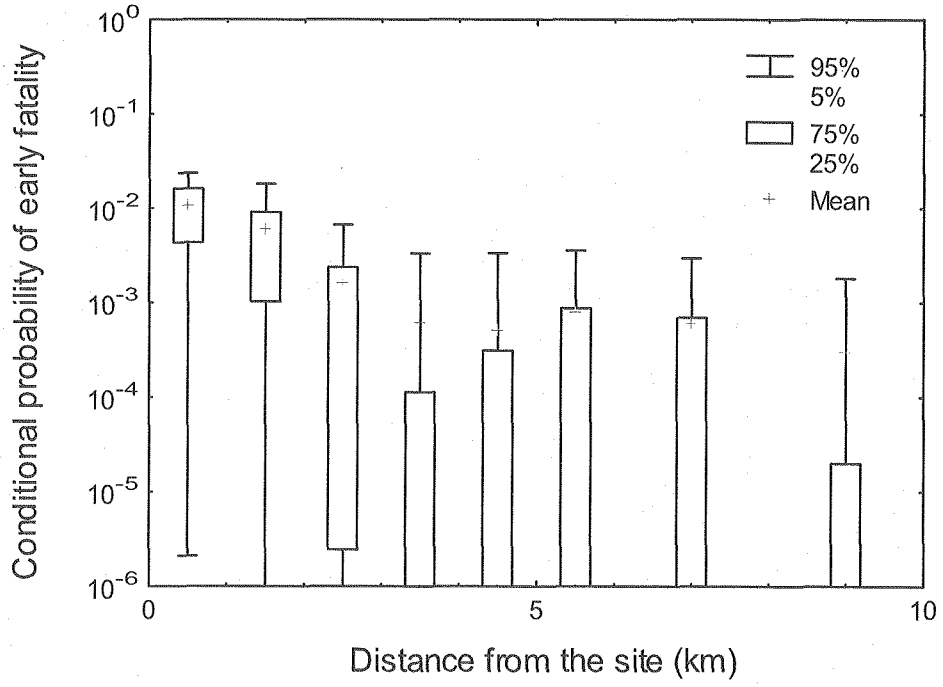

Fig 2.4-6 Uncertainty distributions of the expected values for individual risk of early fatality

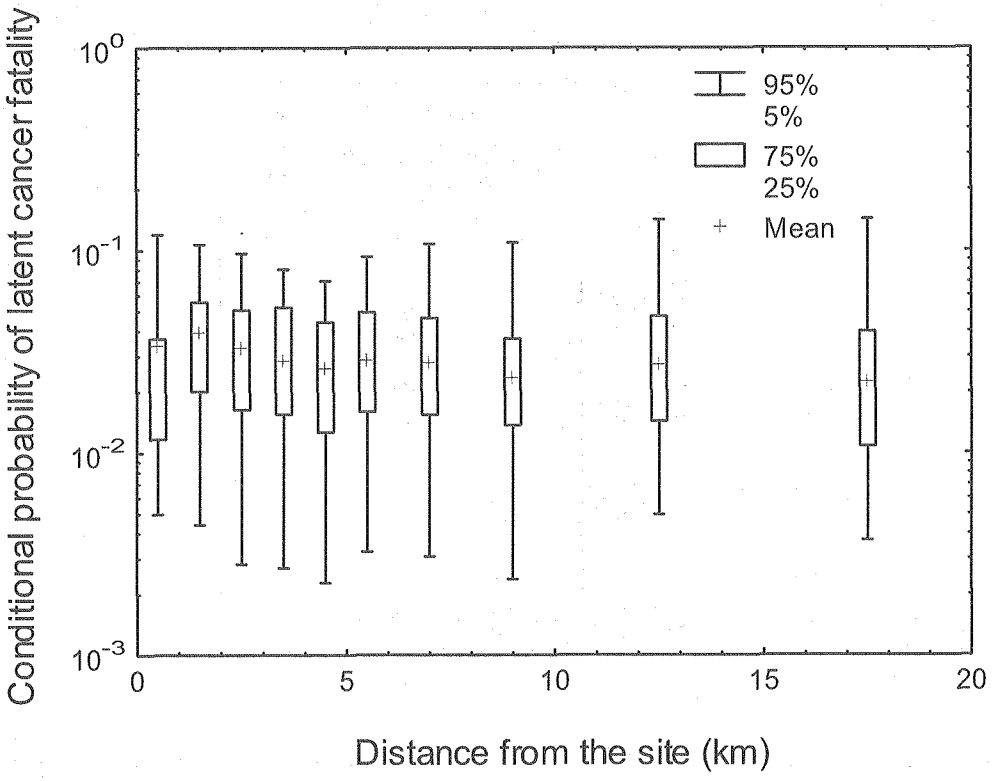

Fig 2.4-7 Uncertainty distributions of the expected values for individual risk of latent cancer fatality

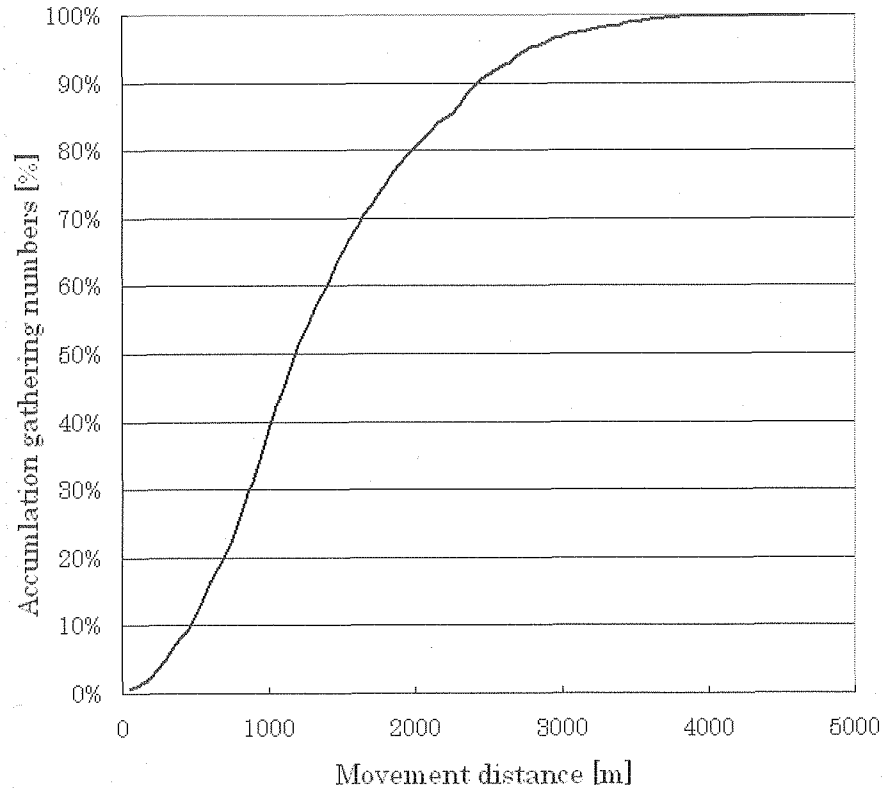

Fig.2.4-8 Distribution of the movement distance for Tokai village

2.5 Analysis and Evaluation of Operating Experience

This section describes the two research activities in last two years: (1) review and compilation of incident reports and (2) examination of samples from BWR core shroud and primary loop recirculation piping.

In the first activity, nuclear incidents that occurred at foreign facilities were systematically reviewed and compiled to identify generic safety issues and characterize these incidents.

In the second activity, in order to investigate the cause of cracks in the reactor core shrouds and primary loop recirculation (PLR) pipes, JAERI conducted the original examinations and reviews of electric company's examinations with the objective to ensure the transparency of the examination as the third-party organization. As the examination results, it is concluded that these cracks initiated in the low carbon stainless steels were stress corrosion cracking.

2.5.1 Review and Compilation of Incident Reports

The primary sources of operating experience data for the analysis and evaluation of incidents are (a) the reports to the Incident Reporting System (IRS), (b) the reports to the International Nuclear Event Scale (INES), both of which have been jointly operated by the Organization of Economic Cooperation and Development/Nuclear Energy Agency (OECD/NEA), and (c) the U. S. Nuclear Regulatory Commission's (U. S. NRC's) generic communications such as Information Notices. The IRS provides the regulatory bodies (and their related organizations) in the member states with the information on only the incidents at nuclear power plants, while the INES provides the information for public communication on events at all types of nuclear facilities.

Approximately 140 incidents reported to the IRS in 2003 and 2004 were reviewed and compiled. Those included incidents involving pipe rupture due to radiolysis gas explosion, leakage from reactor vessel lower head penetrations, potential impact of debris blockage on ECCS recirculation sump, fire in secondary electrical penetration, and damage of fuel assemblies inside a cleaning tank. These incidents were summarized in Japanese and provided to the regulatory bodies, NSC and NISA, and electric utilities.

The reports from the INES have been translated into Japanese, disseminated to the relevant organizations such as NSC, and opened to the public through the Internet[1]. In these two years, approximately 60 INES reports we received from May 1, 2003 to July 31, 2004 were reviewed and translated. During this period, two events rated as level 3 were reported. Those are potential personnel overexposure at irradiation facility and fractured pipe in reprocessing facility. About 20 events involved loss or discovery of radiation sources and about 15 events involved radiation overexposure of personnel or public in industrial facilities using the radiation sources.

As well, we collected and reviewed the event investigation reports issued by the licensee and U. S. NRC and related information on the reactor vessel head degradation at Davis Besse in 2002. A summary report describing the results from the review was published in Japanese[2] and presented at the NSC's annual meeting at the request of NSC.

In addition, we examined quantitative risk trends for the Industry level, using two indicators, that is, the occurrence frequency of precursors and the annual core damage probability, deriving from the results of the U. S. NRC's Accident Sequence Precursor Program which identifies and categorizes precursors to potential severe core damage accident sequences by analyzing the operational events at U. S. nuclear power plants using the PSA technique. As shown in Figs. 2.5-1 and -2, the study indicates that the core damage risk at U. S. nuclear power plants has been lowered and the likelihood of risk significant events has been remarkably decreasing[3].

2.5.2 Examination of Samples from BWR Core Shroud and Primary Loop Recirculation Piping

Recently in the Japanese boiling water reactor (BWR) power plants, many cracking incidences were found in the reactor core shrouds and primary loop recirculation (PLR) pipes. In order to investigate the cause of cracks, electric power companies performed various examinations on the sample material extracted from BWR power plants. JAERI conducted the original examinations and reviews of electric company's examinations with the objective to ensure the transparency of the examination as the third-party organization from October, 2003. As the examination results, it is concluded that these cracks initiated in the low carbon stainless steels were stress corrosion cracking (SCC) [4]. SCC is the degradation phenomenon that the cracking is initiated, propagated and ruptured by lower tensile stress than normal tensile strength of metallic materials exposed in the corrosive environment and is roughly divided into intergranular SCC (IGSCC) and transgranular SCC (TGSCC) by morphologies of fracture surface.

Core shroud has a cylindrical geometry located in reactor pressure vessel and its function is to support the core structure and to make coolant flow route from lower to upper portion inside the core shroud by jet pumps in normal operation. PLR pipe is a circulation system in which reactor cooling water is withdrawn from Reactor Pressure Vessel and is returned to the reactor after increasing pressure by high pressure pump. Cracking incidences were found in the reactor core shroud of the Swiss M hleberg Nuclear Power Station in 1990, the Fukushima Dai-ichi Nuclear Power Station Unit-2 (type 304 stainless steel) in 1994 and the Fukushima Dai-ni Nuclear Power Station Unit-3 (type 316L stainless steel) in 2001. Furthermore, in the Japanese BWR power plants, many cracking incidences were reported in the reactor core shrouds and PLR pipes in 2002 and for identifying the causes of cracking through examinations of the boat samples taken from the cracked regions and various

examinations were carried out.

The samples taken from the cracked region of the core shroud or PLR pipes investigated in JAERI were cut up and the microstructure investigation and fracture surface observation were carried out. Based on the examination results of morphology observation in the cross section and fracture surface, it was apparent that the cracks were caused by SCC. Hardening layer was found from the surface of the core shroud to the depth of about 100-300μm. The cracks were mainly initiated in the hardening layer of core shroud by TGSCC and propagated along the grain boundaries with secondary cracks. Especially, the cracks near the H4 welding portion of core shroud had a tendency to branch complicatedly inside material (Fig. 2.5-3). Based on the examination results concerning presence of tensile residual stress by welding and relatively high dissolved oxygen contents in core coolant and so on, it is assumed that the cracks in the both samples were mainly initiated in the hardening layer by TGSCC and propagated inside by IGSCC [5-11].

References

(1) N. Watanabe and M. Hirano, "World Wide Web for Database of Japanese Translation on International Nuclear Event Scale Reports," J. At. Energy Soc. Japan, Vol.41, No.6, pp.628-638 (1999), [in Japanese].

(2) N. Watanabe, *Review of Incident Involving Reactor Pressure Vessel Head Degradation at U. S. PWR*, JAER-Review 2004-015 (2004), [in Japanese].

(3) N. Watanabe, "Quantitative Risk Trends Deriving from PSA-based Event Analysis – Analysis of Results from U. S. URC's Accident Sequence Precursor Program," Trans. At. Energy Soc. Japan, Vol.3, No.4, pp.396-406 (2004), [in Japanese].

(4) A. Hidaka and M. Suzuki eds., *Proceedings of the Workshop on Reactor Safety research –Focusing on the Integrity of Aged Components- March 17, 2003, Tokai Research Establishment, Tokai-mura*, JAERI-Conf 2003-014, (2003).

(5) The Working Team for Examination of the Samples from Core Shrouds and Primary Loop Recirculation Piping, *Report of Examination of the Sample from Core Shrouds (K3-H7a) at Kashiwazaki-Kariwa Nuclear Power Station Unit-3 (Contract Research)*, JAERI-Tech 2004-002, (2004) , [in Japanese].

(6) The Working Team for Examination Operation of Samples from Primary Loop Recirculation Piping at Onagawa Unit-1, *Report of Examination of the Samples from Primary Loop Recirculation Piping (O1-PLR) at Onagawa Nuclear Power Station Unit-1 (Contract Research)*, JAERI-Tech 2004-003, (2004) , [in Japanese].

(7) The Working Team for Examination of the Sample from Core Shroud and Primary Loop Recirculation Piping, *Report of Examination of the Sample from Core Shroud (1F4-H4) at Fukushima Dai-ichi Nuclear Power Station Unit-4 (Contract Research)*, JAERI-Tech

2004-004, (2004), [in Japanese].

(8) The Working Team for Examination of Samples from Core Shrouds and Primary Loop Recirculation Piping, *Report of Examination of the Sample from Core Shrouds (K1-H4) at the Kashiwazaki-Kariwa Nuclear Power Station Unit-1 (Contract Research)*, JAERI-Tech 2004-011, (2004), [in Japanese].

(9) The Working Team for Examination of Samples from Core Shrouds and Primary Loop Recirculation Piping, *Report of Examination of the Sample from Core Shrouds (O1-H2) at Onagawa Nuclear Power Station Unit-1 (Contract Research)*, JAERI-Tech 2004-012, (2004), [in Japanese].

(10) The Working Team for Examination of the Sample from Core Shroud and Primary Loop Recirculation Piping, *Report of Examination of the Sample from Core Shrouds (2F2-H3) at Fukushima Dai-ni Nuclear Power Station Unit-2 (Contract Research)*, JAERI-Tech 2004-015, (2004), [in Japanese].

(11) The Working Team for Examination Operation of Samples from Core Shroud at Fukushima Dai-ni Unit-3, *Report of Examination of the Samples from Core Shroud (2F3-H6a) at Fukushima Dai-ni Nuclear Power Station Unit-3 (Contract Research)*, JAERI-Tech 2004-044, (2004), [in Japanese].

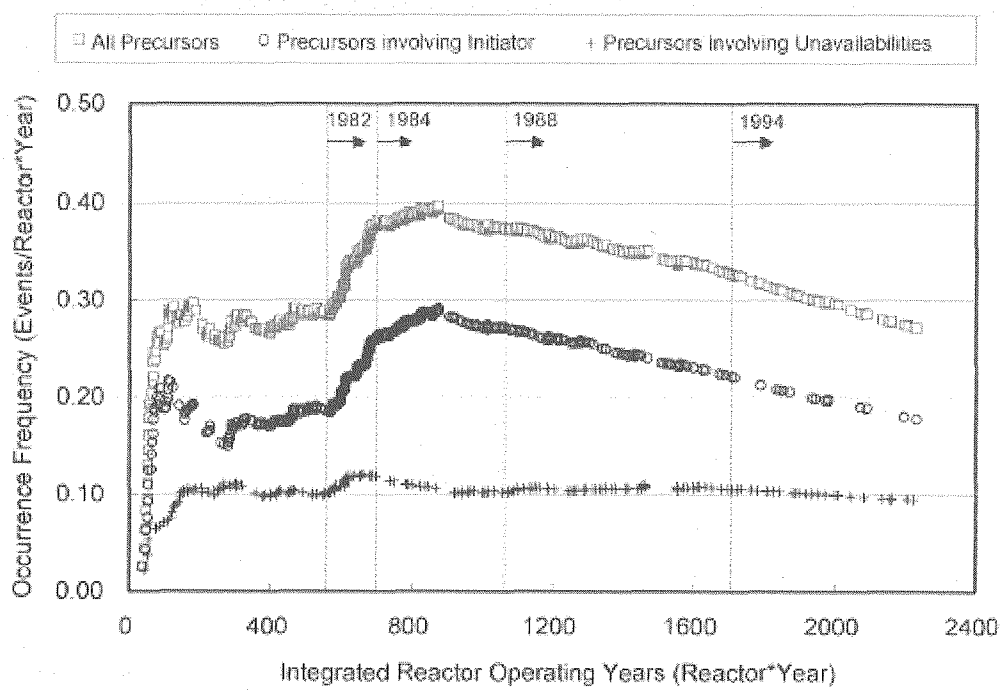

Fig.2.5-1 Occurrence frequency of precursors

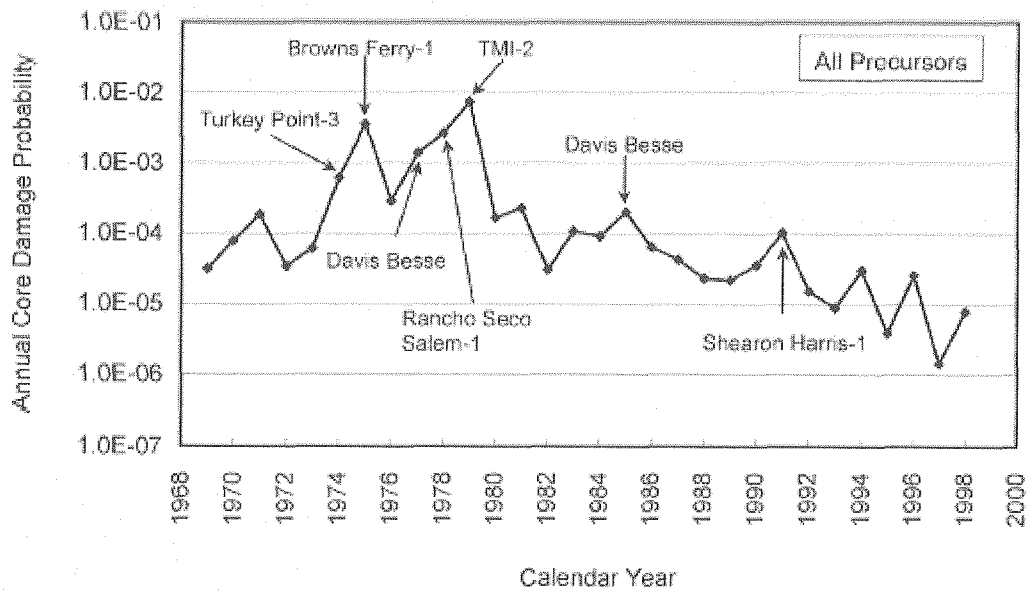

Fig. 2.5-2 Annual core damage probabilities for precursors

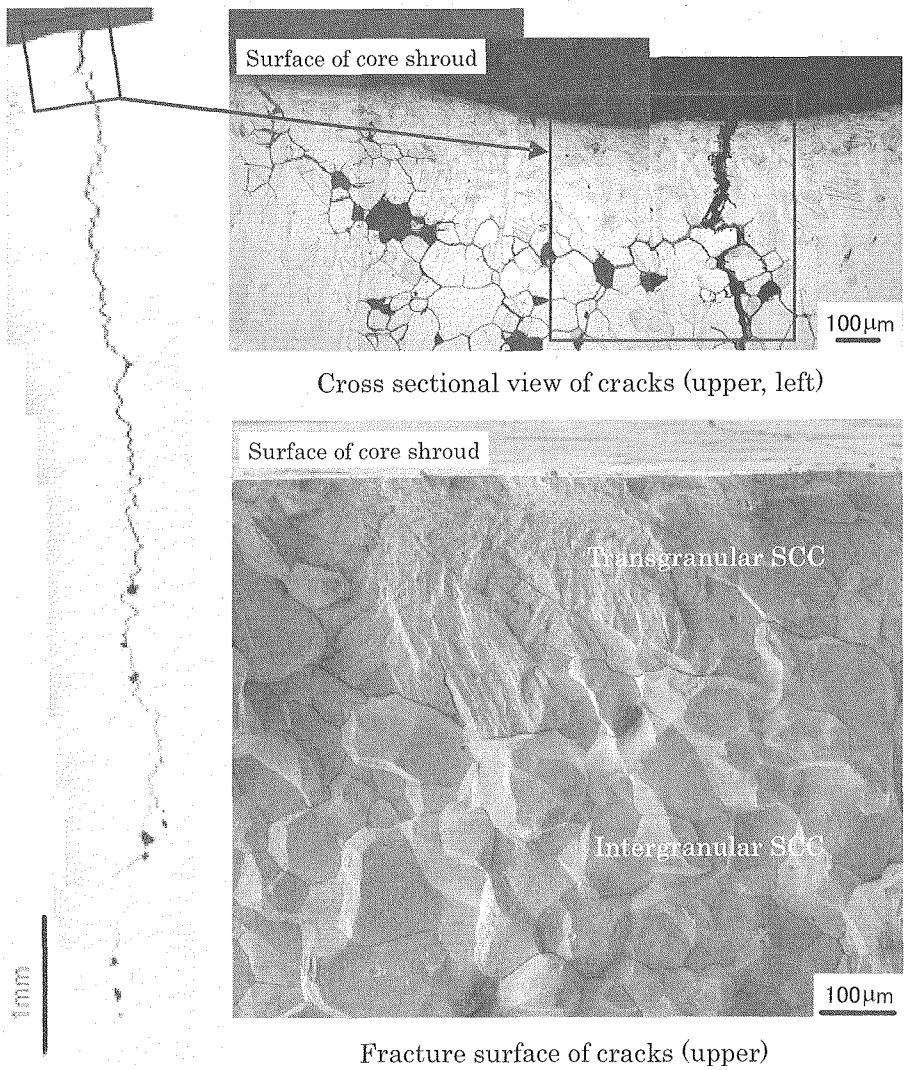

Fig. 2.5-3 Cross sectional microstructure (left and upper) and fracture morphology (lower) of cracks near the welding portion of lower ring of core shroud

3. NUCLEAR FUEL CYCLE SAFETY RESEARCH

In Japan, the construction and operation of commercial nuclear fuel cycle facilities are in progress at the Rokkasho site of the Japan Nuclear Fuel, Ltd. (JNFL), In this site, the Rokkasho reprocessing plant is under commissioning operation. The MOX fuel fabrication plant and recycle fuel interim storage facility are also planned to be constructed. In research and development field, advanced fuel cycle technologies are being pursued in national and civil research institutes.

Given the above situation of the nuclear industry, safety researches on nuclear fuel cycle facilities in JAERI are mainly for reprocessing plant, MOX fuel fabrication plant, recycle fuel interim storage facility and various types of transport casks, focusing on criticality safety, criticality accident evaluation, confinement evaluation at fire and explosion accident, confinement evaluation of reprocessing process, and hypothetic accident analysis of casks. Application of PSA to nuclear fuel cycle facilities is also performed for providing technical bases for introducing the risk informed regulation in Japan.

The following studies are performed.

1) Criticality safety study of reprocessing plant: Acquisition of criticality experiment data and evaluation of temperature coefficients of reactivity for heterogeneous units consisting of fuel rods and fuel solution for application to spent fuel dissolver, which is a typical process equipment of a reprocessing facility.
2) Criticality safety evaluation taking account of fuel burnup: Evaluation of the effect of neutron induced reactions of Nd-147 and Nd-148. Development of a new integrated burnup code system.
3) Criticality safety study on MOX fuel fabrication plant: Evaluation of criticality safety and criticality accident of mixing process.
4) Criticality accident evaluation of reprocessing plant: Study on characteristics of criticality accident through transient criticality experiments assuming criticality accident in reprocessing process equipment containing fuel solution. Measurement and evaluation of radiation doses in these experiments have also been conducted.
5) Safety analysis for transport casks during hypothetical accidents: Analysis of hypothetical accident scenarios of fresh PWR fuel assemblies such as falling out and fire accidents.
6) Safety study on reprocessing process: Safety evaluation study on process confinement by better understanding of the nuclide behavior and development of simulation code for the behavior of nuclides under advanced reprocessing technology for high burnup fuel and MOX fuel.
7) Development of materials for reprocessing equipment: Development of highly corrosion

resistant materials and corrosion monitoring systems for reprocessing equipment.

8) Application study of PSA for nuclear fuel cycle facilities: PSA application study on MOX fuel fabrication facility.

The details and research output of these studies are described in following chapters.

3.1 Research on Criticality Safety of Nuclear Fuel Cycle Facilities

In nuclear fuel cycle facilities such as a reprocessing plant and a MOX fuel fabrication facility where a large amount of fuel material is handled, criticality safety designs of equipment besides stringent management or monitoring of nuclear fuel material are conducted so as not to lead to a criticality accident even in case of unlikely events. Research on design of equipment, management and monitoring of nuclear fuels for prevention of criticality is referred to as criticality safety research. At JAERI, static criticality experiments are performed to measure criticality data, and research on evaluation methods for criticality safety analyses as well as criticality monitoring methods are done as activities of criticality safety research. Furthermore, transient criticality experiments are performed to obtain better understanding on transient characteristics of a criticality accident.

3.1.1 Experimental Study and Analytical Evaluation of Criticality Safety for Reprocessing Facility *1

Temperature effect is a main factor which affects the transient characteristics of a criticality accident. However, no available critical experiment for the temperature effect had been reported before the STACY experiments. A heterogeneous core composed of LWR-type fuel rod array and low-enriched uranyl-nitrate-solution was constituted simulating the dissolver of the reprocessing facility for LWR spent fuel, and critical masses at room temperature were measured by changing uranium concentrations of the solution as the parameter.(1) Moreover, a series of reactivity effects due to changes in fuel temperatures were measured for two kinds of the STACY heterogeneous lattice configurations. The critical solution depths at various solution temperatures were measured, and reactivity effects of temperature changes were evaluated.(2)

The stainless steel core tank with 59 cm inner diameter was blanketed with a thermal insulator as shown in Fig. 3.1-1. The core was constituted in the core tank by arranging the assembly of 5 wt% enriched UO_2 fuel rods in the 6 wt% enriched uranyl nitrate solution. The fuel rods were supported with attachable grid plates held to the grid-plate support, and the support was fixed to the inner-side-wall of the core tank. The grid plate was made of zircaloy-4. The core consisted of two radial regions as follows: the assembly of the UO_2 fuel rods with square lattice filled with the uranyl nitrate solution was arranged in the center of the core tank, and the uranyl-nitrate-solution region surrounded the assembly. The fuel rod had the same dimension as that of PWR while the pellet stuck length was 142 cm. The outer diameter of the clad made of zircaloy-4 and the diameter of the UO_2 pellet were 0.95 cm and 0.82 cm, respectively. Experiments were performed for two types of fuel rod

*1 This work was entrusted from the Ministry of Education, Culture, Sports Science and Technology of Japan.

arrays with different lattice pitches. The two experiment conditions were as follows:

Case name	"2.1cm-pitch"	"1.5cm-pitch"
Lattice pitch (cm)	2.1	1.5
Solution-to-pellet cell volume ratio	7.0	2.9
Number of fuel rods	221	333
Effective diameter of array (cm)	35.2	30.9

The case "2.1cm-pitch" was under over-moderated condition, while the case "1.5cm-pitch" was close to optimum-moderated condition.

Figure 3.1-2 shows variation of critical solution heights with the uranium concentration at room temperature. The critical solution heights of 43 ~ 66 cm were measured for the uranium concentrations of 380 ~ 50 g/L with the accuracy of the solution height of 0.2 mm. Temperature effects were measured at the same uranium concentration of 150 g/L. The solution was heated in stages. Figure 3.1-3 shows critical solution height with solution temperature. From the change of the critical water height with fuel temperature, the reactivity effect was evaluated by a critical-solution-level worth method. The temperature effect was also calculated by using a two-dimensional transport code TWODANT, and a 16 energy-group cross section set collapsed from the SRAC public library based on the JENDL-3.2 cross section library.

Prior to a series of calculations for experiment analyses, the temperature effect on the reactivity for each lattice pitch was examined using perturbation theory. Figure 3.1-4 compares reactivity components for both the cases when the fuel solution was heated from the room temperature to 39.5 °C. The temperature effect of the case "1.5 cm-pitch" is larger than that of the "2.1 cm-pitch", which mainly depends on the fact that the positive reactivity-change of the neutron-absorption-effect at the heterogeneous region of the former case is less than that of the latter case.

Figure 3.1-5 shows the temperature effect for both the experiment and the calculation. The experimental value with 4% uncertainty was estimated to be - 2.0 ¢/°C for the case "2.1cm-pitch", and - 2.5 ¢/°C for the case "1.5cm-pitch". The calculated results gave agreement with the experiments within 10%.

3.1.2 Criticality Safety Evaluation Study Taking Account of Burnup in Nuclear Fuels

(1) Effect of neutron induced reactions of Neodymium-147 and 148 into burnup evaluation

Burnup is an important parameter in criticality safety evaluations of spent nuclear fuel in which burnup credit is taken into account. The Neodymium-148 method, which uses ^{148}Nd as an indicator of burnup, is a widely used method to evaluate the burnup of post irradiation examination (PIE) samples, and it is well known for its good accuracy. However, accuracy of the evaluated burnup values may be affected by the neutron capture reaction of

^{147}Nd and ^{148}Nd.

From this viewpoint, the contribution of neutron capture reactions of ^{147}Nd and ^{148}Nd to the amount of ^{148}Nd was discussed [3]. The change in the amount of ^{148}Nd due to both reactions is less than 0.7% under normal reactor operation conditions. In particular, it is in the 0.1% range if burnup is approximately 30 GWd/t for a BWR and 40 GWd/t for a PWR. Figure 3.1-6 [3] shows the deviation of ^{148}Nd amount against burnup value for the case of PWR.

(2) Development of new integrated burnup code system – SWAT2 *2

Estimation of isotopic composition of spent nuclear fuel is crucial for taking burnup credit into account for criticality safety evaluation. The Japan Atomic Energy Research Institute (JAERI) has developed the burnup code system SWAT [4] for burnup credit applications and associated regulations. For future burnup credit analysis, burnup calculation for whole fuel assembly would be essential to evaluate k_{eff} difference by burnup and isotope distribution within the fuel assembly. SWAT2, the improved version of SWAT, has been developed to incorporate MVP [6], a continuous energy Monte Carlo Code, into SWAT. Figure 3.1-7[4] shows it's calculation flow [5]. This development enables us to treat complicated geometry using neutron flux evaluated by MVP, effective one group cross section data and detailed burnup chain model in ORIGEN2 [7]. Since output of ORIGEN2 can contain not only the amount of isotopes but also activities and decay heat information, SWAT2 has a possibility to evaluate such parameters using a function of a continuous energy Monte Carlo code. This fact may have another importance for safety evaluation purpose. Figure 3.1-8 shows the results of analysis of PIE data. This summarized that SWAT2 can also predict isotopic composition of uranium and plutonium except for ^{238}Pu in spent nuclear fuel within 5%, as shown in the analysis of the data by the revised SWAT.

3.1.3 Criticality Safety Study for MOX Fuel Fabrication Process

The total number of fission released at criticality accident is the most important quantity that should be estimated, because it is the measure of accident scale and exposure dose. From the view of criticality safety, the most distinctive character of MOX fuel fabrication process in fuel processing is the homogenizing process of Oxide Uranium and Plutonium powders. Plutonium's fission is smaller in the delayed neutron fraction than Uranium's, as well as the margin for prompt criticality. The additive used as a lubricant contains hydrogen and acts as a moderator. The behavior of particles of MOX powder or additives at criticality accident is not known well, because there is no experimental result.

---

*2 This work was entrusted from the Ministry of Education, Culture, Sports Science and Technology of Japan.

It has been studied that the numerical modeling of transient phenomena during powder mixing process for the safety evaluation of such powder processing.

(1) Development of a criticality evaluation method considering nuclear fuel powder flowability *3

In conventional criticality evaluations of nuclear fuel powder systems, the particle motion has not been taken into consideration [8]. Therefore, the effects of the particle behavior on nuclear criticality safety are not discussed enough so far. We have developed a novel criticality evaluation methodology by coupling a particle dynamics simulation code with a continuous-energy Monte Carlo transport code. This methodology makes possible to study the relation between the particle motion and nuclear criticality. This criticality evaluation method was applied to the powder system of a MOX fuel fabrication process [9].

Figure 3.1-9 shows the particle dynamics simulation model. In the initial condition, the additive powder was located at the bottom side and MOX powder was settled on the bed of the additive powder. The screw was rotated at 30 rpm. The particle spatial distributions based on the particle dynamics simulation was reflected into the criticality calculation. When the particle distributions were set in the criticality evaluation, the domain was divided as many cells as possible, as shown in Fig. 3.1-10. The particles belonging in each cell were converted into the atomic number densities. The cells were modeled to be homogeneous medias [10].

The simulation result is shown in Fig. 3.1-11. The effective multiplication factor decreased due to the powder free surface deformation induced by the solids mixing. This is because neutron was released more by the surface area expansion due to the deformation. On the other hand, the multiplication factor increases as the MOX powder and the additive powder is mixed, since the additive including lightweight atoms like H and C works as a moderator. As shown in Fig. 3.1-12, when the mixture state is regarded to be homogeneous, there is a linear correlation between the multiplication factor and superficial area in this system.

(2) Effect of mixing state of MOX powder on criticality in homogenization process

In a homogenization process of MOX fuel fabrication, nuclear fuel powder (UO_2 powder and MOX powder) and additive are mixed to make a homogeneous mixture. Since non-uniform mixing condition exists during the mixing process, it is important to identify the most critical mixing state to assure the criticality safety of the process regardless of the mixing state. For mixtures consisting of MOX powder and zinc-stearate (*i.e.*, excluding UO_2 powder), a method to obtain the most critical mixing state was developed [11] based on the

*3 This work was entrusted from the Ministry of Economy, Trade and Industry of Japan.

methodology for obtaining an optimum fuel concentration distribution in fuel solutions or slurries [12]. Figure 3.1-13 shows an example of an optimum distribution of MOX powder volume fraction in a bare sphere of a mixture with the diameter of 72 cm. The initial volume fraction of the MOX powder is uniformly 80%, and the k_{eff} of uniformly distributed mixture is 0.545, and the k_{eff} finally attained is 0.590. In the final distribution, a pure MOX powder without additive surrounds a central region where the atom ratio of hydrogen to heavy metal (*i.e.*, H/(Pu+U)) is ~120, corresponding to an optimal moderation. This study shows that the most critical mixing state may be achieved by forming an optimum moderation region within a mixture.

(3) Development of numerical evaluation codes for criticality accident of MOX powder system *4

Three different types of numerical code, AGNES-P, DOCTRINE and FEDEX-P have been developed [13] for the analysis of the criticality accident of nuclear fuel powder system. It is shown that the calculation result of those developed codes shows good agreement to the other codes such as SKINATH-WP and POWDER as shown in Figs. 3.1-14 and -15.

The developed codes take into account the effect of the phase change of the additive to the homogenizing process of MOX and UO_2 powders. One of typical lubricant powder, Zinc Stearate, is solid at room temperature, melts at about 120 °C, which is higher than the boiling point of water, and dissociates into gas at about 400 °C. Such character could give quite different results from those for water-moderated system.

Figures 3.1-16 and -17 show a preliminary result for a postulated criticality accident at the mixture of MOX and Zinc Stearate powders using AGNES-P and FEDEX-P codes. Much detailed calculations with extended parameters will be performed to investigate the characteristics of the criticality accident at powder system, as well as code evaluation by comparison of the calculated results using each code.

3.1.4 Study on Transient Characteristics of Criticality Accident

Most of criticality accidents in the world occurred with solution fuel such as Uranyl nitrate solution, therefore it has been mainly focused to understand its characteristic. Based on the observed characteristic and measured properties such as power, released energy, temperature and pressure, a numerical code to simulate criticality accident has been developed and evaluated.

(1) Transient characteristics observed in TRACY supercritical experiments [14]

Through a series of TRACY experiments since its first criticality in 1995, a set of time-series data of power, temperature and pressure has been measured and collected

*4 This work was entrusted from the Ministry of Economy, Trade and Industry of Japan.

systematically. Each experiment has been performed with one of its three operational modes to insert reactivity; PW mode, in which the transient rod for neutron absorption, Tr-rod, is withdrawn instantaneously, RW mode, in which Tr-rod is withdrawn slowly and RF mode, in which solution fuel is pumped into the core tank.

From the analysis of such data collection, the characteristic of criticality accident in solution fuel has come out. One of the most basic characters is the relation between the power and the excess reactivity, which is shown in Fig. 3.1-18. As shown in Fig. 3.1-19, the peak power increases with the increase of excess reactivity for PW mode, however, no marked change in peak power can be seen for RF mode. Figure 3.1-20 shows clearly that the peak power increases with the increase of the average insertion rate of reactivity. The dependency of the total released fission on excess reactivity for PW mode is shown in Fig. 3.1-21.

These data are important to understand the characteristic of the criticality accident and it provides the information useful to develop or evaluate the numerical code to evaluate the criticality accident.

(2) Development of criticality accident evaluation code, AGNES [15]

The AGNES2 code has been developed for the evaluation of the criticality accident of solution system and is expected to be useful for the designing of a fuel reprocessing plant, the quick evaluation of the effect of a countermeasure against the accident and the study of the nature of the criticality accident of solution system.

It was observed in the JCO accident that the high power was sustained by the heat loss from solution by the cooling system. That implies the continuous removing of heat energy from the fuel gives rise to large amount of radiation, which is important parameter for the planning of the counter action. Therefore cooling is important problem.

In its recent development work, a new model of cooling has been implemented, in which the heat energy is removed from the container region by the structural materials connected directly to the container and by the natural convection of air.

A virtual structural material is considered to take into account the heat loss by many structural materials. The cooling through this virtual region is modeled as the Newton's law of cooling;

$$q = kA\frac{t_1 - t_0}{x},$$

where q is conduction heat transfer rate, k is the thermal conductivity, A is the area of heat exchange, t_1 is the temperature of the container, t_0 is the temperature of the atmosphere and x is the distance between the container and the atmosphere.

The heat exchange between the container and coolant regions is calculated using the model of the natural convection of air near vertical plane.

One of TRACY experiments is dedicated to show such cooling effect, in which 1.5 $ of excess reactivity was inserted by feeding solution with the rate of 0.15 $/sec and the free excursion is observed for 5 hours after the reactivity insertion. A deep bottom in the power profile at about 2000 seconds and the following oscillation are observed. In this time scale, the heat loss from the fuel solution is dominant for the change of the power. For such experiment, the simulated value using AGNES2's new cooling model shows good agreement with experiment until 4000 second as shown in Fig. 3.1-22.

(3) International comparison of criticality accident evaluation methods [16]

In order to evaluate the numerical code for criticality accident evaluation, an activity of the international comparison of criticality accident evaluation methods began at the expert group on criticality excursion analysis, EGCEA, a group of criticality safety WP of OECD/NEA/NSC. At this activity, some data from the TRACY experiments have been provided as benchmark problems for transient phenomena. This activity is expected to give great benefit for the developmental work of participants.

The basic condition of the TRACY Benchmark Problem I and II is as follows; The fuel solution is uranyl nitrate solution, and its ^{235}U enrichment is 9.98 wt%. The concentration of the total uranium is in the range between 375 g/L and 422 g/L and the acidity of the solution is in the range between 0.58 mol/L and 0.77 mol/L. The core tank is a cylinder made from SUS304, of which inner diameter is 50 cm and its wall thickness is 1 cm.

The benchmark I, TBMI, consists of 5 cases for which reactivity is inserted by pulse withdrawal of the transient rod, and up to 3 $ of excess reactivity is inserted. The benchmark II includes 3 cases for which reactivity inserted by feeding fuel solution from the bottom of the core tank. The maximum power, total fission yields and etc. are the items to be evaluated for comparison.

Figure 3.1-23 shows one of the results calculated using AGNES2. The calculation reproduced the experimental power profile well. For the preliminary analysis of the both benchmarks using AGNES2 code, the difference between the experiment and the calculation in the total released energy is less than 16%.

3.1.5 Study on Criticality Accident Dosimetry

It is necessary for medical treatment to evaluate external doses of heavily exposed patients in criticality accidents. To investigate characteristics of doses in criticality accidents, dose measurement experiments have been performed at TRACY. Experimental items in TRACY are as follows: Measurement of neutron energy spectra by a multi-foil activation method and a recoil proton proportional counter method, measurement of neutron and γ-ray doses by an alanine dosimeter and a thermoluminescence dosimeter (TLD) made of lithium tetra borate ($Li_2B_4O_7$).

(1) Measurement of neutron leakage spectra from the TRACY core*5

A neutron energy spectrum is one of fundamental characteristics to be evaluated for neutron dosimetry since neutron doses depend on the spectrum. The neutron leakage spectra from the TRACY core were measured by two methods: a multi-foil activation method and a recoil proton proportional counter method [17]. For the multi-foil activation method, TRACY was operated in both a transient mode and a static mode. Activation foils (*e.g.*, Au, Cu, In and Ti) were placed on the surface of the TRACY core tank. The neutron energy spectra were estimated by an unfolding code NEUPAC-JLOG using an initial guess spectrum calculated by the MCNP code. The estimated neutron energy spectrum in the transient mode is shown in Fig. 3.1-24. Although the result of the NEUPAC-JLOG code was about 3% higher than that of the MCNP code in thermal energy range, their spectra agreed well in shape each other.

In the recoil proton proportional counter method, a spectrometer consisting of four spherical recoil proton proportional counters, as shown in Fig. 3.1-25, was used. The spectrometer was placed at 2 m away from the surface of the TRACY core tank and TRACY was operated in a static mode. A neutron spectrum was obtained through the unfolding code SPEC-4. The result measured by the recoil proton proportional counter method and that calculated by the MCNP code show good agreement to each other as illustrated in Fig. 3.1-26.

By these two methods for neutron dosimetry, the neutron spectra on the surface of and 2 m away from the surface of the core tank were evaluated. These spectra are useful for study on criticality accident dosimetry at TRACY.

(2) Measurement of neutron dose using a $Li_2B_4O_7$ TLD *5

To investigate neutron dose in criticality accidents, neutron dosimetry experiments were carried out at TRACY [18]. A TLD made of $^{6}Li_2{}^{10}B_4O_7$ and $^{7}Li_2{}^{11}B_4O_7$ was used to separate doses of neutrons and γ-rays. Each TLD has four radiation-detecting elements. Two of them are $^{6}Li_2{}^{10}B_4O_7$ sensitive to both neutron and γ-rays while the others are $^{7}Li_2{}^{11}B_4O_7$ sensitive to γ-rays only. Neutron dose can be obtained by subtracting an average dose of $^{7}Li_2{}^{11}B_4O_7$ from that of $^{6}Li_2{}^{10}B_4O_7$. This TLD is surrounded by a cubic polyethylene moderator block to correct the response in sensitivity of TLD to neutrons. In the experiments, the TLD with the moderator block was placed at 4 m away from the surface of the TRACY core tank. Measured dose in ambient dose equivalent were converted to neutron kerma for water [19] by using a calculated conversion factor. The results of the

*5 This work was entrusted from the Ministry of Education, Culture, Sports Science and Technology of Japan.

measurements and the MCNP calculations are listed in Table 3.1-1. It is found from these measurements that the neutron dose at TRACY normalized with the integrated power in each TRACY operation are almost constant regardless of the operation condition and the integrated power.

(3) Component analysis of γ-rays under criticality accident conditions

Our recent study ascertained that component analysis of γ-rays was necessary for accurate criticality accident dosimetry taking account of γ-ray emission behavior in criticality accidents [20]. The γ-rays are classified into the following four components from the viewpoint of dosimetry: (a) prompt component from fission and neutron-capture reactions during criticality, (b) delayed component from decay of fission products (FPs) during criticality, (c) pseudo component that is a neutron dose registered erroneously in γ-ray dosimeters by neutron-capture reactions, and (d) residual component from FPs and neutron-activated materials after the termination of criticality, as illustrated in Fig. 3.1-27. A component analysis of the γ-rays was tried by dosimetry experiments using a $^{7}Li_{2}{}^{11}B_{4}O_{7}$ TLD and by computational simulations. This analysis quantitatively clarified the dose proportions of these components and also confirmed that these proportions varied with the distance from the TRACY core tank [21].

(4) Experimental estimation of dose distributions in human body under Criticality Accident Conditions

For estimation of dose distributions in a human body under criticality accident conditions, a human dosimetry experiment was carried out using a phantom and two kinds of tissue-equivalent dosimeters. Neutron and γ-ray absorbed doses in muscle tissue were separately measured by combined use of an alanine dosimeter and a $^{7}Li_{2}{}^{11}B_{4}O_{7}$ TLD. This experiment confirmed that the dose distribution of neutrons in the phantom was different from that of γ-rays, as shown in Fig. 3.1-28. This was attributed to the difference between neutrons and γ-rays in their interactions with the phantom, neutron-induced secondary γ-rays in the phantom, and the pseudo γ-ray absorbed dose caused by neutron-capture reactions of impurities (^{6}Li and ^{10}B) remaining in the $^{7}Li_{2}{}^{11}B_{4}O_{7}$ TLD [22].

References

(1) S. Watanabe, T. Yamamoto, H. Hirose, K. Izawa and Y. Miyoshi, "Critical Experiments and Their Benchmark Evaluations on STACY Heterogeneous Core," *Proc. Int. Symposium NUCEF 2005*, Tokai-mura, Japan, Feb. 9-10, 2005, JAERI-Conf 2005-007, p.287 (2005).

(2) S. Watanabe, T. Yamamoto and Y. Miyoshi, "Measurement of Temperature Effect on Low Enrichment STACY Heterogeneous Core", *American Nuclear Society Transactions*, 91, 431 (2004).

(3) K. Suyama and H. Mochizuki, "Effect of Neutron Induced Reactions of Neodymium-147 and 148 on Burnup Evaluation," *J. Nucl. Sci. Technol.*, 42, 661 (2005).

(4) K. Suyama, H. Mochizuki and T. Kiyosumi, "Revised Burnup Code System SWAT: Description and Validation Using Postirradiation Examination Data," *Nucl. Technol.*, 138, 97 (2002).

(5) K. Suyama, H. Mochizuki, H. Okuno and Y. Miyoshi, "Validation of Integrated Burnup Code System SWAT2 by the Analyses of Isotopic Composition of Spent Nuclear Fuel," *Proc. of PHYSOR-2004*, Chicago, USA, April 25-29, 2004, CD-ROM (2004).

(6) Y. Nagaya, K. Okumura, T. Mori and M. Nakagawa, "MVP/GMVP II : General Purpose Monte Carlo Codes for Neutron and Photon Transport Calculations based on Continuous Energy and Multigroup Methods," *JAERI 1348*, Japan Atomic Energy Research Institute (2005).

(7) A. G. Croff, "ORIGEN2 - A Revised and Updated Version of the Oak Ridge Isotope Generation and Depletion Code," *ORNL-5621*, Oak Ridge National Laboratory (1980).

(8) Y. Miyoshi, T. Yamamoto and K. Nakajima, "Simplified Estimation of Criticality Accident of MOX Powder Fuel," *JAERI Research 2002-002*, Japan Atomic Energy Research Institute (2003) [in Japanese].

(9) M. Sakai, T. Yamamoto, M. Murazaki and Y. Miyoshi, "Development of a Criticality Evaluation Method Considering the Particulate Behavior of Nuclear Fuel," *Nucl. Technol.*, 149, 141 (2005).

(10) S. Takahashi, H. Okuno and Y. Miyoshi, "Effect of a Particle Diameter on the Criticality of a MOX powder System," *JAERI-Tech 2005-056*, Japan Atomic Energy Research Institute (2005) [in Japanese].

(11) T. Yamamoto and Y. Miyoshi, "Effect of mixing condition of MOX powder and additive on criticality safety," American Nuclear Society 2004 Winter Meeting and Nuclear Technology Expo, (November 2004), *American Nuclear Society Transactions*, 91, 583 (2004).

(12) H.Okuno and T.Sakai, "Nonuniformity effect on reactivity of fuel in slurry," *Nucl. Technol.*, 122, 265 (1998).

(13) Y. Yamane, T. Yamamoto and Y. Miyoshi, "Development of numerical simulation codes for estimation of number of fission released at criticality accident of MOX powder system," *Proceedings of International Conference on Supercomputing in Nuclear Applications (SNA' 2003)* CD-ROM (2003).

(14) Y. Yamane, K. Nakajima, K. Ogawa, E. Aizawa, H. Yanagisawa and Y. Miyoshi, "Transient Characteristics Observed in TRACY Supercritical Experiments," *Proc. 7th Int. Conf. Nuclear Criticality Safety (ICNC 2003)*, Tokai-mura, Japan, Oct. 20-24, 2003, JAERI-Conf 2003-019, part II, p.791 (2003).

(15) Y. Yamane, K. Nakajima, T. Yamamoto, and Y. Miyoshi, "Development of Criticality Accident Analysis Code AGNES," *Proc. 7th Int. Conf. Nuclear Criticality Safety (ICNC 2003)*, Tokai-mura, Japan, Oct. 20-24, 2003, JAERI-Conf 2003-019, part II, p.740 (2003).

(16) Y. Yamane, T. Yamamoto and Y. Miyoshi, "International Comparison of Criticality Accident Evaluation Methods - Evaluation Plan of Super-critical Benchmark Based on TRACY Experiment-," *Proc. Int. Symposium NUCEF 2005*, Tokai-mura, Japan, Feb. 9-10, 2005, JAERI-Conf 2005-007, p.294 (2005).

(17) T. Nakamura, K. Sakurai and Y. Miyoshi, "Measurement and Evaluation of Leakage Neutron Spectrum at TRACY," *Proc. 7th Int. Conf. Nuclear Criticality Safety (ICNC 2003)*, Tokai-mura, Japan, Oct. 20-24, 2003, JAERI-Conf 2003-019, part II, p.784 (2003).

(18) T. Nakamura, K. Tonoike and Y. Miyoshi, "Dose Evaluation in Criticality Accident Conditions Using Transient Critical Facilities Fueled with a Fissile Solution," *Radiat. Prot. Dosim.*, 110, 483 (2004).

(19) International Commission on Radiation Units and Measurements, "Photon, Electron, Proton and Neutron Interaction Data for Body Tissues," ICRU Report 46, International Commission on Radiation Units and Measurements, (1992).

(20) H. Yanagisawa and H. Sono, J. Katakura, "Re-evaluation of gamma-ray exposure rates during TRACY power burst experiments base on the latest JENDL files," *Proc. 7th Int. Conf. Nuclear Criticality Safety (ICNC 2003)*, Tokai-mura, Japan, Oct. 20-24, 2003, JAERI-Conf 2003-019, part II, p.797 (2003).

(20) H. Sono, H. Yanagisawa, A. Ohno, et al., "Evaluation of gamma-ray dose components in criticality accident situations," *J. Nucl. Sci. Technol.*, 42, 678 (2005).

(22) H. Sono, T. Kojima, N. Soramasu, et al., "Measurement of neutron and gamma-ray absorbed doses inside human body in criticality accident situations using phantom and tissue-equivalent dosimeters," *Proc. Int. Symposium NUCEF 2005*, Tokai-mura, Japan, Feb. 9-10, 2005, JAERI-Conf 2005-007, p.315 (2005).

This is a blank page.

Table 3.1-1 Results of measurements and calculations of neutron dose (at 4 m away from the surface of the TRACY core)

Case ID	Operating condition*	Integrated power (MJ)	Measured neutron kerma (Gy per MJ)	Calculated neutron kerma (Gy per MJ)	Ratio C/E
1	RW	8.4	0.35	0.25	0.73
2	S	10	0.23	0.26	1.15
3	RW	10	0.30	0.25	0.82
4	PW	20	0.27	0.25	0.95
5	PW	14.9	0.29	0.25	0.86
6	S	10.2	0.25	0.27	1.05

* RW: Ramp Withdrawal mode; PW: Pulse Withdrawal mode; S: Static mode

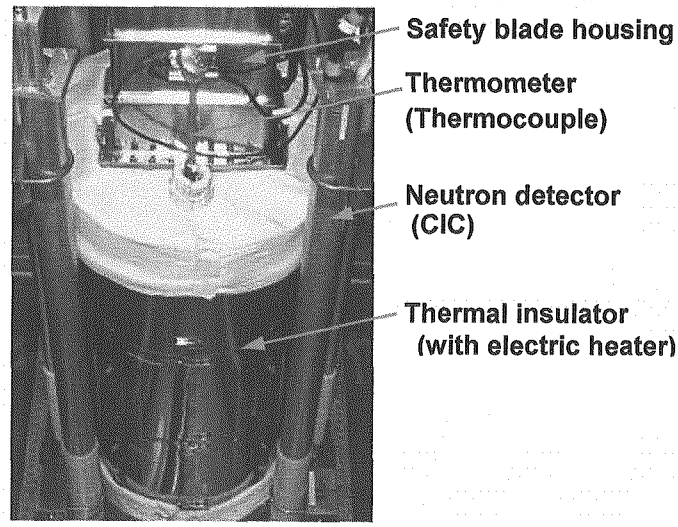

Fig. 3.1-1 STACY core tank with thermal insulator

This is a blank page.

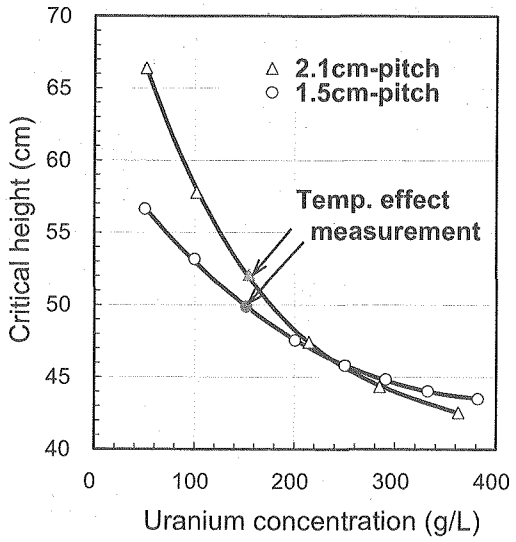

Fig. 3.1-2 Critical height vs. Uranium concentration at room temperature

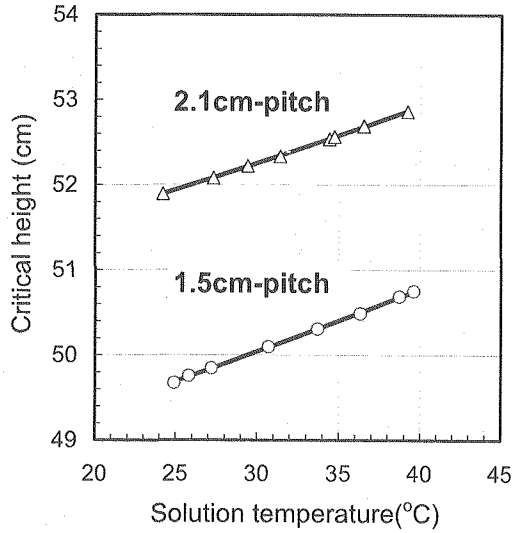

Fig. 3.1-3 Critical height vs. temperature

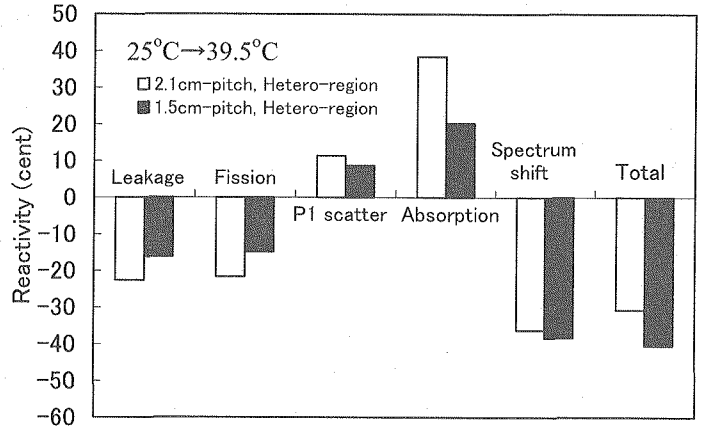

Fig. 3.1-4 Reactivity components of temperature effect

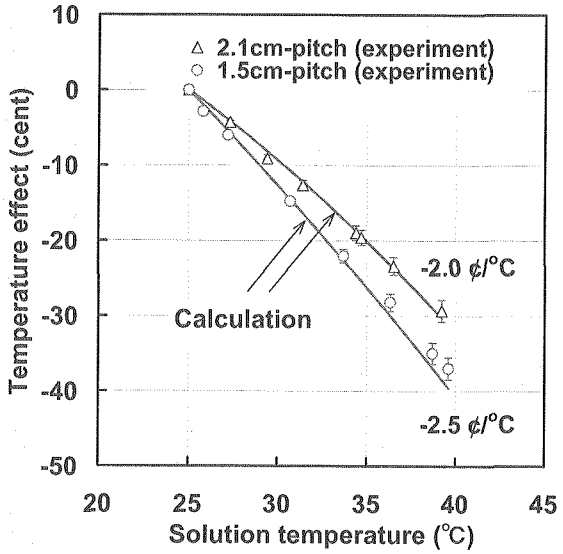

Fig. 3.1-5 Reactivity effect of fuel temperature

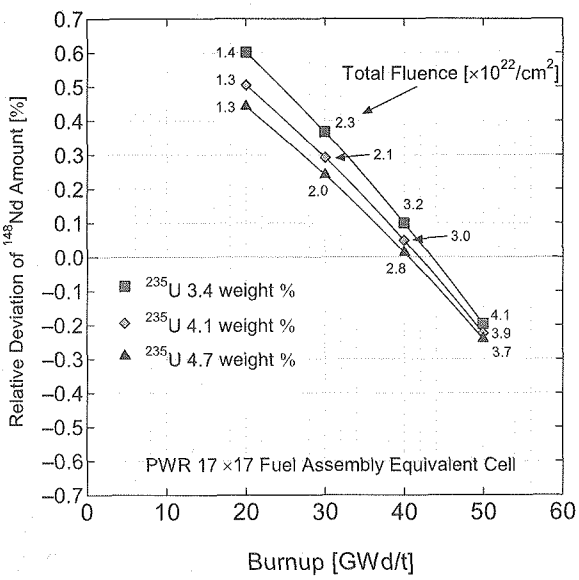

Fig. 3.1-6 Relation between burnup value and Deviation of ^{148}Nd Amount by Neutron Capture Reactions of ^{147}Nd and ^{148}Nd

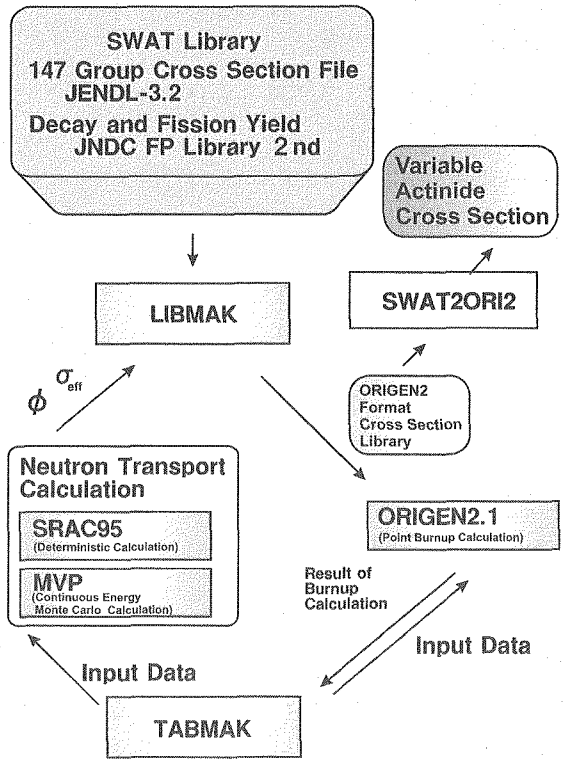

Fig. 3.1-7 Calculation Flow of SWAT2

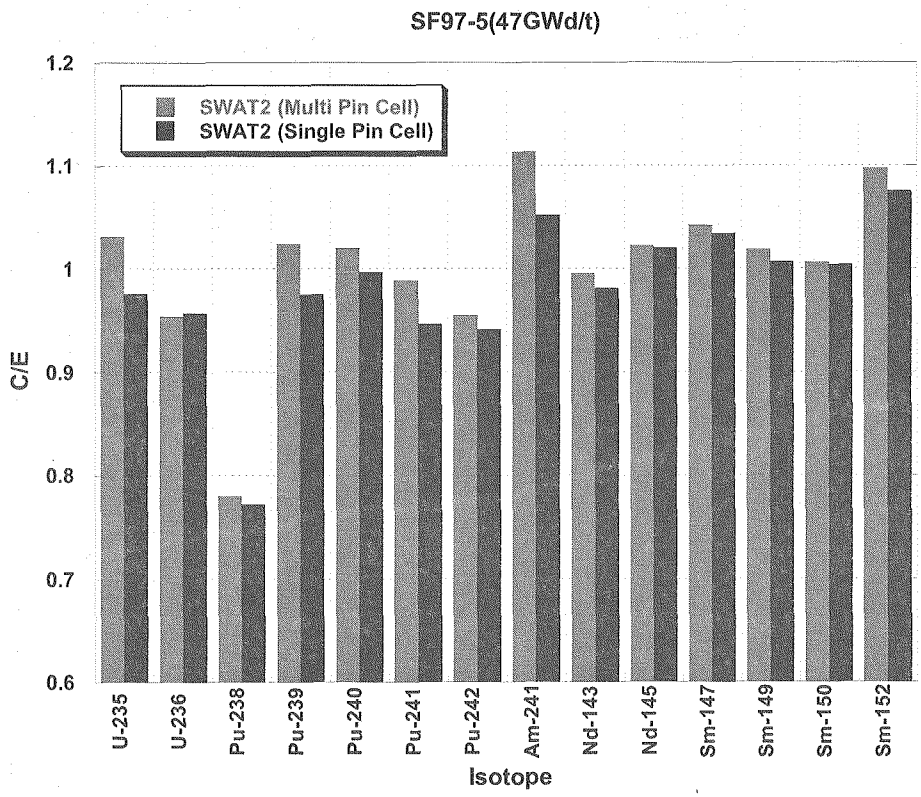

Fig. 3.1-8 Results (C/E values) of PIE Data Analysis by SWAT2

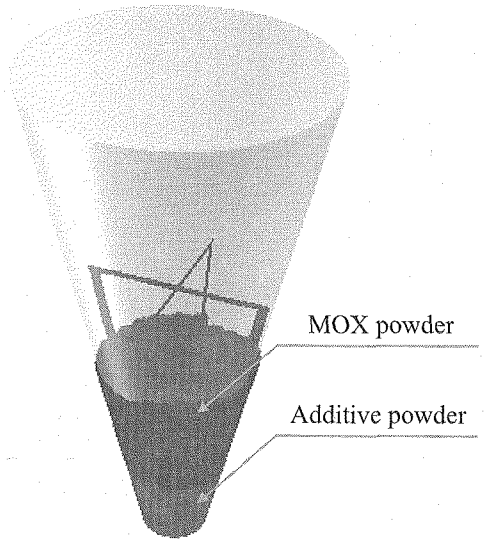

Fig. 3.1-9 Particle dynamics simulation model

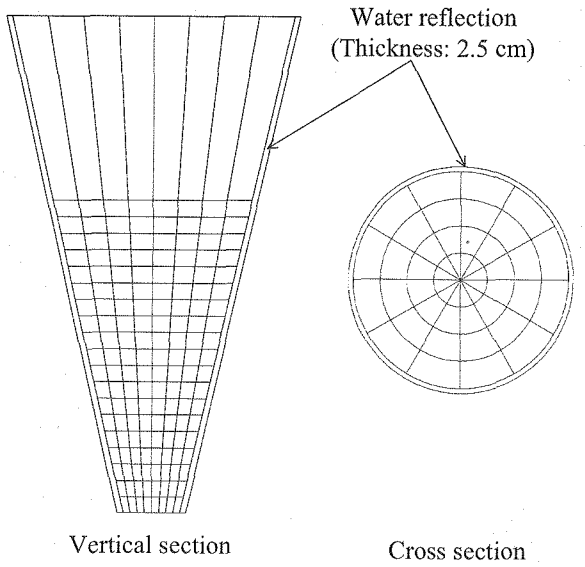

Fig. 3.1-10 Criticality calculation model

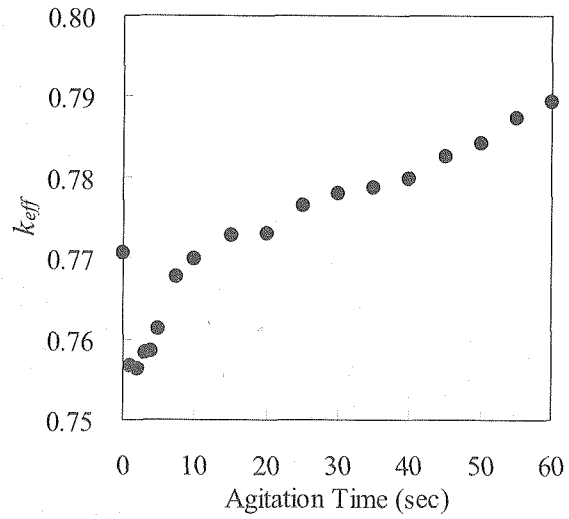

Fig. 3.1-11 Time history of k_{eff} by the solids mixing

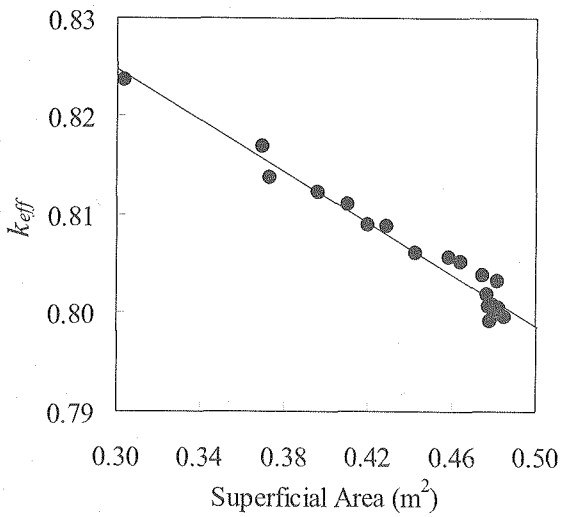

Fig. 3.1-12 Correlation between superficial area and the k_{eff} when the mixture state is regarded to be homogeneous

This is a blank page.

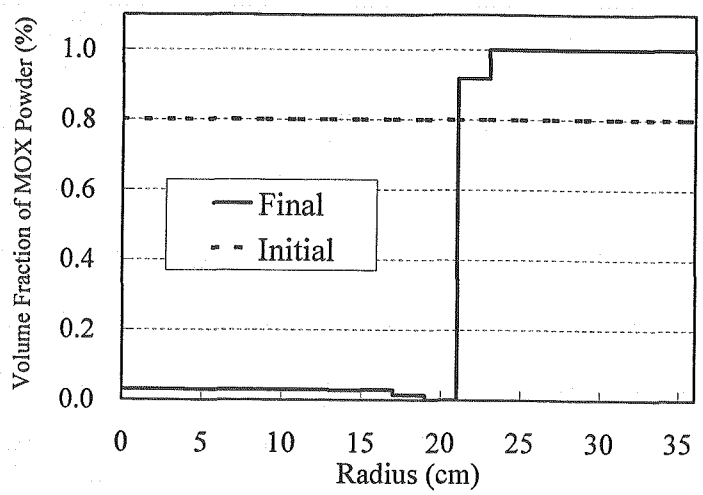

Fig. 3.1-13 Radial distribution of volume fraction of MOX powder in a 72 cm-diameter bare sphere (Approximately 390kg MOX powder and 12 kg zinc-stearate are mixed.)

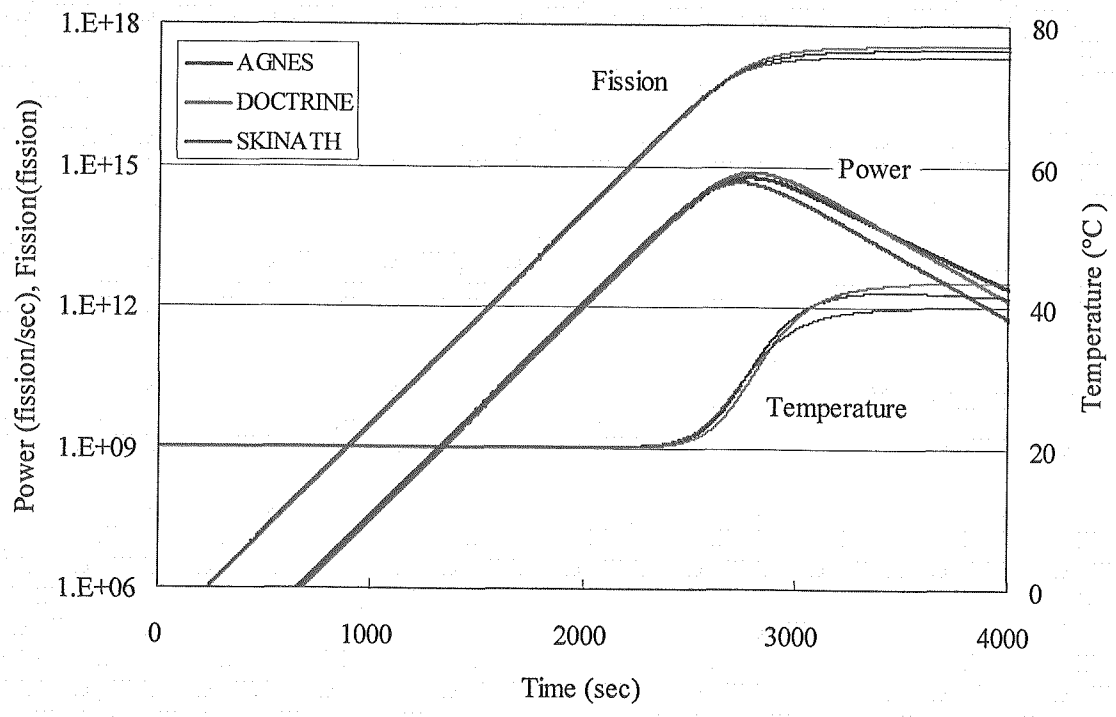

Fig. 3.1-14 Result of one-point codes for Uranium powder system (0.1 $)

This is a blank page.

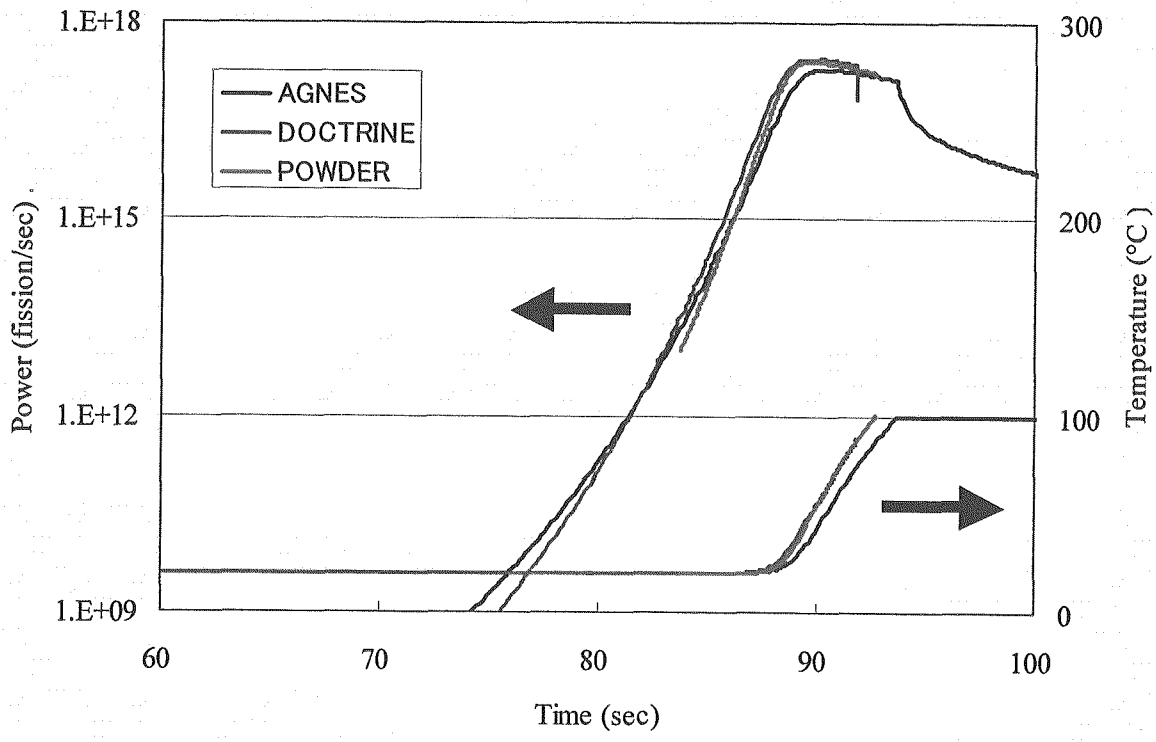

Fig. 3.1-15 Result of one-point codes for Uranium powder system (0.9 $)

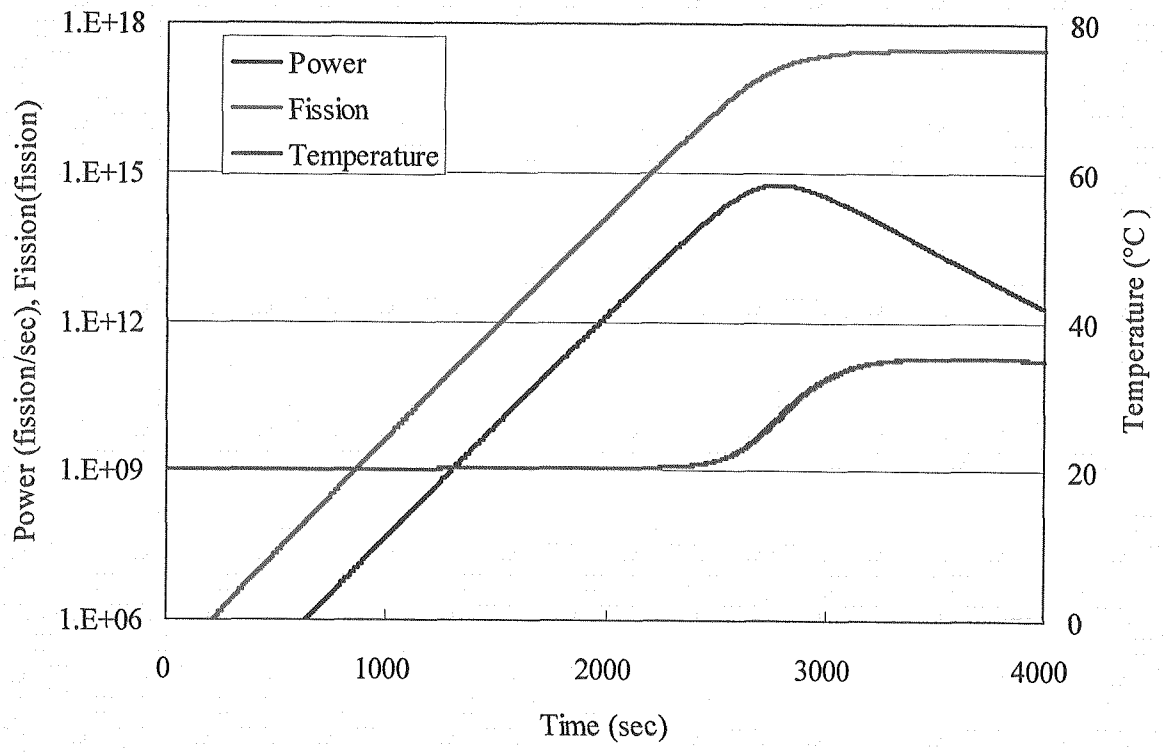

Fig. 3.1-16 Result of AGNES calculation for MOX powder system

This is a blank page.

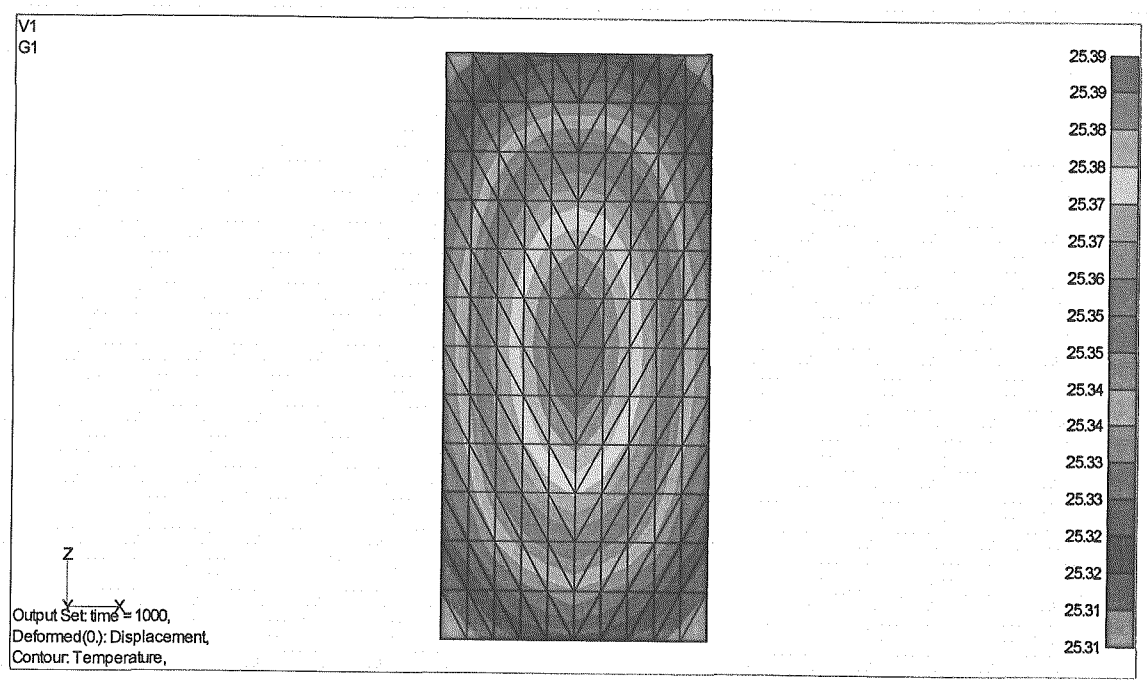

Fig. 3.1-17 Temperature distribution calculated using FEDEX-P for MOX powder system (1000 sec)

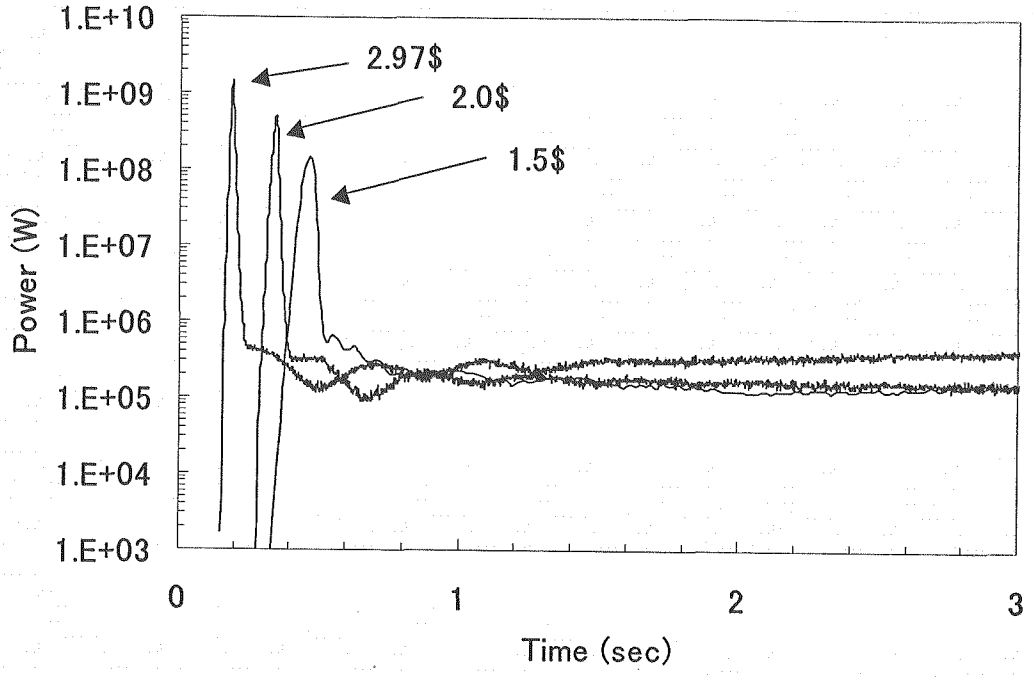

Fig. 3.1-18 TRACY experimental data of power

This is a blank page.

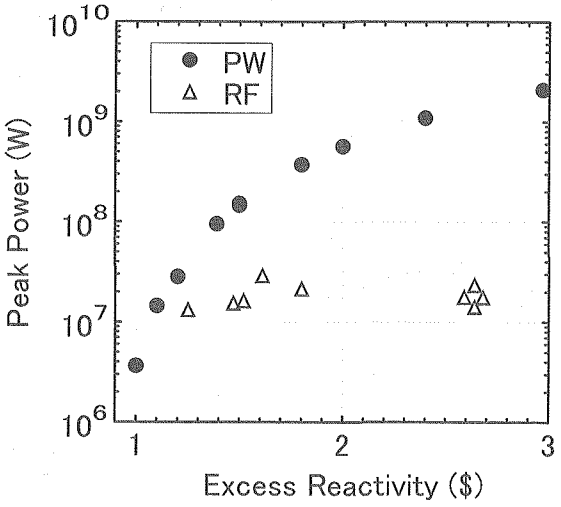

Fig. 3.1-19 Peak power is plotted against excess reactivity

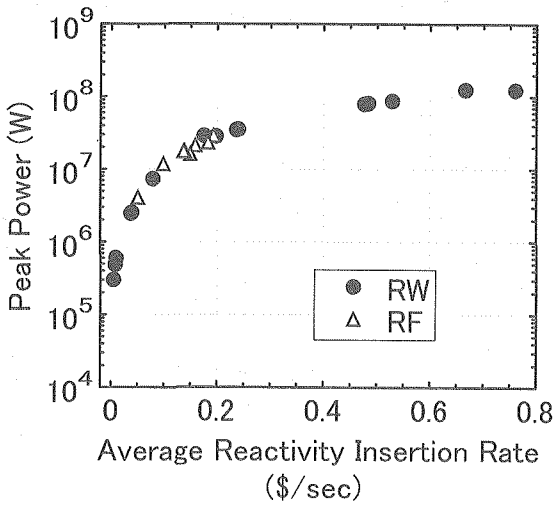

Fig. 3.1-20 Peak power is plotted against average reactivity insertion rate

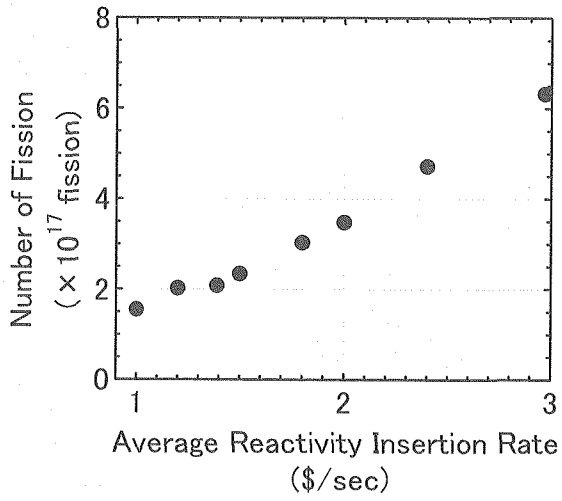

Fig. 3.1-21 Total number of fission is plotted against excess reactivity for PW mode experiments

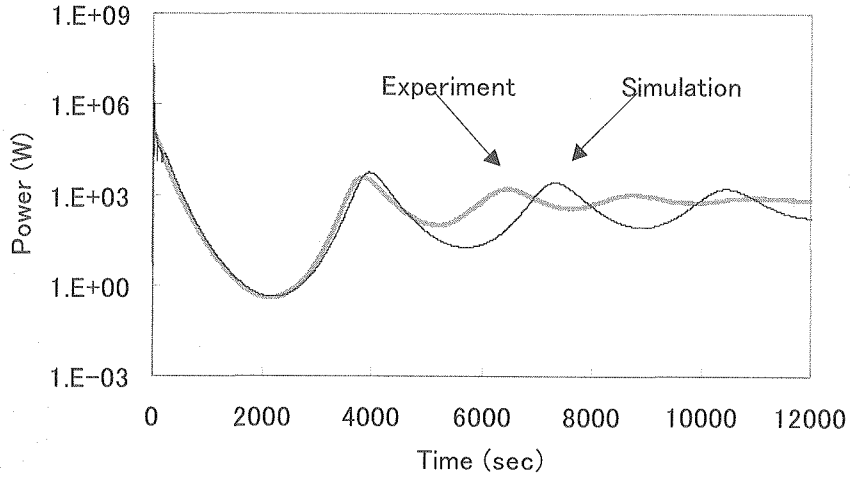

Fig. 3.1-22 A comparison of AGNES2 calculation and experiment for long period (1.5$, 0.15$/s)

This is a blank page.

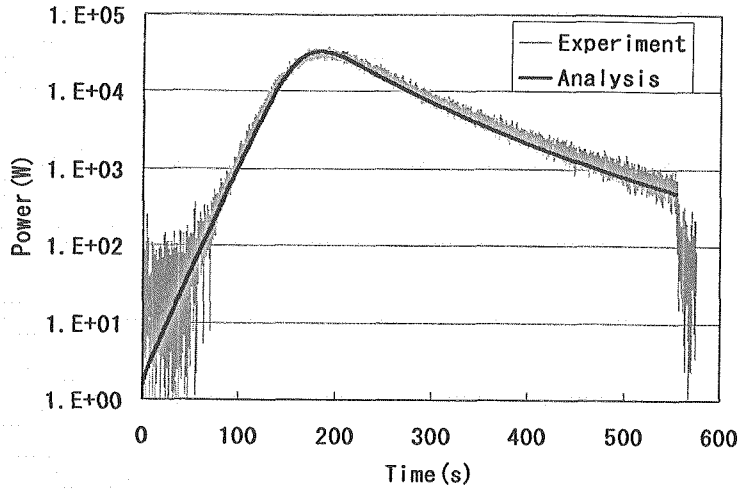

Fig. 3.1-23 A comparison of AGNES2 calculation and experiment (PW mode, 0.3$)

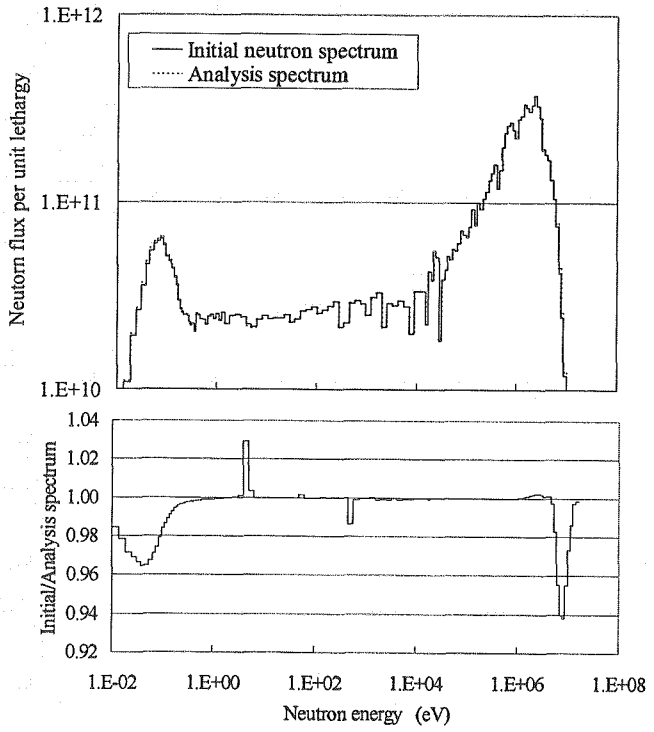

Fig. 3.1-24 Measurement result of neutron spectrum on the surface of the TRACY core in transient mode by multi-foil activation method ("Initial neutron spectrum" and "Analysis spectrum" indicate result of the MCNP calculation and result of the NEUPAC-JLOG calculation, respectively.)

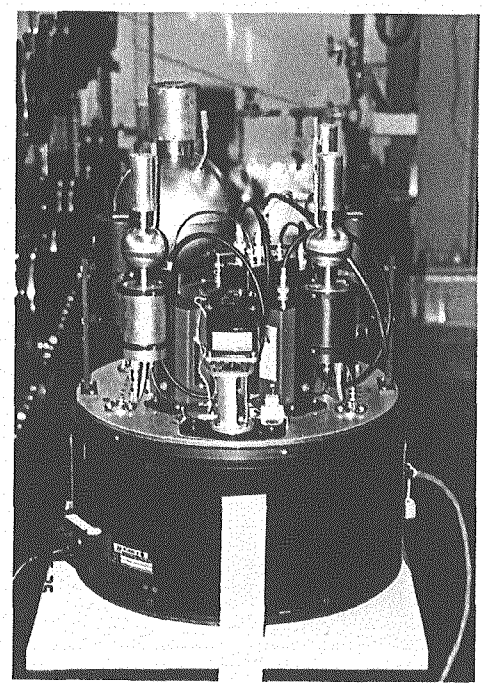

Fig. 3.1-25 An overview of the spectrometer that consists of four recoil proton proportional counters

This is a blank page.

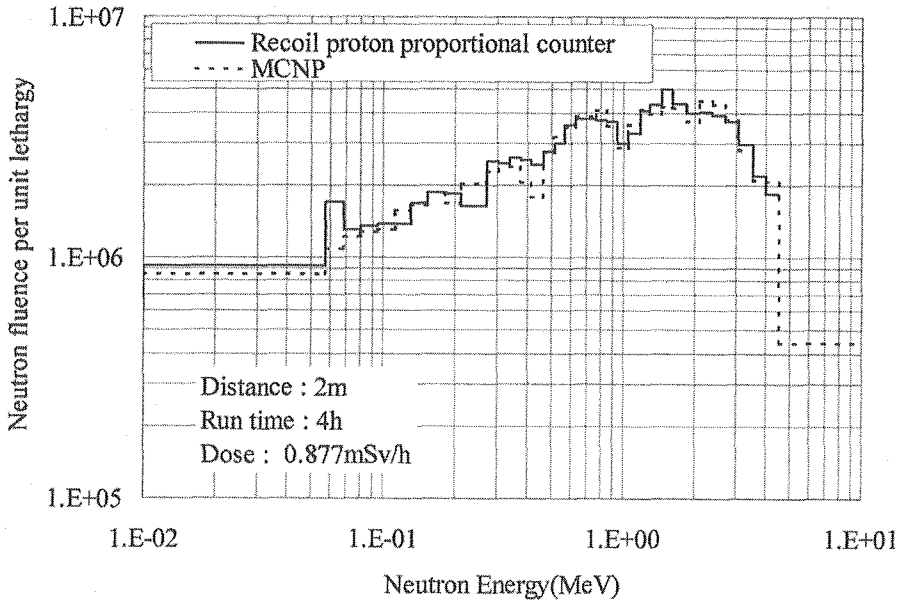

Fig. 3.1-26 Measurement result of neutron spectrum at 2 m away from the surface of the TRACY core in static mode by recoil proton proportional counter method and calculation result of the MCNP code

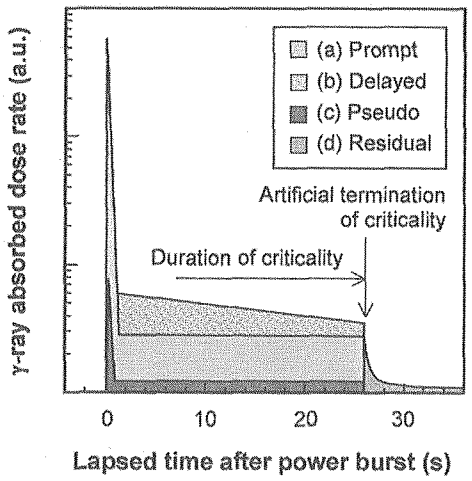

Fig. 3.1-27 Schematic diagram of γ-ray components in a typical criticality accident of fissile solution

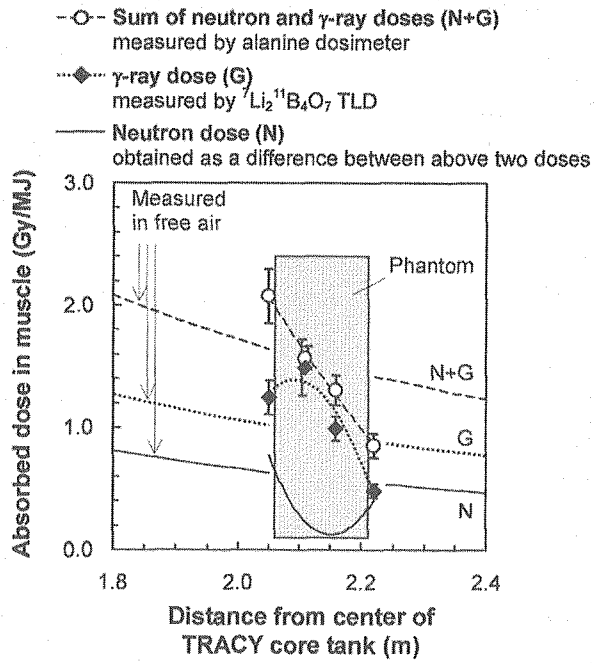

Fig. 3.1-28 Spatial distribution of neutron and γ-ray absorbed doses in phantom (The doses out of the phantom were measured in free air at TRACY by combined use of the alanine dosimeter and the $^{7}Li_2{}^{11}B_4O_7$ TLD.)

3.2 Research on Process Safety of Reprocessing

Reprocessing in the next generation should treat high burn-up spent UO_2 fuel and spent MOX fuel, which contain more minor actinides (MA, Np, Am, Cm, etc.) and fission products (FP) than ever. The chemical processes, dissolution, off-gas treatment, extraction-separation, etc., should satisfy the requirements on economical improvement, capabilities of advanced separation and confinement of those nuclides, MA and FP, inside the processes to reduce environmental hazard.(Fig. 3.2-1) Basic chemistry for elemental separation and separation process of reprocessing were studied as the basis of an aqueous process development for a future fuel cycle. These studies also provide fundamental data for future safety assessment.

3.2.1 Research on Basic Chemistry for Elemental Separation

The basic electrochemistry of actinides, uranium, plutonium and neptunium, was studied using a cyclic voltammetry technique. Formal potential values for redox couples of U(VI)-U(V) complex with organic multidentate ligands,[1] the values for the couples of Pu(IV)-Pu(III)[2] and Np(VI)-Np(V)[3] in nitric acid solution were obtained. The reduction kinetics of Np(VI) to Np(V) by n-butyraldehyde in organic TBP / dodecane solution was studied and a kinetic equation was established.[4, 5] A novel and faster reductant for Np(VI), allylhydrazine, was used in a continuous counter-current back-extraction test, and at least 91 % of Np was selectively recovered from a U(VI)- Pu(IV)-Np(VI) loaded solvent.[6]

An extraction chromatographic technique was studied for separation and recovery of Am and Cm (trivalent minor actinides) from highly active aqueous solution. By using adsorbent impregnating TODGA extractant into porous silica / polymer composite material as a support, Am (tracer concentration) was successfully separated and recovered from synthesized solution together with trivalent lanthanides.[7]

Using a flow-type electrolytic cell with columnar working electrode made of carbon fibers, reduction of Tc(VII) was studied. It was supposed that Tc was reduced to Tc (IV), and it was clarified that the reduced Tc was not adsorbed to anion exchanging resin.[8] The adsorption of technetium to TODGA adsorbent, before and after electrolytic reduction, was also studied. After reduction, the adsorption coefficient of Tc to anion exchanging resin decreased to almost negligible value.[9] Further, the possibility of electro-reductive recovery of Tc form nitric acid solution together with Pd was examined.[10]

As a novel simple separation technique, selective precipitation of hexavalent actinides elements, U(VI), Pu(VI), Np(VI), from a nitric acid solution by N-cyclohexyl-2-pyrrolidone (NCP) was studied. Experiments with transuranium elements showed that Pu(VI) precipitated with NCP[11, 12] but that Np(V) did not.[12] It was also found that Pu(IV) precipitated with NCP. The precipitate, however, re-dissolved if U (VI) co-existed with Pu(IV).[12]

3.2.2 Research on Separation Process of Reprocessing using Spent Fuel

Tests using spent UO_2 and MOX fuel were performed in NUCEF-BECKY (6.2.2) alpha-gamma cell. A test on co-decontamination and U/Pu partition steps of conventional PUREX flow-sheet was performed using mixer-settler contactors (Fig. 3.2-2) in the cell. Using a dissolver solution of spent MOX fuel with burn-up of 40 GWd/t, the behavior data of actinides elements (U, Pu, Np, Am, Cm) were collected (Fig. 3.2-3).[13] Extraction tests under a simplified PUREX flow-sheet were also performed using a dissolver solution of spent UO_2 fuel with burn-up of 44.3 GWd/t, and the possibility of selective Np recovery by using *n*-butyraldehyde as a selective Np(VI) reductant was demonstrated.[5, 14, 15] The feasibility of Tc recovery from a dissolver solution by a PUREX technique was demonstrated from the results of extraction tests and also from the calculation results of a simulation code ESSCAR (Extraction System Simulation Code for Advanced Reprocessing).[14, 16]

Utilization of a process simulation code is an important activity in the safety assessment. To develop a simulation code of a dissolution process, a simple dissolution model was proposed. The model successfully explained the dissolution rate of uranium in spent UO_2 fuel experiments.[17] To simulate an off-gas treatment process, a model of iodine adsorption to silica gel impregnating silver nitrate was proposed, and the model successfully explained the recovery of iodine in spent fuel experiments, too.[18] The extraction process simulation code, ESSCAR, is now in preparation for publication. It can simulate not only the extraction behaviors of radioactive elements, U, Pu, Np, Tc, Zr, etc., but also the extraction behaviors of important chemicals for process safety, hydrazoic acid for example.[19]

References

(1) S.-Y. Kim, T. Asakura, Y. Morita, G. Uchiyama and Y. Ikeda, "Electrochemical Redox Reactions of Uranium(VI) Complexes with Multidentate Ligands in Dimethyl Sulfoxide," Radiochim. Acta, 93, 75-81 (2005).

(2) S.-Y. Kim, T. Asakura and Y. Morita, "10.24 Electrochemical Studies of Plutonium Complexes in Aqueous Nitrate Solutions," Proc. of Int. Symp. NUCEF 2005, Feb. 9-10, 2005, Tokai-mura, Japan, JAERI-Conf 2005-007, 341-344 (2005).

(3) S.-Y. Kim, T. Asakura, Y. Morita, G. Uchiyama and Y. Ikeda, "Electrochemical and Spectroelectrochemical Properties of Neptunium(VI) Ions in Nitric Acid Solution," J. Radioanal. Nucl. Chem., 262(2), 3111-315 (2004).

(4) Y. Ban, T. Asakura and Y. Morita, "Reduction Kinetics of Np(VI) by *n*-Butyraldehyde in Tributyl Phosphate Diluted with *n*-Dodecane," Radiochim. Acta, 92, 883-887 (2005).

(5) H. Mineo, T. Asakura, S. Hotoku, Y. Ban and Y. Morita, "An Advanced Aqueous Reprocessing Process for the Next Generation's Nuclear Fuel Cycle", Proc. of GLOBAL 2003, Nov. 16-20, 2003, New Orleans, USA, p.1250-1255 (CD-ROM) (2003).

(6) Y. Ban, T. Asakura and Y. Morita, "Separation of Np from Pu Using a Salt-free

Reductant for Np(VI) by Continuous Counter-current Back-extraction," Proc. of Global 2005, Oct. 9-13, 2005, Tsukuba, Japan, paper No. 371 (CD-ROM) (2005).

(7) H. Hoshi, Y.-Z. Wei, M. Kumagai, T. Asakura and Y. Morita, "Group Separation of Trivalent Minor Actinides and Lanthanides by TODGA Extraction Chromatography for Radioactive Waste Management," J. Alloy and Compounds, 374, 451-455 (2004).

(8) H. Hoshi, Y.-Z. Wei, M. Kumagai, T. Asakura and Y. Morita, "Electrolytic Reduction of Tc(VII) in Nitric Acid Solution Using Glassy Carbon Electrode," J. Radioanal. Nucl. Chem., 262(3), 601-605 (2004).

(9) H. Hoshi, T. Arai, Y.-Z. Wei, M. Kumagai, T. Asakura and Y. Morita, "10.23 A Study on Adsorption onto TODGA Resin after Electrolytic Reduction in ERIX Process for Reprocessing Spent FBR-MOX Fuel," Proc. of Int. Symp. NUCEF 2005, Feb. 9-10, 2005, Tokai-mura, Japan, JAERI-Conf 2005-007, 335-340 (2005).

(10) T. Asakura, S.-Y. Kim, Y. Morita and M. Ozawa, "Study on Electrolytic Reduction of Pertechnetate in Nitric Acid Solution for Electrolytic Extraction of Rare Metals for Future Reprocessing," J. Nucl. Radiochem. Sci., in press.

(11) N. Koshino, M. Harada, Y. Ikeda, M. Nogami, K. Suzuki, H. Mineo, Y. Morita, K. Yamasaki, T. Chikazawa, Y. Tamaki and T. Kikuchi, "Development of a Simple Reprocessing Process Using Selective Precipitant for Uranyl Ions", Proc. of GLOBAL 2003, Nov. 16-20, 2003, New Orleans, USA, p.492-496 (CD-ROM) (2003).

(12) Y. Morita, Y. Kawata, H. Mineo, N. Koshino, N. Asanuma, Y. Ikeda, K. Yamasaki, T. Chikazawa, Y. Tamaki and T. Kikuchi, "Development of a Simple Reprocessing Process Using Selective Precipitant for Uranyl Ions –Precipitation Behaviors of Plutonium and other Transuranium Elements–," Proc. of Global 2005, Oct. 9-13, 2005, Tsukuba, Japan, paper No. 159 (CD-ROM) (2005).

(13) S. Hotoku, T. Asakura, M. Sato, Y. Ban and Y. Morita, "Spent MOX Fuel Test of Extraction Step," Proceedings of AESJ 2005 Autumn Meeting, Sep. 13-15, 2005, Hachinohe-shi, Japan, J21 (CD-ROM) (2005). [in Japanese]

(14) T. Asakura, S. Hotoku, Y. Ban, M. Matsumura, S.-Y. Kim, H. Mineo and Y. Morita, "Research on PARC Process for Future Reprocessing," Proc. of Int. Conf. ATALANTE 2004 Advances for Future Nuclear Fuel Cycles," June 21-24, 2004, Nimes, France, O12-04, (CD-ROM) (2004).

(15) Y. Morita, T. Asakura, H. Mineo, S. Hotoku and G. Uchiyama, "3.3 Accomplishment of 10-year Research in NUCEF and Future Development -Process Safety and Development Research-," Proc. of Int. Symp. NUCEF 2005, Feb. 9-10, 2005, Tokai-mura, Japan, JAERI-Conf 2005-007, 25-30 (2005).

(16) T. Asakura, S. Hotoku, Y. Ban, M. Matsumura and Y. Morita, "Technetium Separation for Future Reprocessing," J. Nucl. Radiochem. Sci., in press.

(17) H. Mineo, H. Isogai, Y. Morita and G. Uchiyama, "An Investigation into Dissolution Rate of Spent Nuclear Fuel in Aqueous Reprocessing", J. Nucl. Sci. Technol., 41(2), 126-134

(2004).

(18) H. Mineo, M. Gotoh, M. Iizuka, S. Fujisaki, H. Hagiya and G. Uchiyama, "Applicability of a Model Predicting Iodine-129 Profile in a Silver Nitrate Silica-Gel Column for Dissolver Off-Gas Treatment of Fuel Reprocessing", Sep. Sci. Technol., 38(9), 1981-2001 (2003).

(19) T. Asakura, M. Sato, M. Matsumura and Y. Morita, "10.25 Simulation Codes of Chemical Separation Process of Spent Fuel Reprocessing –Tools for Process Development and Safety Research," Proc. of Int. Symp. NUCEF 2005, Feb. 9-10, 2005, Tokai-mura, Japan, JAERI-Conf 2005-007, 345-347 (2005).

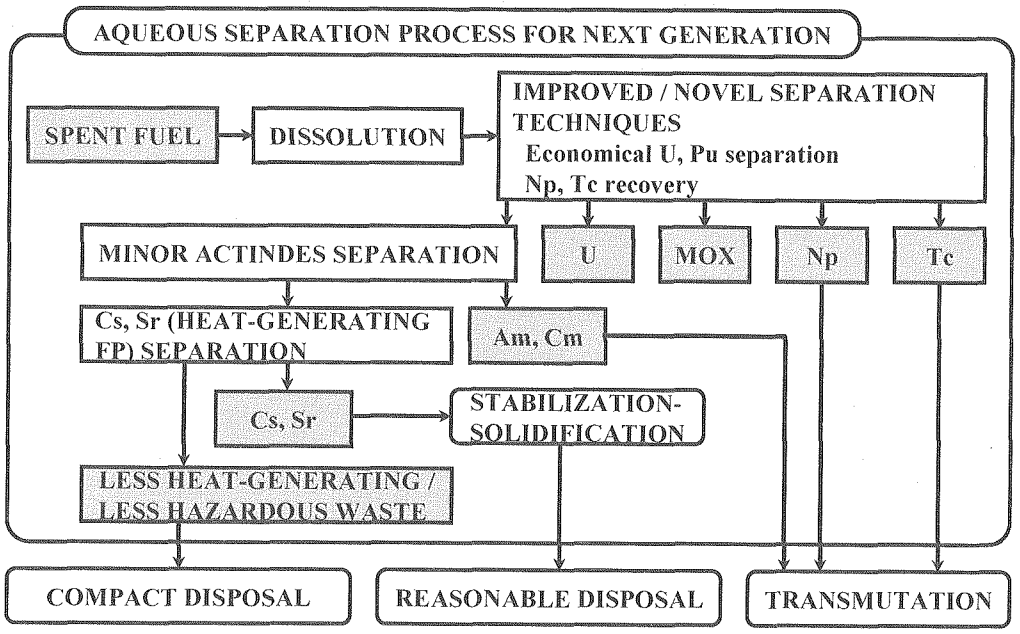

Fig. 3.2-1 Concepts of aqueous separation for reprocessing of next generation

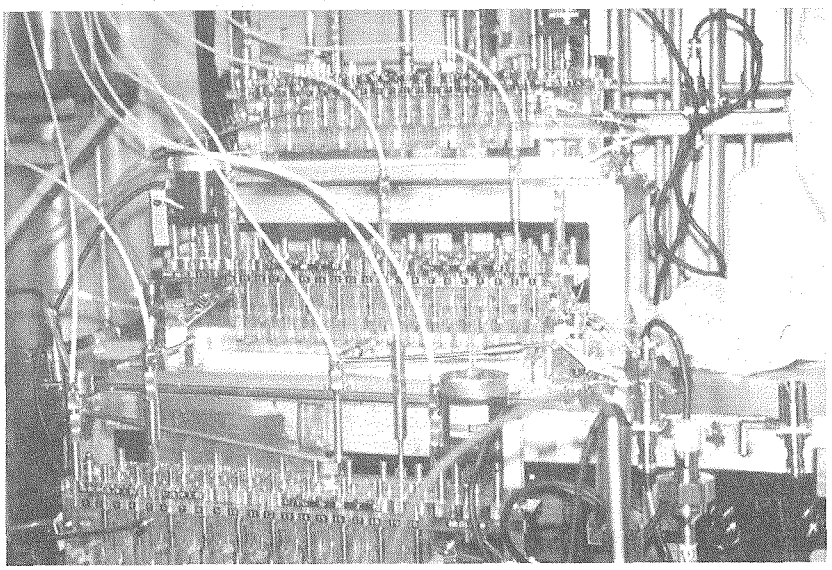

Fig. 3.2-2 Mixer-setter contactors in an αγ cell in NUCEF-BECKY

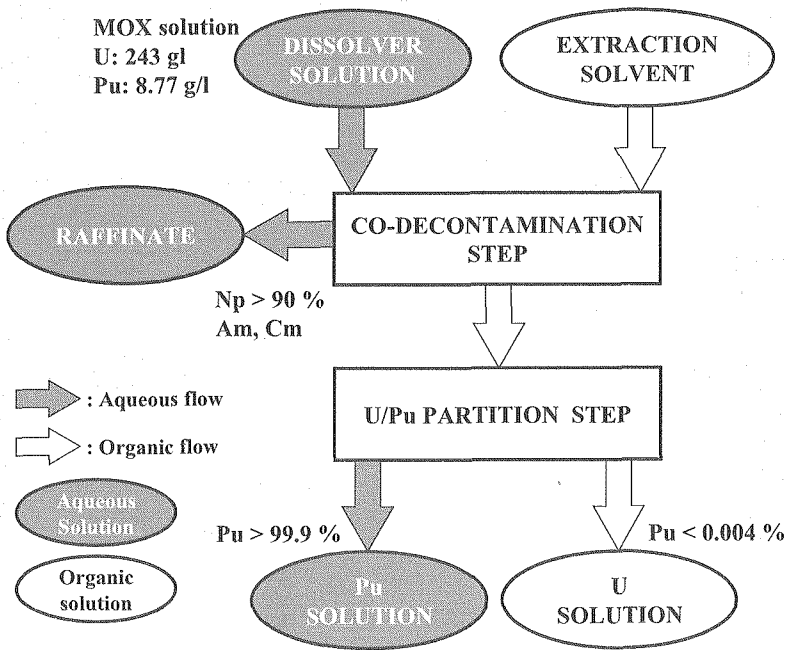

Fig. 3.2-3 Results of a test on co-decontamination and U/Pu partition steps of conventional PUREX flow-sheet using a dissolver solution of spent MOX fuel with burn-up of 40 GWd/t

3.3 Research on Life Prediction and Advanced Technologies for Equipment Materials used in Reprocessing Nitric Acid Process

The corrosion resistance of equipment materials used in nitric acid environments is considered as one of the most important technological issues on the long performance of Purex type commercial reprocessing plants. The Intergranular corrosion of heat transfer tubes in the reduced pressure type evaporators made of stainless steels and the susceptibility to stress corrosion cracking (SCC) of the normal pressure type dissolver/concentrator made of zirconium are the most important critical issues on the reliability of major equipment materials used in the Rokkasho Reprocessing Plant (RRP). The corrosion behavior has been investigated as functions of the heat flux, surface temperature, nitric acid concentration and dissolved metallic ions such as Np and platinum group elements that form strong oxidizer ions. The life prediction study has been carried out by mini-scaled mock-up and laboratory tests. The applicability of new corrosion resistant alloys and on-line corrosion monitoring systems have been also examined as countermeasures for improving the reliability of reprocessing equipment.

3.3.1 Research on Evaporator Materials

The reliability of an evaporator for nitric acid recovery made of stainless steel was evaluated by the mini-scaled mock-up and laboratory tests for evaluating the corrosion controlling factors such as the heat-flux, surface temperature and oxidizer ion contents. The 7th ISI of the mock-up that was carried out on September, 2004, after operated for nearly 48,000 hours. The wall thinning of heat transfer tubes was evaluated as shown in Fig. 3.3-1. Numerical analysis using computational codes has been also conducted using the data obtained from the mock-up and laboratory tests for constructing the data base system. The life prediction system was modified with calculation codes of the three-dimensional thermo-fluid dynamics and corrosion kinetics.

The inhibition effect of two kinds of advanced alloys on the resistance to trans-passive corrosion of heat transfer tubes in evaporators was evaluated. One is a type 310UHP stainless steel added 0.2wt% Ti with sufficient austenite phase stability at low temperature. The resistance to interglanular attack was improved by means of electron beam melting for purifying and two stepped thermo-mechanical treatment so-called the SAR for metallographic structure modification. The other is a Ni base 30Cr-10W-3Si alloy with the high resistance to interglanular attack at a wide range of corrosion potential, by enriching oxide former elements such as Cr, W and Si. For evaluating the applicability of these advanced alloys applied for the reprocessing equipment, the appropriate chemical composition range and manufacturing process were examined. Comparing with type 304ULC, the optimized type 310UHP showed the uniform corrosion rate without local attack in nitric acid solutions under heat flux control, as shown in Fig. 3.3-2. The cracking resistance to TIG welding proc-

ess of type 310UHP with the same filler metal was also examined. The cracking resistance of stainless steel with stable austenite during welding was improved by minimizing the contents of harmful elements such as P,S and alkaline metals. The TIG weld joints had also the good corrosion resistance in the Coriou type corrosion test. The engineering applicability of type 310UHP-Ti to the evaporator was examined by making a mock-up of heater assembly.

Concerning corrosion monitoring system, two types of in-situ techniques with electric resistance method were selected for detecting the wall thinning. The reference corrosion rate was obtained with analyzing the dissolved Ni ion contents and the in-service inspections by Ultrasonic Test (UT) method. One of in-situ monitoring is the Corrosometer with heat flux control system for evaluating the wall thinning of heat conducting tubes. The other is Field Signature Method (FSM) for detecting the wall thinning distribution and crack opening, by measuring the small electrical potential drop between each detection point. On the FSM, the wall thinning lower than 0.1mm was possible to detect with sensitivity of 20% in setting outer side of stainless steel tubes, as shown in Fig. 3.3-3. It was also possible to detect the crack propagation of SCC as the change in field coefficient value. Those monitoring system were installed to the evaporator mock-up for evaluating the practical applicability. The sensitivity of FSM monitoring in mock-up was almost coincident with that obtained by laboratory tests.

3.3.2 Research on Dissolver Materials

Although zirconium has the excellent corrosion resistance in reprocessing nitric acid environments, it has the susceptibility to SCC. The susceptibility is enhanced by both the crystal orientation and the notch effect, because the crack is easy to propagate along with basal plane (0002) of closed packed hexagonal crystal structure (cph) , even if the low stress intensity factor. The surface finish was regulated to UP2-800 and UP3 reprocessing plants in France for inhibiting SCC. Above major factors in relation to SCC of zirconium were examined by laboratory SCC tests in nitric acid simulated to reprocessing equipment.

The effect of surface roughness factor of zirconium on SCC was examined using the constant load test. The test specimen used was a smooth type of square shape with four different surface roughness factor by changing the surface finish. The susceptibility to SCC was evaluated in boiling nitric acid and in silicone oil at the same temperature as reference data. The relationship between rupture time and surface roughness factor (Ra) of specimens is shown in Fig.3.3-4. The rupture time in silicone oil was not reduced by changing the roughness factor. On the other hand, the rupture time reduced with increasing the roughness factor due to SCC. It was also markedly reduced by the existence of a notch. Figure 3.3-5 shows the difference in surface morphology by SEM of specimens after corrosion tests. The crack growth depended on the roughness factor due to SCC was clearly observed in specimens tested in boiling nitric acid. The allowable limit of surface defects during the

practical operation due to the degradation effects such as fretting was estimated to the reprocessing equipment made of zirconium.

The effect of crystal anisotropy of zirconium on the susceptibility to SCC was examined by Slow Strain Rate Test (SSRT) with notch-type specimens in boiling nitric acid as shown in Fig.3.3-6. The crystal anisotropy of specimens depending on the basal plane (0002) was controlled by changing cutting out direction, such as parallel (T), perpendicular (L) and wall thickness (X) to the rolling direction. The typical elongation loss was observed in X specimens because SCC was easy to occur in X specimens. The relationship between the reduction ratio of elongation and the relative ratio of the preferential orientation of (0002) was shown in Fig.3.3-7.

According to those results, the effects of the surface roughness factor and the preferential orientation of (0002) were incorporated in the database system for evaluating the initiation of SCC of zirconium in reprocessing nitric acid environments.

The content sponsored by The Ministry of Economy, Trade and Industry (METI) of Japan was included in this work.

This is a blank page.

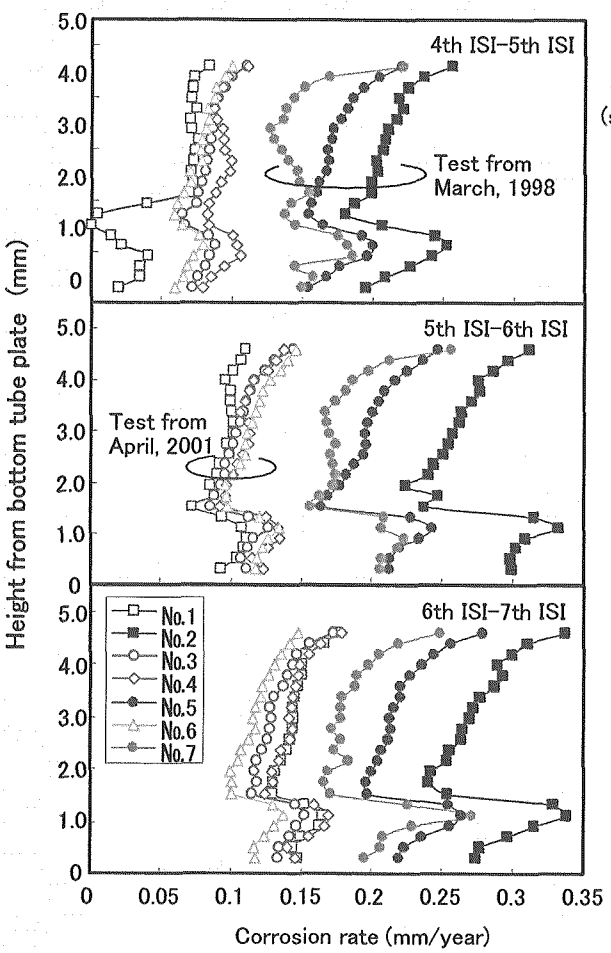

Fig. 3.3-1 Difference in the corrosion rate among heat conducting tubes in mock-up evaporator by UT measurement of each ISI

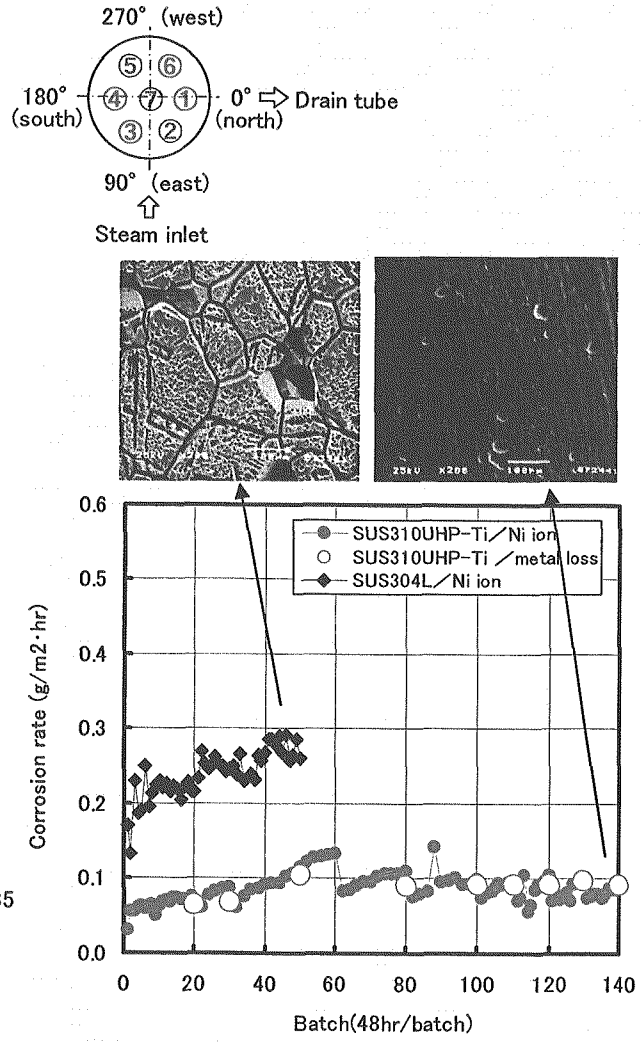

Fig. 3.3-2 Comparison of the corrosion rate between type 310UHP-Ti and type 304ULC stainless steels

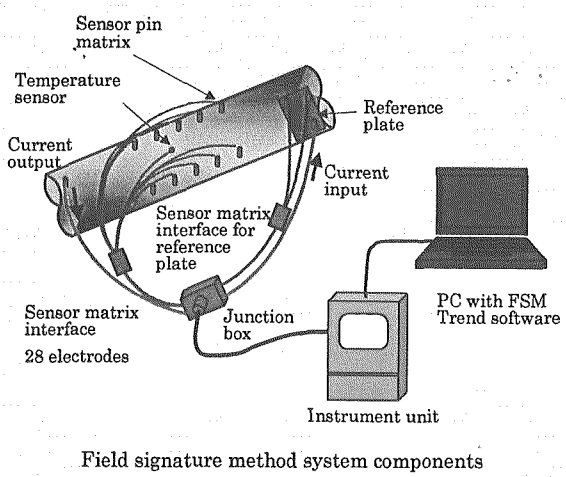

Field signature method system components

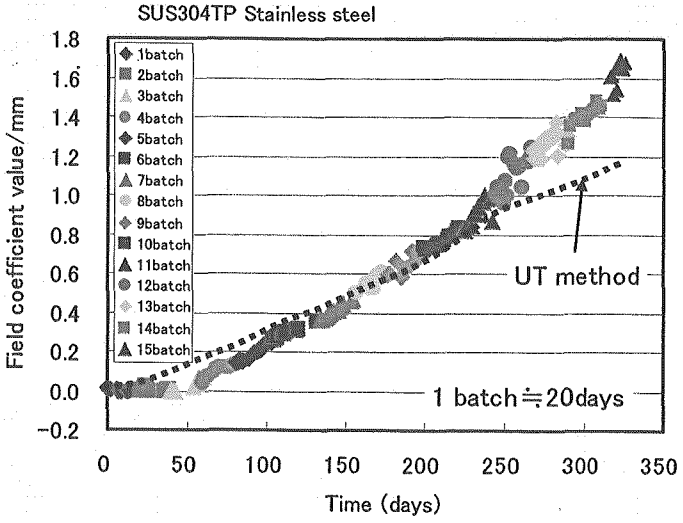

Fig. 3.3-3 Sensitivity in wall thickness of field signature method as corrosion monitor compared with it by UT method

This is a blank page.

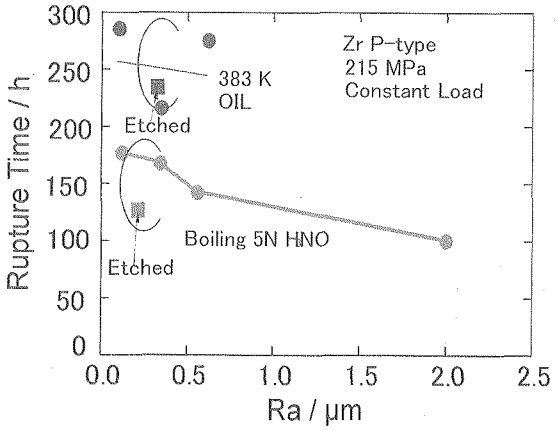

Fig. 3.3-4 Relationship between rupture time and surface roughness factor (Ra) by constant load test

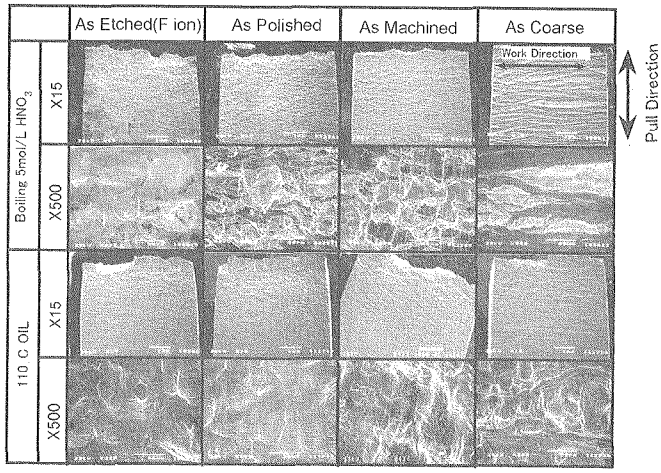

Fig. 3.3-5 Difference in fracture surface morphology of specimens with various surface finish (Coriou corrosion tests)

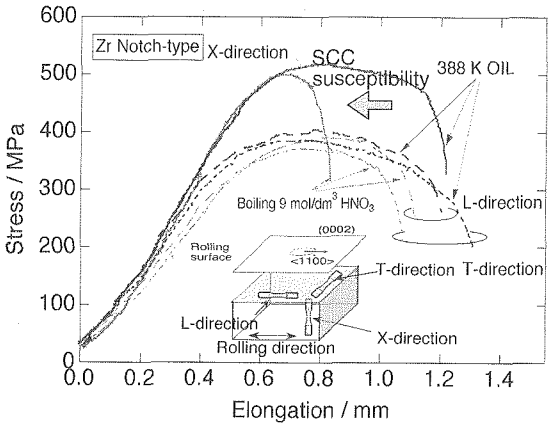

Fig. 3.3-6 Stress-strain curves of notch-type specimens by SSRT with different crystal orientation

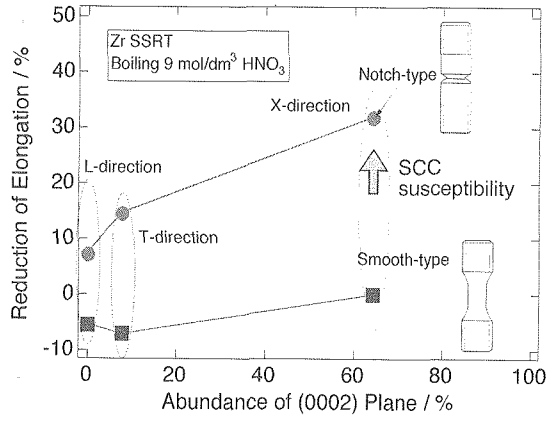

Fig. 3.3-7 Relationship between reduction ratio of elongation by SCC and preferential orientation ratio of (0002) plane.

3.4 Research on PSA of Nuclear Fuel Cycle Facilities

The Probabilistic Safety Assessment (PSA) is a comprehensive and structured method for assessing the safety of a nuclear facility by evaluating the frequencies and consequences of accidents that might threaten public health and safety. Since the first PSA study in the U.S.A., the Reactor Safety Study in 1975, there have been substantial methodological developments and the PSA methods have become a standard tool for safety assessment of nuclear power plants. Compared with the PSA for the nuclear power plants, however, the PSA for nuclear fuel facilities seems to be immature. Characteristics of nuclear fuel cycle facilities are different from nuclear power plant at the viewpoint of PSA. Nuclear materials in various forms exist at different locations in the facility and various accidents are potentially anticipated to threaten them being at risk. Many parts of fabrication process are controlled by operators. PSA procedure for these facilities is being developed taking these characteristics into consideration.

3.4.1 Development of PSA Procedures for MOX Fuel Fabrication Facilities*1

A research project has been initiated to establish a procedure for performing PSA of MOX fuel fabrication in FY2001 in order to assist the regulatory review for commercial MOX fuel fabrication facility. As mentioned above, nuclear materials also exist in various physical forms at different areas in MOX fuel fabrication facility. It is supposed that a variety of accidents may occur with different energy release at these areas. Therefore, it is important to identify potential abnormal events exhaustively and to screen those events efficiently from the point of risk significance. The first version of PSA procedure for these facilities was developed and it was applied for a model plant of MOX fuel fabrication facility to demonstrate its applicability[1-3].

The proposed PSA procedure consists of four major steps, which are hazard analysis, accident scenario analysis, evaluation of frequency and evaluation of consequence, as shown in Fig. 3.4-1. The first step is so called a preliminary PSA, and the latter three steps compose a detailed PSA, which corresponds to level 1 PSA and level 2 PSA for nuclear power plants.

In the first step of the procedure, hazard analysis is carried out for the selection of abnormal events in the facility concerned, which are defined as plant conditions leading to release of radioactive material with failures of preventive measures. In order to identify them without missing any potentially risk significant events, the hazard analysis is carried out through two sub-steps: one for exhaustive identification of potential abnormal events characterized by analyzing facility and the other for efficient screening of those events which may include subtle events from the point of risk significance.

---

*1 This work was entrusted from the Ministry of Economy, Trade and Industry of Japan.

For the first sub-step of hazard analysis, the systematic hazard analysis is useful to reduce efforts of analysts and dependence on knowledge of hazard analysis that analysts should have. The Failure Modes and Effects Analysis (FMEA) is bottom-up type of analysis to examine how failure or malfunction of a part and/or a component composing equipment propagates into a system and appears as an abnormal event. It can be applied easily to batch operation in MOX fuel fabrication facilities. However, FMEA with detailed information of parts and/or components level is a very time consuming task, an FMEA with functional information of equipment composing the facility (called as Functional FMEA) was proposed. A Functional FMEA has an ability to apply to a design phase facility of which detailed design information is not available.

In the second sub-step of the hazard analysis, the screening of the potential abnormal events is carried out by using two dimensional matrix based on the rough estimation of likelihood and maximum unmitigated release of radioactive material (called as Risk Matrix Analysis) to perform the detailed analysis of PSA efficiently. For rough estimation of likelihood of potential abnormal events, a method is used as same basically as the method proposed by U.S. NRC described in the appendix A of standard review plant for the review of an application for a MOX fuel fabrication facility (NUREG-1718). This method does not require detailed reliability analysis. In addition to this feature, the character index is introduced instead of the numerical index for improving the traceability of analysis results, for keeping the information of each reliability factor, which may be masked by summing up of numerical indexes and for giving information on combinations of system failures contributed to the frequency of the potential abnormal event. A guide was prepared to apply reliability index for rough estimation of failure of equipment and human errors through the trial application to model plant and investigation of some database for component failures and human errors. Based on thus obtained likelihood, each abnormal event is categorized into 3 ranges of likelihood, which are "highly unlikely" as less than 10^{-6}/y, "unlikely" as greater than or equal to 10^{-6}/y to less than 10^{-4}/y and "not unlikely" as greater than or equal to 10^{-4}/y, of risk matrix for screening.

The occurrence of criticality accident needs some control failures because MOX fuel fabrication facility is designed on the double contingency principle to prevent criticality accidents. Therefore, a method for estimation of likelihood was specially proposed for criticality accident. The likelihood of criticality accident was obtained as the multiplication of probabilities of deviations from normal operating condition of several criticality control parameters with the assumption of independency among the occurrences of deviations. A criticality condition is investigated with MCNP to clarify acceptable deviations from normal operating condition assuming that the criticality condition is determined by the combination of Pu enrichment, mass inventory of MOX and moderator concentration. A MOX powder handling process is controlled by a computerized system which consists of some mechanical

components, software for data processing and supervision by operators to prevent criticality accident. An evaluation method was also proposed in order to estimate the likelihood of failure probability of such type of the computerized system[2]. The software reliability is necessary to be assessed in this evaluation, it is however assumed to be as reliable as mechanical components that are well pre-examined in the procedure because assessment method for software reliability has not been established.

For rough estimation of consequence of potential abnormal events, maximum radioactive release of each event is estimated by using the Five-Factor Formula proposed by the U.S.NRC in Nuclear Fuel Cycle Facility Accident Analysis Handbook (AAH) (NUREG/CR-6410) assuming that potential abnormal event progresses without preventions and mitigations for environment release. In this estimation, mitigation measures are not taken into account, so that the leak path factors (LPFs) are set to 1. Based on thus obtained quantity of maximum radioactive release, each abnormal event is also categorized into 3 ranges of consequence of risk matrix for screening. The ranges of consequence categories are determined relatively as the range divided between maximum and minimum into three.

Potential abnormal events identified in the previous sub-steps are categorized into the Risk Matrix shown in Fig. 3.4-2. Abnormal events categorized in hatched areas of the matrix are selected as subjects of the subsequent accident sequence analysis.

The detailed PSA is applied to selected abnormal events. The accident scenario analysis identifies the causes of each abnormal event and examines event sequences initiated by the abnormal event by constructing the fault tree (FT) and the event tree (ET). The accident frequencies are evaluated by quantifying FT and ET models. Finally, radioactive material releases to the environment as the accident consequence are evaluated by using the Five-Factor Formula. The Five-Factor Formula in hazard analysis uses LPF=1 for estimation of maximum radioactive release, but LPF in this step is determined by using result of physical model calculation for precipitation, settling, agglomeration and filtration during or after the fire and over pressurization event. Computer codes of CELVA-1D and FIRIN are examined as a method to assess the LPF based on the physical modeling.

3.4.2 Investigation of Applicable Evaluation Methods of Accident Consequence of Nuclear Fuel Cycle Facilities

Two-years research project (fiscal years of 2004-2005) is entrusted to Atomic Energy Society of Japan to provide technical basis of evaluation methods of accident consequence of nuclear fuel facilities. The states-of-the-art of methods and basic experimental data needed for evaluation of accident consequence are investigated applicable to the potential events which may occur in nuclear fuel facilities such as criticality, boiling of radioactive solution, solvent fire, and hydrogen explosion.

Accident scenarios leading to maximum release of radioactive materials to the environment were examined in major processes of a reprocessing plant to identify important physical phenomena governing the release of radioactive materials in each type of events. Based on the results of preliminary search, accident consequence evaluation methods were investigated for four types of typical events.

For criticality event, the analytical results of existing simplified evaluation methods to estimate number of total fissions at major reactor vessels and storage tanks were compared with the experiments or accident records. The experimental background was examined for airborne release factor shown in AAH, which is used in a simplified evaluation method of Five-Factor Formula, applicable to the event of boiling of radioactive solution and hydrogen explosion. It was revealed that the value for airborne release from boiling water surface in AAH was likely to give conservative result. The assessing of integrity of HEPA filter at exhaustive system in nuclear fuel facilities is one of key issues in event of fire. Simplified fire modelings of combustible materials were investigated with the basic experimental data such as heat generation rate, smoke release rate.

Trial evaluation of accident consequences in sample accident scenarios are carried out based on the above investigated result to clarify future research issues in this field.

Reference

(1) K.Yoshida, H.Tamaki, T.Kimoto, et al., "Methodology Development and Application of PSA for MOX Fuel Fabrication Facilities", Proc. of Workshop on PSA for Non-Reactor Nuclear Facilities, OECD/NEA, Paris, (2004).

(2) H.Tamaki, Y.Hamaguchi, K.Yoshida, et al., "Present Status of PSA Methodology Development for MOX Fuel Fabrication Facilities", Proc. of The 7th Int. Conf. GLOBAL 2005, Tsukuba, (2005).

(3) H.Tamaki, K.Yoshida, N.Watanabe, et al., "Hazard Analysis Approach with Functional FMEA in PSA Procedure for MOX Fuel Fabrication Facility", Proc. of Int. Topical Meeting on Probabilistic Safety Analysis PSA'05, San Francisco, (2005).

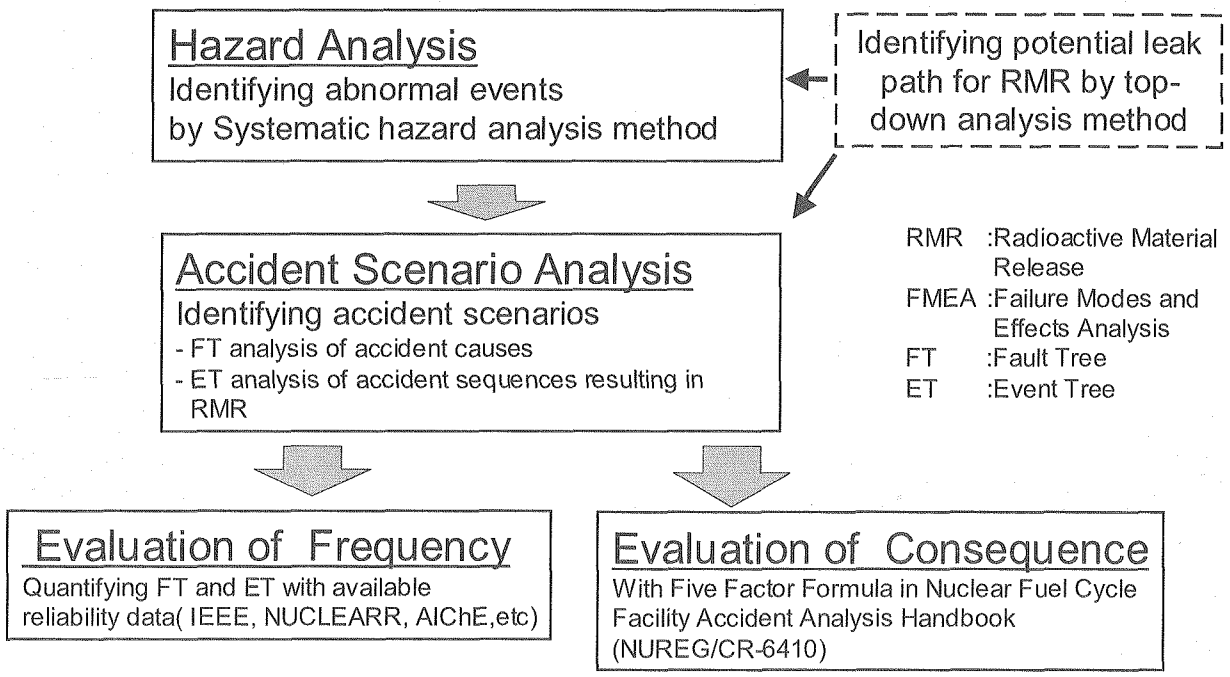

Fig. 3.4-1 PSA Procedure for MOX Fuel Fabrication Facilities

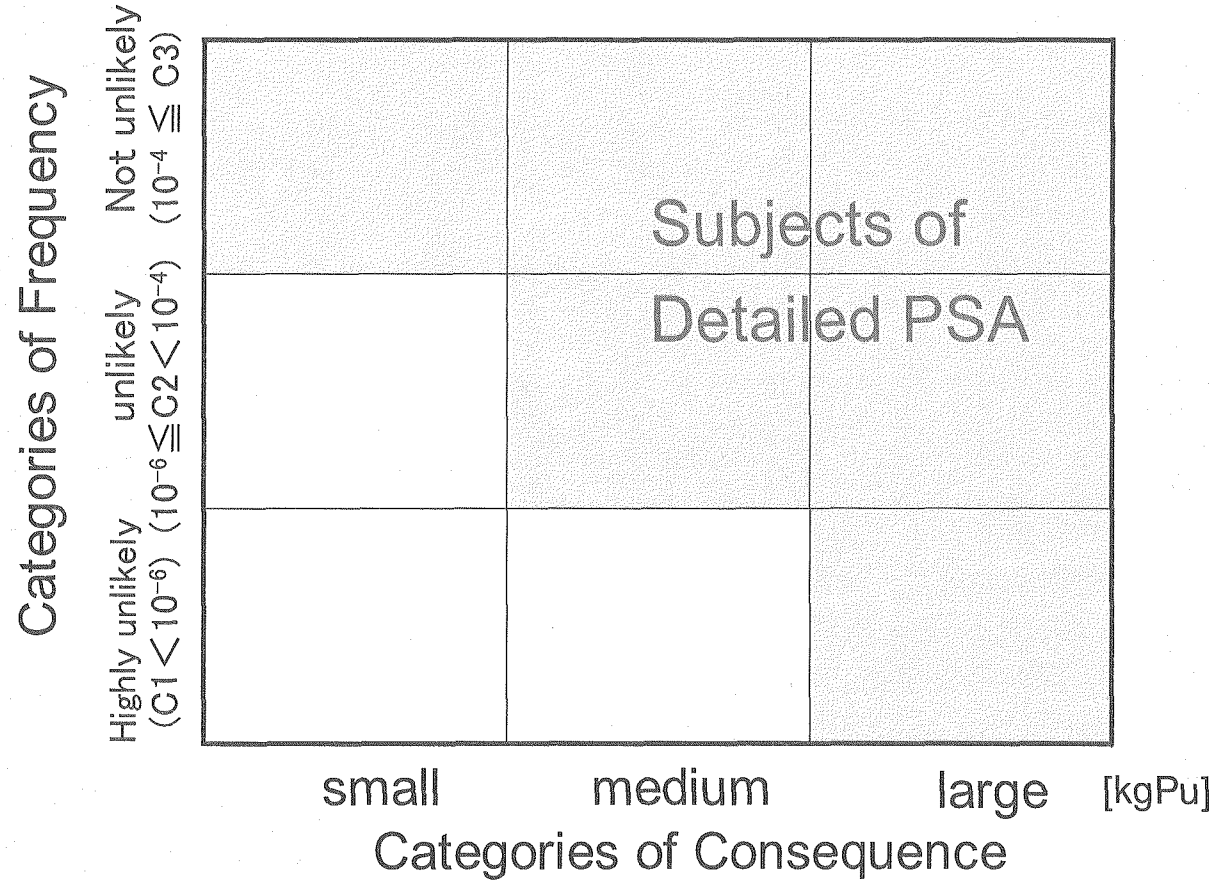

Fig. 3.4-2 Risk Matrix for Screening of abnormal event

3.5 Research on Safety Analysis of Transport Casks

3.5.1 Safety Analysis of Transport Casks in Case of Hypothetical Accidents *1 (1)

Anticipating the transport of increasing amount of nuclear fuel material as well as a variety of radioactive material in the near future to cope with steady development of nuclear fuel cycle industries, decision has been made to conduct safety demonstration analyses of transport casks under severe accident conditions. The safety demonstration analyses were expected to show the safety of the casks, and thus to expel anxiety of general public toward nuclear development in Japan.

Selected as a target of the analysis in fiscal year 2003 was a transport cask for fresh PWR fuel assemblies. For the falling accident scenario, 18 meter drop from public highway to asphalt or concrete road surface on the corner of lid or the edge of the cask was assumed in consideration of the surveys for transport route and actual transport incidents/accidents. For the fire accident scenarios, flame temperature of 800 °C for 90 minutes was hypothetically assumed for the severe accident caused by a rear-ender or a contact with a tank lorry carrying a large amount of flammable material.

The falling out accident analyses were made by applying the impact analysis code LS-DYNA to three-dimensional elements. An outline of deformation resulting from the structural analysis is shown in Fig. 3.5-1. The equivalent inelastic strain was found to be no larger than 10% for the sustainers of the fuel assemblies, which was within the rupture strain of 40% given for the material, leading to the conclusion that there was no serious damage to the fuel assemblies without radioactive material being released to the environment.

The fire accident analyses were carried out by using finite element method (FEM) analysis code ABAQUS for three-dimensional elements. The result shows that the maximum temperature of the outer surface of the fuel assemblies reached 454 °C, as shown in Fig. 3.5-2, which was lower than the temperature 570 °C for cladding to sustain containment.

In fiscal 2004, a transport cask with fresh BWR fuel assemblies was selected as a subject for the analysis. Scenarios for falling and fire accidents were the same as those described in the aforementioned part of this section. Even the most severe condition of corner drop produced less energy than the rupture energy for fuel cladding. The maximum temperature of the outer surface of fuel assemblies reached 478 °C, which was again lower than 570 °C for cladding to sustain containment.

---

*1 This work was entrusted from the Ministry of Economy, Trade and Industry of Japan.

This is a blank page.

Reference

(1) Y. Nomura, K. Kitao, K. Karasawa, *et al.*, "Safety demonstration analyses at JAERI for severe accident during overland transport of fresh nuclear fuel," *Proc. Int. Symposium NUCEF 2005*, Tokai-mura, Japan, Feb. 9-10, 2005, JAERI- Conf 2005-007, Japan Atomic Energy Research Institute, p.170 (2005).

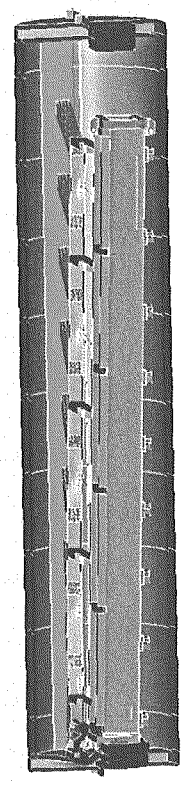

Fig. 3.5-1 Deformation of a container carrying PWR fuel assemblies for a falling scenario

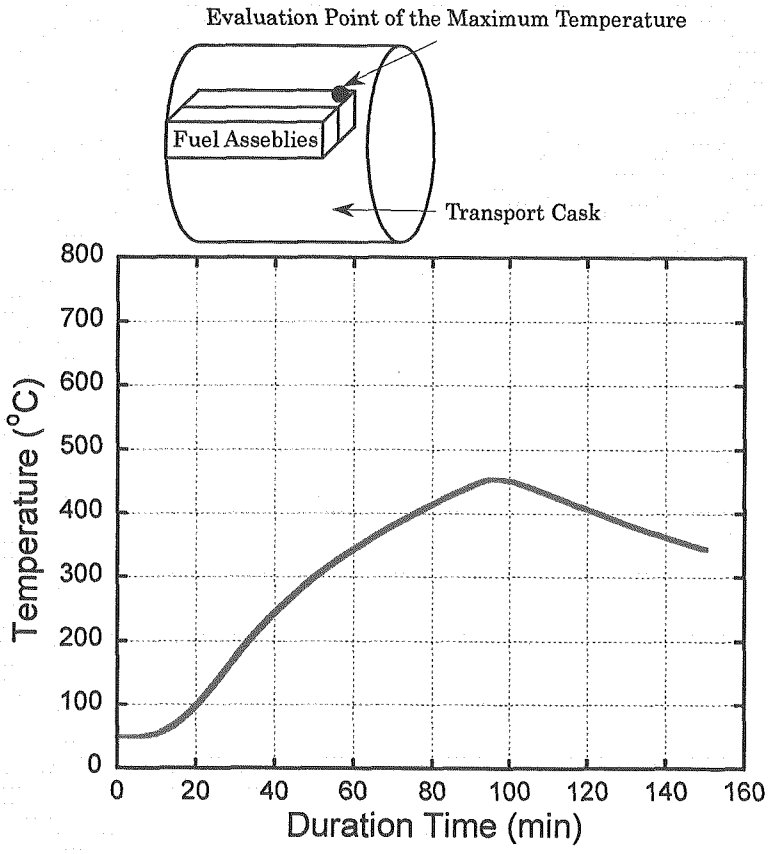

Fig. 3.5-2 Temperature rise at the corner of PWR fuel assemblies for a hypothetical severe fire accident scenario

This is a blank page.

4. SAFETY RESEARCH ON RADIOACTIVE WASTE DISPOSAL AND DECOMMISSIONING OF NUCLEAR FACILITIES

An important part of safety assessments of radioactive waste disposal totally relies on validated computer models and quality assured input data. JAERI has developed safety assessment codes for long-lived radioactive wastes: high-level waste, TRU waste and uranium waste. The developed long-term safety assessment code employs probabilistic approach where uncertainties associated with models and data are quantified. Studies to understand disposal system behavior include chemistry of long-lived radionuclides under deep underground conditions and evolution in performance of engineered barriers. Acquired data are provided for the long-term probabilistic safety assessment calculations and the uncertainty analyses. The deterministic and probabilistic safety assessment code system was applied to determine the clearance level for the near surface disposal of uranium and TRU wastes. The clearance level concentrations for 59 radionuclides were determined.

For assuring the safety of the public and workers during and after decommissioning of nuclear facilities, rules for the decommissioning of nuclear facilities and clearance system have been legislated in the revised Law for the Regulation of Nuclear Source Material, Nuclear Fuel Material and Reactors, which came into force in December 2005. Clearance system here means a set of rules and procedures to divide the a system that divides radioactive waste and materials that are not necessary to treat as radioactive materials. A computer code for calculating the public dose was developed to assess safety during dismantling activities, and development of a dose assessment code for workers was initiated in 2005. Concerning the clearance level system, the verification procedure was demonstrated by using data on the past research reactor dismantling.

4.1 Performance Assessment of Natural Barriers

Safety assessment code, GSRW-PSA has been developed. The probabilistic approach was introduced to groundwater flow analyses based on the statistical distribution on measured hydraulic conductivity. Physical and chemical processes in which radionuclides are involved in the natural barrier are studied through laboratory experiments to understand the mechanisms and to provide data for analyses on radionuclide migration in the safety assessment.

4.1.1 Probabilistic Analysis on Groundwater Flow and Travel Time in Deep Geologic Media*1

The probabilistic safety assessment computer code GSRW-PSA [1] evaluates potential radiological consequences of geologic disposal of HLW. Crystalline bedrock is considered to be one of potential host rocks for geologic disposal of HLW in Japan. For the GSRW-PSA analyses, a hypothetical repository was considered to be constructed in a stable granite rock mass and a depth of the repository was assumed 1,000 m (Fig. 4.1-1).

The radionuclide pathway is described by three major hydraulic units: rock mass, fractured zones and sedimentary layer. The repository is constructed in the bedrock distant from the fractured zones so that short circuit of groundwater from the repository to the biosphere is unlikely to occur and the possibility was ruled out. The domain of radionuclide pathways from the repository to the biosphere was modeled by a combination of two dimensional planes. The pathways were provided by Monte Carlo simulations on groundwater flow analysis (2D finite element analyses) assuming that the hydraulic conductivities of the rock mass and fractured zones are given by the probability density function obtained from Fig. 4.1-2[2]. Two types hydraulic properties for granite rock mass and the fracture zones were assumed in the Monte Carlo simulation: homogeneous and heterogeneous. Parameter variation on the spatially uniform hydraulic conductivity was given based on Fig. 4.1-2 for the homogenous assumption and spatial variation of the hydraulic conductivity for the heterogeneous assumption was estimated from Fig. 4.1-2.

The probabilistic realization of groundwater flow paths for the heterogeneous case is shown in Fig. 4.1-3. According to a series of probabilistic analyses, it was found that the travel time and travel length are sensitive to the uncertainties associated with hydraulic conductivities of geologic media rather than those with other hydraulic properties such as porosity [3].

4.1.2 Radionuclide Migration in Natural Barriers

Geologic disposal of radioactive waste containing long-lived TRU nuclides needs a

*1 This work was entrusted from the Nuclear and Industrial Safety Agency of Japan.

long-term safety assessment. Understanding of radionuclide migration in natural barriers has importance as well as in engineered barriers, and a number of physical processes and chemical reactions involved in the radionuclide migration have been studied. We conducted experimental study on influences of humic substances (HS), highly alkaline conditions and colloids on the radionuclide migration. These reactions have been recognized to have potentially significant influences on radionuclide retardation properties of natural barrier, but have not been modeled to evaluate the migration. Regarding adsorption, interactions of negatively charged metal ions with negatively charged mineral surfaces was investigated.

(1) Influence of humic substances*2

Humic substances (HS) are formed through microbial degradation of biomass and occur ubiquitously in groundwater. They generally have strong affinity to form complexes with TRU nuclides, and accordingly affect sorptive and diffusional behavior of TRU nuclides in geologic media.

Column experiments were performed to study the effects of humic acid on the mobility of ^{237}Np(V), ^{241}Am(III) and ^{63}Ni(II) through crushed granite, in the presence of humic acid [4,5]. The humic acid did not either accelerate or retard the mobility of ^{237}Np through the column. A portion of ^{241}Am was discharged from the column at the same rate as the injected influent, indicating that the portion of ^{241}Am was not retarded in the columns, whereas the rest of ^{241}Am was retarded. The concentration of ^{63}Ni passed through the column increased with the increasing concentration of humic acid.

^{241}Am and ^{63}Ni migrated in columns with retarded and non-retarded portions concurrently, and this behavior cannot be modeled by the conventional instantaneous equilibrium concept. A two species model, which took into account the complexation kinetics of ^{241}Am with humic acid, successfully described the observed migration behavior of ^{241}Am (Fig. 4.1-4). The observed migration behavior of ^{63}Ni was explained by a rate limited transformation model, which took into account non-equilibrium complexation of ^{63}Ni with humic acid.

To study diffusional behavior of ^{241}Am, through-diffusion tests of ^{241}Am in the presence of fulvic acid (FA) were conducted (Fig. 4.1-5 [6]). Fulvic acid is a major HS in groundwater. Diffusion of Am in tuff disks was observed for two FA conditions (Table 4.1-1). RUN-1 is aimed at demonstrating the effect of FA, and RUN-2 at determining the value of effective diffusivity (De) in the presence of FA. A portion of solutions was periodically sampled from the both reservoirs to measure their α-radioactivity.

Figure 4.1-6 shows the concentration of ^{241}Am in the collection reservoir. In the RUN-1, ^{241}Am was not detected in the solution in the collection reservoir by the 55th day in the

*2 This work was entrusted from the Ministry of Education, Culture, Sports, Science and Technology of Japan.

absence of the FA. Diffusion of ^{241}Am was accelerated by adding the FA into the both reservoirs, which indicates that the FA hindered ^{241}Am adsorption on the tuff, and the concentration of ^{241}Am in the solution increased.

At 320 days or later in the RUN-2, the decreasing rate of the concentration of ^{241}Am in the source reservoir became almost equal to the increasing rate in the collection reservoir. It was thought that local sorption equilibrium was attained in the tuff sample and the diffusion of ^{241}Am became steady state. The De was determined by using the concentrations of ^{241}Am in the source reservoirs of the time of 320 days or later and the linear portion of the concentration curves in the collection reservoirs. The De values for RUN-2 were found to be $(4.8\pm1.3)\times10^{-13}$ m^2/s.

(2) Influence of alkaline conditions caused by cement based materials [6] *3

Highly alkaline conditions arise from cement based materials used as waste form matrix and structural materials of repositories. The alkaline environments potentially alter the chemical and physical properties of geologic materials. As diffusion is one of most important processes to describe the behavior of alkaline plume from the repository, diffusivities of alkaline species were measured.

Two different cases of through diffusion tests (Table 4.1-2) were run; a cement-equilibrated, Ca^{2+}-rich aqueous solution was employed in the case A, and an NaOH solution of the same pH in case B. The tests were conducted at 25 °C in a glove box under controlled Ar atmosphere to avoid effects of CO_2. A portion of the aqueous solution in the reservoirs was periodically sampled to measure the pH and concentration of Ca^{2+} and Na^+.

Figure 4.1-7 shows the time course of the concentration of OH^-, Ca^{2+} and Na^+ in the source and collection reservoirs. The effective diffusivity, De, for OH^- in the case A was found to be $(9.7\pm1.0)\times10^{-11}$ m^2/s, which is higher by almost two orders of magnitude than that observed in the case B, $(8.4\pm0.5)\times10^{-13}$ m^2/s. These values are close to De for Ca^{2+}, $(5.1\pm0.3)\times10^{-11}$ m^2/s in the case A and that for Na^+, $(1.0\pm0.4)\times10^{-12}$ m^2/s in the case B. This result indicates that the diffusivity of OH^- in rock is totally determined by those for cationic species coupled with OH^- in aqueous solutions.

(3) Influence of colloids [6] *3

Colloidal particles such as HS and cement colloids can enhance the mobility of metal ions in aquifer. The colloid-facilitated transport is required to be modeled in predicting radionuclide migration. A number of studies have been made on chemical and physical properties of naturally and artificially occurring colloids. Based on the literature review, we selected interactions in which colloids are involved for modeling the colloid-facilitated

*3 This work was entrusted from the Ministry of Education, Culture, Sports, Science and Technology of Japan.

migration. The selected interactions are linear and non-linear equilibrium reactions between radionuclides and colloids, linear and non-linear kinetic reactions between radionuclides and colloids, and filtration with and without capacity limit.

(4) Influence of hydrolysis and carbonate complexation on adsorption of metal ions on minerals

When the pH of pore water in barrier materials increases by dissolution of cement based materials, metal ions, M^{m+}, are often hydrolyzed to form anionic hydroxo complexes, $M(OH)_n^{-(n-m)}$, and the mineral surfaces are negatively charged through the deprotonation of the hydroxide functional groups. Carbonate ions, which are ubiquitous in natural groundwater, also form anionic complex species with metal ions. The increase of the pH of pore water is electrostatically unfavorable for adsorption of metal ions on the mineral surfaces. The safety assessment of a deep geological isolation system requires understanding of the adsorption mechanisms under the condition that both radionuclides and mineral surfaces are mainly negatively charged.

Adsorption of lead (II) on γ-Al_2O_3 was studied at the high pH condition ($11 < pH < 13$) where lead(II) is hydrolyzed from $Pb(OH)_2(aq)$ to $Pb(OH)_3^-$, XPS analysis for the mineral surfaces and molecular orbital calculation [7]. The results suggested that $Pb(OH)_3^-$ can not be adsorbed on the deprotonated $\equiv AlO^-$ surface hydroxide ligand.

Adsorption of actinides, Th, U, Np and Am, onto negatively charged mineral surfaces was also investigated under conditions that actinides were predominantly present as anionic complex species [8]. Distribution coefficients of U(VI), Np(V), Sn(IV), Th(IV) and Am(III) decreased with the increasing pH or with the increasing carbonate concentrations. The monotonous decrease in the distribution coefficients in the investigated pH range suggests that anionic complex species of actinides were not adsorbed on negatively charged mineral surfaces. We calculated speciation of the elements in equilibrated solutions and found that adsorption of the minor neutral species plays a determinant role in the adsorption of actinides under the condition that both actinides and mineral surfaces are mainly negatively charged.

References

(1) S. Takeda and H. Kimura, *Uncertainty analyses for HLW disposal system using probabilistic safety assessment code (GSRW-PSA): Parameter uncertainty and conceptual model uncertainty in natural barrier*, JAERI-Research 2002-014, Japan Atomic Energy Research Institute (2002).

(2) Japan Atomic Energy Research Institute, *The FY15 project report of "The research for long-term assessment methodology of radioactive waste disposal, March 2004,"* JAERI, (2004), [in Japanese].

(3) Japan Atomic Energy Research Institute, *The FY16 project report of "The research for long-term assessment methodology of radioactive waste disposal, March 2005*," JAERI, (2005), [in Japanese].

(4) T. Tanaka *et al.*, "Migration models of neptunium and americium in groundwater under the present condition of humic substances," *Proc. Int'l Symp.: Transfer of Radionuclides in Biosphere, Prediction and Assessment*, JAERI-Conf 2003-010, p. 134 (2003).

(5) T. Tanaka *et al.*, "Influence of humic substances on the ^{63}Ni migration through crushed rock media," *Radiochim. Acta,* 92, 725 (2004).

(6) M. Mukai *et al.*, "Influences of humic substances, alkaline conditions and colloids, on radionuclide migration in natural barrier," *Proc. Int'l Symp. NUCEF 2005*, JAERI-Conf 2005-007, p. 219 (2005).

(7) T. Yoshida *et al.*, "XPS study of Pb(II) adsorption on γ-Al_2O_3 surface at high pH conditions," *J. Nucl. Sci. Technol.* 40, 672 (2003).

(8) T. Yamaguchi *et al.*, "Interactions between anionic complex species of actinides and negatively charged mineral surfaces," *Radiochim. Acta* 92, 677 (2004).

Table 4.1-1 Sample description of through-diffusion tests for ^{241}Am in tuff in the presence of FA in tuff-rock-equilibrated solution

RUN	Source reservoir		Collection reservoir
	^{241}Am (mol/m^3)	FA (g/m^3)	FA (g/m^3)
1	1.4×10^{-5}	0 (<54 days) 30 (55 days <)	0 (<54 days) 30 (55 days <)
2	1.4×10^{-5}	30	30

Table 4.1-2 Sample description of through-diffusion tests for OH^-, Ca^{2+} and Na^+ in alkaline solutions

Case	Source reservoir	Collection reservoir
A	Cement-equilibrated aqueous solution (pH=12.5)	Deionized water
B	NaOH (pH=12.5)	Deionized water

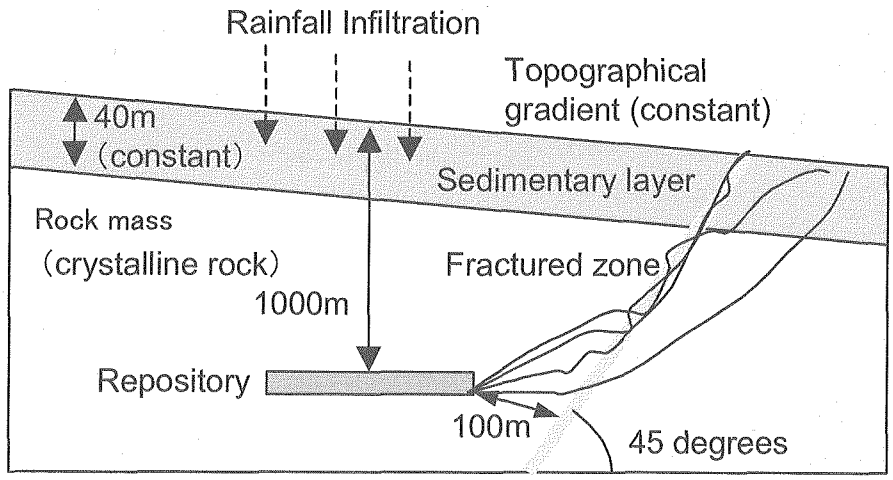

Fig. 4.1-1 Hypothetical HLW repository and fractured zone for GSRW-PSA analyses

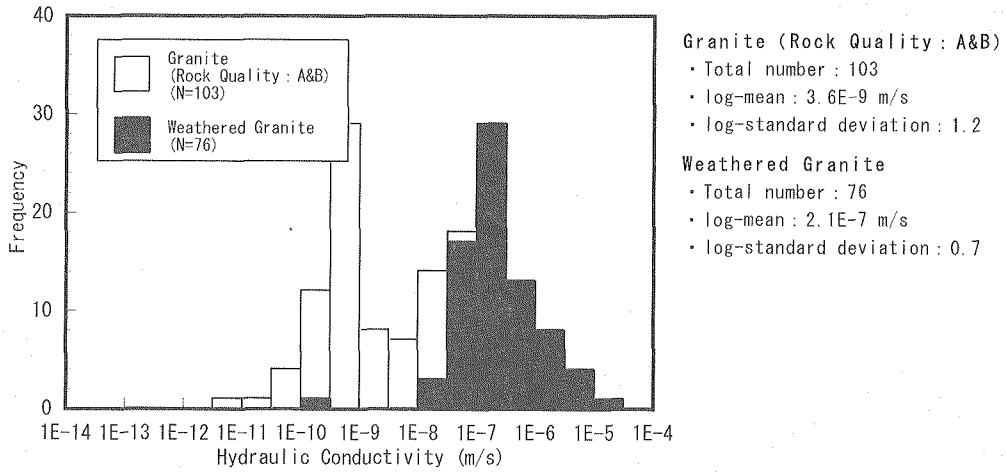

Fig. 4.1-2 The frequency distribution of measured hydraulic conductivities of granite in Japan [2] (The A and B in legend indicate the rock quality index.)

This is a blank page.

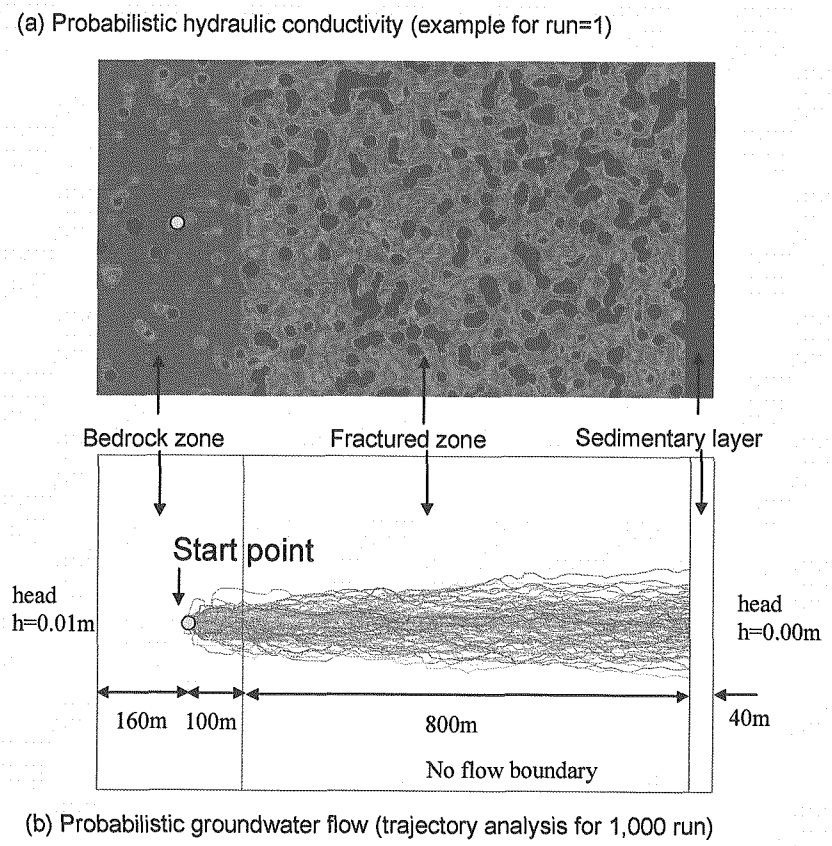

Fig. 4.1-3 (a) Probabilistic realization of spatial distribution of hydraulic conductivities (heterogeneous case) and (b) groundwater flow paths evaluated with 1,000 realizations on the spatial distribution of hydraulic conductivities

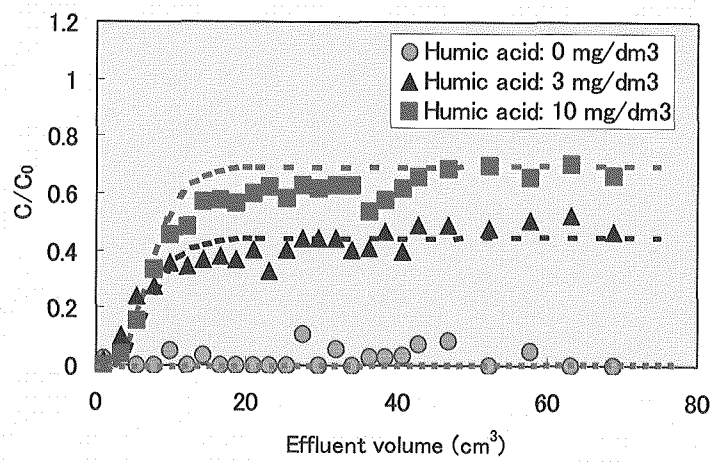

Fig. 4.1-4 Effects of humic acid on migration of ^{241}Am in granite column (Two species model was fitted to the measurement (●, ▲, ■).)

This is a blank page.

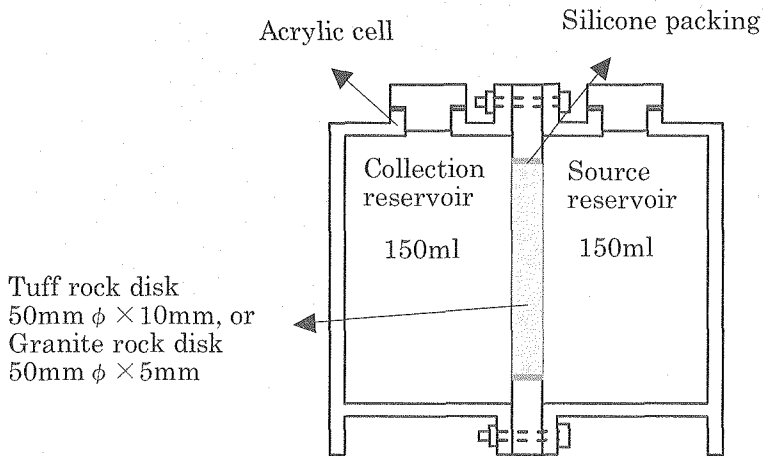

Fig. 4.1-5 Through-diffusion cell (For HA tests, aqueous solution in the source reservoir is doped by Am, which diffuses into the collection reservoir through the tuff rock disk. For alkaline tests, the source reservoir is filled with alkaline solutions to allow alkaline species to diffuse into the collection reservoir through the granite rock disk)

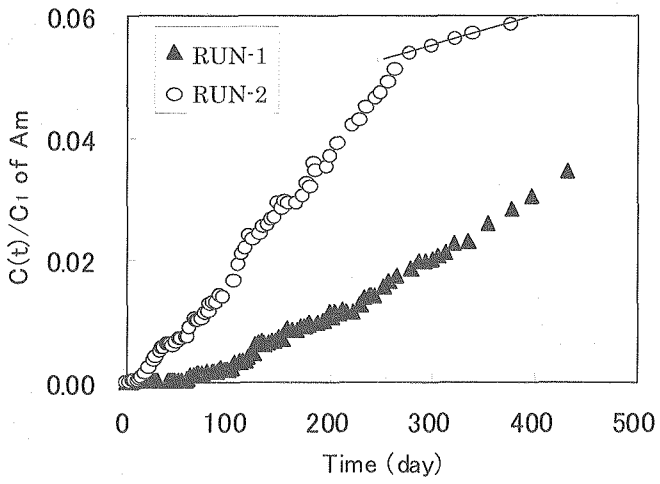

Fig. 4.1-6 Concentration of Am in the collection reservoir (C(t): Concentration of Am in collection reservoir, C_1: Concentration of Am in the source reservoir after the time of 320 days (5.6×10^{-6} mol/m^3))

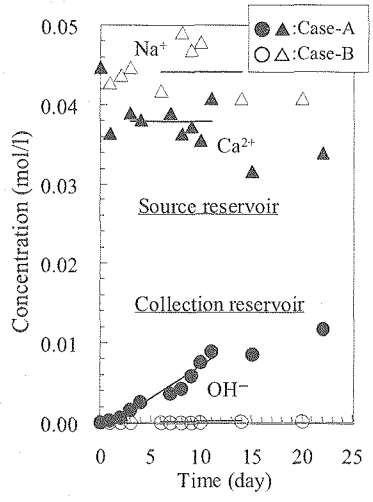

Fig. 4.1-7 Concentrations of OH^-, Ca^{2+} and Na^+ in the source and collection reservoirs (Case A: cement-equilibrated, Ca^{2+}-rich aqueous solution, Case B: NaOH solution of the same pH as the Case A)

4.2 Performance Assessment of Engineered Barriers

Performance of engineered barriers and waste forms and their evolution with time are required to be quantified for the long-term safety assessment of radioactive waste disposal. JAEA has been investigating long-term alteration of bentonite buffer materials. JAEA also studies chemical durability of molten & solidified waste form. Solubility, diffusion in and sorption behavior on engineered barrier materials are studied for selected long-lived radionuclides to provide supporting data for the safety assessment and the uncertainty analysis.

4.2.1 Barrier Performance of Molten & Solidified Wastes

Melting technique is thought to be one of effective methods to produce stable, chemically homogenous, and compacted waste form. The chemical durability of this waste form called molten solidified slag, under disposal environments was studied. Waste repositories are rich in iron and cement based materials, and their effects on waste form durability should be understood. In the fiscal years of 2004 and 2005, static dissolution tests were conducted for simulated SiO_2-CaO-Al_2O_3 slag in the presence of cement and corrosion products of iron.

Figure 4.2-1 shows the results of the static dissolution tests for the slag in the presence of simulated corrosion products of goethite (α-FeOOH), haematite (α-Fe_2O_3) and magnetite (Fe_3O_4) [1]. The dissolution of slag was enhanced in the presence of the corrosion products of iron. This was probably because of the lower concentration of silicon, main component of slag matrix, in the contacting aqueous solutions; dissolved silicon is removed from the solution by sorbing on the corrosion products of iron, and more silicon is supplied from the slag

The similar mechanism is likely to occur for the slag dissolution in the presence of cement based materials. Figure 4.2-2 shows the slag dissolution as a function of time in the presence of cement [2]. The dissolution rate of the slag was unexpectedly kept constant during the tested period up to 144 days. Dissolution of the slag was followed by precipitation of calcium silicate hydrates, which depressed the concentration of silica in the contacting aqueous solution and maintained the solution far from the saturation with respect to silicon. The far-from-saturation state is likely to be a cause of the interminable dissolution of the slag [3].

We have started applying a melting solidification treatment to spent nuclear fuel hulls. They are highly radioactive waste generated from nuclear fuel reprocessing, and a major source of radioactive carbon, ^{14}C. Metallic zirconium, the main component of fuel hull, was melted with metallic copper (Zr/Cu=8/2 in weight) at 1200 °C under an argon atmosphere to form a zirconium-copper alloy ingot [4, 5]. Carbon was remained in the produced zirconium-copper alloy (Table 4.2-1). This result indicates that ^{14}C in spent fuel hull can be immobilized in the alloy through the melting & solidification treatment.

4.2.2 Alteration of Engineered Bentonite Barriers*1

Cement based materials will be used in radioactive waste repositories, and induce highly alkaline environments in the repositories. The alkaline environments will alter montmorillonite, the main constituent of bentonite buffer materials, and are likely to cause the physical and/or chemical properties of the buffer materials to deteriorate. We focus our experimental efforts on predicting long-term variations in hydraulic conductivity of compacted sand-bentonite mixture, a candidate material of the buffer; the variations induce major uncertainties in radionuclide migration analysis and have not been quantitatively understood. The prediction requires mathematical models and a number of input parameters. We conducted experiments to obtain the dissolution rate of montmorillonite in, the diffusivity of hydroxide ions in and the hydraulic conductivity of the compacted sand-bentonite mixtures. A computer code, MC-BENT, which couples mass transport and chemical reactions was developed. We also started experimental and modeling study to estimate the highly alkaline environments induced by cement based materials.

The dissolution rate of montmorillonite was obtained through a time-dependent variation in the quantity of montmorillonite in the compacted sand-bentonite mixtures placed in Si- and Al-adjusted Na-Cl-OH solutions [6,7]. Temperatures were selected to be 50 °C to 170 °C, and concentrations of OH^- of 0.1 to 1.0 mol/dm^3. The X-ray diffraction patterns of specimens indicated the decreases of montmorillonite and crystalline silica with time and the formation of a secondary mineral, analcime ($NaAlSi_2O_6$). The amount of montmorillonite decreased linearly with time, which yields the dissolution rate of montmorillonite as the rate of density decrease (R_A, Mg/m^3/s) from the slope. The obtained dissolution rates are shown in Fig. 4.2-3. The dissolution rate was formulated as $R_A = 3.5(a_{OH^-})^{1.4}\, e^{(-51000/RT)}$, where a_{OH^-} is the OH^- activity in the solution, R the gas constant (8.314 J/mol/K) and T the absolute temperature (K). The dependence on the a_{OH^-} observed in this study for compacted sand-bentonite mixtures is different from the ones expected for loose clay materials which is proportional to the 0.15th – 0.34th power of a_{OH^-} [9, 10]. Possible gaps between a_{OH^-} in bulk of the alkaline solutions and that in the pore water in compacted sand-bentonite mixtures is likely to be a cause of the difference in the a_{OH^-} dependence [11].

The diffusivity of hydroxide ions in compacted sand-bentonite mixtures was measured in the temperature range of 10 to 90 °C as presented in Fig. 4.2-4 and formulated as $D_e = 5.0\times10^{-7}\, \phi^{2.1}\, e^{(-18600/RT)}$ where ϕ is the porosity of the sand-bentonite mixtures [6-8]. The hydraulic conductivity, K (m/s), was also measured for sand-bentonite mixtures of different montmorillonite contents using NaCl solutions of 0.1 to 1.0 mol/dm^3 [8] (Fig. 4.2-5). The data were approximated by $K = 1.2\times10^{-7}\, I^{1.5}\, 10^{-4.2\rho_{mont}}$, where I (mol/dm^3) is the ionic strength of the

*1 This work was entrusted from the Nuclear and Industrial Safety Agency of Japan.

solution and ρ_{mont} the effective montmorillonite dry density (Mg/m^3).

In order to predict the time- and space-dependent hydraulic conductivity of bentonite buffer materials in radioactive waste repositories, a coupled mass-transport / chemical-reaction computer code, MC-BENT, was developed [12, 13]. MC-BENT enables us to estimate long-term alteration of bentonite buffer materials accompanied with space- and time-dependent changes in porosity, hydraulic conductivity and diffusivity. A widely-used and verified geochemical code, PHREEQC, is in charge of the chemical reaction calculations. Instead of using mass transport analysis equipped with PHREEQC, we newly installed a subroutine program by which space-dependent mass transport parameters (diffusivity, hydraulic conductivity and porosity) and their changes with time as a result of dissolution and formation of minerals are available. The subroutine program deals with both diffusion and advection. The finite volume method was applied in MC-BENT to allow variable mesh sizes. We added the capability for calculation of a 2-dimensional system that is essential to dealing with space-dependent hydraulic conductivity. We also added the capability of calculating heat transfer to provide time- and space-dependent temperature because the dissolution rate of montmorillonite and diffusion of alkali components in bentonite buffer strongly depend on the temperature. This code was able to reproduce changes in concentration of major species and montmorillonite contents observed in lab-scale experiments on the bentonite alteration. This is an indication of partial verification of our calculation [8, 12, 13].

The MC-BENT is expanded to incorporate evolution of cement based materials, a source of alkaline groundwater. For that purpose, we need information on the secondary mineral formation in the cement based materials, long-term changes in the porosity, and diffusivity of ions in the evolved cement based materials. We have initiated alteration experiments of hardened cement paste to develop a secondary mineral formation model, and transport-pore clogging experiments to develop a porosity change model [14].

4.2.3 Data Acquisition on Radionuclide Migration*2

(1) Solubility of radionuclides

Effects of pH and ionic strength of aqueous solutions on the solubility of Sn, Zr [15, 16] and Se [17, 18] have been investigated. These elements were selected because ^{126}Sn, ^{93}Zr and ^{79}Se are important radionuclides in safety assessments of groundwater scenario for HLW disposal.

To quantify the solubility in case of repositories in coastal areas, we measured the solubility of Sn at high ionic strengths of 0.1, 1.0 and 2.0 M in the pH range between 4 and 13. The solubility was independent of the pH in the pH range 4 - 8 and increased with pH,

*2 This work was entrusted from the Nuclear and Industrial Safety Agency of Japan.

which is attributed to formation of $Sn(OH)_4(aq)$, $Sn(OH)_5^-$ and $Sn(OH)_6^{2-}$ (Fig. 4.2-6). Therefore, the dissolving reactions of Sn can be described as

$$Sn(OH)_4(s) = Sn(OH)_4(aq), \quad (1)$$

$$Sn(OH)_4(s) + OH^- = Sn(OH)_5^- \text{ and} \quad (2)$$

$$Sn(OH)_4(s) + 2OH^- = Sn(OH)_6^{2-}. \quad (3)$$

The equilibrium constants were determined for each ionic strength and the one for infinite dilution, $I = 0$, and specific ion interaction coefficients between species M and N, ε(M, N), were estimated by the Specific ion Interaction Theory regression. The equilibrium constants were determined to be $\log K_1^0 = -7.0 \pm 0.5$ for the reaction (1), $\log K_2^0 = -1.89 \pm 0.24$ for the reaction (2) and $\log K_3^0 = 1.3 \pm 0.5$ for the reaction (3), and the ion interaction coefficients were determined to be $\varepsilon(Sn(OH)_5^-, Na^+) = -0.15 \pm 0.18$ and $\varepsilon(Sn(OH)_6^{2-}, Na^+) = 1.3 \pm 0.5$.

The solubility of Zr was measured at pH higher than 11. The concentration of Zr increased with pH at pH > 13 with the slope of 2. Therefore, the dissolving reactions of Zr at pH > 13 can be described as

$$Zr(OH)_4(s) + 2OH^- = Zr(OH)_6^{2-} \quad (pH > 13). \quad (4)$$

The concentration of Zr was under the detection limit ($10^{-7.2}$ M = 6.4×10^{-8} M) at pH < 13. The dissolving reactions of Zr at pH < 13 are assumed as

$$Zr(OH)_4(s) = Zr(OH)_4(aq) \text{ and} \quad (5)$$

$$Zr(OH)_4(s) + OH^- = Zr(OH)_5^-. \quad (6)$$

The equilibrium constants at $I = 2$ were determined to be $\log K_4 = -5.22 \pm 0.07$ for the reaction (4), $\log K_5 < -7.2$ for the reaction (5) and $\log K_6 < -6.1$ for the reaction (6) respectively.

The solubility of Se was measured at high ionic strengths of 1.0 and 2.0 M in the pH range between 5 and 13 under the anaerobic conditions. The dominant species of Se were presumed to be HSe^- at the pH range between 5 and 8, and Se_4^{2-} at the pH range between 10 and 13. Therefore, the dissolving reactions of Se can be described as

$$Se(cr) + H^+ + 2e^- = HSe^- \text{ and} \quad (7)$$

$$4Se(cr) + 2e^- = Se_4^{2-}. \quad (8)$$

The equilibrium constants at zero ionic strength were determined to be $\log K_7^0 = -6.6 \pm 0.2$ for the reaction (7) and $\log K_8^0 = -16.6 \pm 0.3$ for the reaction (8), and the specific interaction coefficients were determined to be $\varepsilon(HSe^-, Na^+) = 0.24 \pm 0.09$ and $\varepsilon(Se_4^{2-}, Na^+) = -0.06 \pm 0.20$.

(2) Diffusivity of radionuclides

For a probabilistic safety assessment of groundwater migration scenario for radioactive waste disposal, it is necessary to quantify variations in the diffusivity of radionuclides in engineered barrier system. The diffusivity of radionuclides in bentonite buffer can be affected by porosity, montmorillonite content, chemical composition of pore water, temperature and redox conditions.

We performed a series of diffusion experiments of Sn, Pb, Cs, Sr and I in sand-bentonite

mixtures with the porosity of 40% for 3 types of solutions, 0.01 M NaCl, 0.5 M NaCl and 0.5 M NaOH solutions to clarify the effect of the chemical composition of the pore water on the diffusivity. The diffusivity of Cs was $(1.17\pm0.14)\times10^{-9}$ m²/s, $(3.3\pm1.0)\times10^{-10}$ m²/s and $(3.6\pm1.1)\times10^{-10}$ m²/s, respectively [15]. The diffusivity of I was $(7.6\pm1.7)\times10^{-12}$ m²/s, $(6.0\pm1.2)\times10^{-11}$ m²/s and $(5.3\pm0.6)\times10^{-11}$ m²/s, respectively [19]. The variation in the diffusivity produced by the chemical composition of the pore water was a factor of 4 (0.6 orders of magnitude) for Cs and 1 order of magnitude for I (Fig. 4.2-7). The diffusivity of other elements is being investigated.

To investigate effects of montmorillonite content on the diffusivity, we performed a series of diffusion experiments of Cs and I in 3 types of diffusion medium, altered bentonite, bentonite/sand (1:9) mixture and bentonite/sand (7:3) mixture, with the porosity of 60% under the anaerobic conditions [17, 20]. The diffusivity of Cs was $(4.0\pm1.5)\times10^{-10}$ m²/s, $(7.5\pm1.3)\times10^{-11}$ m²/s and $(5.2\pm0.4)\times10^{-10}$ m²/s, respectively, and was increased with the montmorillonite content. The variation in the diffusivity was caused by surface diffusion of Cs on the montmorillonite, and it was determined to be a factor of 7 in proportion to montmorillonite content. In contrast, the diffusivity of I was decreased with the montmorillonite content, $(7.5\pm0.4)\times10^{-11}$ m²/s, $(1.4\pm0.1)\times10^{-10}$ m²/s and $(5.8\pm0.2)\times10^{-11}$ m²/s, respectively. The variation in the diffusivity of I was caused by anion exclusion in confined pore space in the compacted media, and it was estimated to be a factor of 3 (Fig. 4.2-7).

(3) Sampling and treatment of rock cores and groundwater under reducing environments of deep underground

For investigations of geochemical properties such as rock-radionuclide interactions and diffusivity of radionuclides in the deep underground, it is necessary to provide undisturbed rock cores maintaining reducing environments of deep underground and in situ groundwater. We have started our experimental study with establishing a method of sampling and treatment of undisturbed rock cores and groundwater under maintained reducing environments of deep underground for sorption experiments [21]. Undisturbed rock cores and contacting groundwater were sampled from a Neogene's sandy mudstone layer at depth of 100 to 200 m and transferred into an Ar gas atmospheric glove box with minimized exposure to the air. The reducing conditions of the sampled groundwater and rock cores were examined in the Ar atmospheric glove box by measuring pH and Eh of the groundwater sample. The rock cores and the groundwater are used to investigate sorption of key elements on the rock. Variation in the distribution coefficients with the concentration of $NaNO_3$ and NaCl will be determined.

4.2.4 Analysis of Uncertainties with Solubility and Dissolution Rate of Waste Glass*3

(1) Uncertainty analysis on solubility of radionuclides

Solubility is a key parameter for safety assessment of geologic disposal of radioactive waste. The uncertainty of the solubility value consists of that associated with thermodynamic data and that with groundwater chemistry. JAEA has developed a computer code to estimate the uncertainty of solubility of radionuclides from those two factors. The uncertainty was calculated for the Se and Np solubilities by using data on pore water chemistry in buffer materials and representative thermodynamic database, EQ3/6-TDB and JNC-TDB.

The results of the uncertainty analysis show that the highly effective parameters of groundwater chemistry are identified as Eh, pH and the iron concentration for Se, and Eh, pH and the carbonate concentration for Np. A difference in uncertainty of the Se solubility between calculations employing EQ3/6-TDB and JNC-TDB is due to the uncertainty value given to the equilibrium constant for iron selenide, $FeSe_2$. For Np, the difference occurs due to the different assumption on the solubility limiting solid, Np(IV) carbonate complex, $Np(CO_3)_4^{4-}$, in EQ3/6-TDB and carbonato-hydroxo complex, $Np(CO_3)_2(OH)_2^{2-}$, in JNC-TDB. The difference in the solubility values is shown in Fig. 4.2-8 [22].

(2) Uncertainty analysis: Effects of waste glass uncertainty on radionuclide migration

JAEA has developed a probabilistic safety assessment code GSRW-PSA for HLW disposal system. An uncertainty and sensitivity analysis program was installed to quantify the effects of evolution of waste glass on radionuclide migration rates. Time dependent dissolution/alteration parameters of waste glass are given to the program. The GSRW-PSA was applied to ^{135}Cs.

The ^{135}Cs flux at the engineered/natural barrier boundary is sensitive to the time dependence of glass dissolution parameters. The flux at the natural barrier/biosphere boundary is not sensitive. This is because migration of ^{135}Cs is highly sensitive to sorption onto the host rock, natural barrier, and accordingly the variation in glass dissolution parameters is masked [23].

References

(1) T. Mizuno, *et al.*, "Aqueous corrosion of a SiO_2-Al_2O_3-CaO slag in the presence of iron oxides," Annual Meeting of the Atomic Energy Society of Japan, M19, Tokai Univ. (2005), [in Japanese].

(2) T. Maeda, *et al.*, "Dissolution of slag in the presence of cement," Annual Meeting of the Atomic Energy Society of Japan, M18, Tokai Univ. (2005), [in Japanese].

*3 This work was entrusted from the Nuclear and Industrial Safety Agency of Japan.

(3) T. Maeda, *et al.*, "Dissolution behavior of slag in the presence of cement," *Nihon-Genshiryoku-Gakkai Shi* (*J. At. Energy Soc. Jpn.*), 4[4], 242 (2005), [in Japanese].

(4) T. Mizuno, *et al.*, "Immobilization of carbon 14 contained in spent fuel hulls through melting-solidification treatment," *Proc. Int. Conf. ATALANTE2004*, Nimes, France, Jun. 21-24, 2004, p.3-20 (2004).

(5) T. Mizuno, *et al.*, "Development of immobilization technique of carbon-14 contained in spent fuel hulls through melting-solidification treatment; investigation of carbon retention in the ingot," Fall Meeting of the Atomic Energy Society of Japan, F4, Kyoto Univ. (2004), [in Japanese].

(6) S. Nakayama, *et al.*, "Dissolution of montmorillonite in compacted bentonite by highly alkaline aqueous solution and diffusivity of hydroxide ions," *Appl. Clay Sci.*, 27, 53 (2004).

(7) T. Yamaguchi, *et al.*, "Experimental study on dissolution of montmorillonite in compacted sand-bentonite mixture under Na-Cl-OH pore-water conditions," *Proc. Int. Workshop on Bentonite-Cement Interaction in Repository Environ.*, April 14-16, 2004, Tokyo, NUMO-TR-04-05, p. A3-54 (2004).

(8) T. Yamaguchi, *et al.*, "Experimental and modeling study on long-term alteration of compacted bentonite with alkaline groundwater," *presented at 2nd Intl. Meeting Clays in Natural & Engineered Barriers for Radioactive Waste Confinement*, Tours, France, Mar. 14-18, 2005, to be published in Appl. Clay Sci. (2005).

(9) T. Sato, *et al.*, "Dissolution mechanism and kinetics of smectite under alkaline conditions," *Proc. Int. Workshop on Bentonite-Cement Interaction in Repository Environ.*, April 14-16, 2004, Tokyo, NUMO-TR-04-05, p. A3-38 (2004).

(10) T. Tanaka, *et al.*, "Long-term Alteration of Bentonite - for Safety Evaluation of Deep Geological Disposal," *Proc. Int. Symp NUCEF 2005*, Tokai, Japan, Feb. 9-10, 2005, JAERI-Conf 2005-007, Japan Atomic Energy Research Institute, p. 105 (2005).

(11) Y. Sakamoto, *et al.*, "Dissolution of montmorillonite in compacted sand-bentonite mixtures by alkaline solution," *presented at the 13th International Clay Conference 2005*, Tokyo, Japan, Aug. 21-27, 2005, Poster: P25-41 (2005).

(12) M. Takazawa, *et al.*, "Modeling of variation in permeability of compacted bentonite with alkaline fluid for long-term safety assessment of geological disposal system," *Proc. Int. Workshop on Bentonite-Cement Interaction in Repository Environ.*, April 14-16, 2004, Tokyo, NUMO-TR-04-05, p. A3-59 (2004).

(13) M. Takazawa, *et al.*, "Experimental and modeling study to predict long–term alteration of bentonite buffer materials with alkaline groundwater," *Proc. Int. Symp NUCEF 2005*, Tokai, Japan, Feb. 9-10, 2005, JAERI-Conf 2005-007, Japan Atomic Energy Research Institute, p. 236 (2005).

(14) K. Negishi, *et al.*, "Experimental and modeling study on effect of cement degradation on

alteration of bentonite buffer material," *presented at the 13th International Clay Conference 2005*, Tokyo, Japan, Aug. 21-27, 2005, Poster: P25-37 (2005).

(15) T. Yamaguchi, et al., "Experimental study on long-term safety assessment considering uncertainties for geological disposal of radioactive wastes: JAERI status at 2005," Proc. of GLOBAL 2005 Intl. Conf., Oct. 9-13, 2005, Tsukuba, in press? (2005).

(16) T. Yamaguchi, et al., "Evaluation of uncertainty associated with parameters for long-term safety assessment of geological disposal," Proc. Intl. Symp. NUCEF 2005, Feb. 9-10, 2005, Tokai, JAERI-Conf 2005-007, p. 150 (2005).

(17) Y. Iida, et al., "Data acquisition on migration of radionuclides under deep geological environments," Proc. Intl. Symp. NUCEF 2005, Feb. 9-10, 2005, Tokai, JAERI-Conf 2005-007, p. 230 (2005).

(18) Y. Iida, et al., "Experimental Study for Evaluation of Selenium Solubility (1) Selenium Solubility at High Ionic Strength." Annual Meeting of the Atomic Energy Society of Japan, M54, Tokai Univ. (2005).

(19) Japan Atomic Energy Research Institute, "H16, Research on long-term safety assessment methodology for radioactive waste disposal," Japan Atomic Energy Research Institute, (2005), [in Japanese].

(20) Y. Iida, et al., "Diffusivity of radionuclides in altered sand-bentonite mixtures." Fall Meeting of the Atomic Energy Society of Japan, L49, Hachinohe Institute of Technology. (2005), [in Japanese].

(21) K. Ebashi, et al., "Sampling and treatment of rock cores and groundwater under reducing environments of deep underground," Proc. Intl. Symp. NUCEF 2005, Feb. 9-10, 2005, Tokai, JAERI-Conf 2005-007, p. 242 (2005).

(22) S. Takeda, *et al.*, "Estimate of solubility uncertainties on probabilistic geochemical calculation", 2005 Annual Meeting of the Atomic Energy Society of Japan, Tokai Univ. (2005), [in Japanese].

(23) K. Yotsuji, *et al.*, "Estimation of uncertainties associated with long-term dissolution scenario of waste glass", 2005 Fall Meeting of the Atomic Energy Society of Japan, Hachinohe Institute of Technology (2005), [in Japanese].

Table 4.2-1 Concentration of carbon before/after melting and retention of carbon in zirconium-copper alloy ingot specimens

Ingot	Concentration of carbon (mg/kg)		Retention Ratio (C_1/C_0)
	before melting (C_0)	after melting (C_1)	
No.1	72 ± 23	87 ± 26	1.20 ± 0.37
No.2	72 ± 23	83 ± 40	1.16 ± 0.56
No.3	72 ± 23	70 ± 27	0.97 ± 0.38

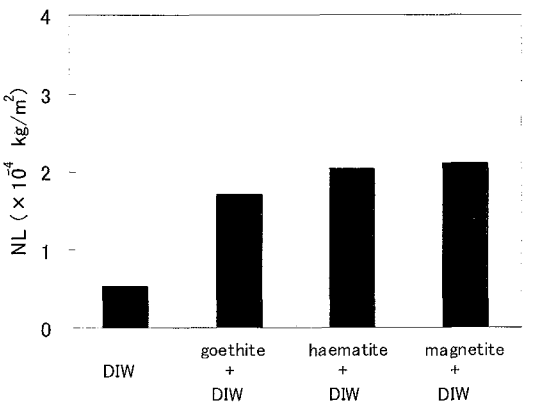

Fig.4.2-1 Normalized mass loss (NL) of boron for the slag specimen leached in deionized water (DIW) at 90 °C for 56 days in the presence and absence of corrosion products of iron (goethite, haematite and magnetite) (NL of boron is the index of the slag dissolution.)

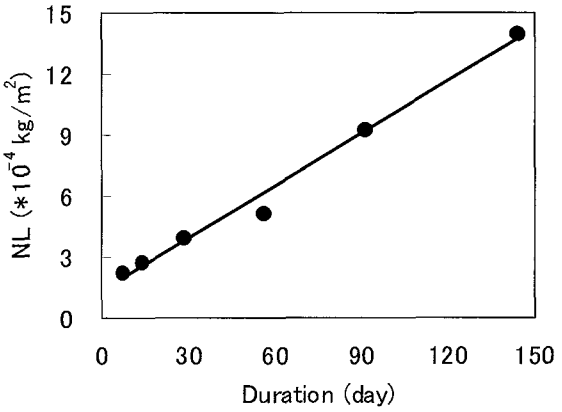

Fig.4.2-2 Normalized elemental mass loss (NL) of boron during leach tests for the slag specimens in the presence of cement at 90 °C (NL of boron is the index of the slag dissolution.)

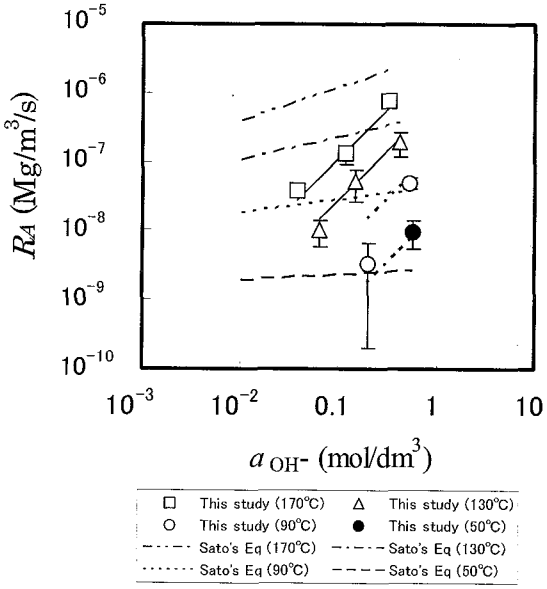

Fig. 4.2-3 Dependence of the montmorillonite dissolution rate, R_A (Mg/m^3/s), on temperature and on activity of OH^-, a_{OH^-}

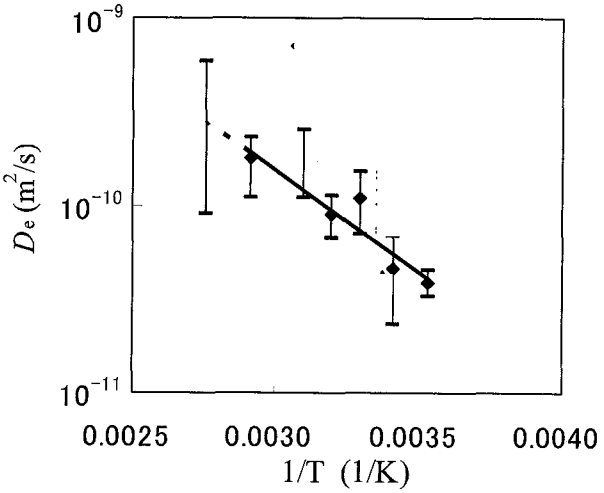

Fig. 4.2-4 Effective diffusivity, D_e (m^2/s), of hydroxide ions in compacted sand-bentonite mixtures at the temperature of 10 – 90 °C

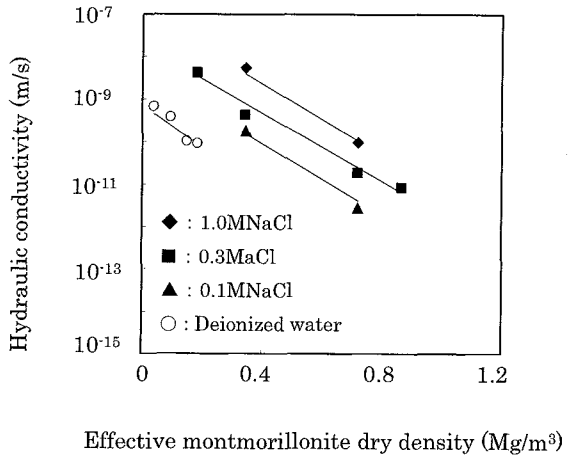

Fig. 4.2-5 Correlation between hydraulic conductivity of sand-bentonite mixtures and effective montmorillonite dry density for different NaCl concentrations in water

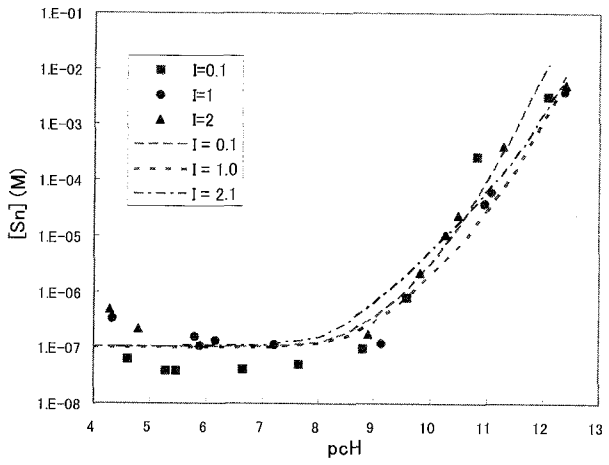

Fig. 4.2-6 Effects of pH (pcH) and ionic strength (I) on the solubility of Sn (The solubility was independent of pH in the pH range 4 - 8 and increased with pH at pH > 9, which is attributed to formation of $Sn(OH)_4(aq)$, $Sn(OH)_5^-$ and $Sn(OH)_6^{2-}$.)

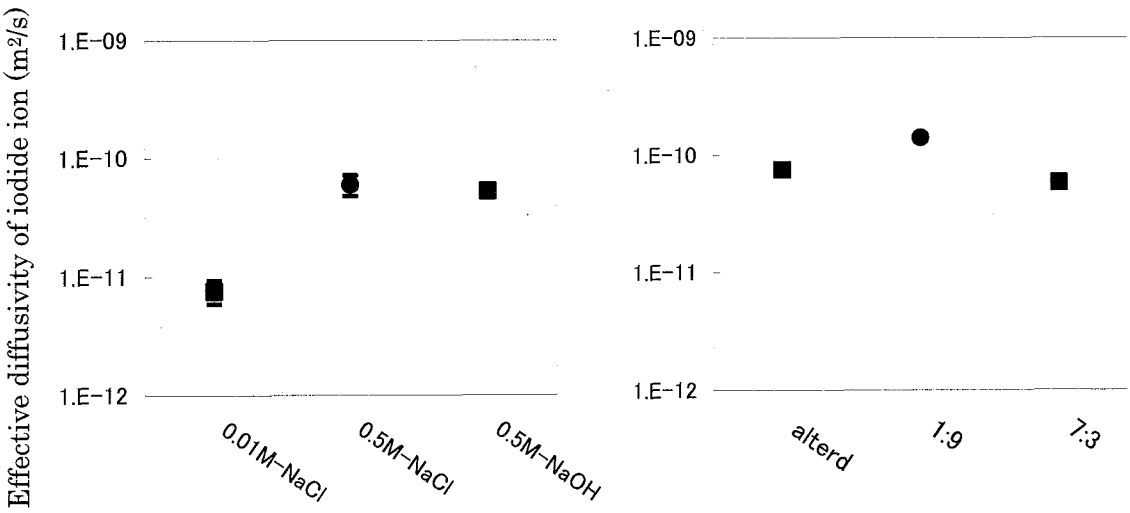

Fig. 4.2-7 Effects of chemical composition of contacting solutions (left) and montmorillonite content of diffusion medium (right) on the diffusivity of iodide ion (The variation in the diffusivity produced by the chemical composition of the contacting solutions was 1 order of magnitude and that by the montmorillonite content was a factor of 3.)

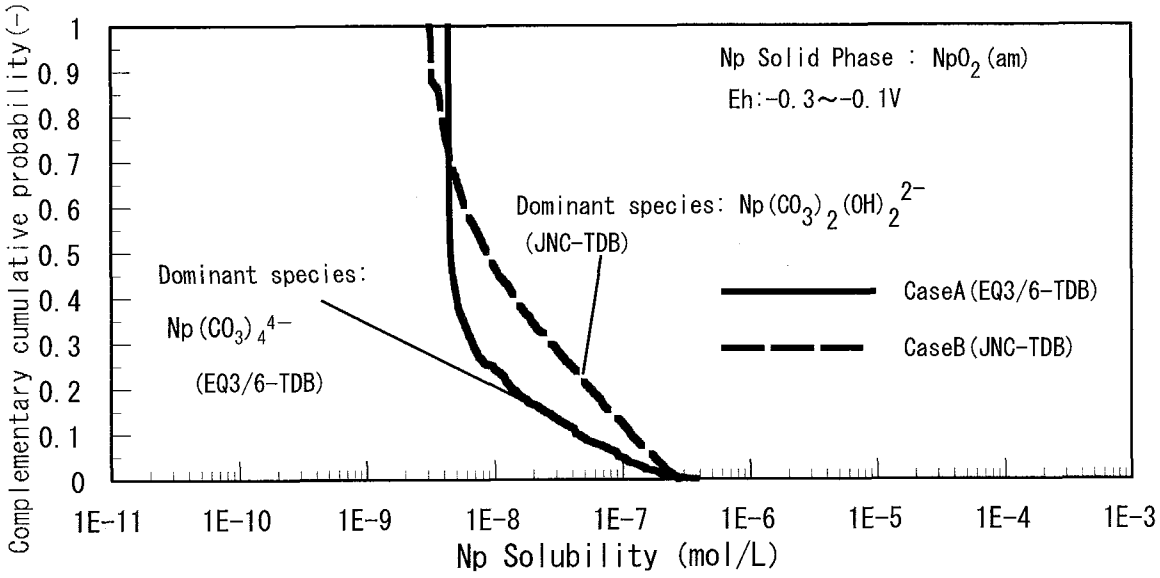

Fig.4.2-8 Uncertainty of Np solubility calculated using thermodynamic data in EQ3/6-TDB and JNC-TDB (The probability of the solubility exceeding 10^{-8} mol/L is remarkably higher in case B than in case A. This is because JNC-TDB used in case B includes data for $Np(CO_3)_2(OH)_2^{2-}$ and this species can dominate the concentration of Np under the groundwater composition assumed in the calculation.)

4.3 Determination of Clearance Level for Uranium and TRU Wastes*1

The deterministic and probabilistic safety assessment code, PASCLR, has been developed to derive the clearance level for uranium wastes and TRU waste. PASCLR calculates the radionuclide concentrations equivalent to the individual dose criterion (10 μSv/y) for disposal and recycle scenarios. The pathways of interest for the scenarios are schematically shown in Fig. 4.3-1 [1]. The clearance levels for 59 nuclides contained in uranium and TRU wastes were estimated from deterministic analyses. The probabilistic analysis was used to estimate parameter uncertainties for some selected exposure pathways.

The result of deterministic and probabilistic analyses for ^{234}U is shown in Fig. 4.3-2. Important exposure pathways for ^{234}U are inhalation of radon gas and ingestion of agricultural products in the disposal scenario. The radionuclide concentrations equivalent to 10 μSv/y obtained by deterministic analyses correspond to about 15^{th} percentile value in the cumulative distribution function, which was given by the probabilistic analyses. This comparison of probabilistic and deterministic analyses indicates that the parameter values used in the deterministic analysis are conservative. The most important exposure pathway for radionuclides of 4N to 4N+3 series other than ^{234}U, ^{235}U and ^{238}U was identified to be inhalation during unloading scrap metals in the recycle scenario [2].

References

(1) S. Takeda, *et al.*, "Development of PASCLR Code System to derive Clearance Levels of Uranium and Trans Uranium Wastes: User's Manual", JAEA-Data/Code, 2005 (in printing).

(2) M. Munakata, *et al.*, "Evaluation of clearance level of uranium and TRU waste", The 2^{nd} meeting of Application of Safety Assessment Methodologies for Near Surface Waste Disposal Facilities (ASAM), (2004).

*1 This work was entrusted from the Nuclear and Industrial Safety Agency of Japan.

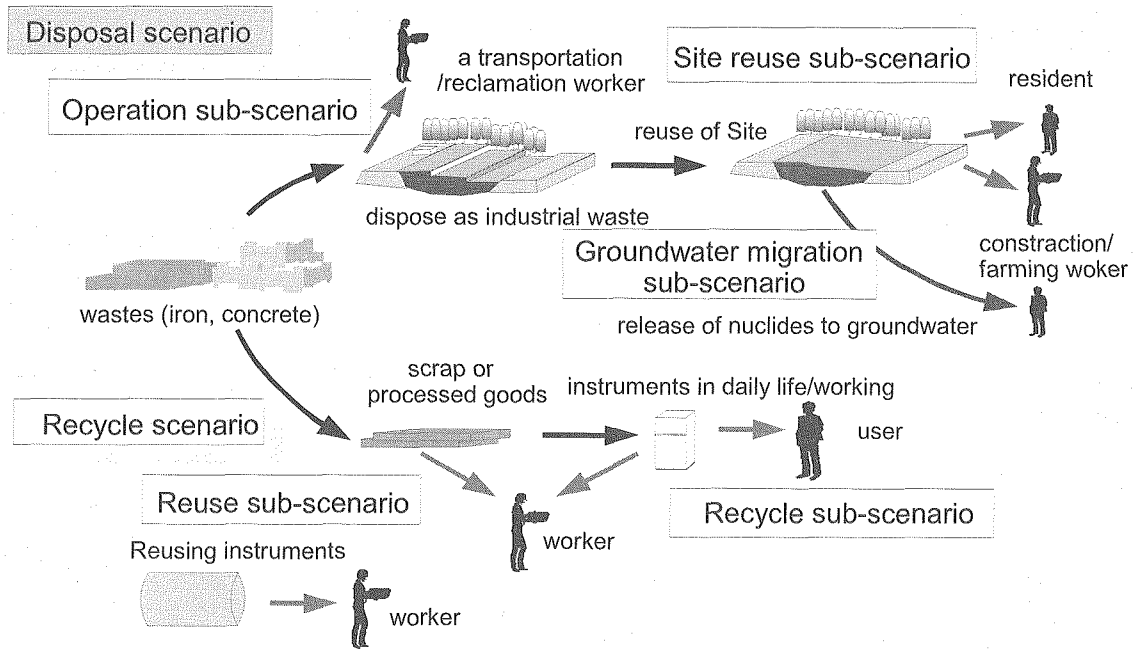

Fig. 4.3-1 Disposal and recycle scenarios for the clearance level calculation of uranium and TRU wastes

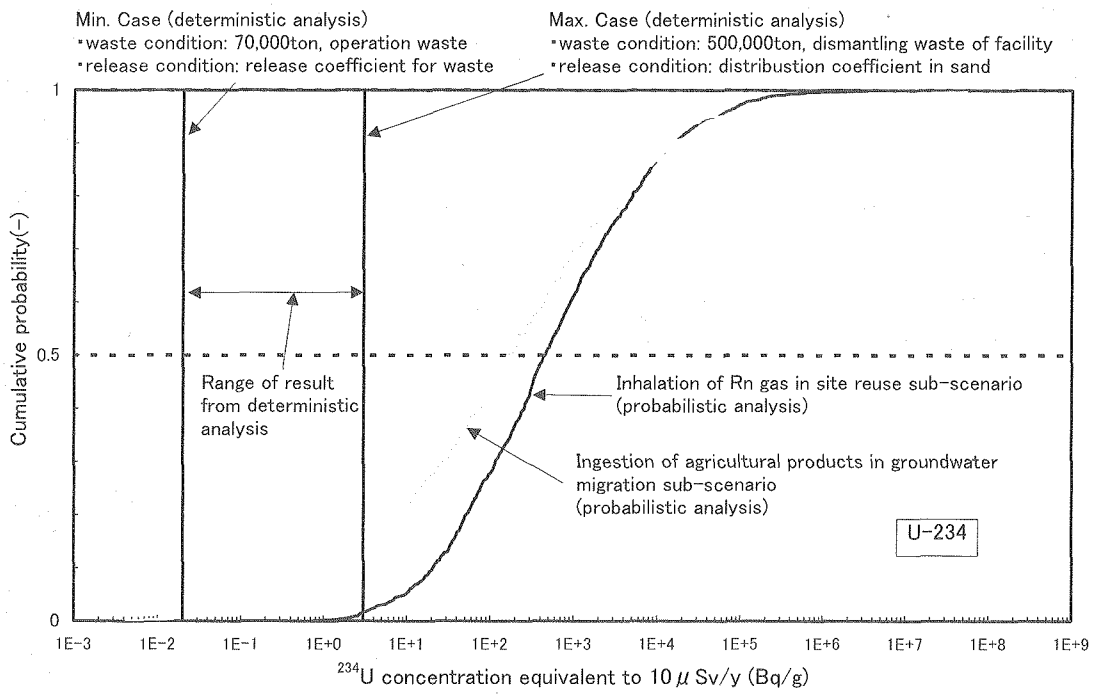

Fig. 4.3-2 Cumulative distribution function for the ^{234}U concentration equivalent to 10 μSv/y (The deterministic analyses were performed under some different conditions, e.g. amounts of waste disposed of and parameters for radionuclide release in the site reuse sub-scenario.)

4.4 Safety Evaluation for Decommissioning of Nuclear Facilities*1

The Nuclear Reactor Regulation Law was revised in May 2005 on the decommissioning of nuclear facilities and clearance system for arising waste. The revised part came into force in December, 2005, and decommissioning will be conducted according to the compliance requirements by the Law. A computer code, DecDose, for calculating the public dose was developed to assess safety during dismantling activities, and development of a dose assessment code for workers was initiated in 2005. Part of the clearance level verification procedure was demonstrated by using the past JPDR dismantling data to categorize arising materials out of radiological regulatory control.

4.4.1 Development of Dose Assessment Code for Decommissioning of Nuclear Power Plant

A dose assessment code, DecDose, has been developed [1] for use in regulatory review of applicant safety analyses. DecDose calculates public exposure doses for both the normal and accidental situations during dismantling nuclear power plants. For the normal situation, the annual discharge of radionuclides to the atmosphere and the ocean, which depends on the inventory and dismantling method applied, is calculated (Fig. 4.4-1). DecDose treats multiple exposure pathways including cloudshine, inhalation, surface ground deposition, ingestion of seafood after the release of radionuclides to the environment, and direct and skyshine radiation from temporarily stored radioactive waste. For the accidental situations, the short term exposure through cloudshine and inhalation caused by all of potential accidents is calculated. The radionuclide inventory is the amount of radionuclides that are accumulated on filters and stored in waste containers during normal dismantling activities, and is assumed to be released to the atmosphere with the progression of the accidental events,.

4.4.2 Simulation of Clearance Level Verification Work

JAEA has discussed fundamental concept of clearance level verification methodology and developed the procedure in 2003. A simulation study has been conducted since 2004 to examine the practicability of the developed procedure by using the waste arising from the dismantled Japan Power Demonstration Reactor, JPDR (1963-1996). The clearance verification procedure consists of three phases: preliminary survey, measurement and categorization, and storage and management. Our simulation study was devoted to the first 2 phases. As for the preliminary survey, we characterized target materials such as metal and concrete by referring survey results of JPDR facilities and its operational history.

The second phase, "measurement and categorization", includes selection of radionuclides to be evaluated and conversion of measured counting rates to concentration for the selected radionuclides. The conversion factor depends on physical characteristics of target waste

*1 This work was entrusted from the Nuclear and Industrial Safety Agency of Japan.

(dimension, shape and material), type of detector, and counting configuration. The computer simulation result (Fig. 4.4-2) shows that the conversion factor (Bq/g/cps) depends on the outer diameter of pipes.

In the verification simulation carried out for the dismantling wastes that had been generated from JPDR, radionuclides to be evaluated were selected according to the two-step selection method, which is based on a relative measure of significance and is proposed by Japan [2]. We, then, assigned radionuclide composition ratios, evaluated radionuclide concentrations by using the conversion factors, and evaluated the significance for clearance judgment. The conducted verification simulation showed practicability of proposed clearance procedure.

References

(1) T. Shimada, *et al.*, "Development of public dose assessment code for decommissioning of nuclear reactors (DecDose)" *Proceedings of The 10th International Conference on Environmental Remediation and Radioactive Waste Management*, Glasgow, United of Kingdom, Sept. 4-8, 2005, p.E-161 (2005).

(2) International Atomic Energy Agency, "Monitoring for compliance with exclusion, exemption, and clearance values," IAEA Safety Report Series, to be published.

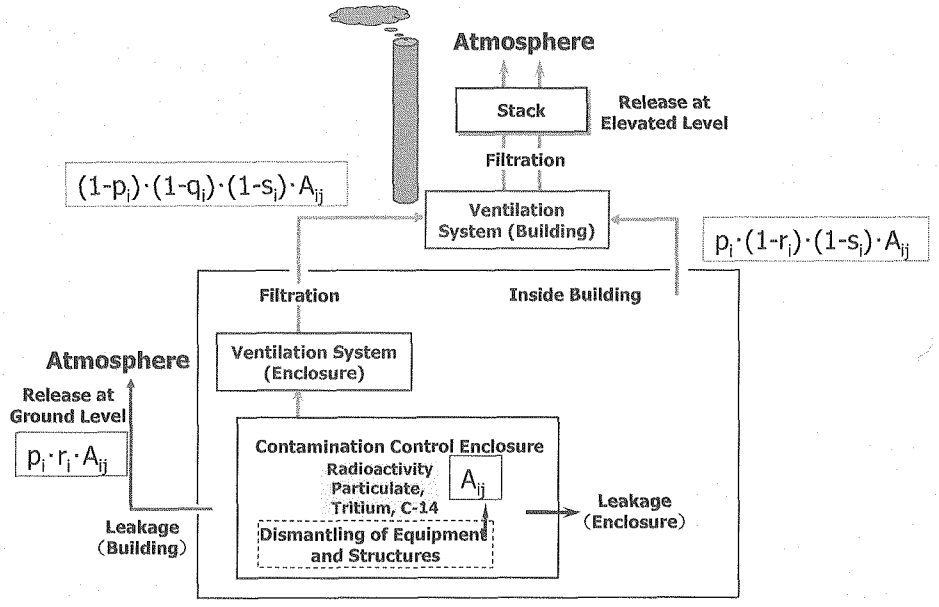

A_{ij} : Amount of radionuclide dispersed to the enclosure during dismantling using method j
p_i : leakage ratio from contamination control enclosure
q_i : filtering efficiency of local filter
s_i : filtering efficiency of building filter
r_i : leakage ratio from building

Fig. 4.4-1 Discharging routes of radionuclides from the building to the atmosphere in DecDose

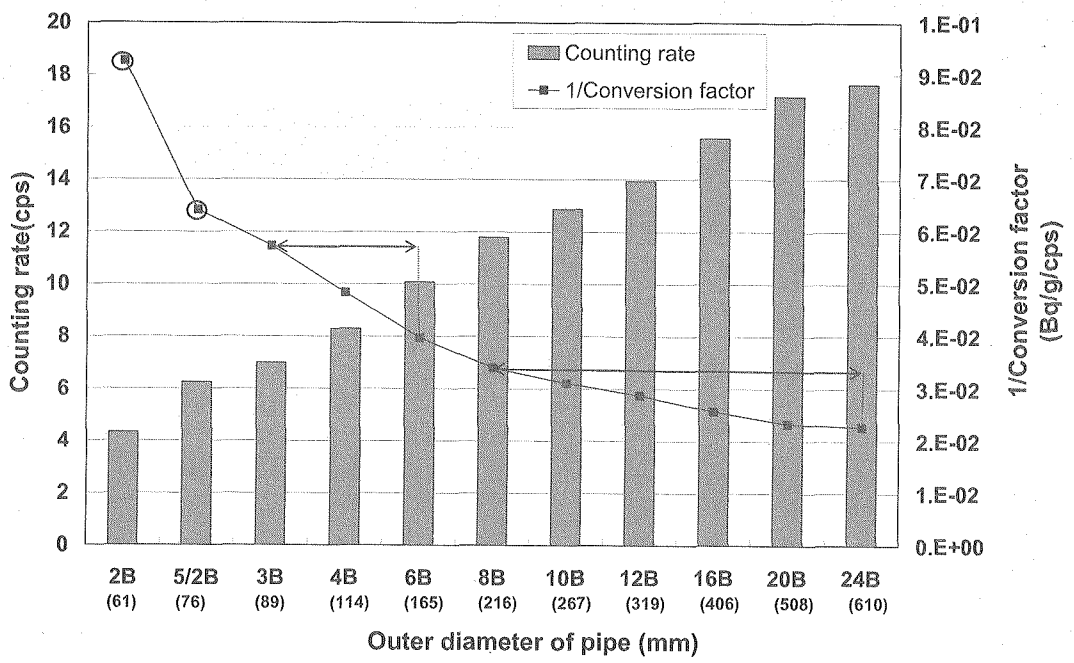

Fig. 4.4-2 Conversion factors from the measured counting rate (cps) to the radionuclide concentration (Bq/g) for pipes of different diameter (In practice, pipes are categorized into four groups; 8B-24B, 3B-6B, 5/2B and 2B. To ensure conservative assessments, the conversion factor for the pipe 8B is applied to the pipes of 8B-24B, that for the pipe 3B to the pipes of 3B-6B, that for the pipe 5/2B to the pipe 5/2B and that for pipe 2B to pipe 2B.)

5. RESEARCH ON ENSURING SAFETY OF NUCLEAR INSTALLATION WITH SOCIO-TECHNICAL APPROACH

Appropriate decision making, at various social levels, based on correct comprehension of situation is crucial for ensuring safety of nuclear installation. The decision makers involved are not only at the level of workers, but also at levels of company's management, regulatory officers of national and local government, and public citizen. It is essential for decision makers to have deep understanding of the functional structure of the technical system and acceptable operation boundaries for safety (safety boundaries). The information communications and sharing among the levels play an important role. Research on information systems for the communication has been carried out in JAERI, especially for plant safe operation at workers level, for safety management at management levels, and for safety related decision making at public citizen level. Concerning communication system for plant safe operation, an innovative function-boundary oriented human machine interface system based on Ecological Interface Design (EID) concept was developed, and its evaluation experiment was conducted. The interface system has been further extended into an innovative education/ training system DETRAS (Distanced Education/Training System on Reactor Simulator over Internet), which could be utilized for enhancing deep functional understanding of the system by management people, regulatory officer and public citizen as well as operators. Concerning communication system in organizational management, the JCO criticality accident in 1999 was analyzed in detail to reveal characteristics of a typical modern complex system.

5.1 Development of an Innovative Ecological Interface System [1-3]

The new developed interface system consists of six VDT terminals and two large display units(100 inch wide). The VDT terminals for each work station are placed adjacent to each other, so that operators can easily refer to the information on the two or more terminals in parallel. On the two large display units, graphical formats representing higher level of information at means-ends network, such as "Energy Balance in Reactor System" and "Mass Flow Distribution in Secondary System", are presented. As shown in Fig.5.1-1, the display page consists of five different areas such as (1)Information Display Area, where some sixty display formats can be called to be placed; (2)Monitor Area, where operation modes and their status are shown, (3)Alarm Indicator Area, in which active alarms are listed in a text format; (4)Control Panel Area, through which control actions on the reactor system are taken. There are about three hundred pages, each of which corresponds to equipment or switch controllable on the simulated reactor system. In this area, immediate prerequisite conditions for control and effects due to the change of the equipment state are placed together with objects representing switch; (5)Menu Area, in which menu buttons calling/changing

graphical display formats to the Information Display Area are placed. There are two types of menu, namely a)static menu and b)dynamic menu.

Adding to the graphical formats included in the existing simulator interface, five graphical display formats representing higher level information items at means-ends network were newly created. The display formats having been created are: (1)Energy Balance in Reactor System (see Fig.5.1-1), (2)Mass Balance in Primary System, (3)P-T Diagram with the Functional Relation of Related Process Parameters, (4)Mass Flow Distribution in Secondary System, and (5)State Diagram of Steam Generator. Among these, the display format of P-T Diagram is an extension of the diagram included in the existing interface system by adding P-T diagram representing a state of pressurizer and the functional relation of process parameters related.

Verification of the interface system was empirically conducted, that is, designers, by themselves, actually take several maneuvering actions on the simulator with several scenarios such as startup and shutdown of the reactor system as well as some abnormal situations including malfunction occurrence and, then, identify the problems and difficulties encountered in taking the actions with the interface. The problems and difficulties encountered are analyzed and are taken as a source of necessary modification of the interface system. Validation of the interface was then conducted with participation of experts for operating the NPP. The new interface was validated as actually supporting operators. Furthermore, it was found that the new interface was very effective also in promoting deep understanding of the system functional structure.

5.2 Development of an Innovative Distanced Education/ Training System over Internet [4-6]

JAERI, then, has extended the project for integrating the ecological interface system into an innovative education/ training system which utilizes the well advanced communication technology including broad-band Internet technology. Conceptual structure of DETRAS is shown in Fig.5.2-1 DETRAS consists of simulator center, and remote operation environment which is connected with the simulator operation center through internet and utilized for remote operation of a reactor simulator[4]. The simulator operation center is equipped with reactor simulators, PCs for monitoring and instructions, and PCs for control and web server. In the situation required, instructors could be present in the simulator operation center in order to support user's operation of a reactor simulator. Reactor simulators are implemented on MS-Windows 2000/ XP PCs, each of which is also equipped with communication server to control sending and receiving simulator data and simulator-control data between remote operation environment and simulator operation center. A user (individual or organization), who would like to operate the reactor simulator, could set up a remote operation environment on his/her PC (MS-Windows 2000/XP) by downloading and installing reactor operation interface (GUI and control) program and remote area communication server

process program for communication with the simulator operation center. The user could chose one of the following three types of remote operation environment which is suitable to his/her computer resource and objectives.

(a) Operation environment for remote training center with large display units and several CRTs for display and control,

(b) Multi CRTs operation environment , and

(c) Single CRT operation environment for individual's learning .

For each type of the remote operation environment, an operation interface (GUI and control program), which is dedicated to each environment respectively, could be provided.

DETRAS has a capability of full scope simulation of nuclear reactor behavior and structure. A user could choose simulation speed among 1 x, 2 x , 4 x and 8 x real time. Utilizing this function, a user could carry out simulation of start-up and shut-down repeatedly which would require long hours of real time. A user could restart simulation from the time point memorized (re-start function), and reproduce the simulation process from the desired time point (back-track function). Monitoring and Instruction

(1) User monitoring: An instructor could, monitor on his CRTs, the display pages used by the user and the mouse-cursor position.

(2) Instruction: The user could see, on his/her CRTs, a instructed point given with mouse-cursor by the instructor. With two-way audio-communication capability, the instructor could give users verbal instruction.

A prototype system of DETRAS was designed and implemented. And verification test was conducted with a modeled simulator center at JAERI Tokai site and remote operation environment outside of JAERI. The functions and performance of DETRAS was verified.

5.3 Analysis of the JCO Criticality Accident [7-9]

The JCO criticality accident in Tokai-mura, was analyzed using a framework based on cognitive systems engineering. Analyses were made from the point of view of both the system and actors, which include analysis in terms of the safety boundaries against criticality accident. It was found that incorrect mental models about the work system played a critical role in bringing on the accident and that such models were formed and influenced through several factors, such as, in terms of criticality safety, a poor system of education and training, lack of information in procedures and instructions, and no warning signs at workplaces. From these results we derived a set of immediate countermeasures and generalized lessons in order to prevent such an accident in future.

References

(1) Y. Yamaguchi and F. Tanabe, "Creation of Interface System for nuclear reactor

operation - Practical Implication of Implementing EID Concept on Large Complex System –", *Proc. of the IEA2000/HFES2000 Congress*, Vol.3 ,pp.571-574 (2000).

(2) Y. Yamaguchi and F. Tanabe, "Creation and Evaluation of an Ecological Interface System for Operation of Nuclear Reactor System", Enlarged Halden Program Group Meeting, Norway, (2002).

(3) Y. Yamaguchi and F. Tanabe, "Integration of Ecological Approach into a NPP Control Room and It's Empirical Evaluation, presented at the workshop meeting on innovative human system interface", Halden, Norway, 1-2 September, (2003)

(4) Y. Yamaguchi and F. Tanabe, "Development of Distanced Education/ Training System on Reactor Simulator over Internet DETRAS", *Transaction of Fall Meeting of Atomic Energy Sosciety of Japan*, September, (2005), [in Japanese].

(5) Y. Yamaguchi, Y. Imai and F. Tanabe, "Development of Prototype System of Distanced Education/ Training System on Reactor Simulator over Internet", *Proc. of Human Interface Symposium 2005*, September, (2005), [in Japanese].

(6) Y. Yamaguchi, Y. Imai and F. Tanabe, "Development of Distanced Education/ Training System on Reactor Simulator over Internet (DETRAS)", *Proc. of Enlarged Halden Programme Meeting*, Lirrehammer, Norway, October, (2005).

(7) F. Tanabe and Y. Yamaguchi, An Analysis of the JCO Criticality Accident: Lessons Learned for Safety Design and Management, Chapter 10, in "Emerging Demands for the Safety of Nuclear Power Operations", Ed. Itoigawa, Wilpert and Fahlbruch, CRS Press ,(2005).

(8) F. Tanabe and Y. Yamaguchi, "Human Factors Problems in Causes of the JCO Criticality Accident", *Proc. of the 46th Annual Meeting of the Japanese Ergonomics Society,* June, (2005), [in Japanese].

(9) F. Tanabe and Y. Yamaguchi, "Safety Boundaries Perception and Communication-Cause Analysis of the JCO Criticality Accident", *Proc. of the 22nd Annual Meeting of the Japanese Cognitive Science Society,* July, (2005), [in Japanese].

This is a blank page.

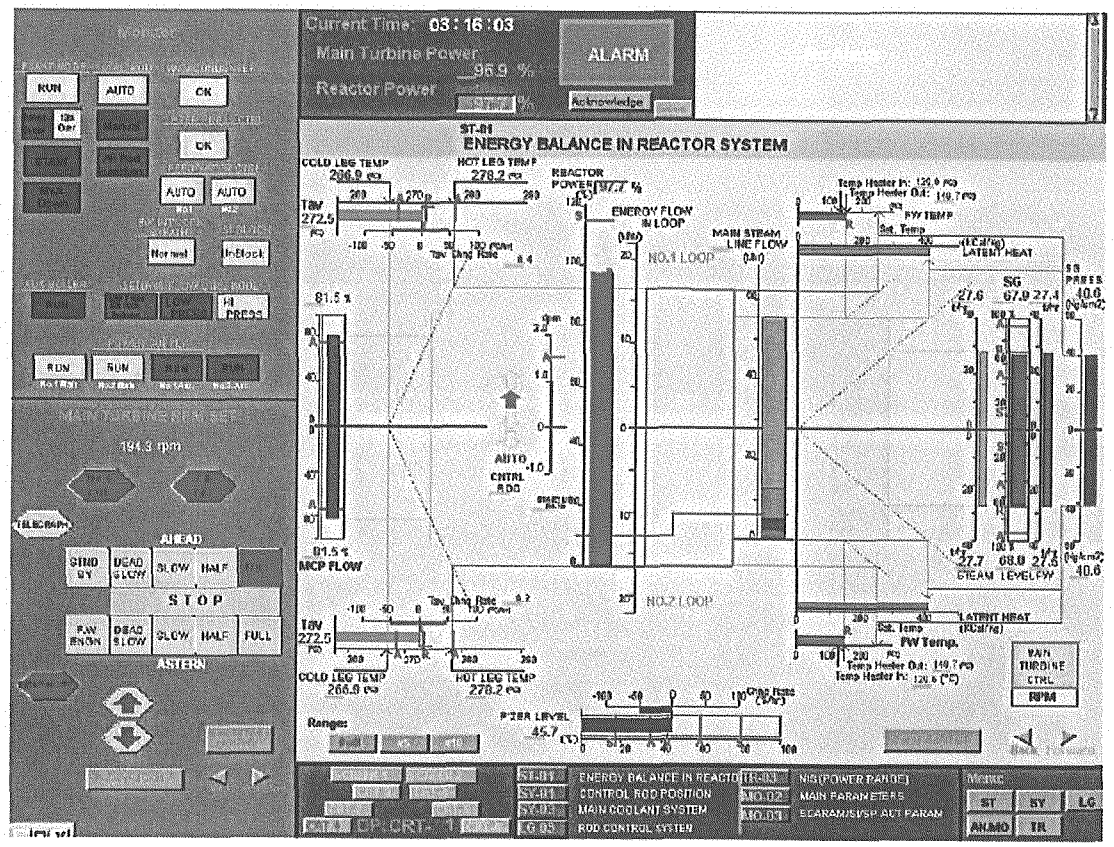

Figure 5.1-1 Example of new display pages and display format (system energy balance)

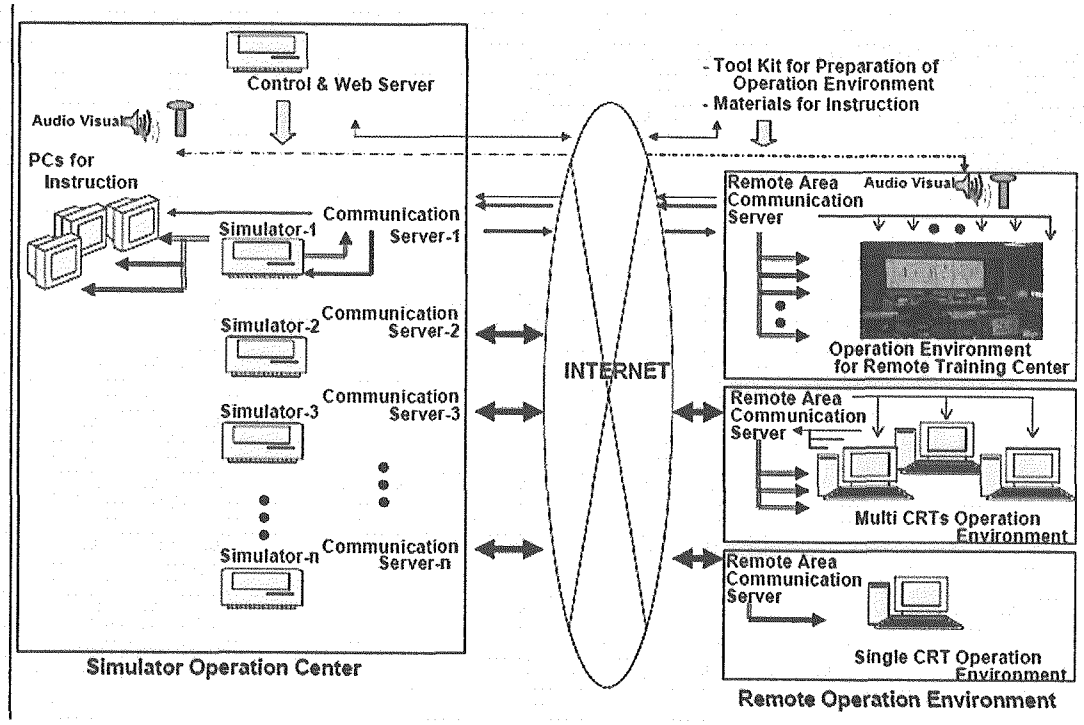

Figure 5.2-1 Conceptual structure of DETRAS (Distanced Education/Training System on Reactor Simulator over Internet)

This is a blank page.

6. TEST FACILITIES FOR SAFETY RESEARCH

Several large-scale test facilities had been utilized to perform nuclear safety research in JAERI, the predecessor of JAEA.

For examinations using high-radioactive material, JAERI had three hot laboratories, the Reactor Fuel Examination Facility (RFEF) for the post-irradiation examination of LWR fuel, the Research Hot Laboratory (RHL) for the post-irradiation examination of nuclear fuels and materials, and the Waste Safety Testing Facility (WASTEF) for examinations concerning corrosion behavior of the nuclear plant material and disposal of radioactive wastes from nuclear research facilities and other plants. The outline and utilization of these facilities are shown in the following section 6.1.

For fundamental researches on the nuclear fuel cycle and the radioactive waste management, JAERI had the Nuclear Fuel Cycle Safety Engineering Research Facility (NUCEF). The facility consists of the Static Experiment Critical Facility (STACY), the Transient Experiment Critical Facility (TRACY) and the Back-end Fuel Cycle Key Elements Research Facility (BECKY). STACY and TRACY are critical experiment facilities for criticality safety research in the nuclear fuel cycle. BECKY is an R&D facility on chemical separation in reprocessing, partitioning of high-level radioactive waste, management of TRU-containing waste and basic chemistry on TRU elements. The outline and utilization of the NUCEF are shown in the section 6.2.

For irradiation tests of nuclear fuels and materials, JAERI had the Japan Materials Testing Reactor (JMTR). The reactor is a tank-in-pool type, cooled and moderated by light water with maximum thermal power of 50MW. Irradiation tests have been recently conducted mainly for material research and development of light water reactor, fusion reactor, and for fundamental research of materials irradiation damage. The outline and utilization of the JMTR are shown in the section 6.3.

Some other facilities in JAERI relating nuclear safety research are briefly described from section 2.1 to 2.4, which are the Nuclear Safety Research Reactor (NSRR) for research on fuel behavior under the reactivity initiated accident, the Large Scale Test Facility (LSTF) and the Thermal-Hydraulic Neutronic Coupling loop (THYNC) for research on thermal hydraulics behavior under the operational/accidental condition of LWR, the Verification Experiments of radionuclide Gas/Aerosol release facility (VEGA) for experiments on radionuclide release from irradiated fuel during severe accidents of LWR.

6.1 Hot Laboratories

For the nuclear safety research program, there are three hot laboratories at JAERI, i.e., the Reactor Fuel Examination Facility (RFEF), the Waste Safety Testing Facility (WASTEF) and the Research Hot Laboratory (RHL).

The RFEF is principally performing post irradiation examinations (PIEs) on the reliability and safety of operating power reactor fuel assemblies for PWR, BWR and ATR.

The WASTEF was formerly carrying out safety examination on disposal of high-level waste. However, since the R & D program on waste was finished in FY 1998, main emphasis is placed on chemical hot examinations and PIEs of nuclear materials.

The RHL had been mainly performing PIEs for irradiated fuels and materials, and was taken out of service in the end of FY 2002 due to the fulfillment of its missions. At the present, the RHL is under decommissioning, and the parts of its area have the renewal program to store the un-irradiated fuel samples.

From FY 2003, the PIEs for the nuclear safety research are performed by using the RFEF and the WASTEF on the basis of an each its characteristics, i.e. the RFEF for the fuel field examinations and the WASTEF for material field ones.

Major activities of each facility are described in 6.1.1 through 6.1.3.

6.1.1 Reactor Fuel Examination Facility, RFEF

The RFEF was established in 1979 for performing PIEs of spent reactor fuels in LWR and ATR in order to investigate the fuel safety and reliability. It is equipped with 6 beta-gamma concrete cells with 3 lead ones and 2 alpha-gamma concrete cells with 2 lead ones.

PIEs of the fuel assembly of BWR and PWR are being performed under contract with the utilities and the fuel vender. Re-assembling of MOX fuel assembly irradiated in the "Fugen" reactor had been performed.

For support of R&D works in JAERI, the high burn-up UO_2 and MOX fuels (the highest burn-up is 79 GWd/t), which were irradiated in European nuclear power plants, were transported to RFEF in 2004. Subsequently, fabrication of test rods for the Reactivity Initiated Accident (RIA) tests in the Nuclear Safety Research Reactor (NSRR) and PIEs are carried out under the Advanced LWR Fuel Performance and Safety Research Program. In addition, fabrication of test rods for the RIA tests, PIEs, and the Loss of Coolant Accident (LOCA) tests have been performed with high burn-up fuel claddings irradiated at nuclear power plants in Japan. Concerning Verification Experiments of radionuclides Gas & Aerosol release (VEGA) experiments on radionuclide release and transport during severe accidents, the experiments using irradiated fuel were successfully completed and the gamma scanning tests for filters and piping were performed as a part of the post-test analyses. VEGA experiments had been continued until FY 2004. Moreover, destructive PIEs of rock-like oxide (ROX) fuels, carbonite fuels and nitride fuels have been progressed. Additionally,

re-assembling and PIEs of the spent fuel assemblies of nuclear ship "Mutsu" have been progressed.

Regarding to the development of new PIE technology, a measuring method of hydrogen concentration by backscattered electron image analysis (BEI method) has been improved. The BEI method is very useful for the measurement of local hydrogen concentration in fuel claddings. In the RFEF, a sample preparation and image analysis procedures of the BEI method were improved to measure hydrogen concentration efficiently and precisely [1]. In future, the confirmation tests with claddings of higher hydrogen concentrated, hydrides segregated and irradiated will be performed.

6.1.2 Waste Safety Testing Facility, WASTEF

The facility was established in 1981 to investigate the safety storage and disposal of high level wastes (HLW) from reprocessing of spent fuel. It is equipped with 3 beta-gamma concrete cells, 2 alpha-gamma concrete cells, one lead cell and 9 glove boxes.

Main activities of hot operation in recent years are as follows ;

- Corrosion tests in hot environment under the heat flux control condition for reprocessing plant materials such as an evaporator, a dissolver and so on
- SSRT (Slow Strain Rate Tensile) testing under the simulated operating condition of BWR for investigating the IASCC (Irradiation assisted stress corrosion cracking) phenomenon.
- Burn-up measurement using the micro fragments for evaluation of the integrity and reliability of high burn-up spent fuel.

In addition, in radioactive waste disposal field, diffusion test in bentonite under the simulated environment of geological disposal for evaluating the migration behavior of radio-nuclides and fabrication of molten solidified products doped with TRU elements were still ongoing. Leaching tests on the simulated products had been also conducted for confirming the expected performance.

Newly activities have been continually carried out for safety research of material field. A new technique in mechanical test had been developed for evaluating the integrity of LWR fuel cladding tube, the fracture toughness test is carried out by using an EDM (Electrical Discharge Machine) a fatigue testing machine and so on. In addition, the ring tension test will be conducted for evaluating the circumferential mechanical property on cladding tube in near future.

Moreover, to obtain the detailed information of the irradiated microstructure, the field-emission type transmission electron microscope (FE-TEM) and the focused ion beam (FIB) micro-sampling system were installed at WASTEF. TEM specimen from the optional points of mechanical-tested radioactive specimens can be fabricated by this system. Figure 6.1-1 shows the FE-TEM and FIB micro-sampling system. Additionally, the Auger electron spectroscopy system is available to study the 2D and 3D element distribution and

geometrical aspects in micro areas on irradiated material surfaces.

6.1.3 Research Hot Laboratory, RHL

The RHL was constructed in 1961 to perform the examinations of irradiated fuels and materials as the first one in JAPAN. The facility was expanded in 1966 to provide the surveillance data of fuels, pressure vessel steel and graphite materials for the Magnox reactor in Tokai-village. It was equipped with 10 heavy concrete cells, and 38 lead cells. The RHL had been contributed to research program in JAERI.

However, the RHL was selected the one of target facility 'A middle-range decommissioning plan for the facility in Tokai Research Establishment' as the rationalization program for decrepit facilities in JAERI. Therefore, all PIEs had been finished in March 2003 and the dismantling works of hot cells have been started.

The recent status of the RHL, the decommissioning program is progressing with safety operation of the facility. The apparatuses were removed out from the hot cells. The authorization work of the dismantling program for regulation committee is in progress.

The 4 lead cells (called semi-hot cell) and the 14 lead cells (called Junior-cell) had been dismantled in FY 2003 to 2004. The examination apparatuses in the other lead cells (called steel cell) were moved out and decontamination of the cells for the preparation of dismantling work had been performed in FY 2005. The dismantling work for 18 lead cells had been finished.

The examinations performed in RHL will be succeeding to the RFEF and the WASTEF. The partial area of RHL facility will be provided for the temporary storage of un- irradiated nuclear materials used for our previous research works.

Reference

(1) A. Onozawa, *et al*, "Improved Technique of Hydrogen Concentration Measurement in Fuel Cladding by Backscattered Electron Image Analysis", *Proceedings of 2005 JAEA-KAERI Joint Seminar on Advanced Irradiation and PIE Technologies*, Oarai, Japan, Nov.16-17, p.S2-12(2005).

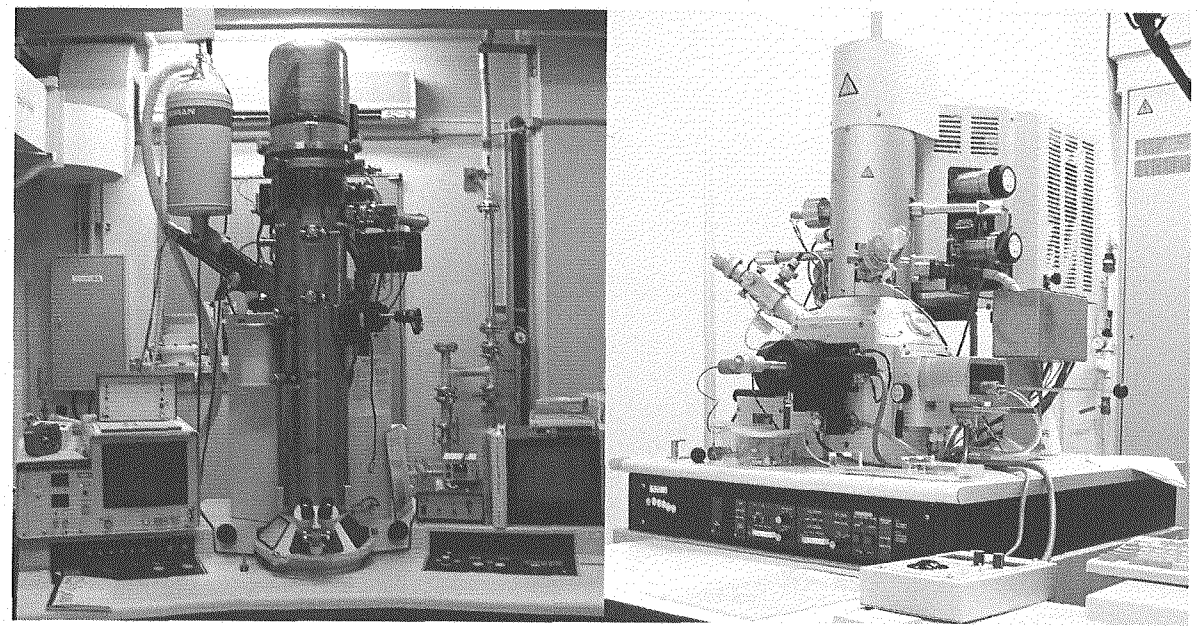

Figure 6.1-1 FE-TEM(left) and FIB micro-sampling system (right)

This is a blank page.

6.2 Nuclear Fuel Cycle Safety Engineering Research Facility, NUCEF

NUCEF is a large-scale facility for fundamental researches on safety and technological advancement in the field of nuclear fuel cycle and radioactive waste management. A cutaway view of NUCEF is illustrated in Fig. 6.2-1. The facility consists of two buildings: Experiment Buildings A and B. The Experiment Building A has two critical facilities, named STACY and TRACY, and a fuel treatment system for these critical facilities. Various critical experiments using STACY and TRACY have been performed since 1995.[1] The Experiment Building B, named BECKY, is a complex research facility in which various $\alpha\gamma$ cells, glove boxes and hoods are installed. Studies on chemical separation in a reprocessing process, partitioning of the high-level radioactive wastes, management of transuranium (TRU) wastes and basic chemistry on TRU elements have been conducted in BECKY since 1995.[2,3,4] Major specifications of the facilities are summarized in Table 6.2-1.

6.2.1 STACY and TRACY

STACY is a critical facility to obtain basic data on criticality safety of fissile solution systems under various core configurations. A series of critical experiments using a heterogeneous core system which consisted of 5-wt%-enriched UO_2 pin rods and a 6-wt%-enriched uranyl nitrate solution[5] was conducted in FY 2003. After obtaining criticality data of a 6-wt%-enriched uranyl nitrate solution in a homogeneous core system[6] in FY 2004, a new series of criticality experiments was started in FY 2005 to obtain reactivity worth data of fission products (FPs) for burn-up credit studies of spent fuel. In this series, the heterogeneous core system was reinstalled and pseudo FP elements such as Sm, Rh, Cs, and Eu (nonradioactive), which significantly affect reactivity worth, were added to the fuel solution in serial order. The configuration of the heterogeneous core system is shown in Fig. 6.2-2. The number of the STACY operations was 45 in FY 2003, 41 in FY 2004 and 30 in the first half of FY 2005, and amounted to 518 as of September, 2005.

TRACY is a pulse-type reactor to simulate criticality accident conditions using low-enriched (^{235}U enrichment 10 wt%) uranyl nitrate solution for studies on neutronic characteristics and radiation dosimetry. A water-reflected core system[7] has been newly used as well as a bare core system[8] since FY 2003. The configuration of the water-reflected core system is shown in Fig. 6.2-3. The number of the TRACY operations was 25 for the bare core system and 15 for the water-reflected core system in FY 2003, 54 for the bare core system and 7 for the water-reflected core system in FY 2004 and 27 for the bare core system in the first half of FY 2005, and amounted to 324 as of September, 2005.

The properties of the fuel solution such as solution density and uranium concentration have been periodically measured about once a week, because ventilation air flows in fuel storage tanks slightly vaporizes water in the solution and thereby uranium concentration and acid molarity of the solution increase gradually.

In the fuel treatment system, a 6-wt%-enriched uranyl nitrate solution was prepared for the STACY experiment series using pseudo FP elements. Solubility of each FP element in uranyl nitrate solution was determined to evaluate the maximum permissible concentration of FP elements in the STACY experiments.

For the undermentioned research on TRU high-temperature chemistry, gram-ordered ^{241}Am (1.60 g) was separated and converted into oxide from plutonium-solvent extraction raffinate.

6.2.2 BECKY

In $\alpha\gamma$ cells shielded with high-density concrete, a series of experiments for the safety assessment and improvement of a reprocessing process has been performed since 1998 using the spent fuel of a light water reactor ranging from 8 to 44.3 GWd/t.[2] In 2004, new experiments using MOX spent fuel started in the cells. In order to obtain the data concerning dissolution characteristics of Pu and properties of residual substance and solution, small scale dissolution tests and bench scale dissolution tests were conducted using several grams and approximately 500 g of MOX spent fuel with a burn-up of 40 GWd/t from the Advanced Thermal Reactor "Fugen", respectively. The experimental apparatus utilized for the small scale dissolution test is shown in Fig. 6.2-4.

Researches on radionuclide migration necessary for long-term performance assessment of a geological disposal system have been performed in the glove boxes. In order to acquire the experimental migration data for establishing probabilistic safety assessment methodologies, an existing glove box system was improved by installing an argon gas circulation system to conduct the experiments under inert gas atmosphere.[9] Sorption tests of radionuclides on rock samples, which were taken from deep underground with original reducing environments maintained, started in the system.

In the experimental facility for TRU high temperature chemistry (TRU-HITEC), studies on minor-actinide-bearing fuels and pyrochemical processes have been performed since 2003. The facility,[10] shown in Fig. 6.2-5, consists of three $\alpha\gamma$ cells shielded with steel and polyethylene and a globe box shielded with leaded acrylic resin, where a high purity argon gas atmosphere is maintained. Hot tests with gram-ordered ^{241}Am started in December, 2004. Experiments to obtain the fundamental behavior data of minor actinide elements such as Np, Am, and Cm in fuels/targets and molten salts at high temperature are now on-going.

Development of the high-sensitivity detection of fissile material by 14 MeV Neutron Direct Interrogation Method,[11] which aims at establishing a nondestructive measurement technique for rational and safe disposal of radioactive waste, is successfully carried out. Until now, excellent improvement of the detection sensitivity regardless of the position in waste packages is accomplished using the developed method compared with a existing active neutron method. It is expected that this measurement method will be utilized as a measure

to discriminate radioactive waste from non-radioactive waste for wastes contaminated with fissile materials.

References

(1) Y. Miyoshi, "Accomplishment of 10-year Research in NUCEF and Future Development, —Criticality Safety Research—," *Proc. Int. Symp. NUCEF 2005*, Tokai-mura, Japan, Feb. 9-10, 2005, JAERI-Conf 2005-007, p.19 (2005).

(2) Y. Morita, T. Asakura, H. Mineo, *et al.*, "Accomplishment of 10-year Research in NUCEF and Future Development, —Process Safety and Development Research—," *Proc. Int. Symp. NUCEF 2005*, Tokai-mura, Japan, Feb. 9-10, 2005, JAERI-Conf 2005-007, p.25 (2005).

(3) S. Nakayama, T. Tanaka and T. Yamamoto, "Accomplishment of 10-year Research in NUCEF and Future Development, —Waste Disposal Safety Research—," *Proc. Int. Symp. NUCEF 2005*, Tokai-mura, Japan, Feb. 9-10, 2005, JAERI-Conf 2005-007, p.31 (2005).

(4) K. Minato, "Accomplishment of 10-year Research in NUCEF and Future Development, —Actinides Science Research—," *Proc. Int. Symp. NUCEF 2005*, Tokai-mura, Japan, Feb. 9-10, 2005, JAERI-Conf 2005-007, p.37 (2005).

(5) H. Sono, Y. Fukaya, H. Yanagisawa, *et al.*, *Analyses of Neutronic Characteristics of STACY Heterogeneous Core with 1.5-cm-Lattice-Pitch Fuel Pins*, JAERI-Tech 2003-065, Japan Atomic Energy Research Institute (2003), [in Japanese].

(6) H. Yanagisawa and H. Sono, *Evaluation of Neutronic Characteristics of STACY 80-cm-diameter Cylindrical Core Fueled with 6% Enriched Uranyl Nitrate Solution*, JAERI-Tech 2003-057, Japan Atomic Energy Research Institute (2003).

(7) H. Sono, H. Yanagisawa and Y. Miyoshi, *Evaluation of Neutronic Characteristics of TRACY Water-reflected Core System*, JAERI-Tech 2003-096, Japan Atomic Energy Research Institute (2003) , [in Japanese].

(8) H. Sono, H. Yanagisawa, K. Nakajima, *et al.*, "Analyses of Criticality and Reactivity for TRACY Experiment Based on JENDL-3.3 Data Library," *Proc. 7th Int. Conf. Nuclear Criticality Safety (ICNC2003)*, Tokai-mura, Japan, Oct. 20-24, 2003, JAERI-Conf 2003-019, Vol. I, p.308 (2003).

(9) M. Akai, N. Ito, T. Yamaguchi, *et al.*, *Geochemistry Research Equipment for TRU Waste Elements*, JAERI-Tech 2004-058, Japan Atomic Energy Research Institute (2004).

(10) K. Minato, M. Akabori, T. Tsuboi, *et al.*, *Development of Module for TRU High Temperature Chemistry (Joint Research)*, JAERI-Tech 2005-059, Japan Atomic Energy Research Institute (2005).

(11) M. Haruyama, M. Takasei, H. Tobita, *et al.*, "High-Sensitive Detection by Direct

Interrogation of 14 MeV Acc Neutrons, (I) —Uranium-Contaminated Metal Matrix in a Waste Dram—," *Trans. At. Energy Soc. Japan*, Vol.3, No.2, p.185 (2004), [in Japanese].

Table 6.2-1 Major specifications of facilities in NUCEF.

(a) STACY and TRACY

	STACY	TRACY
Thermal power	-Max. 200 W	-Max. 10 kW (delayed critical operation) -Max. 5,000 MW (transient operation)
Excess reactivity	-Max. 0.8 $	-Max. 0.8 $ (delayed critical operation) -Max. 3 $ (transient operation)
Maximum fuel inventory	-Uranyl nitrate solution 4 or 6 wt% enrichment 350 kgU 10 wt% enrichment 150 kgU -Plutonium nitrate solution 60 kgPu -UO_2 fuel rod 5 wt% enrichment 400 kgU	-Uranyl nitrate solution 10 wt% enrichment 150 kgU
Reactivity control method	-Feed and drainage of solution (safety rods for shutdown)	-Feed and drainage of solution -Withdrawal of transient rod
First criticality	-February 1995	-December 1995

(b) BECKY

	Research on Chemical Separation Process	Research on Radioactive Waste Management and TRU Chemistry
Research activities	-Improvement of reprocessing process -Development of partitioning process of high-level liquid waste	-Studies on long-term degradation of engineered barriers and chemical/ geochemical behavior of radionuclides -Studies on fundamental properties of TRU-containing compounds at high temperature -Development of nondestructive measurement technique
Experiment method	-Laboratory-scale experiments using LWR spent fuel , MOX spent fuel, high-level liquid waste and radioisotopes	-Laboratory-scale experiments using nuclear fuel materials and radioisotopes -Drum irradiation using an active neutron assay system
Major equipment	-αγ cells shielded with high-density concrete -Glove boxes	-Atmosphere-controlled and conventional glove boxes -TRU-HITEC (Steel αγ cells) -Active neutron assay system
Usable major radioactive materials and permitted maximum annual usage	-LWR and MOX spent fuels : 880 TBq -Plutonium : 1.45 kg -Uranium : 10 kg(natural), etc. -Thorium : 1 kg -Radioisotopes: ^{237}Np, ^{241}Am, ^{99}Tc, ^{129}I, ^{79}Se, ^{93}Zr, ^{126}Sn, etc.	

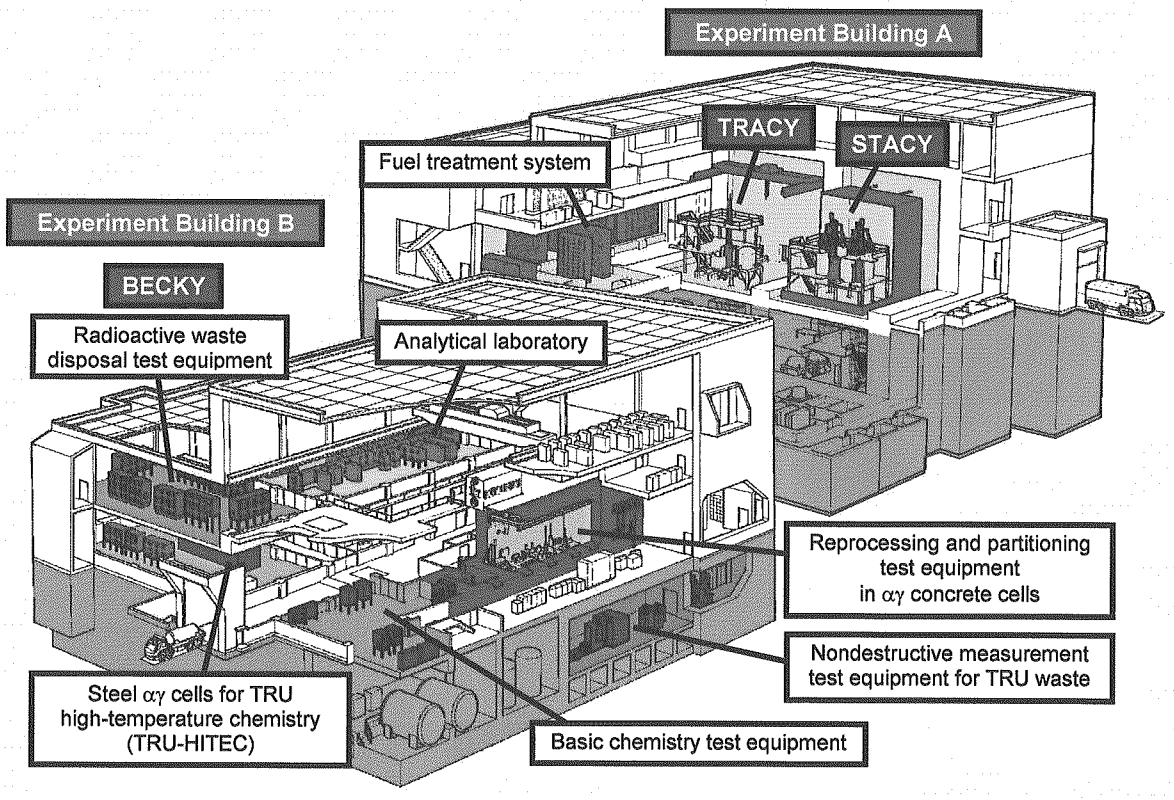

Fig. 6.2-1 Cutaway view of NUCEF

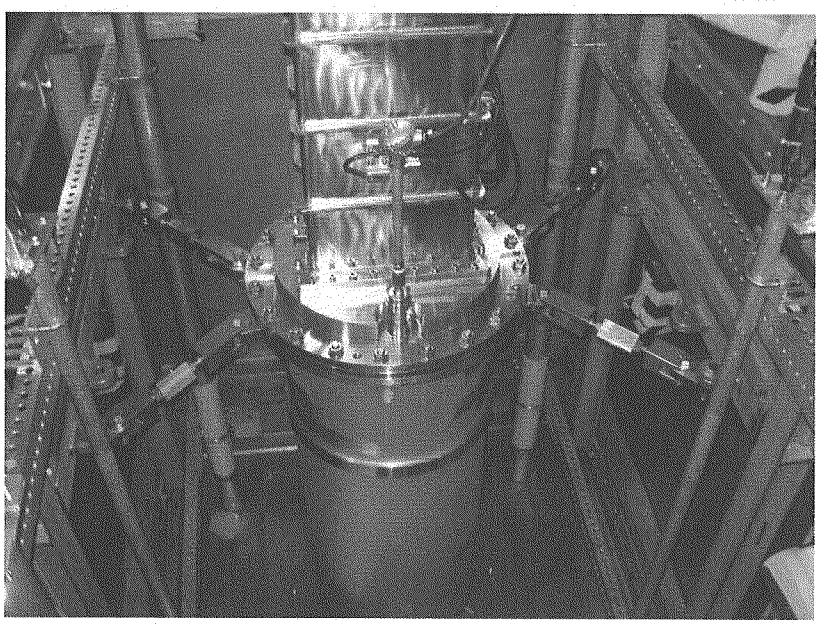

Fig. 6.2-2 STACY heterogeneous core system (The core consists of hundreds of 5-wt%-enriched UO_2 pin rods and a 6-wt%-enriched uranyl nitrate solution.)

This is a blank page.

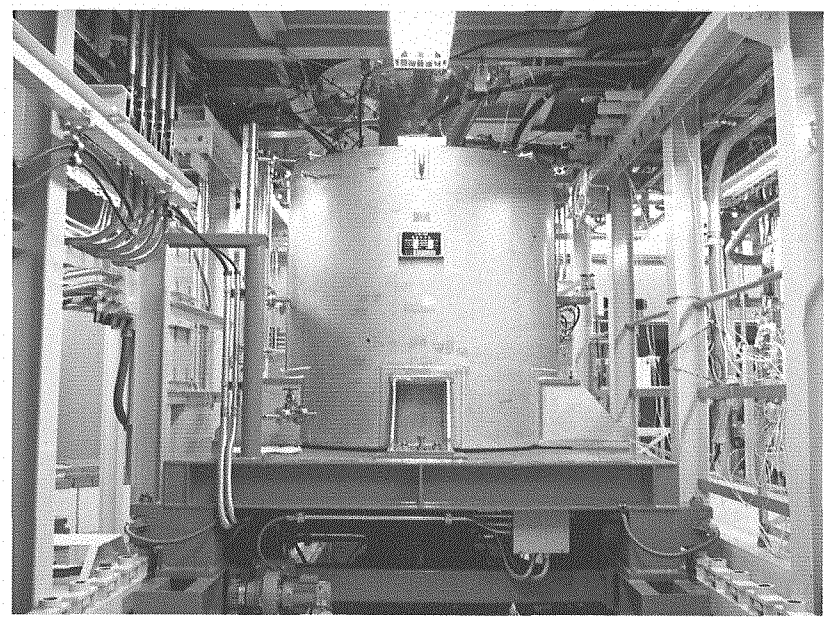

Fig. 6.2-3 TRACY water-reflected core system (The core is surrounded with two-part divided water tanks.)

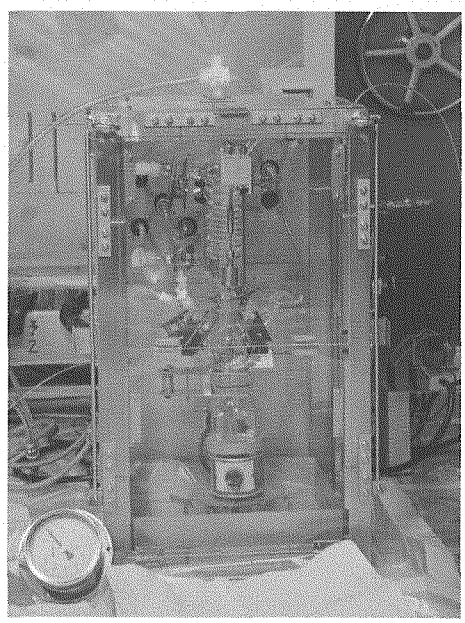

Fig. 6.2-4 Experimental apparatus for the small scale dissolution test in αγ concrete cells

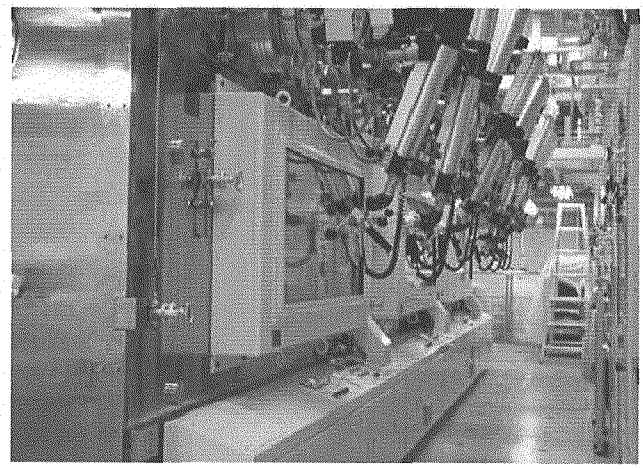

Fig. 6.2-5 Front view of TRU-HITEC

This is a blank page.

6.3 Japan Materials Testing Reactor and Hot Laboratory

The Japan Materials Testing Reactor (JMTR) is the multi-purpose testing reactor for irradiation tests of nuclear fuels and materials. The reactor is a tank-in-pool type, cooled and moderated by light water with maximum thermal power of 50 MW. During last thirty-four years since the JMTR started materials irradiation tests in 1971, many types of irradiation capsules, large irradiation test loops and in-core instrumentation devices were developed and used. Irradiation tests have been recently conducted mainly for material research and development of light water reactor, fusion reactor and fundamental research of materials irradiation damage.

In the hot laboratory connected to the JMTR with the water canal, various post irradiation examinations (PIEs) are carried out for specimens of nuclear fuels and materials which are highly radioactive after the irradiation in JMTR and/or other reactors. The hot cell in the hot laboratory and the reactor are also connected through a water canal which is used to transfer capsules irradiated in JMTR to the hot laboratory for PIEs, and to transfer capsules re-assembled in the hot cell to JMTR for re-irradiation. The layout of the the JMTR, the hot laboratory and their related facilities is shown in Fig. 6.3-1

6.3.1 Japan Materials Testing Reactor, JMTR

(1) Outline of JMTR

The JMTR achieved the first criticality in March, 1968. The JMTR is being operated at rated thermal power of 50 MW since 1971. The core configuration of the JMTR is shown in Fig.6.3-2. The reactor core consists of the fuel region and the reflector region. The fuel region consists of standard fuel elements and control rods, etc., and is located in the center of the reactor core. The reflector region surrounds the fuel region, and consists of beryllium reflectors and aluminum reflectors, etc. The low gamma dose irradiation region by the gamma ray shielding plate made of Zircaloy-2 is placed in north part of the reactor core. In the JMTR, approx. 60 irradiation holes include 6 holes of the fuel region are available to irradiation tests with irradiation capsules.

The fast neutron flux (E>1 MeV) in the current core configuration is approximately $3\times 10^{18}m^{-2}s^{-1}$ at maximum in the fuel region, and it decreases to the level of 1/2000 of the maximum in the peripheral (farthest) irradiation positions in the core. The thermal neutron flux (E<0.683 eV) is approximately $4\times 10^{18}m^{-2}s^{-1}$ at maximum in the first and the second reflector layers surrounding the fuel region, and it decrease to the level of 1/30 of the maximum in the peripheral irradiation positions. These wide distributions of neutron flux provide flexible irradiation fields for various needs of irradiation tests.

JMTR has wide variety of irradiation facilities in order to meet requirement of irradiation tests. The irradiation facilities consist of many types of irradiation capsules, hydraulic rabbit irradiation facility, the power ramping test facility and Advanced Water

Chemistry Controlled Irradiation Research Device. Irradiation capsules are the most flexible irradiation tools to fulfill the various kinds of irradiation needs for nuclear fuel and material research. Hydraulic rabbit irradiation facility is mainly used for short time irradiation tests for such as fundamental research. The power ramping test facility was installed in 1984, since then ninety-nine power ramping tests were totally carried out in the JMTR by JAERI's research for nuclear fuel safety and the national research project for high burn-up BWR fuels. The facility operation has been currently suspended since 2001.

New irradiation test facility "Advanced Water Chemistry Controlled Irradiation Research Device" for IASCC study consists of saturated temperature capsules (SATCAPs), the out-of-pile water control unit (WCU) and the connecting units to connect SATCAPs with the WCU as shown in Fig. 6.3-3. The WCU can feed controlled water up to five SATCAPs at maximum for effective proceeding of irradiation test program.

(2) Operation of JMTR

With regard to recent operation of JMTR, 5 cycles, 6 cycles and 2 cycles were achieved in fiscal year 2003, 2004 and the first half of fiscal year 2005 respectively, and the total operating time in two and a half years was approximately 8300 hours.

Requirement of high neutron fluence irradiation related to ageing research of light-water reactor was increased. Therefore, in order to extend the operating period of one-cycle from 26 to 31 days, reactor core was improved by adding two fuel elements and the operation period with the improved core was extended to 31 days in Nov. 2003. Consequently, the operation days in fiscal year 2004 extended to 181 days.

(3) Irradiation test

The total number of capsules and hydraulic rabbits irradiated in fiscal year 2003, 2004 and the first half of fiscal year 2005 were 131 capsules and 32 rabbits, 145 capsules and 29 rabbits and 41 capsules and 8 rabbits, respectively.

With regard to nuclear safety research of light water reactor, additional-irradiation of high burn-up PWR fuels, irradiation tests of pressure vessel materials, reactor core materials and concrete and irradiation tests for IASCC study were carried out.

(4) Development of capsule for in-pile IASCC testing

In the field of IASCC research, SCC tests under neutron irradiation are one of the key technologies to obtain information concerning synergistic effects of the applied stress, water chemistry and neutron/gamma irradiation. Therefore, the in-pile crack growth and crack initiation test techniques were developed using saturated temperature capsule[1]. In order to apply the stress to initiate or propagate SCC on test specimens, metal bellows was employed in the testing unit. By this method, applied stress can be controlled by controlling a pressure

difference between inner and outer of metal bellows. CT specimens or UCL specimens are equipped in a capsule and loaded by shrinking of bellows. To fabricate in-situ test capsules in a hot cell, a remote welding technique as well as specimen installation technique was established. In-pile IASCC testing using the capsule was started in fiscal year 2004 and will be completed in fiscal year 2006.

(5) Water chemistry evaluation for IASCC study

In the in-pile IASCC test, water chemistry such as dissolved oxygen (DO), dissolved hydrogen (DH), hydrogen peroxide (H_2O_2) contents is one of the most important parameter as same as neutron/gamma fluence or stress condition. Therefore, the water radiolysis code for the irradiation loop system (WRAC-JM) was developed based on the water radiolysis in a crevice code (WRAC)[2]. In the WRAC-JM code, the direct generation of radiolytic species due to radiation energy deposition in the water, secondary generation and disappearance caused by their interaction and interaction with the capsule surface were introduced. By this analysis code, precise water chemistry at optional point can be evaluated. In other words, important information for IASCC irradiation tests can be obtained by this analysis code.

6.3.2 Hot Laboratory of[TT1] JMTR

The hot laboratory of JMTR was put into service in 1971 to perform PIEs of specimens irradiated mainly in JMTR. A plane view of the hot laboratory is shown in Fig. 6.3-4. A wide variety of PIEs for the research and development of nuclear fuels and materials is available in three kinds of hot cells (eight concrete cells, five steel cells and seven lead cells) in the hot laboratory. Four microscope lead cells are also connected to the concrete cell No.8.

Since the concrete cell No.1 in the hot laboratory is connected with the reactor by a canal pool, irradiated capsules including several kinds of specimens are easily transferred from JMTR to the concrete cell No.1 through the canal pool. Irradiated capsules are dismantled in the concrete cell No.2 to pull irradiated specimens out from them. The PIEs carried out in the concrete cells are gamma scanning, X-ray radiography, eddy current testing, compression test and IASCC growth testing. The optical micrographic examination and hardness test are performed in the microscope lead cells. Samples for them are prepared in the concrete cell No.8.

The PIEs carried out in the lead cells are the stress corrosion cracking (SCC) test, slow strain rate testing (SSRT), tensile test, Charpy impact test and small punch (SP) test. Heat treatment of specimens by an electric furnace and fractography by a scanning electron microscope (SEM) are also performed in the lead cells.

The PIEs in the steel cells are the visual inspection, dimensional measurement, low cycle

fatigue test, tensile test, fracture toughness test and crack growth test.

Concerning the nuclear safety research, following PIEs were conducted in the hot laboratory of JMTR from April 2003 to September 2005. Tensile test, hardness test, fracture toughness test, SSRTs, fatigue test, Charpy impact test, compression test, fracture surface observation and metallographic test were performed on the irradiated stainless and pressure vessel steels. Useful results were obtained on the reliability and safety of structural materials of nuclear components, on the stress corrosion cracking of core internal materials and on the aging of structural materials. IASCC growth test technique of irradiated in-core structural materials, remote-welding technique for assembling in-pile IASCC capsule in hot cell and remote operation technique of atomic force microscope (AFM) are currently developed in the hot laboratory and described in the following paragraphs.

(1) IASCC growth test technique of irradiated in-core structural materials

In March 2004, a new IASCC test machine having two autoclaves for producing the test condition of high temperature water was installed in the concrete cell No.6. Crack growth tests and SSRTs on irradiated steels, by using different test jigs, have been conducted in the machine. A photograph of the test machine installed in the hot cell is shown in Fig. 6.3-5. The maximum operational parameters for SSRTs and crack growth tests in a simulated BWR environment, are as follows; load capacity: 10 kN, temperature: 573 K, pressure: 10 MPa, and flow rate: 30 little per hour. The 0.5T-CT type test specimens with 12.7, 6.4 or 5.6 mm in thickness can be applied to the IASCC growth test by this machine. IASCC growth tests of four irradiated CT specimens have already been finished until August 2005.

(2) Remote-welding technique for assembling in-pile IASCC capsule in hot cell

In order to assemble the in-pile IASCC capsule equipped with a test unit mounted the pre-irradiated CT specimens for the crack growth test in JMTR, the remote-welding technique of the capsule tube was particularly needed for the butt joint of capsule tube with large diameter. Therefore, a technique for new remote-controlled welding machine whose torch was fixed over the tube had been developped from August 2003 to January 2004. A schematic drawing of the machine is shown in Fig. 6.3-6. The capsule tube from 40 to 65 mm in diameter can be welded by the machine. The rotating speed of the capsule tube during welding can be controlled from 60 to 200 sec/round. Four in-pile IASCC capsules equipped with the pre-irradiated CT specimens were remotely assembled in the hot cell for performing crack growth tests under the neutron irradiation in JMTR. The irradiation test of two in-pile IASCC capsules has been already finished successfully in JMTR.

(3) Development of remote-controlled atomic force microscope (AFM)

In 2004, the remote-controlled AFM apparatus was developed to perform nano-scopic

examinations of irradiated specimens in the hot cell as a new examination technique. It was developed with former Research Group for Reactor Structural Materials of Tokai Establishment under the JAERI-JNC (Japan Nuclear Cycle Development Institute) joint research program from 2003 to 2005[3, 4], which was titled: A study on degradation of structural materials used under the irradiation environment in nuclear research. The purpose of this study was to develop the method for the damage evaluation and detection in earlier stage of irradiation damage progress. The AFM apparatus can observe electrochemical corrosion characteristics focused on grain boundary in irradiated specimens as nano-scopic three-dimensional surface configuration. This is one of the effective PIE methods to evaluate the irradiation damage which induces to intergranular IASCC[5], for instance. The apparatus was installed in the No.6 lead cell of JMTR HL as shown in Fig. 6.3-7. Scanning area of the apparatus is from 500 x 500 nm^2 to 800 x 800 μm^2. The vertical resolution is 0.3nm in minimum. A cantilever unit, a detective sensor of the apparatus, is about 6.5 x 4.5 x 1 mm^3. Optical microscope with CCD camera is also equipped, the area of 500 x 400 μm^2 can be observed. Because the cantilever unit is too small to handle by the manipulator, remote-controlled cantilever exchange system was installed, which was essential to modify a market produced AFM to completely remote-controlled type. In 2005, AFM observation results on neutron irradiated specimen with creep loaded have been obtained by using the AFM apparatus. In a future work of JMTR HL, this apparatus will be useful for nano-scopit detection and evaluation of irradiation damages in structural materials used in nuclear power plants.

References

(1) Y.Kaji, et al., "Present status of In-pile IASCC Growth Tests at JMTR" The 32th Enlarged Halden Programme Group Meeting., Proceedings (2005).

(2) T.Satoh, Y.Satoh and S.Uchida, "Water Chemistry in a Crack Tip under Irradiation, (II)" Journal of Nuclear Science and Technology.,40[5], pp.334-342 (2003).

(3) T. Hoshiya, F. Ueno, et al., "JNC-JAERI United Research Report, A study on degradation of structural materials under irradiation environment in nuclear reactors", JNC TY9400 2004-026 & JAERI-Research 2004-016, (2004), [in Japanese].

(4) F. Ueno, Y. Nagae, et al., "JAERI-JNC United Research Report, A study on degradation of structural materials under irradiation environment in nuclear reactors", JAERI-Research 2005-023 & JNC TY9400 2005-013, , (2005), [in Japanese].

(5) Y. Nemoto, Y. Miwa, et al., "AFM evaluation of grain boundary corrosion behavior on ion irradiation stainless steel", Int. Symp. on Materials Chemistry in Nuclear Environment (Material Chemistry '02), March 13-15, 2002, Tsukuba, JAERI-Conf 2003-001, pp.397-404 (2003).

This is a blank page.

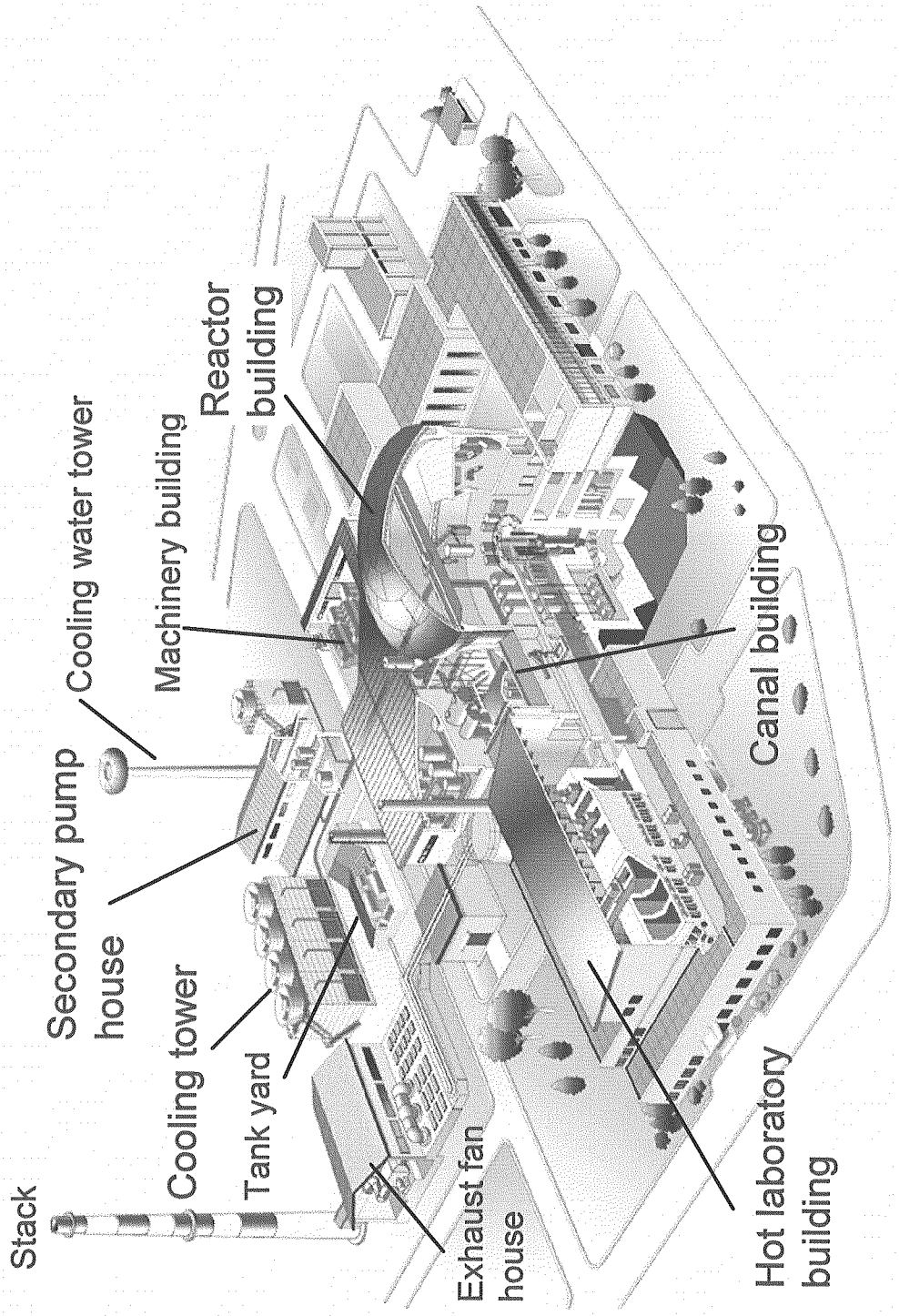

Fig. 6.3-1 Outline of Japan Materials Testing Reactor (JMTR)

This is a blank page.

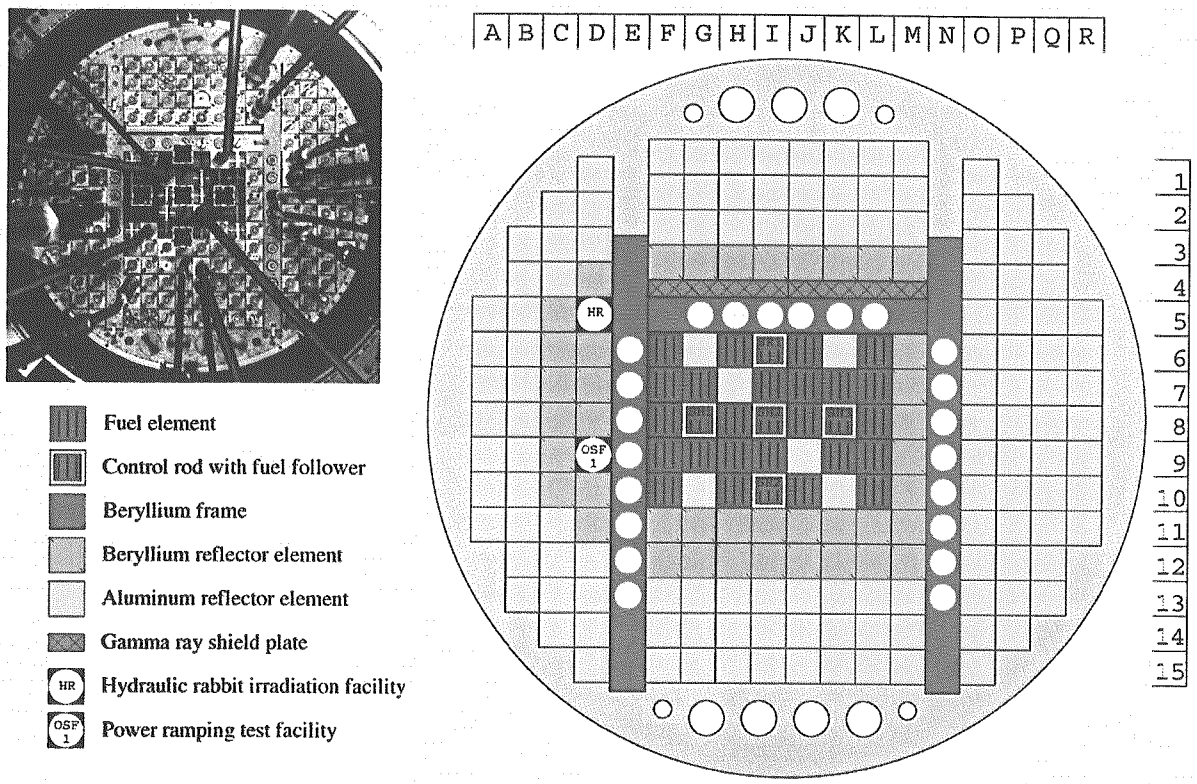

Fig.6.3-2 Core arrangement of the JMTR

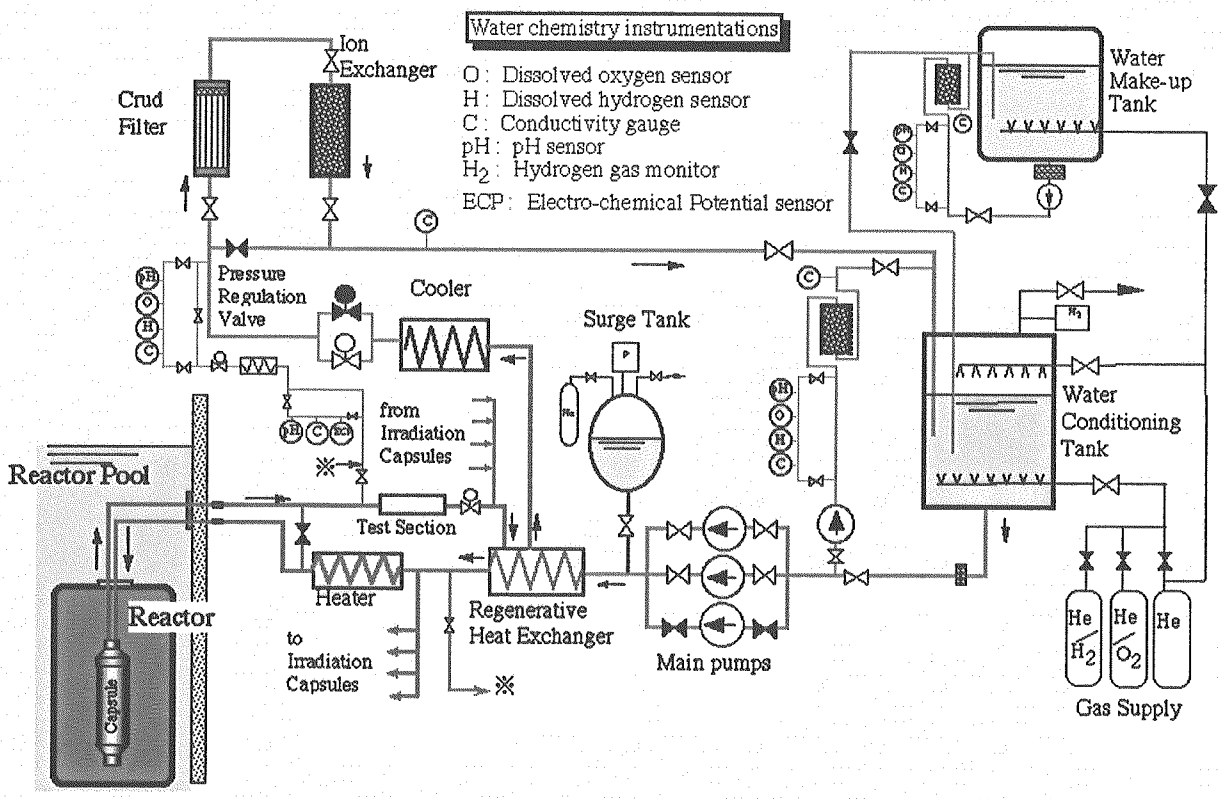

Fig. 6.3-3 Schematic diagram of the advanced water chemistry controlled irradiation research device for material irradiation under the simulated BWR condition

This is a blank page.

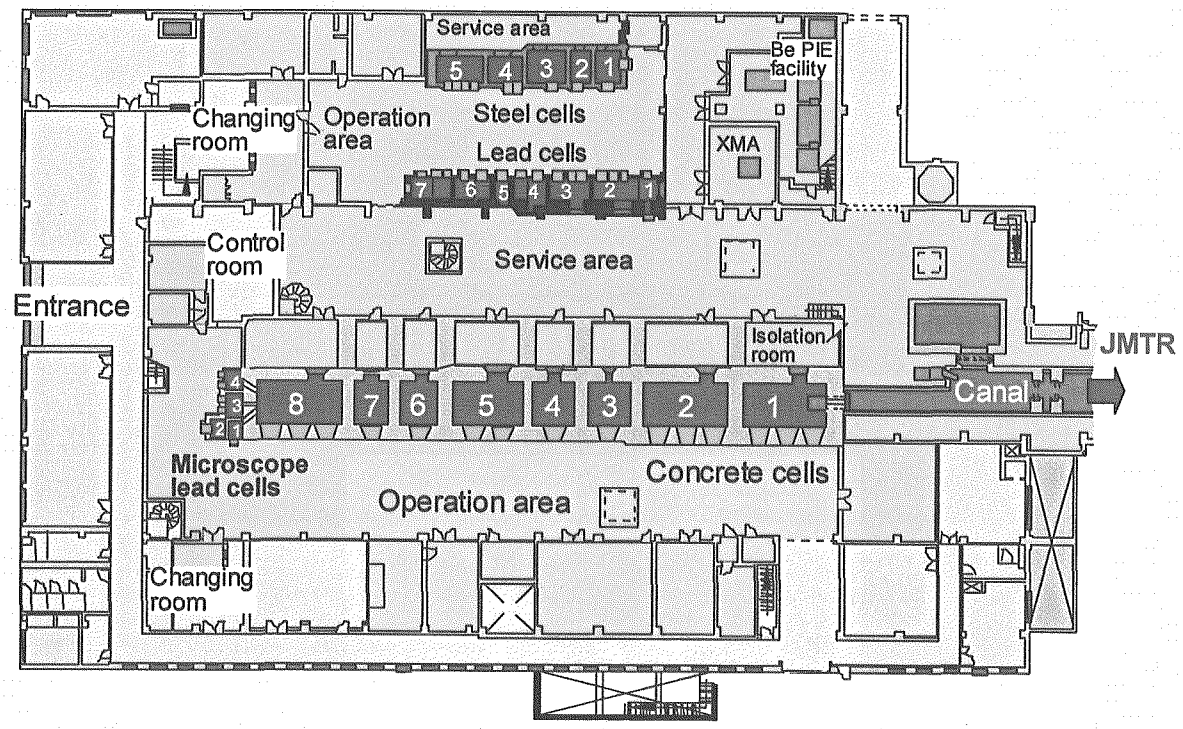

Fig. 6.3-4 Plane view of JMTR hot laboratory

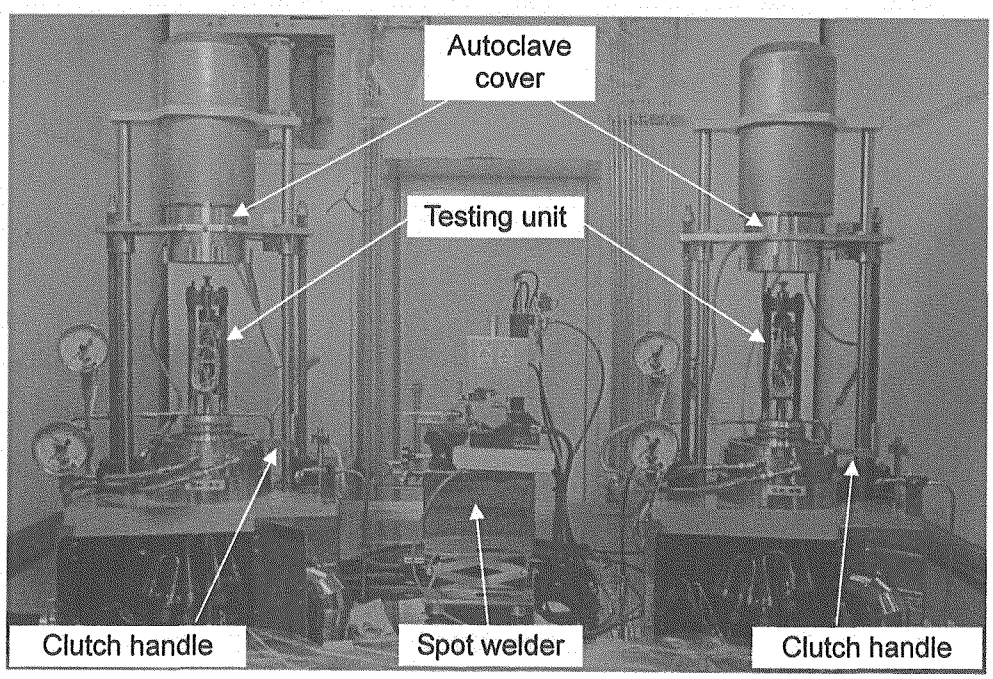

Fig. 6.3-5 SCC growth test facility installed in hot cell

This is a blank page.

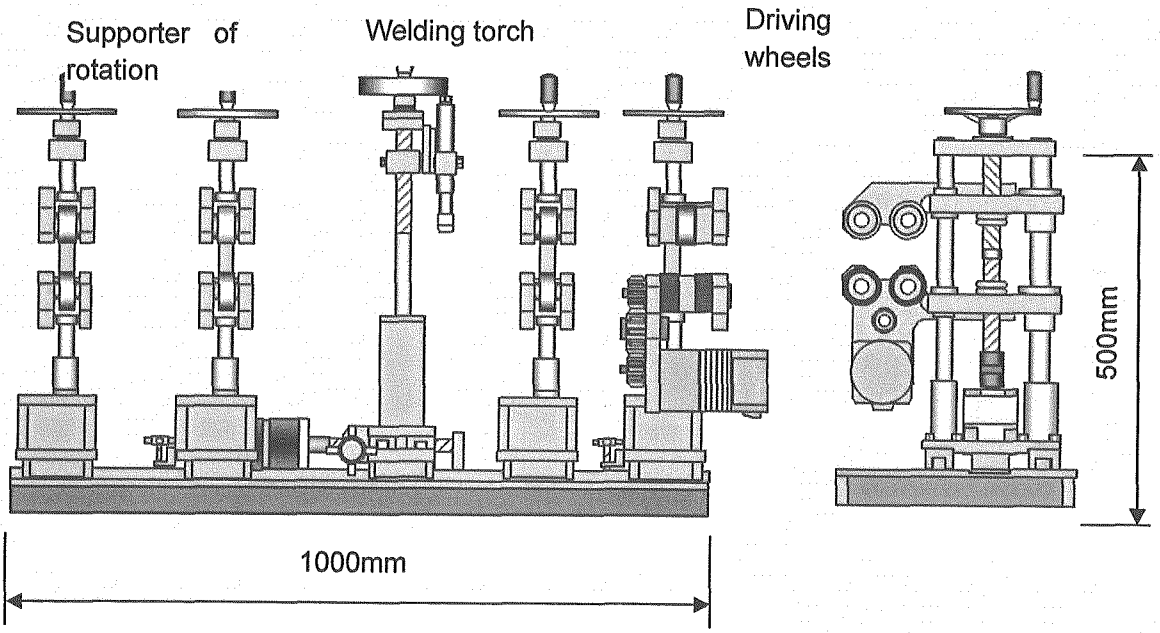

Fig. 6.3-6 Schematic drawing of capsule welding apparatus

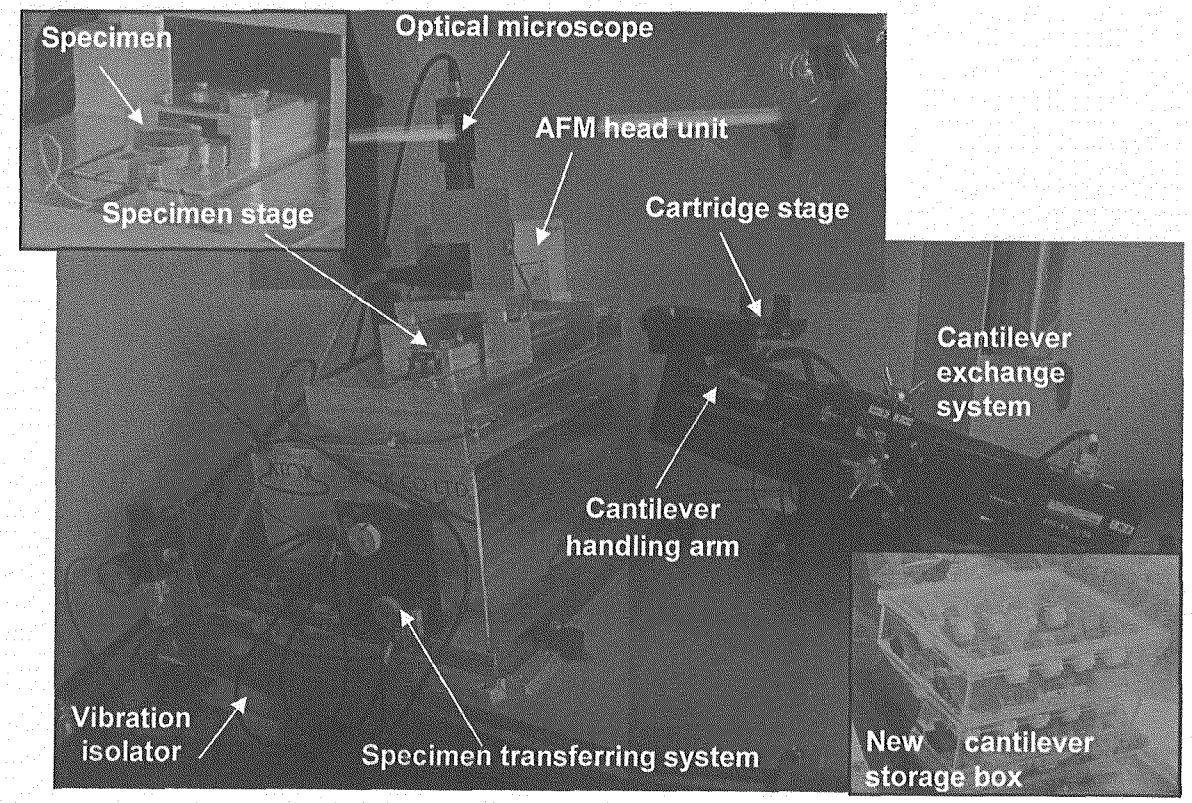

Fig. 6.3-7 Remote-controlled AFM installed in hot cell

This is a blank page.

7. INTERNATIONAL COLLABORATION

JAERI, the predecessor of JAEA, recognized that improving the safety of nuclear facilities was a common global goal and was necessary to achieve public acceptance of nuclear energy. With this impetus, JAERI assigned international collaboration as a significant role in its nuclear safety research activities. This collaborative effort allowed the sharing of data and information among the participating countries by conducting cooperative research to obtain scientific and technical knowledge. International collaborative research activities are listed in Table 7-1. In addition, JAERI actively took a responsible role by providing technical experts and assistance to the international community through the International Atomic Energy Agency (IAEA) and the Organization for Economic Cooperation and Development (OECD) to enhance and further ensure the safety of nuclear facilities around the world.

Table 7-1 International cooperative agreements in the field of nuclear safety research

Items	Participants (Host Organization)	Place	Period	Objectives
OECD Halden Reactor Project	13 Organizations from 14 Countries	Norway/Halden	Apr. 1967- Dec. 2008	Research on performance and reliability of fuel.
Cooperative Research Program in the Field of Peaceful Use of Nuclear Energy	JAERI KAERI	Korea/Taejon	Aug. 2004- Aug. 2007	Information exchange on research of probabilistic safety assessment, development of testing technology for thermal-hydraulics, severe accident.
Implementing Agreement between USNRC and JAERI in the Area of Probabilistic Risk Assessment Research	JAERI USNRC	USA/Washington DC	Aug. 2002- Sep. 2005	Information exchange on research of probabilistic safety assessment (PSA).
Implementing Agreement between USNRC and JAERI in the Field of Nuclear Reactor Safety Research	JAERI USNRC	USA/Washington DC	Sep. 2003- Sep. 2005	Information exchange on research of thermal-hydraulic safety and related code development, severe accident, plant aging, high-burnup fuel for LWRs.
Co-operation Agreement of Nuclear Safety and Radiation Protection	JAERI IRSN	France/Cadarache	Dec. 2003 - Dec. 2008	Information exchange on research in the areas of nuclear safety and radiation protection, i.e. fission products release and criticality safety.
Amendment No.1 to the Implementing Agreement for Cooperation in the Field of Reactors Research	JAERI CEA	France/Cadarache, Saclay	May 2004 - Sep. 2007	Information exchange on research in the areas of advanced water-cooled reactor systems, accelerator driven systems and other systems, i.e. thermal-hydraulic and neutronics coupling, fuel-coolant interactions, probabilistic component reliability evaluation, reactor physics and thermal hydraulincs.
Agreement on the OECD ROSA Project to resolve Thermal-Hydraulic Safety Issues relevant for Water Reactors, through Experiments in the ROSA Large Scale Test Facility	16 Organizations from 13 Countries (JAERI)	France/Paris	April 2005 - March 2009	Research on resolving thermal-hydraulic safety issues relevant to LWRs through experiments with the test facility ROSA/LSTF.